R/V Mirai Cruise Report

MR20-05C (MR20-Nishino)

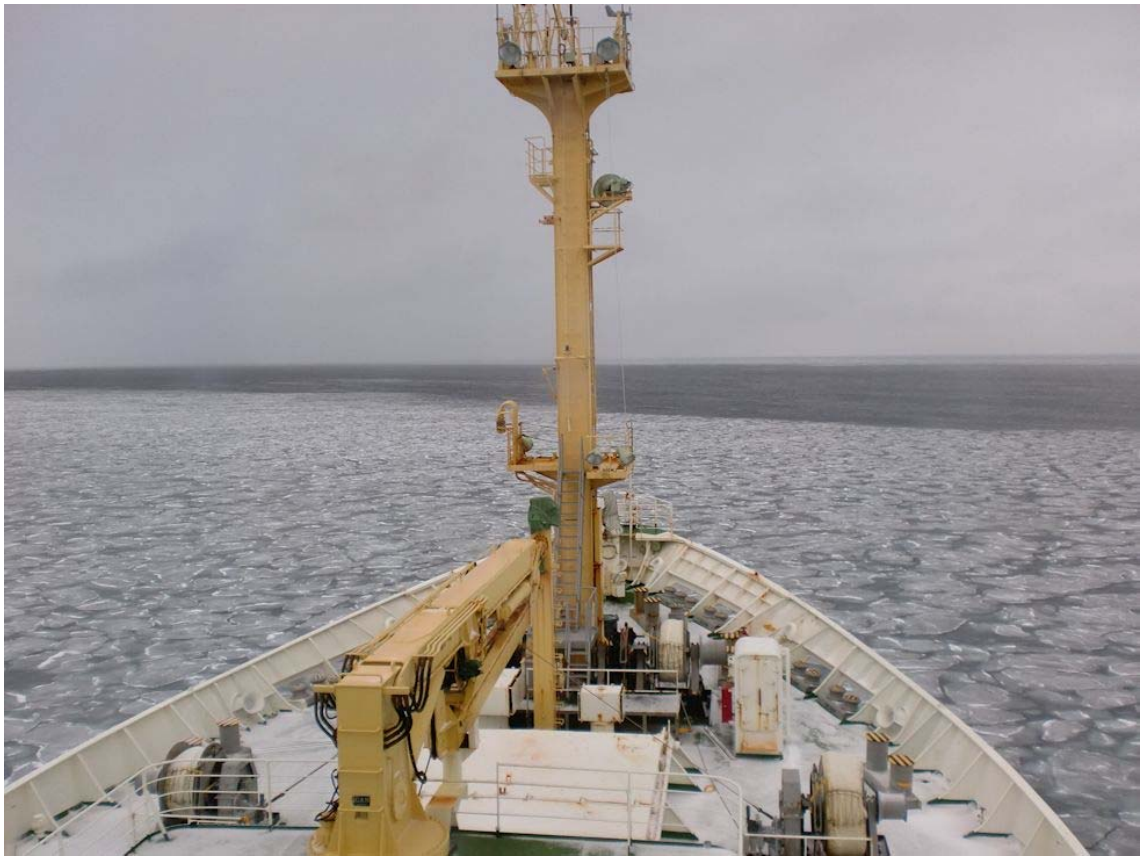

Arctic Challenge for Sustainability II (ArCS II)

Arctic Ocean, Bering Sea, and North Pacific Ocean
19 September 2020 – 2 November 2020

Japan Agency for Marine-Earth Science and Technology

(JAMSTEC)

Contents

1. Cruise Summary

1.1. Objectives

Since spatial and temporal variability is inherently large in the Arctic Ocean, we urgently need baseline data for the Arctic Ocean as a whole to prepare for the further changes to come. Critically needed understandings would be advanced from a coordinated multi-ship, multi-nation pan-Arctic ship-based sampling campaign, based on shared state-of-the-art protocols for data collections and sharing and carefully planned ship tracks during the same period. This could allow for a synoptic view of the totality of hydrographic and ecosystem changes taking place in the Arctic Ocean and facilitate advancing model development using integrated data sets to predict the future state of the Arctic. To obtain such baseline data, we have planned a pan-Arctic research program, the Synoptic Arctic Survey (SAS), with a goal of conducting it in 2020 and 2021.

1.2. Overview

Under the SAS program, we conducted the Arctic Ocean cruise from 19 September to 2 November 2020 using the Research Vessel (R/V) Mirai (Figure 1.2-1). We left Shimizu on 19 September and had a quarantine near the coast of Japan for 14 days (19 September–2 October). Then, we passed through the Bering Strait toward the north on 6 October and carried out the Arctic Ocean survey for 16 days (6–21 October). On 21 October, we passed through the Bering Strait southward and came back to Shimizu on 2 November. This cruise was supported by the project of Arctic Challenge for Sustainability II (ArCS II), which was funded by the Ministry of Education, Culture, Sports, Science and Technology of Japan (MEXT).

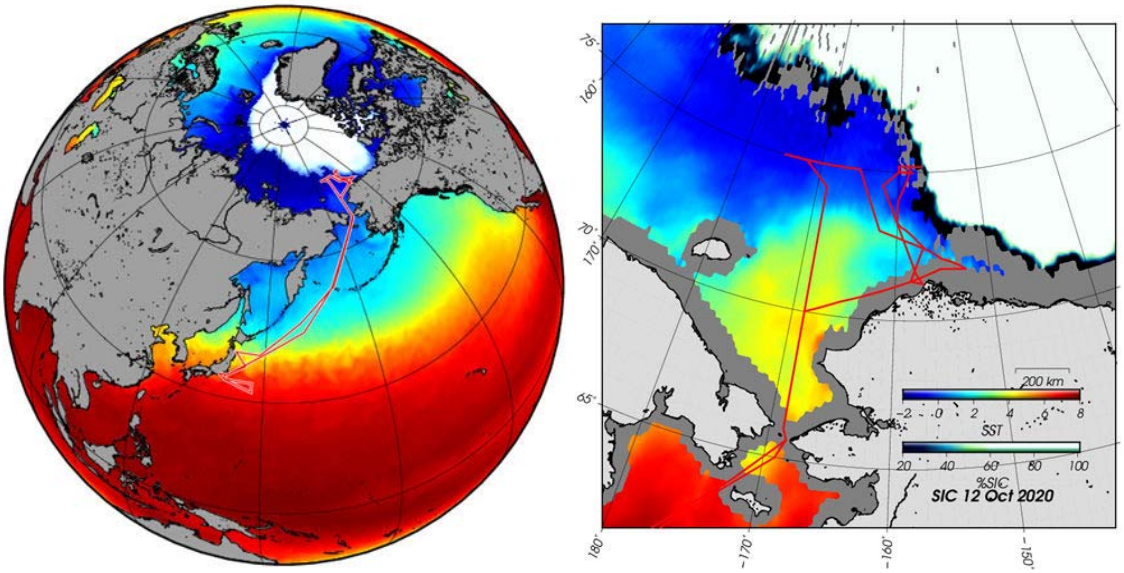

Figure 1.2-1. Cruise track (red lines), sea ice concentration (SIC) on 12 October 2020, and sea surface temperature (SST) averaged over the period of observation.

According to a report from National Snow and Ice Data Center (NSIDC), sea ice extent for October 2020 was 5.28 million square kilometers, placing it lowest in the satellite record for the month. This was 3.07 million square kilometers below the 1981 to 2010 October average and 450,000 square kilometers below the record low mark for October set in 2019. Our research areas in the Canada Basin were covered by sea ice on the Alaskan side, but ice free on the Siberian side (Figure 1.2-2).

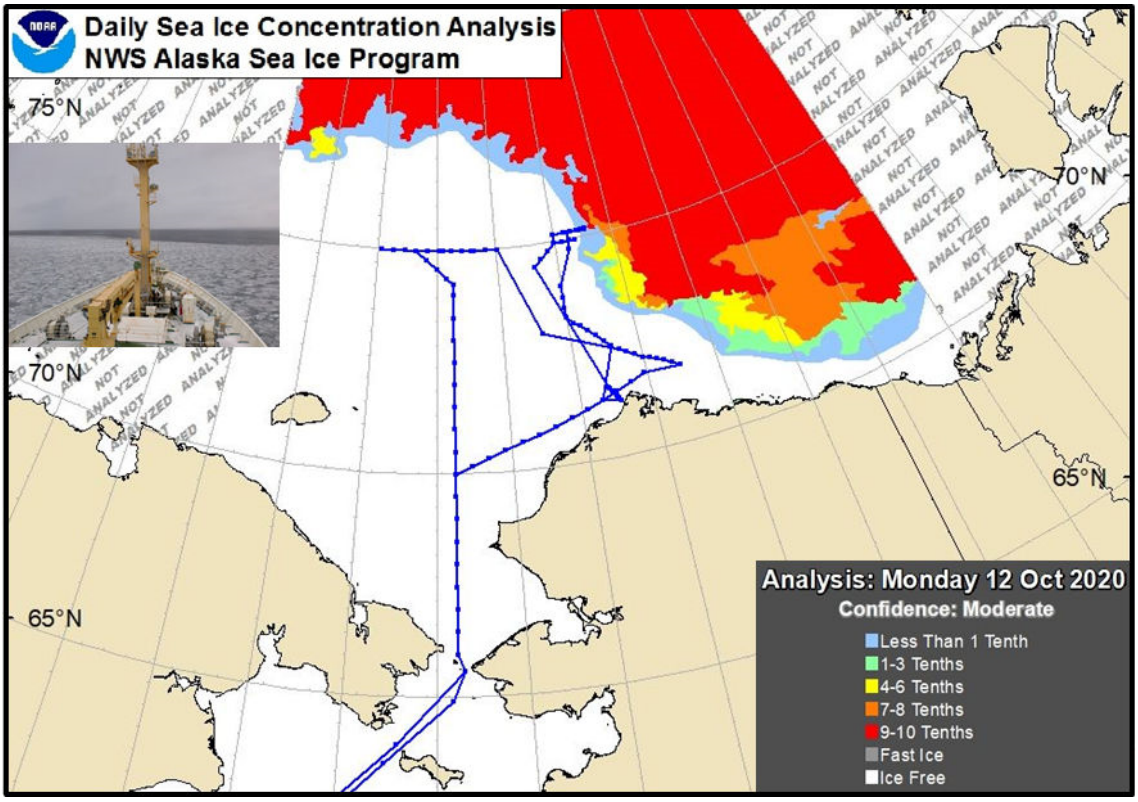

Figure 1.2-2. Colors indicate sea ice concentration on 12 October 2020. The inserted photo was taken on 12 October 2020, when we approached to an ice-edge area (75° 11' N, 157° 07' W) in the Canada Basin. Blue lines represent the cruise tracks of R/V Mirai. The sea ice data is obtained from Daily Sea Ice Concentration Analysis, NWS Alaska Sea Ice Program, NOAA.

The research areas included the EEZ and the territorial sea of the USA. We conducted meteorological and hydrographic surveys including marine biogeochemical samplings from the Chukchi Sea shelf to marginal ice zones of the Canada Basin (Figure 1.2-3). The observational items were Conductivity-Temperature-Depth (CTD)/Lowered Acoustic Doppler Current Profiler (LADCP)/water samplings; eXpendable CTD (XCTD); portable CTD (RINKO-Profiler); ocean microstructure measurements by Turbulence Ocean Microstructure Acquisition Profiler (TurboMAP); wave measurements; drifting buoy deployments; flying drone operations; bio-optics measurements; plankton nets (NORPAC, ring, and closing nets); plastic samplings (neuston net); sediment samplings (Smith-McIntyre grab); incubation experiments; ship-board ocean current and surface

water monitorings; meteorological measurements and samplings; trace gases, aerosol, greenhouse gas, and water vapor isotope observations; satellite observations; Doppler radar; sea ice radar; and sea bottom topography, gravity, and magnetic field measurements. We tried to recover a mooring off Pt. Barrow (but it was left there because of difficulties in dragging operations). Furthermore, a sediment trap was deployed in the Northwind Abyssal Plain, where is on the pathway of the Pacific-origin water, to monitor its transport and impact on marine ecosystem. In a marginal ice zone (MIZ), we conducted sub-mesoscale observations using XCTD, RINKO-Profiler, and TurboMAP. We also tried to use flying drones to assess the conditions of sea ice and waves (but they were cancelled due to bad weather). Various drifting buoys (wave buoys and a drifting buoy with a thermistor chain) were launched in the MIZ to measure the ocean waves, currents, and temperature. Intensive oceanographic surveys off Pt. Barrow were carried out in collaboration with an international framework, Distributed Biological Observatory (DBO).

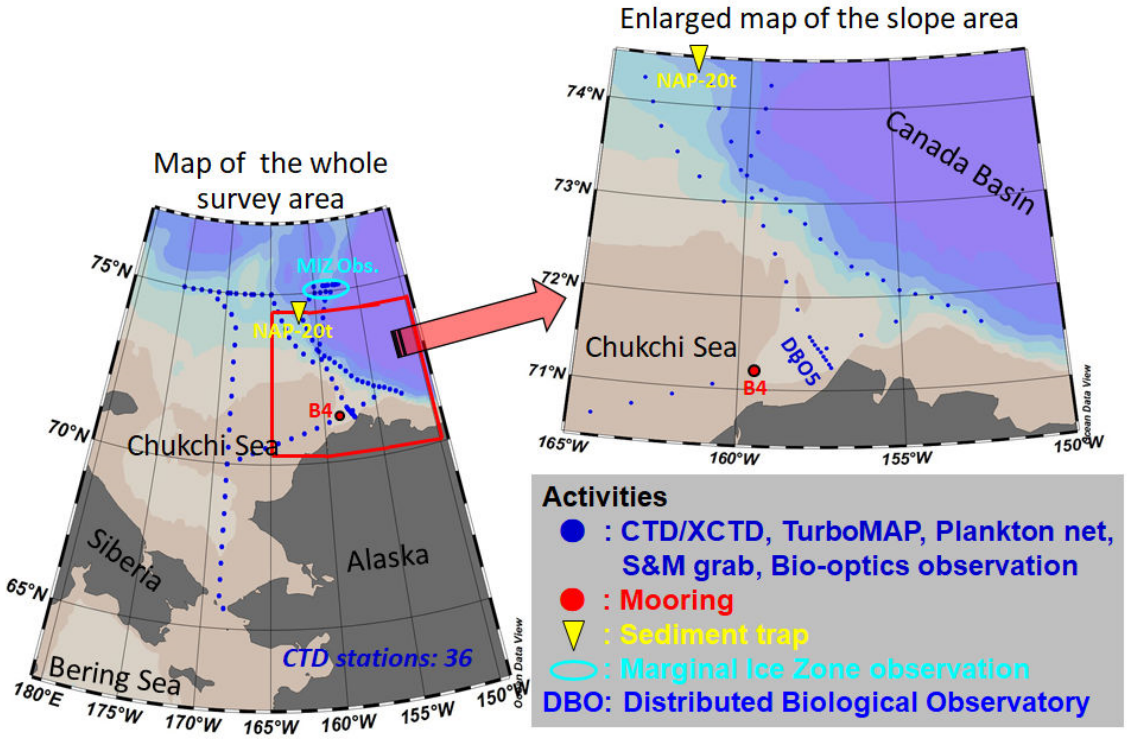

Figure 1.2-3. Map of the research areas in the Arctic Ocean (left) and an enlarged drawing from the Chukchi shelf slope to the Canada Basin (right). Blue dots indicate stations where we conducted observations using Conductivity-Temperature-Depth (CTD) sensors with Lowered Acoustic Doppler Current Profiler (LADCP) and water sampling bottles; eXpendable CTD (XCTD) sensors; Turbulence Ocean Microstructure Acquisition Profiler (TurboMAP); plankton nets; Smith-McIntyre (S&M) grab; and bio-optics instruments. A red dot and yellow triangle represent mooring and sediment trap sites, respectively. A light blue ellipse represents an area of marginal ice zone (MIZ) observation, where we conducted sub-mesoscale observations using XCTD, RINKO-

Profiler, and TurboMAP. Various drifting buoys were launched in the MIZ. We also carried out intensive oceanographic surveys off Pt. Barrow under an international collaboration (Distributed Biological Observatory; DBO).

In this cruise, we had 36 CTD stations including 25 water sampling sites. Three of 36 CTD stations with water samplings were in the subtropical North Pacific and one with water sampling was set in the subarctic North Pacific. Other CTD stations were in the Arctic Ocean. We also had 92 observation sites for XCTDs, 23 for a TurboMAP, 13 for a RINKO-Profiler, 13 for bio-optics, 28 for a NORPAC net, 24 for a ring net, 1 for a closing net, 6 for a neuston net, 9 for a S&M grab, 5 for wave buoys, 1 for a drifting buoy with a thermistor chain, 1 for a mooring, and 1 for a sediment trap. Continuous meteorological, oceanographic, and geophysical observations/samplings were carried out on the cruise track.

In addition, to promote understanding on the Arctic research of the general public, the onboard researchers participated in information dissemination using social networking services (SNS). Short texts and photos were posted either on the R/V Mirai 2020 Arctic cruise official website (https://www.nipr.ac.jp/arcs2/mirai2020/) and JAMSTEC Twitter account (@JAMSTEC_PR), or the Sasakawa Peace Foundation official Facebook and Twitter account (@SPF_PR). The posts covered various topics such as observation activities and day-to-day life on the R/V Mirai.

The above-mentioned missions were successfully completed thanks to great efforts made by the captain, ice pilot, officers, crew, and all the participants in this cruise (Photo 1.2-1). Based on the data obtained in this cruise, we will be able to shed light on the Arctic change and its controlling factors, and will contribute to the global climate change studies.

Photo 1.2-1. Commemorative photograph for the participants of R/V Mirai Arctic Ocean cruise in 2020.

In this cruise, the following 11 research themes were proposed:

- Studies on board

● Representative of the Science Party [Affiliation]: Shigeto Nishino [JAMSTEC]
○ Title of proposal: Synoptic Arctic Survey (SAS): A coordinated multi-ship, multi-nation pan-Arctic ship-based sampling campaign
● Representative of the Science Party [Affiliation]: Takuji Waseda [The University of Tokyo]
○ Title of proposal: Observation of wave-ice-ocean-atmosphere interaction in the marginal ice zone
● Representative of the Science Party [Affiliation]: Yusuke Kawaguchi [The University of Tokyo]
○ Title of proposal: Observational study of eddy, waves and turbulence in the sea-ice shrinking Arctic Ocean
● Representative of the Science Party [Affiliation]: Takuhei Shiozaki [The University of Tokyo]
○ Title of proposal: Changes in nitrogen cycle in the Arctic Ocean
● Representative of the Science Party [Affiliation]: Sohiko Kameyama [Hokkaido University]
○ Title of proposal: Study on the dynamics of methane and DMSP in the Arctic Ocean
● Representative of the Science Party [Affiliation]: Kohei Matsuno [Hokkaido University]
○ Title of proposal: Relationship between sea-ice reduction and horizontal distribution on zooplankton community in the pacific sector of Arctic Ocean
● Representative of the Science Party [Affiliation]: Nobuyoshi Fukuhara [NHK (Japan Broadcasting Corporation)]
○ Title of proposal: Onboard news gathering by media

- Studies not on board

● Representative of the Science Party [Affiliation]: Daisuke Hirano [Hokkaido University]
○ Title of proposal: Study of oceanic and sea-ice variability off the northern coast of Alaska
● Representative of the Science Party [Affiliation]: Fumikazu Taketani [JAMSTEC]
○ Title of proposal: Ship-based observations of trace gases and aerosols over the Arctic Ocean, Bering Sea, and North Western Pacific Ocean
● Representative of the Science Party [Affiliation]: Yasunori Tohjima [National Institute for Environmental Studies]
○ Title of proposal: Observations of atmospheric greenhouse gases and related species in the Arctic Ocean and the western North Pacific
● Representative of the Science Party [Affiliation]: Hotaek Park [JAMSTEC]
○ Title of proposal: Observation of water vapor isotope in the Arctic

1.3. Basic information

Name of vessel	R/V Mirai L x B x D 128.58m x 19.0m x 13.2m Gross Tonnage: 8,706 tons Call Sign JNSR
Cruise code	MR20-05C
Undertaking institute	Japan Agency for Marine-Earth Science and Technology (JAMSTEC)
Chief scientist	Shigeto Nishino Japan Agency for Marine-Earth Science and Technology (JAMSTEC)
Cruise periods	19 September 2020 – 2 November 2020
Ports call	28 September 2020, Hachinohe (arrival and leave due to an emergency patient disembarkation)
Research areas	The Arctic Ocean, Bering Sea and North Pacific Ocean

1.4. Cruise tracks

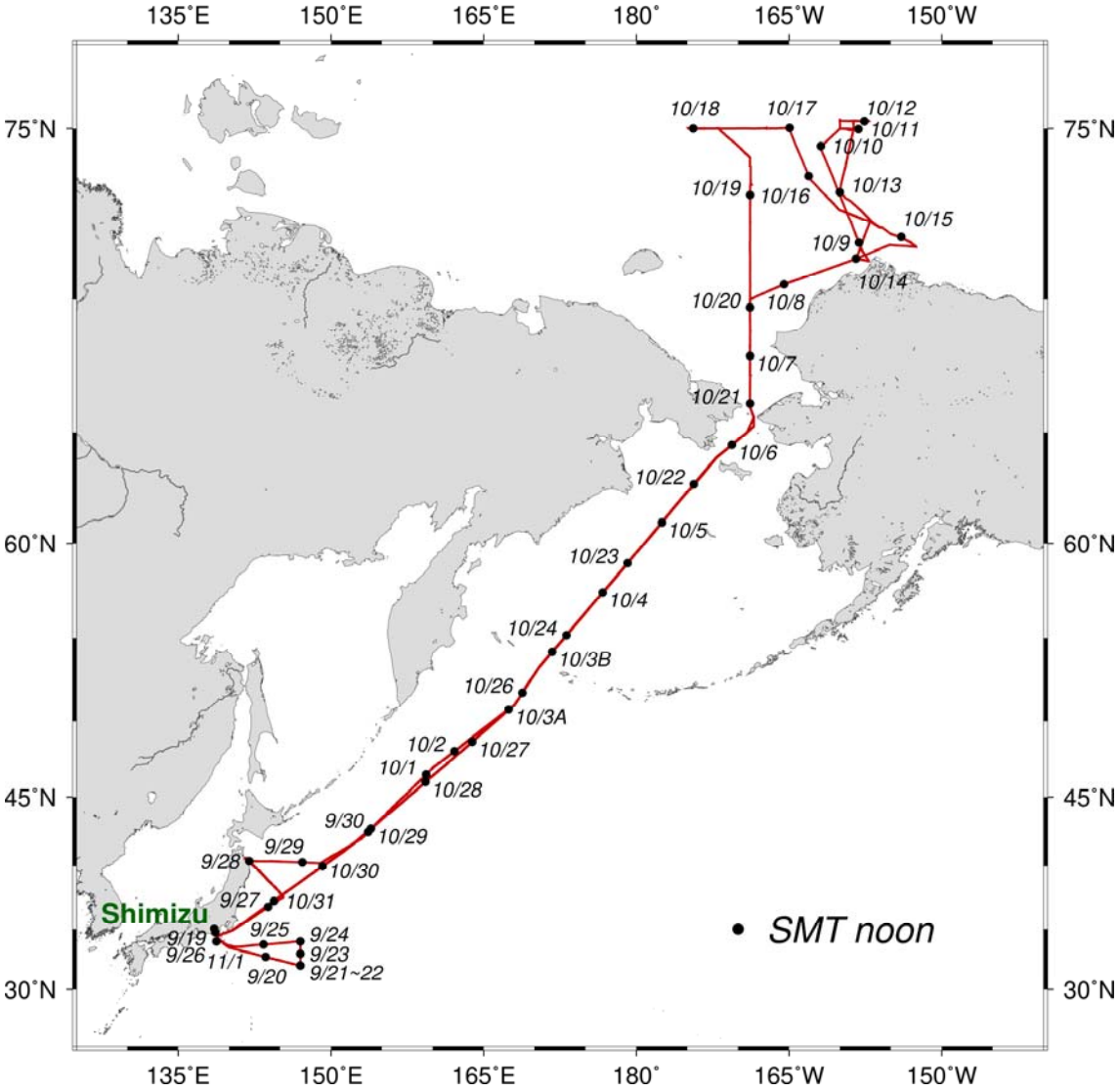

Figure 1.4-1. Cruise track of MR20-05C in the whole research areas.

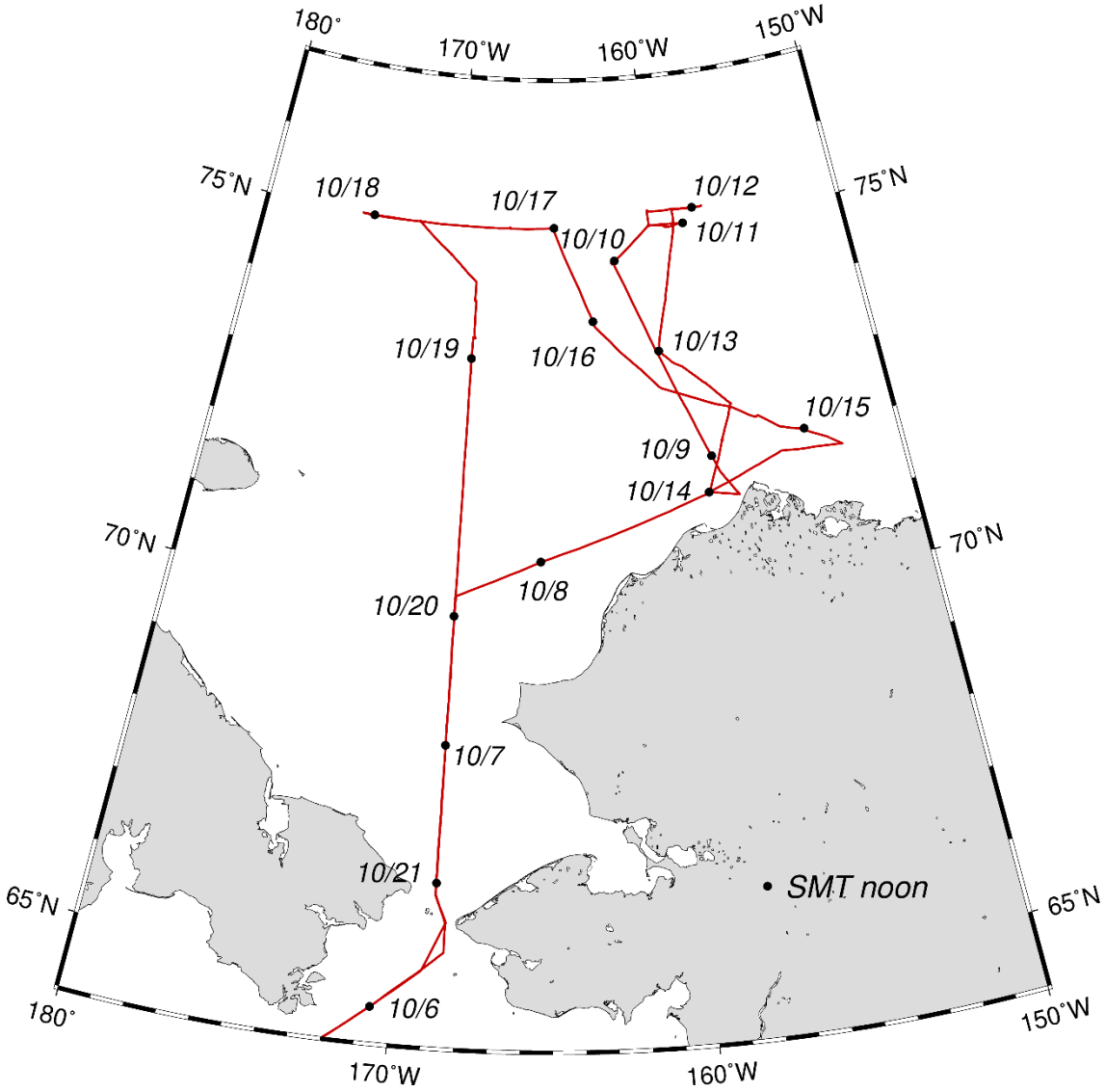

Figure 1.4-2. Cruise track of MR20-05C in the Arctic ocean.

1.5. List of participants

Table 1.5-1. List of participants of MR20-05C.

No.	Name	Organization	Position
1	Shigeto Nishino	Japan Agency for Marine-Earth Science and Technology (JAMSTEC)	Senior Research Scientist
2	Amane Fujiwara	Japan Agency for Marine-Earth Science and Technology (JAMSTEC)	Research Scientist
3	Takuhei Shiozaki	Atmosphere and Ocean Research Institute, The University of Tokyo	Associate Professor
4	Miaki Muramatsu	Japan Agency for Marine-Earth Science and Technology (JAMSTEC)	Assistant Researcher
5	Syunya Sano	Japan Agency for Marine-Earth Science and Technology (JAMSTEC)	Assistant Researcher
6	Junko Toyoshima	Ocean Policy Research Institute, Sasakawa Peace Foundation	Research Scientist
7	Tatsuya Kawakami	Faculty of Fisheries Sciences, Hokkaido University	Postdoctoral Researcher
8	Keita Nishizawa	Graduate School of Frontier Sciences, The University of Tokyo	Graduate Student
9	Eun-Yae Son	Atmosphere and Ocean Research Institute, The University of Tokyo	Graduate Student
10	Koki Tokuhiro	Graduate School of Fisheries Sciences, Hokkaido University	Graduate Student
11	Yuri Fukai	Graduate School of Environmental Science, Hokkaido University	Graduate Student
12	Xinyuan Zheng	Graduate School of Environmental Science, Hokkaido University	Graduate Student
13	Nobuyoshi Fukuhara	KIN Inc.	TV Director
14	Tetsuro Yasuda	Timeless Vision Pro Inc.	CEO
15	De Silva Liyanarachchi Waruna Arampath	Weathernews Inc.	Sea Ice Expert
16	David Snider	Martech Polar Consulting Ltd.	Ice Pilot
17	Ryo Oyama	Nippon Marine Enterprises, Ltd.	Technical Staff

No.	Name	Organization	Position
18	Soichiro Sueyoshi	Nippon Marine Enterprises, Ltd.	Technical Staff
19	Wataru Tokunaga	Nippon Marine Enterprises, Ltd.	Technical Staff
20	Masanori Murakami	Nippon Marine Enterprises, Ltd.	Technical Staff
21	Masahiro Orui	Marine Works Japan Ltd.	Technical Staff
22	Jun Matsuoka	Marine Works Japan Ltd.	Technical Staff
23	Keisuke Matsumoto	Marine Works Japan Ltd.	Technical Staff
24	Shinsuke Toyoda	Marine Works Japan Ltd.	Technical Staff
25	Ko Morita	Marine Works Japan Ltd.	Technical Staff
26	Hiroaki Sako	Marine Works Japan Ltd.	Technical Staff
27	Yuya Hitomi	Marine Works Japan Ltd.	Technical Staff
28	Nagisa Fujiki	Marine Works Japan Ltd.	Technical Staff
39	Hiroshi Hoshino	Marine Works Japan Ltd.	Technical Staff
30	Misato Kuwahara	Marine Works Japan Ltd.	Technical Staff
31	Tomomi Sone	Marine Works Japan Ltd.	Technical Staff
32	Erii Irie	Marine Works Japan Ltd.	Technical Staff
33	Yuta Oda	Marine Works Japan Ltd.	Technical Staff
34	Yuko Miyoshi	Marine Works Japan Ltd.	Technical Staff
35	Marin Sato	Marine Works Japan Ltd.	Technical Staff
36	Syungo Oshitani	Marine Works Japan Ltd.	Technical Staff
37	Aine Yoda	Marine Works Japan Ltd.	Technical Staff
38	Shintaro Amikura	Marine Works Japan Ltd.	Technical Staff

No.	Name	Organization	Position
39	Haruka Sato	Marine Works Japan Ltd.	Technical Staff

2. Meteorology

2.1. C-band weather radar

(1) Personnel

Fumikazu Taketani (JAMSTEC) – Principal investigator, Not on board
Masaki Katsumata (JAMSTEC) – Not on board
Ryo Oyama (Nippon Marine Enterprises, Ltd.; NME) – Operation leader
Souichiro Sueyoshi (NME)
Wataru Tokunaga (NME)
Masanori Murakami (NME)
Yoichi Inoue (MIRAI Crew)

(2) Objectives

The objective of weather radar observations is to investigate the structures and evolutions of precipitating systems over the high-latitude region including arctic ocean.

(3) Instrumentation and methods

(a) Radar specifications

The C-band weather radar on board the R/V Mirai was used. Basic specifications of the radar are as follows:

Frequency:	5370 MHz (C-band)
Polarimetry:	Horizontal and vertical (simultaneously transmitted and received)
Transmitter:	Solid-state transmitter
Pulse Configuration:	Using pulse-compression
Output Power:	6 kW (H) + 6 kW (V)
Antenna Diameter:	4 meters
Beam Width:	1.0 degrees
Inertial Navigation Unit:	PHINS (IXBLUE S.A.S)

(b) Available radar variables

Radar variables, which were converted from the power and phase of the backscattered signal at vertically- and horizontally-polarized channels, were as follows:

Radar reflectivity:	Z
Doppler velocity:	Vr
Spectrum width of Doppler velocity:	SW
Differential reflectivity:	Z_{DR}
Differential propagation phase:	Φ_{DP}
Specific differential phase:	K_{DP}
Co-polar correlation coefficients:	ρ_{HV}

(c) Operation methodology

The antenna was controlled to point the commanded ground-relative direction, by controlling the azimuth and elevation to cancel the ship attitude (roll, pitch and yaw) detected by the laser gyro. The Doppler velocity was also corrected by subtracting the ship movement in beam direction.

For the maintenance, internal signals of the radar were checked and calibrated at the beginning and the end of the cruise. Meanwhile, the following parameters were checked daily; (1) frequency, (2) mean output power, (3) pulse width, and (4) PRF (pulse repetition frequency).

During the cruise, the radar was operated as in Table 2.1-1. A dual PRF mode was used for a volume scan. For RHI and surveillance PPI scans, a single PRF mode was used.

(4) Preliminary results

The C-band weather radar observations were conducted through the cruise, except in the area where the operations were prohibited by Japanese license.

Note that the observation was paused in the following periods.

(a) Due to trouble on the air conditioner for the radar room:
Oct.10, 1542UTC – 1618UTC

(b) Due to trouble on the receiver system:
Oct.23, 1408UTC – 1451UTC
Oct.23, 1938UTC – 2000UTC
Oct.24, 0117UTC – 0206UTC

The obtained data will be analyzed after the cruise.

(5) Data archive

These data obtained in this cruise will be submitted to the Data Management Group (DMG) of JAMSTEC, and will be opened to the public via "Data Research System for Whole Cruise Information in JAMSTEC (DARWIN)" in JAMSTEC web site.
<http://www.godac.jamstec.go.jp/darwin/e>

Table 2.1-1. Scan modes of C-band weather radar.

	Surveillance PPI Scan	Volume Scan						RHI Scan
Repeated Cycle (min.)	30	6						6
Times in One Cycle	1	1						3
PRF(s) (Hz)	400	dual PRF (ray alternative)						1250
		667	833	938	1250	1333	2000	
Azimuth (deg)	Full Circle							Option
Bin Spacing (m)	150							
Max. Range (km)	300	150		100		60		100
Elevation Angle(s) (deg.)	0.5	0.5		1.0, 1.8, 2.6, 3.4, 4.2, 5.1, 6.2, 7.6, 9.7, 12.2, 15.2		18.7, 23.0, 27.9, 33.5, 40.0		0.0 ~ 60.0

2.2. Surface meteorological observations

(1) Personnel

Shigeto Nishino (JAMSTEC) – Principal investigator
Ryo Oyama (Nippon Marine Enterprises, Ltd.; NME) – Operation leader
Souichiro Sueyoshi (NME)
Wataru Tokunaga (NME)
Masanori Murakami (NME)
Yoichi Inoue (MIRAI Crew)

(2) Objectives

Surface meteorological parameters are observed as a basic dataset of the meteorology. These parameters provide the temporal variation of the meteorological condition surrounding the ship.

(3) Instruments and methods

Surface meteorological parameters were observed during this cruise. In this cruise, the two systems for the observation were used.

i. MIRAI Surface Meteorological observation (SMet) system

Instruments of SMet system are listed in Table 2.2-1 and measured parameters are listed in Table 2.2-2. Data were collected and processed by KOAC-7800 weather data processor made by Koshin-Denki, Japan. The data set consists of 6 seconds averaged data.

ii. Shipboard Oceanographic and Atmospheric Radiation (SOAR) measurement system

SOAR system designed by BNL (Brookhaven National Laboratory, USA) consists of major five parts.

a) Analog meteorological data sampling with CR1000 logger manufactured by Campbell Scientific Inc. Canada – wind pressure, and rainfall (by a capacitive rain gauge) measurement.
b) Digital meteorological data sampling from individual sensors - air temperature, relative humidity and precipitation (by optical rain gauge (ORG)) measurement.
c) Radiation data sampling with CR1000X logger manufactured by Campbell Inc. and radiometers with ventilation unit manufactured by Hukseflux Thermal Sensors B.V. Netherlands – short and long wave downward radiation measurement.
d) Photosynthetically Available Radiation (PAR) sensor manufactured by Biospherical Instruments Inc. (USA) - PAR measurement.

e) Scientific Computer System (SCS) developed by NOAA (National Oceanic and Atmospheric Administration, USA) - centralized data acquisition and logging of all data sets.

SCS recorded radiation, air temperature, relative humidity, CR1000 and ORG data. SCS composed Event data (JamMet) from these data and ship's navigation data every 6 seconds. Instruments and their locations are listed in Table 2.2-3 and measured parameters are listed in Table 2.2-4.

For the quality control as post processing, we checked the following sensors, before and after the cruise.

i. Young Rain gauge (SMet and SOAR)
Inspect of the linearity of output value from the rain gauge sensor to change Input value by adding fixed quantity of test water.

ii. Barometer (SMet and SOAR)
Comparison with the portable barometer value, PTB220, VAISALA

iii. Thermometer (air temperature and relative humidity) (SMet and SOAR)
Comparison with the portable thermometer value, HM70, VAISALA

(4) Observation period
19 Sep. 2020 - 01 Nov. 2020

(5) Preliminary results
Figure 2.2-1 shows the time series of the following parameters;
Wind (SOAR)
Air temperature (SMet)
Relative humidity (SMet)
Precipitation (SOAR, ORG)
Short / Long wave radiation (SOAR)
Pressure (SMet)
Sea surface temperature (SMet)
Significant wave height (SMet)

(6) Data archives
These data obtained in this cruise will be submitted to the Data Management Group (DMG) of JAMSTEC, and will be opened to the public via "Data Research System for Whole Cruise Information in JAMSTEC (DARWIN)" in JAMSTEC web site.
<http://www.godac.jamstec.go.jp/darwin/e>

(7) Remarks (Times in UTC)

i) The following periods, Sea surface temperature of SMet data were available.

07:13UTC 19 Sep. 2020 - 01:27UTC 28 Sep. 2020

07:47UTC 28 Sep. 2020 - 01:32UTC 01 Nov. 2020

ii) The following time, increasing of SMet capacitive rain gauge data were invalid due to MF/HF radio transmission.

04:21UTC 19 Sep. 2020 - 04:25UTC 19 Sep. 2020

03:19UTC 29 Oct. 2020 - 04:58UTC 29 Oct. 2020

iii) The following period, the downwelling shortwave radiation data of SMet contained 10-40[W/m^2] bias in during the night.

07:38UTC 27 Sep. 2020 - 11:49UTC 07 Oct. 2020

01:55UTC 22 Oct. 2020 - 11:00UTC 29 Oct. 2020

iv) The following time, Wave data were invalid.

20:55UTC 10 Oct. 2020 - 23:55UTC 10 Oct. 2020

Table 2.2-1. Instruments and installation locations of SMet system.

Sensors	Type	Manufacturer	Location (altitude from surface)
Anemometer	KS-5900	Koshin Denki, Japan	Foremast (25 m)
Tair/RH	HMP155	Vaisala, Finland	Compass deck (21 m)
with aspirated radiation shield	43408 Gill	R.M. Young, U.S.A.	starboard and port side
Thermometer: SST	RFN2-0	Koshin Denki, Japan	4th deck (-1m, inlet -5m)
Barometer	Model-370	Setra System, U.S.A.	Captain deck (13 m) Weather observation room
Capacitive rain gauge	50202	R. M. Young, U.S.A.	Compass deck (19 m)
Optical rain gauge	ORG-815DS	Osi, USA	Compass deck (19 m)
Radiometer (short wave)	MS-802	Eko Seiki, Japan	Radar mast (28 m)
Radiometer (long wave)	MS-202	Eko Seiki, Japan	Radar mast (28 m)
Wave height meter	WM-2	Tsurumi-seiki, Japan	Bow (10 m) Stern (8m)

Table 2.2-2. Parameters of MIRAI SMet system.

Parameter	Units	Remarks
1 Latitude	degree	
2 Longitude	degree	
3 Ship's speed	knot	MIRAI log
4 Ship's heading	degree	MIRAI gyro
5 Relative wind speed	m/s	6sec./10min. averaged
6 Relative wind direction	degree	6sec./10min. averaged
7 True wind speed	m/s	6sec./10min. averaged

8 True wind direction	degree	6sec./10min. averaged
9 Barometric pressure	hPa	adjusted to sea surface level 6sec. averaged
10 Air temperature (starboard)	degC	6sec. averaged
11 Air temperature (port)	degC	6sec. averaged
12 Dewpoint temperature (starboard)	degC	6sec. averaged
13 Dewpoint temperature (port)	degC	6sec. averaged
14 Relative humidity (starboard)	%	6sec. averaged
15 Relative humidity (port)	%	6sec. averaged
16 Sea surface temperature	degC	6sec. averaged
17 Precipitation intensity (optical rain gauge)	mm/hr	hourly accumulation
18 Precipitation (capacitive rain gauge)	mm/hr	hourly accumulation
19 Downwelling shortwave radiation	W/m^2	6sec. averaged
20 Downwelling infra-red radiation	W/m^2	6sec. averaged
21 Significant wave height (bow)	m	hourly
22 Significant wave height (stern)	m	hourly
23 Significant wave period (bow)	second	hourly
24 Significant wave period (stern)	second	hourly

Table 2.2-3. Instruments and installation locations of SOAR system.

Sensors (Meteorological)	Type	Manufacturer	Location (altitude from surface)
Anemometer	05106	R.M. Young, USA	Foremast (25 m)
Barometer with pressure port	PTB210 61002 Gill	VAISALA, Finland R.M. Young, USA	Foremast (23 m)
Rain gauge	50202	R.M. Young, USA	Foremast (24 m)
Tair/RH with aspirated radiation shield	HMP155 43408 Gill	VAISALA, Finland R.M. Young, USA	Foremast (23 m)
Optical rain gauge	ORG-815DR	Osi, USA	Foremast (24 m)

Sensors (Radiation)	Type	Manufacturer	Location *
Radiometer (short wave) with ventilation unit	SR20 VU01	Hukseflux Thermal Sensors B.V., Netherlands	Foremast (25 m)
Radiometer (long wave) with ventilation unit	IR20 VU01	Hukseflux Thermal Sensors B.V., Netherlands	Foremast (25 m)

Sensor (PAR&UV)	Type	Manufacturer	Location (altitude from surface)
PAR&UV sensor	PUV-510	Biospherical Instrum ents Inc., USA	Navigation deck (18m)

Table 2.2-4. Parameters of SOAR system (JamMet).

Parameter	Units	Remarks
1 Latitude	degree	
2 Longitude	degree	
3 SOG	knot	
4 COG	degree	
5 Relative wind speed	m/s	
6 Relative wind direction	degree	
7 Barometric pressure	hPa	
8 Air temperature	degC	
9 Relative humidity	%	
10 Precipitation intensity (optical rain gauge)	mm/hr	
11 Precipitation (capacitive rain gauge)	mm/hr	reset at 50 mm
12 Down welling shortwave radiation	W/m^2	
13 Down welling infra-red radiation	W/m^2	
14 Defuse irradiance	W/m^2	
15 “SeaSnake” raw data	mV	
16 SSST (SeaSnake)	degC	
17 PAR	$microE/cm^2/sec$	
18 UV 305 nm	$microW/cm^2/nm$	
19 UV 320 nm	$microW/cm^2/nm$	
20 UV 340 nm	$microW/cm^2/nm$	
21 UV 380 nm	$microW/cm^2/nm$	

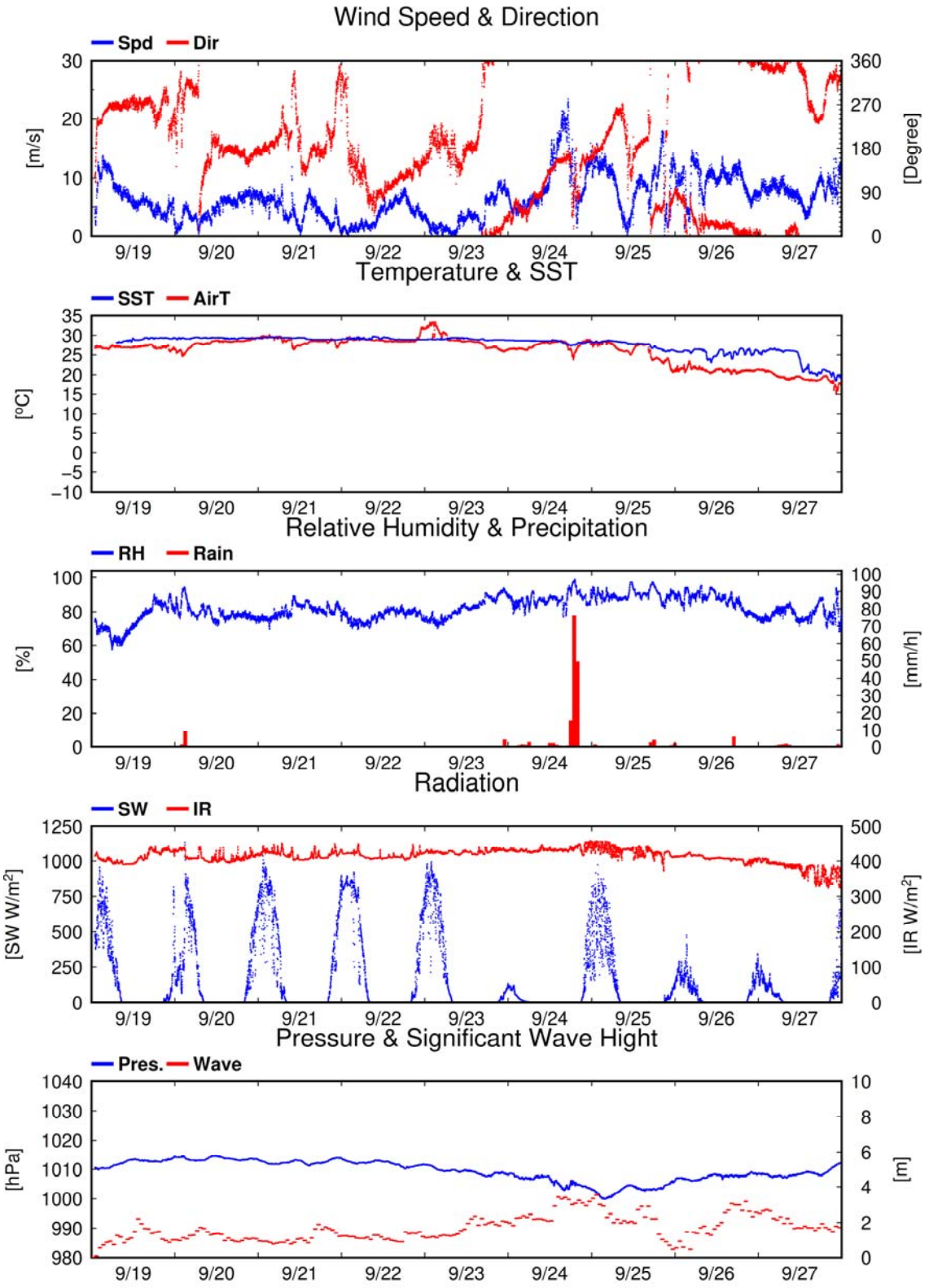

Figure 2.2-1. Time series of surface meteorological parameters during this cruise.

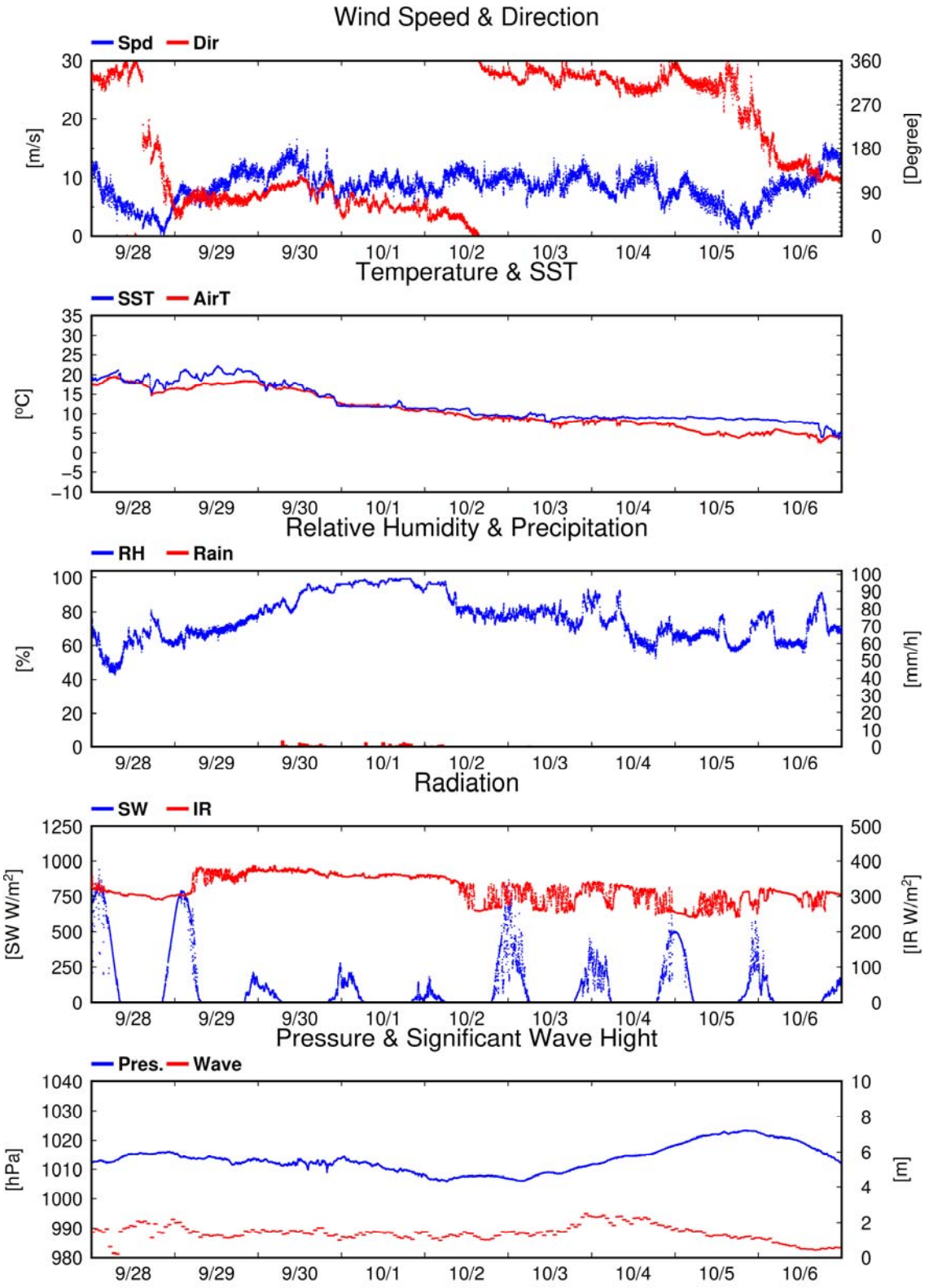

Figure 2.2-1. (Continued)

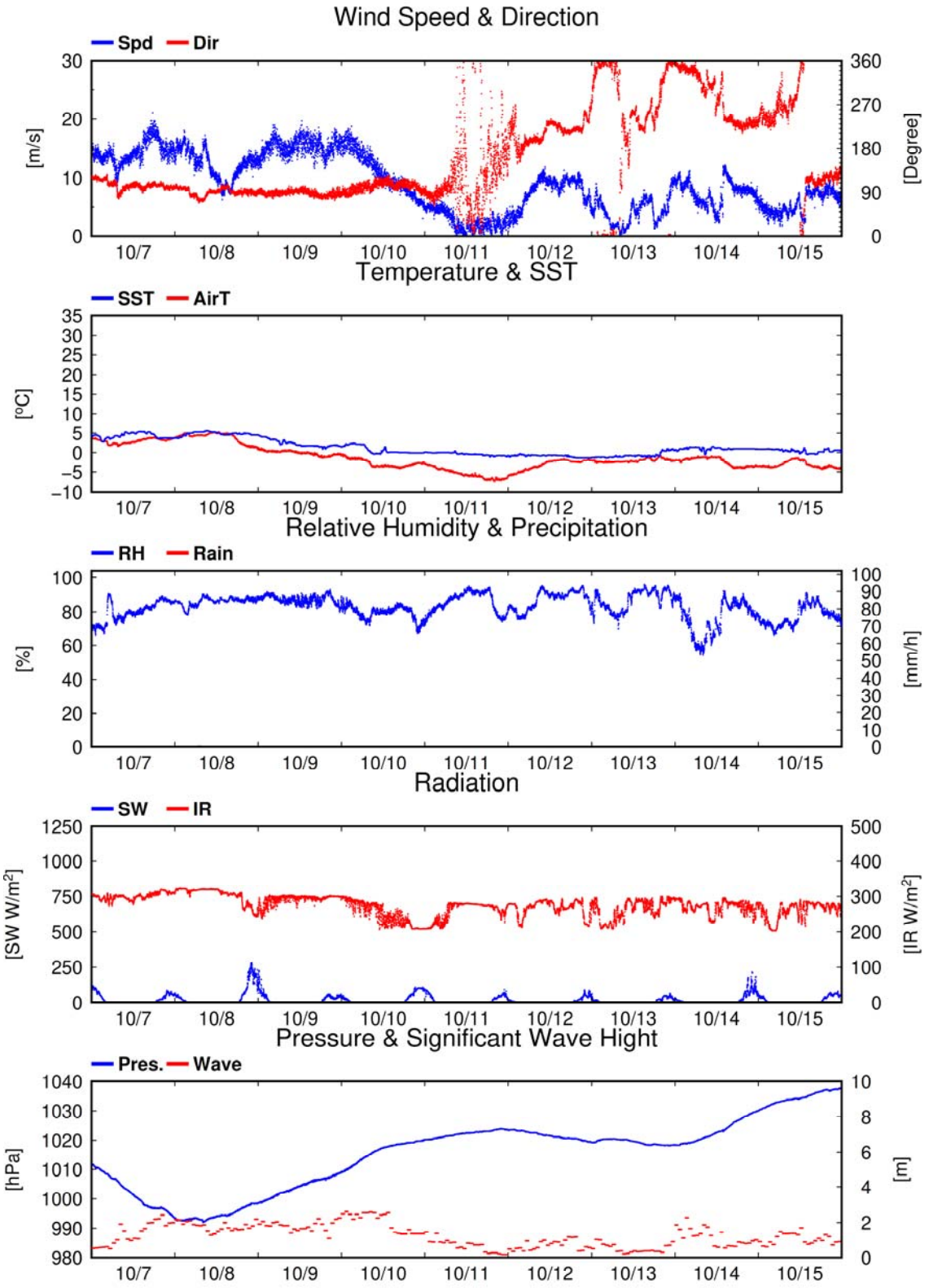

Figure 2.2-1. (Continued)

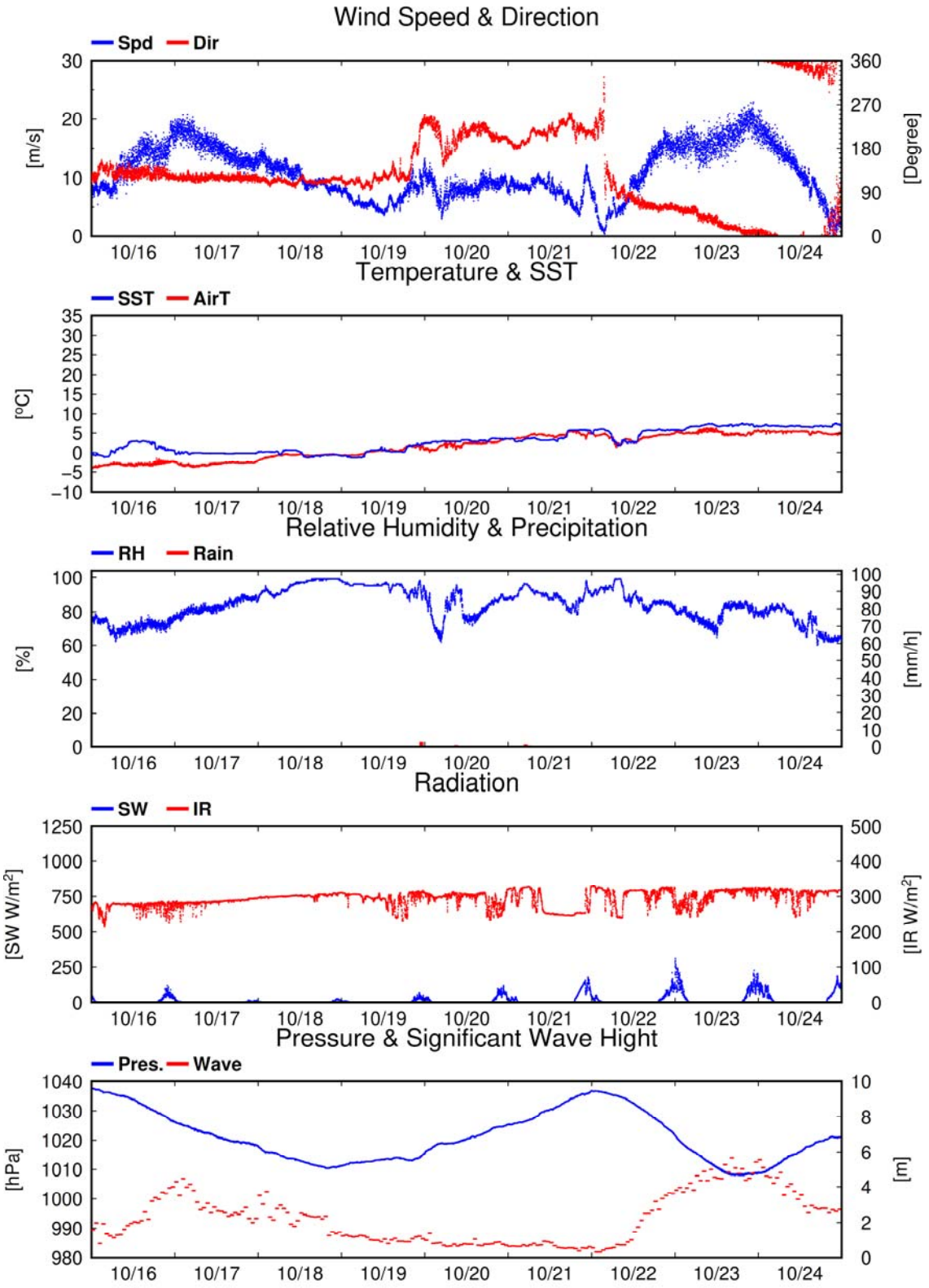

Figure 2.2-1. (Continued)

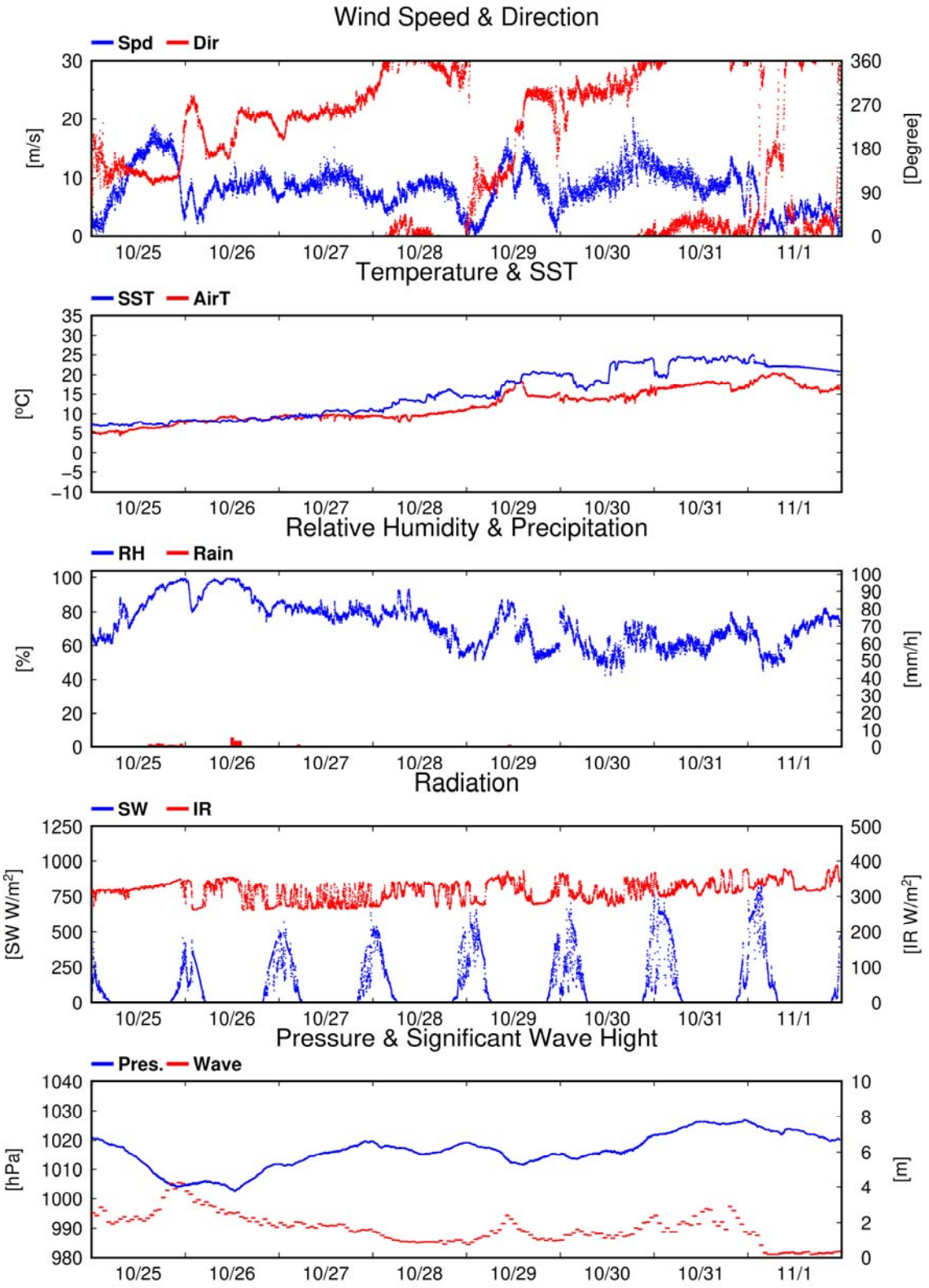

Figure 2.2-1. (Continued)

2.3. Ceilometer

(1) Personnel

Shigeto Nishino (JAMSTEC) – Principal investigator
Ryo Oyama (Nippon Marine Enterprises, Ltd.; NME) – Operation leader
Souichiro Sueyoshi (NME)
Wataru Tokunaga (NME)
Masanori Murakami (NME)
Yoichi Inoue (MIRAI Crew)

(2) Objectives

The information of cloud base height and the liquid water amount around cloud base is important to understand the process on formation of the cloud. As one of the methods to measure them, the ceilometer observation was carried out.

(3) Parameters

1. Cloud base height [m].
2. Backscatter profile, sensitivity and range normalized at 10 m resolution.
3. Estimated cloud amount [oktas] and height [m]; Sky Condition Algorithm.

(4) Instruments and methods

Cloud base height and backscatter profile were observed by ceilometer (CL51, VAISALA, Finland). The measurement configurations are shown in Table 2.3-1. On the archive dataset, cloud base height and backscatter profile are recorded with the resolution of 10 m.

Table 2.3-1. The measurement configurations.

Property	Description	
Laser source	Indium Gallium Arsenide (InGaAs) Diode	
Transmitting center wavelength	910±10 nm at 25 degC	
Transmitting average power	19.5 mW	
Repetition rate	6.5 kHz	
Detector	Silicon avalanche photodiode (APD)	
Responsibility at 905 nm	65 A/W	
Cloud detection range	0 ~ 13 km	
Measurement range	0 ~ 15 km	
Resolution	10 m in full range	
Sampling rate	36 sec.	
Sky Condition	Cloudiness in octas (0 ~ 9)	
	0	Sky Clear
	1	Few
	3	Scattered
	5-7	Broken
	8	Overcast
	9	Vertical Visibility

(5) Observation period

19 Sep. 2020 - 01 Nov. 2020

(6) Preliminary results

Figure 2.3-1 shows the time-series of the lowest, second and third cloud base height during the cruise.

(7) Data archives

These data obtained in this cruise will be submitted to the Data Management Group (DMG) of JAMSTEC, and will be opened to the public via "Data Research System for Whole Cruise Information in JAMSTEC (DARWIN)" in JAMSTEC web site.
<http://www.godac.jamstec.go.jp/darwin/e>

(8) Remarks (Times in UTC)

Window cleaning

01:22UTC 26 Sep. 2020
20:28UTC 03 Oct. 2020
19:28UTC 13 Oct. 2020
20:50UTC 21 Oct. 2020
23:11UTC 29 Oct. 2020

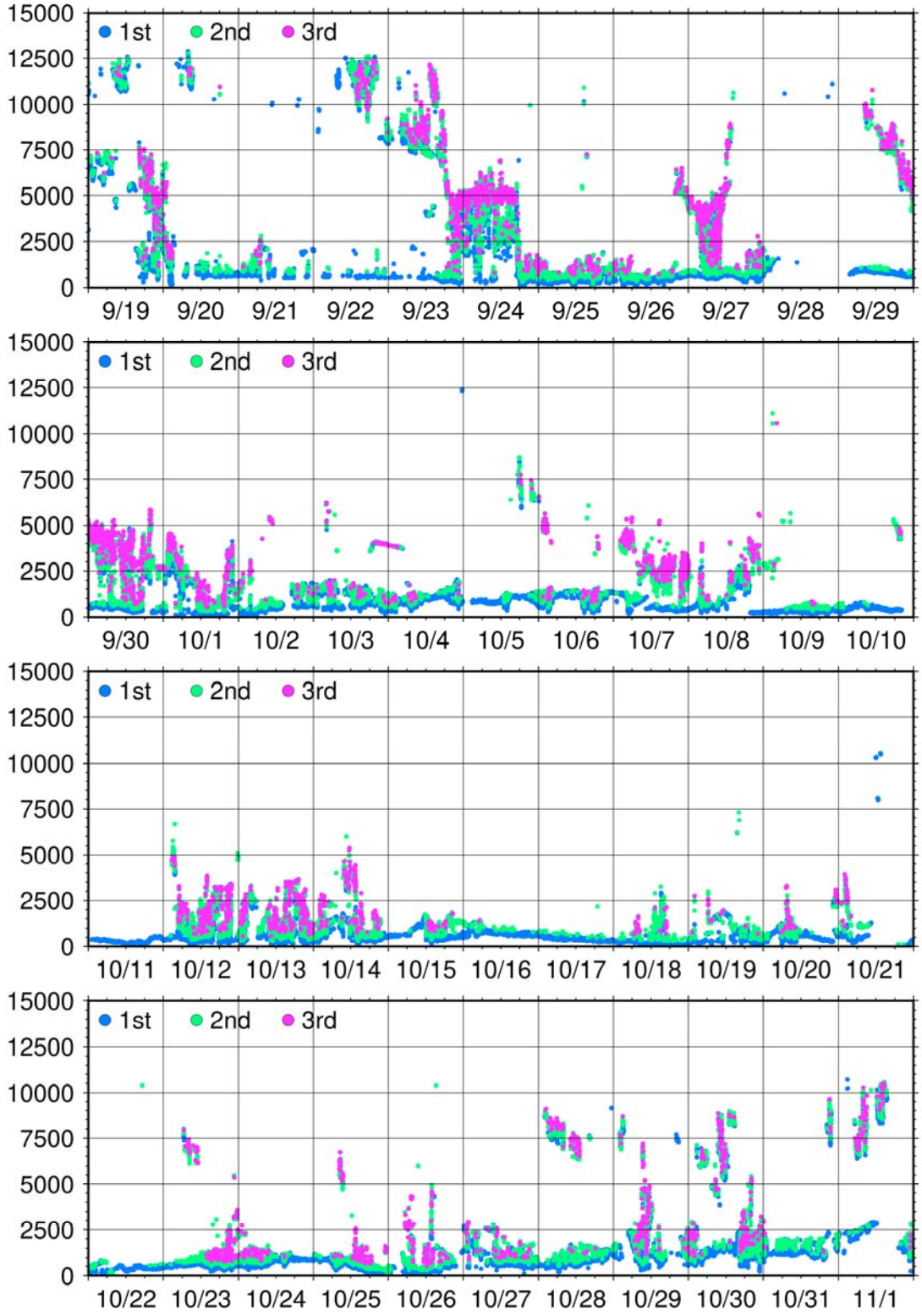

Figure 2.3-1. Time series of cloud base height during this cruise.

2.4. Arctic monitoring system

(1) Personnel

Genki Sagawa (Weathernews Inc.) – Principal investigator, Not on board

Waruna De Silva (Weathernews Inc.)

(2) Objectives

Providing visualized data on analysis and forecast by the Arctic monitoring system to support MIRAI's Arctic navigation. Evaluating the system to examine actual requirements for ideal ice navigation in future.

(3) Parameters

There is no parameter observed by the system.

(4) Instruments and methods

Figure 2.4-1 shows a network configuration diagram of the Arctic Monitoring System. A Mac mini works as a server of the system. It regularly accesses to a cloud storage (Amazon S3) outside of MIRAI through the proxy server, and fetch data on up-to-date analysis and forecast stored in the storage. The system also works as a web server of a map visualization application, which can be viewed by using web browsing softwares, as Microsoft Edge or Google Chrome, from devices connecting to MIRAI LAN. A sample image of the application is shown in Figure 2.4-2.

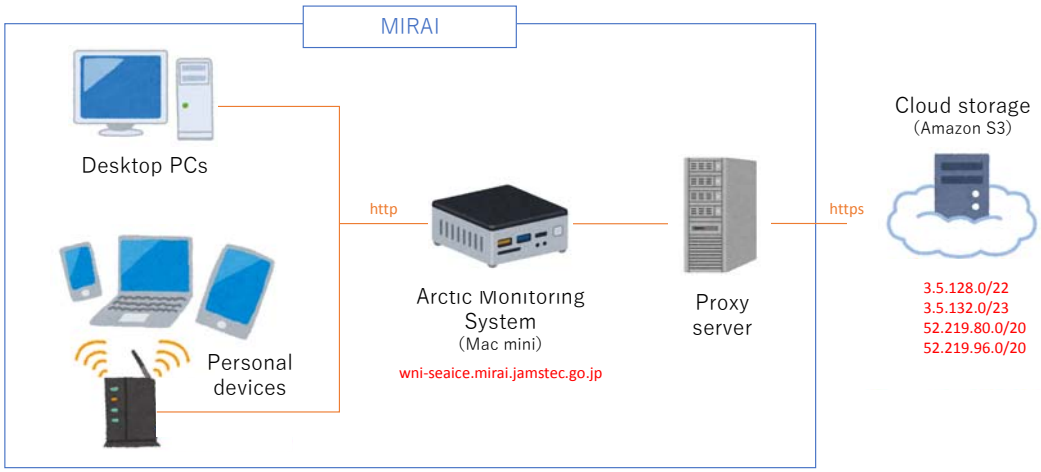

Figure 2.4-1. Network configuration diagram of the Arctic Monitoring System.

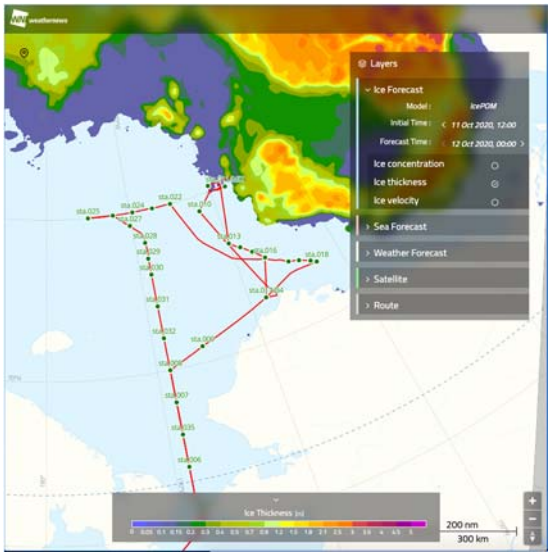

Figure 2.4-2. WNI sea ice monitoring system. Figure also shows the forecasted sea ice thickness on 2020-10-12, station lists and near real time ship track.

To safe and efficient navigation in the ice infested water, sea ice monitoring system and precise medium range forecast of sea ice distribution are vital requirements. Therefore, to make the research activities in the Arctic Ocean with R/V MIRAI and future ice breaker vessel, the Japan Agency for Marine-Earth Science and Technology (JAMSTEC) has a collaboration project with weathernews (WNI) to develop a sea ice monitoring system as shown in Figure 2.4-2.

The WNI Arctic monitoring system provided data are used for the navigation and voyage planning. There are 6 main functions in the WNI Arctic monitoring system.

1. High-resolution IcePOM model 10-day sea ice forecast
    a. Concentrtion
    b. Thickness
    c. Velocity
2. Sea forecast High-resolution IcePOM model 10-day ocean forecast
    a. Sea surface temperature (SST)
3. ECMWF 10-day weather forecast
    a. Temperature at 2m
    b. Sea level Pressure
    c. Wind velocity at 10m
4. Route
    a. Ship track (near real time)
    b. Stations list
    c. XCTDs locations
5. Sentinel 1A/1B satellite SAR images
6. Distance calculator

The high-resolution IcePOM model 10-day sea ice forecast of concentration, thickness and ice velocity and ocean forecast of sea surface temperature data use for avoiding the thick sea ice during the cruise. ECMWF 10-day weather forecast of temperature, mean sea level pressure and wind velocity to understand the upcoming weather. Sentinel 1A/1B satellite SAR images to help deploying buoys and navigation. SAR data also revealed the marginal ice zone eddy development during the cruise as shown in Figure 2.4-3. Near-real time ship route, station list and XCTD locations are helpful to plan the voyage easily. And finally, distance calculator for planning the observation points during the cruise.

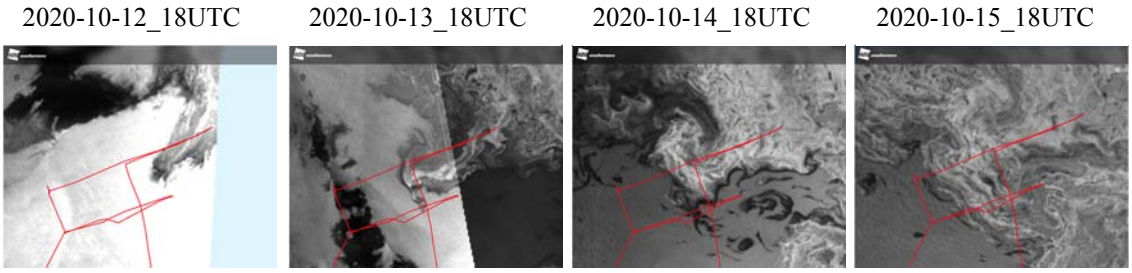

Figure 2.4-3. Marginal ice zone eddy development. Red line is MIRAI ship track.

2.5. Atmospheric observation over the Arctic ocean

2.5.1. Gas and particles observation

(1) Personnel

Fumikazu Taketani (JAMSTEC) – Principal investigator, Not on board
Takuma Miyakawa (JAMSTEC) – Not on board
Yugo Kanaya (JAMSTEC) – Not on board
Masayuki Takigawa (JAMSTEC) – Not on board
Chunmao Zhu (JAMSTEC) – Not on board
Hisahiro Takashima (JAMSTEC/Fukuoka Univ.) – Not on board
Operation for all instruments was supported by Nippon Marine Enterprises, Ltd. (NME)

(2) Objectives

To investigate roles of aerosols in the marine atmosphere in relation to climate change
To investigate processes of biogeochemical cycles between the atmosphere and the ocean.

(3) Parameters

CO, O_3, particle number concentration, aerosol fluorescent property, AED, Rain, NO2.

(3) Methods

(3-1) CO and O_3 mixing ratios

Ambient air was continuously sampled on the compass deck and drawn through ~20-m-long Teflon tubes connected to a gas filter correlation CO analyzer (Model 48C, Thermo Fisher Scientific) and a UV photometric ozone analyzer (Model 205, 2B Tech), located in the Research Information Center. The data will be used for characterizing air mass origins.

(3-2) Particle number concentration

The number concentration of ament particles was measured by mixing condensation particle counter (MCPC) (Model 1720, Brechtel).

(3-3) Fluorescent property

Fluorescent properties of aerosol particles were measured by a single particle fluorescence sensor, Waveband Integrated bioaerosol sensor (WIBS4) (WIBS-4A, Droplet Measurement Technologies). Two pulsed xenon lamps emitting UV light (280 nm and 370 nm) were used for excitation. Fluorescence emitted from a single particle within 310−400 nm and 420−650 nm wavelength windows was recorded.

(3-4) Aerosol extinction coefficient (AEC)

Multi-Axis Differential Optical Absorption Spectroscopy (MAX-DOAS), a passive remote sensing technique measuring spectra of scattered visible and ultraviolet (UV) solar radiation, was used for atmospheric aerosol and gas profile measurements. Our MAX-DOAS instrument consists of two main parts: an outdoor telescope unit and an indoor spectrometer (Acton SP-2358 with Princeton Instruments PIXIS-400B), connected to each other by a 14-m bundle optical fiber cable. The line of sight was in the directions of the portside of the vessel and the scanned elevation angles were 1.5, 3, 5, 10, 20, 30, 90 degrees in the 30-min cycle. The roll motion of the ship was measured to autonomously compensate additional motion of the prism, employed for scanning the elevation angle. For the selected spectra recorded with elevation angles with good accuracy, DOAS spectral fitting was performed to quantify the slant column density (SCD) of NO2 (and other gases) and O4 (O2-O2, collision complex of oxygen) for each elevation angle. Then, the O4 SCDs were converted to the aerosol optical depth (AOD) and the vertical profile of aerosol

extinction coefficient (AEC) using an optimal estimation inversion method with a radiative transfer model. Using derived aerosol information, retrievals of the tropospheric vertical column/profile of NO2 and other gases were made.

(3-5) Rain sampling

Rain sample was corrected using a hand-made sampler installed on compass deck. These sampling logs are listed in Table 2.5.1-1. To investigate the nutrients and Black carbon concentration in the rain, these samples are going to be analyzed in laboratory.

For MCPC instruments, the ambient air was commonly sampled from the compass deck by a 3-m-long conductive tube through the dryer to dry up the particles, and then introduced to instrument installed at the environmental research room. WIBS-4 instrument installed the shelter at the compass deck. MAXDOAS was installed at the deck above stabilizer of ship.

(4) Observation log

Table 2.5.1-1: Logs of Rain sampling by rain sampler

(5) Data archive

These data obtained in this cruise will be submitted to the Data Management Group (DMG) of JAMSTEC, and will be opened to the public via "Data Research System for Whole Cruise Information in JAMSTEC (DARWIN)" in JAMSTEC web site.
<http://www.godac.jamstec.go.jp/darwin/e>

(6) Acknowledgments

We thank the crew of the R/V Mirai, and staff of Nippon Marine Enterprises, Ltd. for their support with observations throughout the cruise.

Table 2.5.1-1. Logs of Rain sampling by rain sampler.

ID	Date Collected				Latitude			Longitude		
	YYYY	MM	DD	hh:mm:ss (UTC)	Deg.	Min.	N/S	Deg.	Min.	E/W
MR2005C-R001	2020	09	20	1:47	32	47.54	N	143	19.23	E
MR2005C-R002	2020	09	21	5:30	32	02.12	N	146	58.01	E
MR2005C-R003	2020	09	24	5:41	34	0.87	N	147	00.51	E
MR2005C-R004	2020	09	25	5:30	33	41.17	N	147	00.51	E
MR2005C-R005	2020	09	26	4:30	34	32.1	N	142	21.62	E
MR2005C-R006	2020	09	27	4:30	37	07.89	N	144	25.34	E
MR2005C-R007	2020	09	27	22:15	39	46.18	N	142	42.47	E
MR2005C-R008	2020	09	28	22:55	40	16.87	N	146	15.13	E
MR2005C-R009	2020	09	30	21:15	45	55.00	N	158	27.23	E
MR2005C-R010	2020	10	02	3:50	48	25.49	N	162	47.22	E
MR2005C-R011	2020	10	02	20:30	50	20.09	N	166	37.86	E
MR2005C-R012	2020	10	03	20:20	53	44.08	N	171	04.83	E
MR2005C-R013	2020	10	14	19:45	71	19.33	N	158	23.46	W
MR2005C-R014	2020	10	18	21:10	75	00.17	N	174	59.63	W
MR2005C-R015	2020	10	20	19:30	70	00.9	N	168	49.51	W
MR2005C-R016	2020	10	26	21:15	49	08.15	N	164	36.89	E
MR2005C-R017	2020	10	29	22:25	40	18.37	N	149	48.47	E
MR2005C-R018	2020	10	30	23:25	37	41.09	N	145	06.91	E

2.5.2. Lidar

(1) Personnel

Fumikazu Taketani (JAMSTEC) – Principal investigator, Not on board
Masaki Katsumata (JAMSTEC) – Not on board
Kyoko Taniguchi (JAMSTEC) – Not on board
Ryo Oyama (Nippon Marine Enterprises, Ltd.; NME) – Operation leader
Souichiro Sueyoshi (NME)
Wataru Tokugawa (NME)
Masanori Murakami (NME)
Yoichi Inoue (MIRAI Crew)

(2) Objectives

The objective of this observation is to capture the vertical distribution of clouds, aerosols, and water vapor in high spatio-temporal resolution.

(3) Instruments and methods

The Mirai Lidar system transmits a 10-Hz pulse laser in three wavelengths: 1064nm, 532nm, 355nm. For cloud and aerosol observation, the system detects Mie scattering at these wavelengths. The separate detections of polarization components at 532 nm and 355 nm obtain additional characteristics of the targets. The system also detects Raman water vapor signals at 660 nm and 408nm, Raman nitrogen signals at 607 nm and 387nm at nighttime. Based on the signal ratio of Raman water vapor to Raman nitrogen, the system offers water vapor mixing ratio profiles.

(4) Observation log

19 September 2020 to 1 November 2020

(5) Preliminary results

All data will be reviewed after the cruise to maintain data quality.

(6) Data archives

These data obtained in this cruise will be submitted to the Data Management Group (DMG) of JAMSTEC, and will be opened to the public via "Data Research System for Whole Cruise Information in JAMSTEC (DARWIN)" in JAMSTEC web site.
<http://www.godac.jamstec.go.jp/darwin/e>

2.5.3. GNSS precipitable water

(1) Personnel

Fumikazu Taketani (JAMSTEC) – Principal investigator, Not on board

Masaki Katsumata (JAMSTEC) – Not on board

Operation for all instruments was supported by Nippon Marine Enterprises, Ltd. (NME)

(2) Objectives

Getting the GNSS satellite data to estimate the total column integrated water vapor content of the atmosphere.

(3) Instruments and Methods

The GNSS satellite data was archived to the receiver (Trimble NetR9) with 5 sec interval. The GNSS antenna (Margrin) was set on the roof of aft wheel house. The observations were carried out all through the cruise.

(4) Preliminary Results

The data have been obtained all through the cruise. We will calculate the total column integrated water from observed GNSS satellite data after the cruise.

(5) Data Archive

Raw data is recorded as T02 format and stream data every 5 seconds. Corrected data will be submitted to JAMSTEC Marine-Earth Data and Information Department and will be archived there.

(6) Acknowledgment

The onboard operation was supported by Nippon Marine Enterprises, Ltd.

2.5.4. Disdrometers

(1) Personnel

Fumikazu Taketani (JAMSTEC) – Principal investigator, Not on board

Masaki Katsumata (JAMSTEC) – Not on board

Operation for all instruments was supported by Nippon Marine Enterprises, Ltd. (NME)

(2) Objectives

The disdrometer can continuously obtain size distribution of raindrops. The objective of this observation is (a) to reveal microphysical characteristics of the rainfall, depends on the type, temporal stage, etc. of the precipitating clouds, (b) to retrieve the coefficient to convert radar-observed parameters (especially from C-band radar in Section 2.1) to the information of the precipitating particle such as precipitation rate, particle size distribution, etc.

(3) Instrumentations and Methods

Two "Laser Precipitation Monitor (LPM)" (Adolf Thies GmbH & Co) are utilized. It is an optical disdrometer. The instrument consists of the transmitter unit which emit the infrared laser, and the receiver unit which detects the intensity of the laser come thru the certain path length in the air. When a precipitating particle fall thru the laser, the received intensity of the laser is reduced. The receiver unit detect the magnitude and the duration of the reduction and then convert them onto particle size and fall speed. The sampling volume, i.e. the size of the laser beam "sheet", is 20 mm (W) x 228 mm (D) x 0.75 mm (H).

The numbers of particles are categorized by the detected size and fall speed and counted every minutes. The categories are shown in Table 2.5.4-1.

The LPMs are installed on the top (roof) of the anti-rolling system, as shown in Figure 2.5.4-1. Both are installed at the corner at the bow side and the starboard side. One (in aft) equipped the "wind protection element" to reduce the effect of the wind on the measurement, and to estimate the effectiveness of the "element" by comparing data from two sensors.

(4) Preliminary Results

The data have been obtained all through the cruise. The further analyses for the precipitation amount, precipitation-size-distribution parameters, etc., will be carried out after the cruise.

(5) Data Archive

These data obtained in this cruise will be submitted to the Data Management Group (DMG) of JAMSTEC, and will be opened to the public via "Data Research System for Whole Cruise Information in JAMSTEC (DARWIN)" in JAMSTEC web site.

<http://www.godac.jamstec.go.jp/darwin/e>

(6) Acknowledgment

The onboard operation was supported by Nippon Marine Enterprises, Ltd.

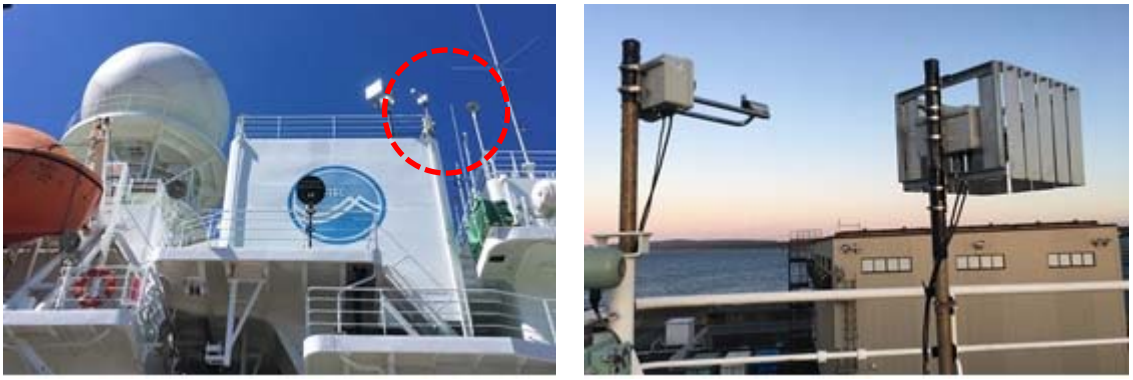

Figure 2.5.4-1. Onboard LPM sensors. (Left) The location of the sensors, as designated by the red broken circle. (Right) The sensors. Right one (aft one) equipped wind protection element to reduce the effect of the wind, while left one (fore one) did not.

Table 2.5.4-1. Categories of the particle size and the fall speed.

Particle Size		
Class	Diameter [mm]	Class width [mm]
1	≥ 0.125	0.125
2	≥ 0.250	0.125
3	≥ 0.375	0.125
4	≥ 0.500	0.250
5	≥ 0.750	0.250
6	≥ 1.000	0.250
7	≥ 1.250	0.250
8	≥ 1.500	0.250
9	≥ 1.750	0.250
10	≥ 2.000	0.500
11	≥ 2.500	0.500
12	≥ 3.000	0.500
13	≥ 3.500	0.500
14	≥ 4.000	0.500
15	≥ 4.500	0.500
16	≥ 5.000	0.500
17	≥ 5.500	0.500
18	≥ 6.000	0.500
19	≥ 6.500	0.500
20	≥ 7.000	0.500
21	≥ 7.500	0.500
22	≥ 8.000	unlimited

Fall Speed		
Class	Speed [m/s]	Class width [m/s]
1	≥ 0.000	0.200
2	≥ 0.200	0.200
3	≥ 0.400	0.200
4	≥ 0.600	0.200
5	≥ 0.800	0.200
6	≥ 1.000	0.400
7	≥ 1.400	0.400
8	≥ 1.800	0.400
9	≥ 2.200	0.400
10	≥ 2.600	0.400
11	≥ 3.000	0.800
12	≥ 3.400	0.800
13	≥ 4.200	0.800
14	≥ 5.000	0.800
15	≥ 5.800	0.800
16	≥ 6.600	0.800
17	≥ 7.400	0.800
18	≥ 8.200	0.800
19	≥ 9.000	1.000
20	≥ 10.000	10.000

2.5.5. Micro rain radar

(1) Personnel

Fumikazu Taketani (JAMSTEC) – Principal investigator, Not on board

Masaki Katsumata (JAMSTEC) – Not on board

Operation for all instruments was supported by Nippon Marine Enterprises, Ltd. (NME)

(2) Objectives

The micro rain radar (MRR) is a compact vertically-pointing Doppler radar, to detect vertical profiles of rain drop size distribution. The objective of this observation is to understand detailed vertical structure of the precipitating systems.

(3) Instruments and Methods

The MRR-2 (METEK GmbH) was utilized. The specifications are in Table 2.5.5-1. The antenna unit was installed at the starboard side of the anti-rolling systems (see Figure 2.5.5-1), and wired to the junction box and laptop PC inside the vessel.

The data was averaged and stored every one minute. The vertical profile of each parameter was obtained every 100 meters in range distance (i.e. height) up to 3100 meters. The recorded parameters were; Particle size distribution, radar reflectivity, path-integrated attenuation, rain rate, liquid water content and fall velocity..

Figure 2.5.5-1. Photo of the antenna unit of MRR.

Table 2.5.5-1. Specifications of the MRR-2.

Transmitter power	50 mW
Operating mode	FM-CW
Frequency	24.230 GHz (modulation 1.5 to 15 MHz)
3dB beam width	1.5 degrees
Spurious emission	< -80 dBm / MHz
Antenna Diameter	600 mm
Gain	40.1 dBi

s

(4) Preliminary Results

The data have been obtained all through the cruise. The further analyses will be after the cruise.

(5) Data Archive

These data obtained in this cruise will be submitted to the Data Management Group (DMG) of JAMSTEC, and will be opened to the public via “Data Research System for Whole Cruise

Information in JAMSTEC (DARWIN)" in JAMSTEC web site.
<http://www.godac.jamstec.go.jp/darwin/e>

(6) Acknowledgment

The onboard operation was supported by Nippon Marine Enterprises, Ltd.

2.6. Greenhouse gases observation

(1) Personnel

Yasunori Tohjima (National Institute for Environmental Studies; NIES)
– Principal investigator, Not on board
Fumikazu Taketani (JAMSTEC) – Not on board
Shinji Morimoto (Tohoku University) – Not on board
Hideki Nara (NIES) – Not on board
Daisuke Goto (National Institute of Polar Research; NIPR) – Not on board
Prabir Patra (JAMSTEC) – Not on board

(2) Objectives

The Arctic region, being considered to be more sensitive to the global climate change than the rest of the world, is warming about twice as fast as the global average. Additionally, several studies suggested that the global warming would potentially enhance emissions of the greenhouse gases including CO_2 and CH_4 from the carbon pools in the Arctic permafrost into the atmosphere. Therefor there are growing concerns about feedback mechanism between the global warming and the greenhouse gas emissions from the Arctic region. The objective of this study is to detect the increases in the atmospheric greenhouse gas levels associated with the ongoing global warming in the Arctic region in the early stage. The continuous observations of the atmospheric CO_2 and CH_4 mixing ratios during this MR20-05C cruise would allow us to detect the enhanced mixing ratios associated with the regional emissions and to estimate the distribution of the regional emission sources. The atmospheric CO mixing ratios, which were also observed at the same time, can be used as an indicator of the anthropogenic emissions associated with the combustion processes.

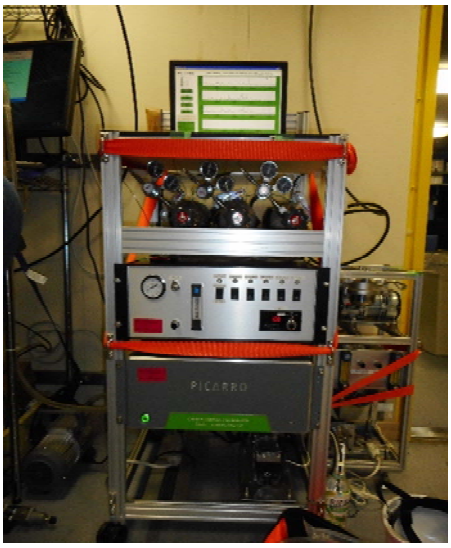

Photo 2.6-1. Continuous measurement system of the atmospheric CO_2, CH_4, and CO based on a cavity ring-down spectrometer (CRDS) used during MR20-05C cruise.

(3) Parameters

Mixing ratios of atmospheric CO_2, CH_4, and CO.

(4) Instruments and methods

Atmospheric CO_2, CH_4, and CO mixing ratios were measured by a wavelength-scanned cavity ring-down spectrometer (WS-CRDS, Picarro, G2401, see Photo 1). An air intake, capped with an inverted stainless steel beaker covered with stainless steel mesh, was placed on the right-side of the upper deck. A diaphragm pump (GAST, MOA-P108) was used to draw in the outside air at a flow rate of ~8 L min^{-1}. Water vapor in the sample air was removed to a dew pint of about 2°C and about -35°C by passing it through a thermoelectric dehumidifier (KELK, DH-109) and a Nafion drier (PERMA PURE, PD-50T-24), respectively. Then, the dried sample air was introduced into the WS-CRDS at a flow rate of 100 ml min^{-1}. The WS-CRDS were automatically calibrated every 49 hours by introducing 3 standard airs with known CO_2, CH_4 and CO mixing ratios. The analytical precisions for CO_2, CH_4 and CO mixing ratios are about 0.02 ppm, 0.3 ppb and 3 ppb, respectively.

(5) Station list or Observation log

The continuous observations of CO_2, CH_4 and CO mixing ratios were conducted during the entire cruise.

(6) Preliminary results

The time series of the atmospheric CH_4, CO_2, and CO mixing ratios observed during the entire cruise are shown in Figure 2.6-1.

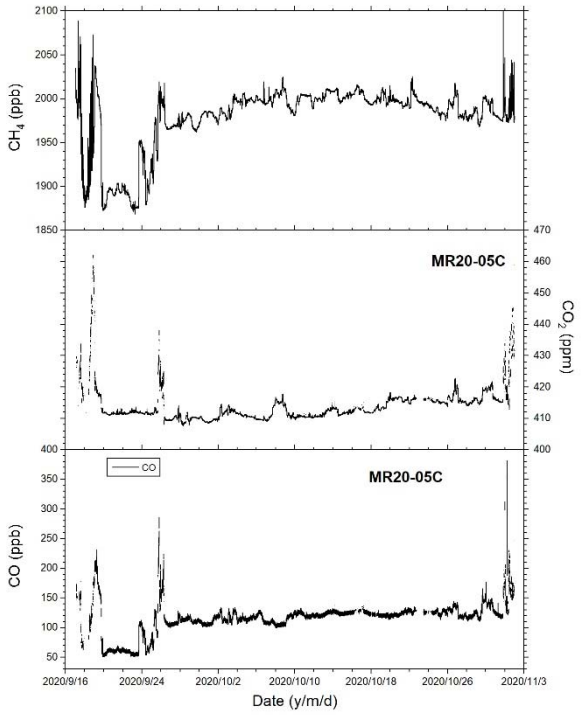

Figure 2.6-1. The time series of the atmospheric (top) CH_4, (middle) CO_2, and (bottom) CO mixing ratios observed during the entire period of MR20-05C cruise.

(7) Data archives

These data obtained in this cruise will be submitted to the Data Management Group (DMG) of JAMSTEC, and will be opened to the public via "Data Research System for Whole Cruise Information in JAMSTEC (DARWIN)" in JAMSTEC web site.
<http://www.godac.jamstec.go.jp/darwin/e>

2.7. Isotope analyses of water vapor

(1) Personnel

Hotaek Park (JAMSTEC) – Principal investigator, Not on board

(2) Background and objective

The Arctic sea ice extent of this year has recorded the largest decline secondary since the start of satellite observation. The opened sea surface enhances the Arctic warming through stronger positive feedbacks identified as increased cyclone and clouds, further warming by ice-albedo feedbacks, especially significant in autumn and winter, and increased precipitation over the pan-Arctic. The resultant wetter atmosphere and increased precipitation likely strengthen water cycle in the Arctic Ocean, and the moisture transport to the neighbor terrestrial region through the atmospheric dynamics can affect the water cycle there. In reality, the observed Arctic river discharges show significant increases in spring snowmelt season and the autumn. The increased autumnal moisture induced by the declined sea ice is able to bring higher snow depth in the season. The snow is likely correlated to the increased spring discharge. The snow has also an insulation function, warming permafrost. The permafrost thawing can increase the connectivity of the melted water to river discharge. Likewise, the linkage between the Arctic sea ice and the terrestrial hydrology suggests the potential impacts of the declining sea ice on the terrestrial hydrologic processes.

Numerical models are a useful tool to identify the linkage of the declining sea ice and the terrestrial hydrology, while the modeling is requiring the validation of the simulated results against observations. Isotope is characterized by the usefulness to do backward tracing the source area of precipitated water. The combination of numerical model simulation and isotope observation makes it possible to explore the relationship of the declining sea ice and the terrestrial water cycle. Therefore, a consecutive observation of the isotope of atmospheric water vapor was conducted during the MR20 Arctic cruise. This document reports the isotopic properties observed at the cruise.

(3) Parameters

Isotope ratios of Oxygen and Hydrogen and water vapor concentration

(4) Instrument and method

The isotope of atmosphere water vapor was monitored by a Cavity Ringdown

Spectrometer (L2130-i, Isotopic H_2O, Picarro, Figure 2.7-1), which simultaneously observes the isotope ratios of oxygen and hydrogen with 1–2 Hz frequency, including water vapor concentration. The observed data are archived on the storage of the spectrometer, operated by Windows system. Two standard liquids, for example with isotope values of -0.21 permil and -30.76 permil in oxygen, are individually injected for 15 minutes every 12-hour, in which the derived linear regression equation is used to calibrate the monitored values by the spectrometer.

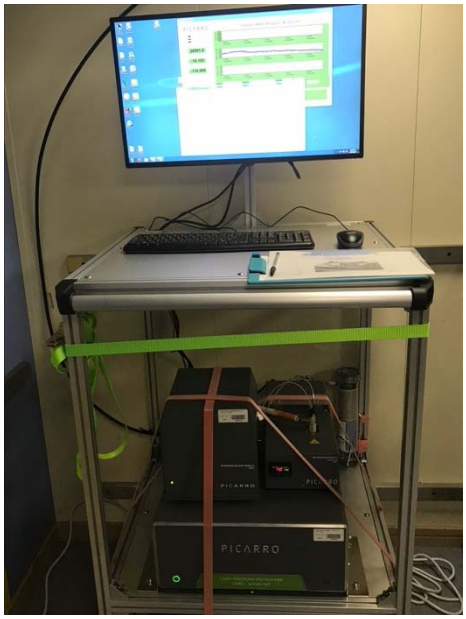

Figure 2.7-1. Isotope spectrometer system.

(5) Preliminary results

The observed isotope ratios were averaged to hourly time steps (Figure 2.7-2), exhibiting results observed in the Arctic Ocean during the period of October 6–23, 2020. The isotope ratios are generally decreasing and then increasing with the elapse of dates. The daily variability represents influences of air temperature, reflecting the ship cruising routes from south to north and in turn to south. In reality, the isotope of oxygen significantly correlated with air temperature, as identified in the analysis of 2019 Arctic cruise. The isotopes show large diurnal and daily variability (Figure 2.7-2). Here discussed for the two days (i.e., October 12 and 13) that indicated the largest differences in the isotopic ratios in the consecutive time series. The isotope of oxygen recorded the minimum -29 permil on October 12 that recorded -6°C in air temperature and then dramatically recovered to -18 permil during 20 hours, responding to the change in air temperature. As the ship entered in the Arctic Ocean, the air temperature generally indicated the freezing state from October 10 and 18. The oxygen ratios during the period have distributed at the range lower than -20

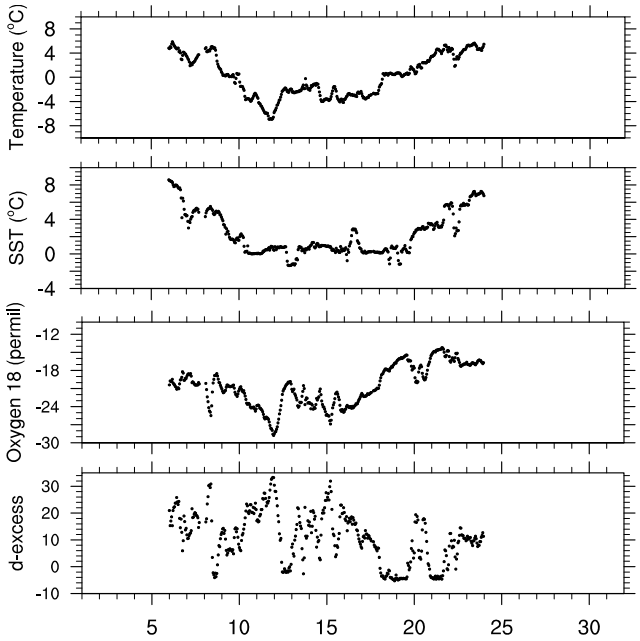

Fig. 2.7-2. Variability of air temperature, sea surface temperature, and isotopes of oxygen and hydrogen during October 6 and 23, 2020.

permil. The analysis of the cruise of 2019 indicated the significant impact of wind direction on the variability of isotope ratios. However, their significant relationship was not identified in this year cruise.

Both oxygen and hydrogen indicated significantly high correlation. Their relationship yielded the slope of 6.1 and 5.9 in 2019 and 2020, respectively (Figure 2.7-3). The slopes distribute within the ranges of 5 and 7 obtained at the northernmost terrestrial sites. However, the slope 6 derived by the two-year cruise is lower than the value 8 of global meteoric water line (GMWL), which represent the sensitivity of isotope to air temperature.

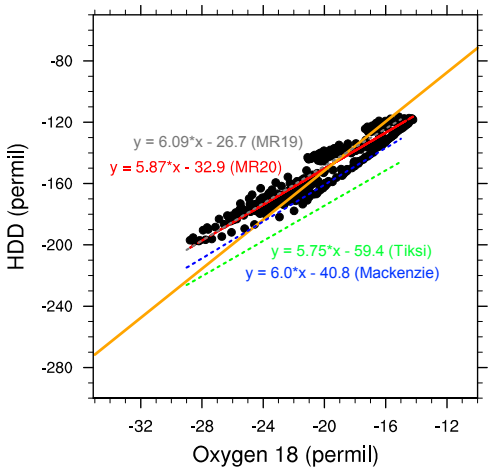

Fig. 2.7-3. Relationship between the observed oxygen and hydrogen at the cruises of 2019 and 2020, including the isotopic relationship obtained at the two terrestrial sites.

(6) Data archive

The data obtained in this cruise will be submitted to the Data Management Group of JAMSTEC, and will be opened to the public via "Data Research System for Whole Cruise Information in JAMSTEC (DARWIN)" in JAMSTEC web site. http://www.godac.jamstec.go.jp/darwin/e.

3. Physical Oceanography

3.1. CTD casts and water sampling

(1) Personnel

Shigeto Nishino (JAMSTEC) – Principal investigator
Amane Fujiwara (JAMSTEC)
Shinsuke Toyoda (Marine Works Japan Ltd.; MWJ) – Operation leader
Shungo Oshitani (MWJ)
Ko Morita (MWJ)
Aine Yoda (MWJ)
Yuya Hitomi (MWJ)
Miaki Muramatsu (JAMSTEC)
Syunya Sano (JAMSTEC)

(2) Objective

Investigation of oceanic structure and water sampling.

(3) Parameters

Temperature (Primary and Secondary)
Salinity (Primary and Secondary)
Pressure
Dissolved Oxygen (Primary "RINKO III" and Secondary "SBE43")
Fluorescence (Primary and Secondary)
Beam Transmission
Turbidity
Nitrate
Photosynthetically Active Radiation
Altimeter
Deep Ocean Standards Thermometer

(4) Instruments and Methods

CTD/Carousel Water Sampling System, which is a 36-position Carousel Water Sampler (CWS) with Sea-Bird Electronics, Inc. 12-liter sample Bottles were used for sampling seawater (#1 - #10 aced washed and Viton O-ring. #11, #12 aced washed and Viton O-ring from Stn.005). The sensors attached on the CTD were temperature (primary and secondary), conductivity (primary and secondary), pressure, dissolved oxygen (primary: RINKO III, secondary: SBE43), fluorescence (primary and secondary), beam transmission, turbidity, nitrate, photosynthetically active radiation, altimeter and Deep Ocean Standards Thermometer. Salinity was computed by measured values of pressure, conductivity and temperature. The CTD/CWS was deployed from starboard on working deck.

Specifications of the sensors are listed below.

CTD: SBE911plus CTD system

Under water unit:

SBE9plus (S/N: 09P54451-1027, Sea-Bird Electronics, Inc.)

Pressure sensor: Digiquartz pressure sensor (S/N:117457)

Calibrated Date: 08 Jul 2020

Carousel water sampler:

SBE32 (S/N: 3227443-0391, Sea-Bird Electronics, Inc.)

Temperature sensors:

Primary: SBE03-04/F (S/N: 031525, Sea-Bird Electronics, Inc.)

Calibrated Date: 01 Jun. 2019

Secondary: SBE03-04/F (S/N: 031359, Sea-Bird Electronics, Inc.)

Calibrated Date: 27 Jun. 2019

Conductivity sensors:

Primary: SBE04C (S/N: 042435, Sea-Bird Electronics, Inc.)

Calibrated Date: 25 Jun. 2019

Secondary: SBE04C (S/N: 042854, Sea-Bird Electronics, Inc.)

Calibrated Date: 26 Jun. 2019

Dissolved Oxygen sensor:

Primary: RINKOIII (S/N: 0287_163011BA, JFE Advantech Co., Ltd.)

Calibrated Date: 25 Jun. 2020

Secondary: SBE43 (S/N: 430401 Sea-Bird Electronics, Inc.)

Calibrated Date: 02 Jul. 2019

Fluorescence:

Primary:

Chlorophyll Fluorometer (S/N: 3618, Seapoint Sensors, Inc.)

Gain setting: 30X, 0-5 ug/l

Calibrated Date: None

Offset: 0.000

Secondary:

Chlorophyll Fluorometer (S/N: 3700, Seapoint Sensors, Inc.)

Gain setting: 3X, 0-50 ug/l

Calibrated Date: None

Offset: 0.000

Transmission meter:

C-Star (S/N CST-1726DR, WET Labs, Inc.)

Calibrated Date: 12 Jun. 2020

Turbidity:

Turbidity Meter (S/N: 14953)

Gain setting: 100X

Scale factor: 1.000

Calibrated Date: None

Casts used: 001M001, 001M002, 002M002, 003M001

Nitrate:

Deep SUNA (S/N 895, Satlantic, Inc.)

Calibration Date: 16 Jun. 2020

Casts used: 002M001, 004M001 – 036M001

Photosynthetically Active Radiation:

PAR sensor (S/N: 1025, Satlantic Inc.)

Calibrated Date: 06 Jul. 2015

Altimeter:

Benthos PSA-916T (S/N: 1100, Teledyne Benthos, Inc.)

Submersible Pump:

Primary: SBE5T (S/N: 055816, Sea-Bird Electronics, Inc.)

Secondary: SBE5T (S/N: 054598, Sea-Bird Electronics, Inc.)

Bottom contact switch: (Sea-Bird Electronics, Inc.)

Deep ocean standards thermometer:

SBE35 (S/N: 0053, Sea-Bird Electronics, Inc.)

Calibrated Date: 10 Jun. 2019

Deck unit: SBE11plus (S/N 11P54451-0872, Sea-Bird Electronics, Inc.)

Configuration file: MR2005C_A.xmlcon

001M001, 001M002, 002M002, 003M001

MR2005C_B.xmlcon

002M001, 004M001 – 036M001

The CTD raw data were acquired on real time using the Seasave-Win32 (ver.7.26.7.121) provided by Sea-Bird Electronics, Inc. and stored on the hard disk of the personal computer. Seawater was sampled during the up cast by sending fire commands from the personal computer.

For depths where vertical gradients of water properties were exchanged to be large, the bottle was exceptionally fired after waiting from the stop for 60 seconds to enhance exchanging the water between inside and outside of the bottle. 30 seconds below thermocline to stabilize then fire.

Data processing procedures and used utilities of SBE Data Processing-Win32 (ver.7.26.7.129) and SEASOFT were as follows:

(The process in order)

DATCNV: Convert the binary raw data to engineering unit data. DATCNV also extracts bottle information where scans were marked with the bottle confirm bit during acquisition. The duration was set to 4.4 seconds, and the offset was set to 0.0 seconds.

TCORP (original module): Corrected the pressure sensitivity of the temperature (SBE3) sensor.
S/N 031525: 1.714e-008 (degC/dbar)
S/N 031359: -2.29885054e-007 (degC/dbar)

RINKOCOR (original module): Corrected the time dependent, pressure induced effect (hysteresis) of the RINKOIII profile data.

RINKOCORROS (original module): Corrected the time dependent, pressure induced effect (hysteresis) of the RINKOIII bottle information data by using the hysteresis corrected profile data.

BOTTLESUM: Create a summary of the bottle data. The data were averaged over 4.4 seconds.

ALIGNCTD: Convert the time-sequence of sensor outputs into the pressure sequence to ensure that all calculations were made using measurements from the same parcel of water. Dissolved oxygen data are systematically delayed with respect to depth mainly because of the long time constant of the dissolved oxygen sensor and of an additional delay from the transit time of water in the pumped pluming line. This delay was compensated by 5 seconds advancing dissolved oxygen sensor (SBE43) output (dissolved oxygen voltage) relative to the temperature data. RINKOIII voltage (User polynomial 0) was advanced 1 second and transmission data was advanced 2 seconds.

WILDEDIT: Mark extreme outliers in the data files. The first pass of WILDEDIT obtained the accurate estimate of the true standard deviation of the data. The data were read in blocks of 1000 scans. Data greater than 10 standard deviations were flagged. The second pass computed a standard deviation over the same 1000 scans excluding the flagged values. Values greater than 20 standard deviations were marked bad. This process was applied to

pressure, depth, temperature (primary and secondary), conductivity (primary and secondary), dissolved oxygen voltage (SBE43).

CELLTM: Remove conductivity cell thermal mass effects from the measured conductivity. Typical values used were thermal anomaly amplitude alpha = 0.03 and the time constant 1/beta = 7.0.

FILTER: Perform a low pass filter on pressure and depth data with a time constant of 0.15 second. In order to produce zero phase lag (no time shift) the filter runs forward first then backward

WFILTER: Perform a median filter to remove spikes in the fluorescence data (primary and secondary), transmission data, transmission beam attenuation, transmission voltage, turbidity and nitrate. A median value was determined by 49 scans of the window.

SECTIONU (original module of SECTION): Select a time span of data based on scan number in order to reduce a file size. The minimum number was set to be the starting time when the CTD package was beneath the sea-surface after activation of the pump. The maximum number of was set to be the end time when the package came up from the surface.

LOOPEDIT: Mark scans where the CTD was moving less than the minimum velocity of 0.0 m/s (traveling backwards due to ship roll).

DESPIKE (original module): Remove spikes of the data. A median and mean absolute deviation was calculated in 1-dbar pressure bins for both down and up cast, excluding the flagged values. Values greater than 4 mean absolute deviations from the median were marked bad for each bin. This process was performed twice for temperature, conductivity and dissolved oxygen (RINKOIII and SBE43) voltage.

DERIVE: Compute dissolved oxygen (SBE43).

BINAVG: Average the data into 1 decibar bins and 1 sec bins.

BOTTOMCUT (original module): Deletes discontinuous scan bottom data, when it's created by BINAVG.

DERIVE: Compute salinity, potential temperature, and sigma-theta.

SPLIT: Separate the data from the input .cnv file into down cast and up cast files.

(5) Station list

During this cruise, 40casts of CTD observation were carried out. Date, time and locations of the CTD casts are listed in Table 3.1-1.

(6) Preliminary Results

During this cruise, we judged noise, spike or shift in the data of some casts. These were as follows.

001M002: Beam Transmission
down 4200 - down 4244 dbar, up 350 - up 106 dbar: noise

002M001: Beam Transmission
down 816 dbar - down 822 dbar: spike

Nitrate
down 753 dbar - down 1123 dbar, up 1122 dbar - up 697 dbar: overrange

002M002: Secondary Temperature, Secondary Salinity
down 42 dbar: spike

004M001: Secondary Temperature, Secondary Salinity
down 46 dbar: spike

Nitrate
down 64 dbar - down 1001 dbar, up 1000 dbar - up 42 dbar: overrange

004M002: Beam Transmission
down 246 dbar, down 247 dbar: spike

Nitrate
down 54 dbar - down 801 dbar, up 800 dbar - up 37 dbar: overrange

006M001: Primary Salinity
down 27 dbar: spike

008M001: Primary Temperature, Primary Salinity
down 31 dbar: spike

009M001: Primary Salinity, SBE43 voltage
up 10 dbar - up 1 dbar: shift

012M001: SBE43 voltage
Down 703 dbar - down 1326 dbar: noise

018M001: Secondary Salinity
down 21 dbar: spike

035M001: Primary Temperature, Primary Salinity
down 14 dbar: spike

(7) Data archive

These data obtained in this cruise will be submitted to the Data Management Group (DMG) of JAMSTEC, and will be opened to the public via "Data Research System for Whole Cruise Information in JAMSTEC (DARWIN)" in JAMSTEC web site.
<http://www.godac.jamstec.go.jp/darwin/e>

Table 3.1-1. MR20-05C CTD cast table.

Stnnbr	Castno	Date(UTC)	Time(UTC)		BottomPosition		Depth	Wire	HT Above	Max	Max	CTD	Remark
		(mmddyy)	Start	End	Latitude	Longitude	(m)	Out (m)	Bottom (m)	Depth	Pressure	Filename	
001	1	092120	22:40	23:36	32-00.00N	147-00.00E	5970.0	795.7	-	794.9	802.0	001M001	
001	2	092220	03:13	07:23	32-00.00N	146-59.96E	5969.0	5943.4	9.2	5947.8	6074.0	001M002	
002	1	092320	00:03	01:55	32-59.83N	146-59.92E	5997.0	1111.2	-	1112.1	1123.0	002M001	
002	2	092320	03:32	03:56	32-59.55N	146-59.81E	5998.0	146.8	-	149.9	151.0	002M002	no LADCP data no sampling water
003	1	092320	23:34	03:43	34-00.13N	146-59.69E	5825.0	5799.3	9.1	5802.8	5925.0	003M001	
004	1	100120	04:23	05:48	47-00.03N	160-01.95E	5230.0	989.9	-	990.3	1001.0	004M001	
004	2	100120	09:40	10:40	47-01.01N	160-02.67E	5217.0	792.0	-	792.8	801.0	004M002	
005	1	100720	07:04	07:09	65-38.36N	168-27.67W	52.6	42.1	4.3	47.5	48.0	005M001	no sampling water
006	1	100720	14:11	14:16	67-00.18N	168-49.86W	46.3	37.5	5.3	40.6	41.0	006M001	no sampling water
007	1	100820	07:26	07:53	69-00.83N	168-49.77W	51.3	39.3	4.8	46.5	47.0	007M001	
008	1	100820	13:30	13:34	69-59.97N	168-49.74W	40.3	29.8	5.4	33.7	34.0	008M001	no sampling water
009	1	100820	22:34	22:58	70-30.02N	165-29.73W	43.9	32.2	5.6	37.6	38.0	009M001	
010	1	101020	17:50	18:44	74-31.58N	161-55.64W	1688.0	789.2	-	792.2	802.0	010M001	
010	2	101020	21:34	23:18	74-33.03N	161-53.06W	1721.0	1706.4	9.1	1706.0	1731.0	010M002	
011	1	101120	20:55	22:12	74-58.81N	158-07.55W	841.0	828.0	10.3	825.7	836.0	011M001	
012	1	101220	05:14	07:06	75-10.95N	160-00.17W	1985.0	1966.6	10.2	1962.9	1993.0	012M001	
013	1	101320	21:08	22:41	73-17.32N	160-00.66W	1212.0	1194.6	6.5	1193.1	1209.0	013M001	
014	1	101420	01:38	02:09	73-03.17N	159-00.42W	839.0	783.5	10.3	784.3	794.0	014M001	no sampling water
015	1	101420	04:28	05:47	72-47.32N	157-59.98W	773.0	750.8	10.8	750.8	760.0	015M001	
016	1	101420	09:14	09:42	72-28.48N	157-00.05W	690.0	671.4	10.1	670.9	679.0	016M001	no sampling water
017	1	101520	03:53	04:30	71-19.18N	158-26.24W	114.8	106.6	4.8	109.8	111.0	017M001	
018	1	101520	15:08	15:29	71-40.78N	152-29.90W	416.0	383.1	8.7	387.6	392.0	018M001	no sampling water
019	1	101520	18:01	18:25	71-47.73N	152-59.44W	477.0	458.3	8.9	458.7	464.0	019M001	no sampling water
020	1	101520	20:59	22:08	71-58.34N	153-59.67W	740.0	723.6	9.1	724.2	733.0	020M001	
021	1	101620	01:28	01:45	72-03.92N	154-59.79W	393.0	373.4	11.0	375.8	380.0	021M001	no sampling water
022	1	101720	21:50	22:59	75-00.87N	164-57.48W	552.0	534.5	9.1	539.6	546.0	022M001	
023	1	101820	02:27	03:13	75-00.17N	167-14.30W	262.0	249.9	9.3	256.1	259.0	023M001	
024	1	101820	08:34	09:17	75-00.04N	169-38.22W	236.0	220.3	9.0	226.5	229.0	024M001	
025	1	101820	21:13	22:05	75-00.21N	174-59.64W	266.0	260.7	3.7	266.0	269.0	025M001	
026	1	101920	02:30	03:22	75-00.05N	172-00.23W	383.0	367.0	10.0	370.8	375.0	026M001	
027	1	101920	08:28	09:07	74-36.00N	170-11.94W	208.0	197.7	5.2	200.8	203.0	027M001	
028	1	101920	14:48	14:58	74-00.04N	168-50.13W	178.6	169.1	5.7	172.1	174.0	028M001	no sampling water
029	1	101920	20:51	21:23	73-29.97N	168-48.83W	115.6	105.1	5.5	108.8	110.0	029M001	
030	1	102020	00:18	00:45	73-00.08N	168-49.55W	64.2	54.4	4.7	58.4	59.0	030M001	
031	1	102020	07:34	07:55	72-00.00N	168-49.98W	50.4	42.1	4.2	45.5	46.0	031M001	
032	1	102020	13:30	13:34	71-00.05N	168-49.94W	44.0	33.8	5.6	37.6	38.0	032M001	no sampling water
033	1	102020	21:03	21:24	69-59.98N	168-48.79W	39.4	31.0	5.2	33.7	34.0	033M001	
034	1	102120	03:09	03:31	69-00.22N	168-49.64W	51.7	41.5	5.3	45.5	46.0	034M001	
035	1	102120	09:16	09:45	68-00.00N	168-49.98W	57.5	49.2	4.4	52.5	53.0	035M001	
036	1	102120	18:04	18:10	67-00.18N	168-49.79W	46.1	37.9	5.2	40.6	41.0	036M001	no sampling water

3.2. LADCP

(1) Personnel

Yusuke Kawaguchi (The University of Tokyo)
– Principal investigator, Not on board
Shigeto Nishino (JAMSTEC)
Eun Yae Son (The University of Tokyo)
Shinsuke Toyoda (Marine Works Japan Ltd.; MWJ) – Operation leader
Syungo Oshitani (MWJ)
Yuya Hitomi (MWJ)
Ko Morita (MWJ)
Aine Yoda (MWJ)
Miaki Muramatsu (JAMSTEC)
Syunya Sano (JAMSTEC)

(2) Objective

To investigate ocean current velocity and vertical shear

(3) Parameters

The device retrieves depth, horizontal velocity (u), meridional velocity (v).

(4) Objectives and methodology

The lowered ADCP (LADCP), Workhorse Monitor WHM300 (Teledyne RD Instrument, San Diego, California, USA) was utilized at the every CTD point in MR20-05C to get a shear data at the same time. LADCP system consist of two ADCP of upward-and downward looking transducer and a 45V battery package. The LADCP system were set for recording before the CTD cast and its data were recovered right after CTD cast. Velocity conversion from the two transducers were done by LDEO LADCP software (version 10; Visbeck 2002). For the data conversion, navigation data and CTD data were applied for the improvement of data quality.

Detailed configuration is below:

Bin size: 8.0 m

Number of bins: 25

Pings per ensemble: 1

Ping interval: 1.0 sec

(5) Station log

Station number is same with CTD files. Each station has 2 data with separated folder named MASTR (down-looking ADCP) and SLAVE (up-looking ADCP).

(6) Caution on utilization

During the operation, several warnings were appeared by ping ensemble difference. It basically coming from the start time difference between MASTER ADCP (down-looking) and SLAVE ADCP (up-looking). The issue came from the difference in baudrate of MASTER and SLAVE ADCPs. If both MASTER and SLAVE do not have 115000, SLAVE wakes up earlier before send a script file via MASTER.

Second caution on LADCP data utilization is some profiles showed bad ping correlation. Most of issues were occurred at the shallow area <500 m.

Third matter is beam4 has been weakened during the observation. The original MASTER ADCP showed weak beam (No.4). However, correlation among beams were high enough to use. Additionally, we tried to use back up ADCP sensor, however, this ADCP showed high voltage consumption. Therefore, we changed ADCP again to have MASTER as original SLAVE which showed good beam performance and original MASTER was set to SLAVE.

For the last, when run LDEO software, it shows low-voltage warning, however, real voltage was above 40V. This matter comes from assumption of voltage usage, which made by LDEO software. It calculates median voltage count ×0.33, which was not a proper constant for our ADCPs. Therefore, the warning can be ignored. Warning can be seen in Table 3.2-1.

Table 3.2-1. List of LADCP log on caution.

Cast No.	Date	Battery log	Obs. depth	MASTER SN	SLAVE SN	LDEO remark
001M001	21/09/2020	new	802	13591	12971	no fix ping rate
001M002	22/09/2020		6074	13591	12971	no fix ping rate
002M001	22/09/2020		1123	13591	12971	no fix ping rate
003M001	23/09/2020	new	5925	13591	12971	no fix ping rate
004M001	01/10/2020		1001	13591	12971	
004M002	01/10/2020		801	13591	12971	
005M001	07/10/2020		48	13591	12971	cannot process
006M001	07/10/2020	new	41	13591	12971	
007M001	08/10/2020		47	13591	12971	weak down looking beam 4
008M001	08/10/2020		34	13591	12971	cannot process
009M001	08/10/2020		38	13591	12971	

Cast No.	Date	Battery log	Obs. depth	MASTER SN	SLAVE SN	LDEO remark
010M001	10/10/2020		802	13591	12971	weak down looking beam 4
010M002	10/10/2020		1731	13591	12971	weak down looking beam 4
011M001	11/10/2020	new	836	13591	12971	weak down looking beam 4
012M001	12/10/2020		1993	13591	12971	weak down looking beam 4
013M001	13/10/2020		1209	13591	12973	weak down looking beam 4
014M001	14/10/2020		794	13591	12973	weak down looking beam 4
015M001	14/10/2020		760	13591	12973	weak down looking beam 4
016M001	14/10/2020	new	679	13591	12973	weak down looking beam 4
017M001	15/10/2020	new	111	12973	12971	
018M001	15/10/2020		392	12973	12971	
019M001	15/10/2020	new	464	12973	12971	
020M001	15/10/2020		733	12971	13591	broken up looking beam 4
021M001	16/10/2020	new	380	12971	13591	broken up looking beam 4

(7) Data archive

These data obtained in this cruise will be submitted to the Data Management Group (DMG) of JAMSTEC, and will be opened to the public via "Data Research System for Whole Cruise Information in JAMSTEC (DARWIN)" in JAMSTEC web site.

<http://www.godac.jamstec.go.jp/darwin/e>

Reference

Visbeck, M. (2002): Deep velocity profiling using Acoustic Doppler Current Profilers: Bottom track and inverse solutions, J. Atmos. Oceanic Technol., 19, 794–807.

3.3. XCTD

(1) Personnel

Shigeto Nishino (JAMSTEC) – Principal investigator
Takuji Waseda (The University of Tokyo) – Not on board
Keita Nishizawa (The University of Tokyo)
Yusuke Kawaguchi (The University of Tokyo) – Not on board
Eun-Yae Son (The University of Tokyo)
Ryo Oyama (Nippon Marine Enterprises, Ltd.; NME) – Operation leader
Soichiro Sueyoshi (NME)
Wataru Tokunaga (NME)
Masanori Murakami (NME)
Yoichi Inoue (MIRAI Crew)

(2) Objective

To obtain vertical profiles of sea water temperature and salinity (calculated from temperature, pressure (depth), and conductivity).

(3) Parameters

The ranges and accuracies of parameters measured by the XCTD (eXpendable Conductivity, Temperature & Depth profiler) are as follows;

Parameter	Range	Accuracy
Conductivity	0 ~ 60 [mS/cm]	+/- 0.03 [mS/cm]
Temperature	-2 ~ 35 [deg-C]	+/- 0.02 [deg-C]
Depth	0 ~ 1000 [m]	5 [m] or 2 [%] (either of them is major)

(4) Instruments and Methods

We observed vertical profiles of sea water temperature and salinity measured by XCTD-1 probes manufactured by Tsurumi-Seiki Co. (TSK). The electric signal from the probe was converted by MK-150N (TSK), and was recorded by AL-12B software (Ver.1.1.4, TSK). We launched 92 probes by using the automatic launcher. The XCTD observation log is shown in Table 3.3-1.

(5) Observation log

Table 3.3-1. XCTD observation log.

No.	Station No.	Date [YYYY/MM/DD]	Time [hh:mm]	Latitude [deg]	Longitude [deg]	Dep. [m]	SST [deg-C]	SSS [PSU]	Probe S/N
1	Stn.04 (K2)	2020/10/01	04:37	47-00.0372N	160-01.9725E	5229	11.959	32.711	18086024
2	X001	2020/10/07	09:08	66-00.1881N	168-49.7872W	53	4.518	31.643	20015337
3	X002	2020/10/07	11:26	66-29.9972N	168-50.2090W	51	5.085	31.552	20015340
4	X003	2020/10/07	17:18	67-29.9704N	168-49.8517W	50	4.804	31.681	20015343
5	X004	2020/10/08	00:26	68-00.1964N	168-50.4112W	57	3.753	32.675	20025857
6	X005	2020/10/08	02:56	68-30.0119N	168-49.5523W	53	4.380	31.704	20025858
7	X006	2020/10/08	10:35	69-30.0032N	168-49.7660W	51	5.241	30.669	20015341
8	X007	2020/10/08	16:57	70-10.0473N	167-44.1452W	49	4.911	30.619	20025856
9	X008	2020/10/08	19:21	70-20.0010N	166-37.1396W	45	4.722	30.519	20015338
10	X009	2020/10/09	02:22	70-38.3133N	164-18.7458W	46	3.902	30.576	20025853
11	X010	2020/10/09	05:07	70-46.6475N	163-07.8741W	44	3.345	30.693	20015335
12	X011	2020/10/09	07:51	70-54.7378N	161-56.9786W	43	2.627	30.629	20015344
13	X012	2020/10/09	10:25	71-02.9641N	160-46.1021W	50	2.429	29.943	20015334
14	X013	2020/10/09	13:06	71-11.0832N	159-35.1779W	69	1.690	28.930	20025854
15	X014	2020/10/09	19:25	71-14.8355N	157-11.0387W	48	1.009	31.026	20025850
16	X015	2020/10/09	19:42	71-17.1843N	157-14.3828W	55	1.254	30.759	20025849
17	X016	2020/10/09	19:59	71-19.7912N	157-19.9850W	89	1.418	30.475	20025851
18	X017	2020/10/09	20:22	71-22.1795N	157-24.7751W	109	1.602	30.022	20025855
19	X018	2020/10/09	20:45	71-24.8566N	157-29.8356W	122	1.778	29.723	20015790
20	X019	2020/10/09	21:00	71-27.2680N	157-34.9919W	110	1.750	29.561	20015791
21	X020	2020/10/09	21:15	71-29.8182N	157-40.4787W	82	1.791	29.580	20015788
22	X021	2020/10/09	21:29	71-32.2095N	157-45.2123W	71	1.871	29.757	20015789
23	X022	2020/10/09	21:44	71-34.6870N	157-50.2679W	64	1.853	29.644	20015787
24	X023	2020/10/09	23:22	71-52.3613N	158-13.4704W	60	1.646	29.995	20025852
25	X024	2020/10/10	01:00	72-10.0448N	158-36.2353W	54	1.679	29.655	20015797
26	X025	2020/10/10	02:38	72-27.7221N	158-58.8395W	53	2.284	30.008	20015794
27	X026	2020/10/10	04:17	72-45.3607N	159-23.9974W	126	2.079	31.174	20025847
28	X027	2020/10/10	05:52	73-02.9984N	159-47.7363W	266	1.999	30.403	20025848
29	X028	2020/10/10	07:27	73-20.7110N	160-13.0317W	1210	1.019	28.663	20015793
30	X029	2020/10/10	09:00	73-38.3631N	160-36.4490W	1097	-0.228	28.198	20015792
31	X030	2020/10/10	10:47	73-59.1075N	161-07.0618W	465	-0.257	28.187	20015795
32	X031	2020/10/10	12:03	74-13.6510N	161-28.2507W	1407	0.683	28.816	20015798
33	X032	2020/10/11	08:49	74-40.9342N	161-17.0718W	1815	0.237	28.214	20025842
34	X033	2020/10/11	10:04	74-50.4249N	160-38.5097W	1465	-0.305	26.838	20025840
35	X034	2020/10/11	16:01	74-59.8018N	159-58.6839W	1972	-0.526	26.384	20015799
36	X035	2020/10/11	17:09	74-59.8076N	159-18.2868W	1754	-0.822	25.438	20025843
37	X036	2020/10/12	17:31	75-10.9968N	159-00.0930W	930	-0.980	25.448	20015800

No.	Station No.	Date [YYYY/ MM/DD]	Time [hh:mm]	Latitude [deg]	Longitude [deg]	Dep. [m]	SST [deg-C]	SSS [PSU]	Probe S/N
38	X037	2020/10/12	19:04	75-10.8351N	157-49.7777W	1437	-1.208	25.356	20025838
39	X038	2020/10/12	19:22	75-10.7294N	157-36.9768W	1536	-1.279	25.468	20025839
40	X039	2020/10/12	19:42	75-10.6950N	157-25.0952W	1560	-1.338	25.627	20025845
41	X040	2020/10/12	19:50	75-10.7216N	157-19.5374W	1496	-1.343	25.759	20025841
42	X041	2020/10/12	20:06	75-10.8250N	157-09.2396W	1211	-1.339	25.789	20025846
43	X042	2020/10/12	21:18	75-11.4257N	157-06.4603W	1161	-1.342	25.859	20025867
44	X043	2020/10/12	23:46	75-10.5530N	157-36.6806W	1543	-1.317	25.556	20025865
45	X044	2020/10/13	02:17	75-10.9480N	158-21.6744W	1151	-1.161	25.340	20025844
46	X045	2020/10/13	03:21	75-10.6829N	158-39.9882W	1054	-1.126	25.338	20015796
47	X046	2020/10/13	05:50	74-59.9256N	158-40.5095W	958	-1.136	25.305	20025862
48	X047	2020/10/13	08:27	74-45.0136N	158-51.2042W	691	-1.081	25.714	20025861
49	X048	2020/10/13	11:10	74-30.0045N	159-04.7236W	894	-0.809	25.101	20025864
50	X049	2020/10/13	13:43	74-14.9973N	159-16.1094W	776	-0.750	25.375	20025837
51	X050	2020/10/13	16:11	74-00.0033N	159-28.8247W	1641	-0.870	26.043	20025860
52	X051	2020/10/13	18:02	73-45.0148N	159-41.1832W	2733	-1.001	25.701	20025859
53	X052	2020/10/13	19:22	73-29.9873N	159-53.5428W	1919	-0.842	28.474	20025863
54	X053	2020/10/14	00:32	73-08.2838N	159-29.7900W	801	0.562	29.255	20025866
55	X054	2020/10/14	03:17	72-55.2039W	158-30.1209W	971	1.163	30.214	20025870
56	X055	2020/10/14	07:49	72-37.7547N	157-30.0123W	349	0.461	29.764	20025869
57	X056	2020/10/15	06:39	71-27.4634N	157-19.4418W	123	0.814	30.138	20068364
58	X057	2020/10/15	08:28	71-35.8565N	156-14.5298W	160	0.306	30.553	20068363
59	X058	2020/10/15	10:16	71-43.9937N	155-09.5958W	280	0.564	30.146	20025868
60	X059	2020/10/15	19:30	71-52.6102N	153-29.9856W	385	0.772	30.469	18086025
61	X060	2020/10/16	00:24	72-00.8245N	154-29.9553W	698	-0.195	29.291	19040346
62	X061	2020/10/16	02:38	72-10.6567N	155-30.0372W	407	-0.709	28.898	18086026
63	X062	2020/10/16	03:37	72-14.9985N	156-00.0108W	392	-1.175	27.848	18086027
64	X063	2020/10/16	05:04	72-19.8892N	156-29.9892W	440	-0.868	28.358	18086028
65	X064	2020/10/16	18:12	72-59.9921N	160-44.4968W	99	2.488	31.663	20068365
66	X065	2020/10/16	19:58	73-14.9999N	161-36.9771W	231	1.514	30.512	20068361
67	X066	2020/10/16	21:32	73-29.9459N	161-25.3885W	165	0.554	29.286	20068362
68	X067	2020/10/16	23:03	73-44.9904N	163-04.9600W	194	0.625	28.982	20068360
69	X068	2020/10/17	00:20	73-59.9898N	163-27.3976W	284	-0.547	27.202	19061568
70	X069	2020/10/17	01:36	74-14.9889N	163-49.0844W	379	-0.313	27.699	19061569
71	X070	2020/10/17	02:54	74-30.0082N	164-13.3692W	501	0.097	28.052	19061572
72	X071	2020/10/17	04:14	74-45.0140N	164-37.0948W	557	-0.484	27.711	19061573
73	X072	2020/10/17	19:06	74-59.9227N	165-00.4841W	544	-0.219	28.263	19061565
74	X073	2020/10/18	00:32	75-00.2528N	165-59.9928W	490	0.139	28.583	19061566
75	X074	2020/10/18	01:50	75-00.0598N	166-59.9920W	340	0.096	27.856	19061563
76	X075	2020/10/18	05:50	75-00.0109N	167-59.9867W	167	-0.020	28.378	19061567
77	X076	2020/10/18	07:15	75-00.0266N	169-00.1422W	216	0.549	29.013	19061562
78	X077	2020/10/18	11:21	75-00.0251N	170-00.0137W	258	0.380	28.662	19061564

No.	Station No.	Date [YYYY/ MM/DD]	Time [hh:mm]	Latitude [deg]	Longitude [deg]	Dep. [m]	SST [deg-C]	SSS [PSU]	Probe S/N
79	X078	2020/10/18	12:58	74-59.8026N	171-00.0348W	318	-0.762	27.547	19061571
80	X079	2020/10/18	23:34	75-00.0533N	173-59.9815W	291	-0.728	28.248	19061570
81	X080	2020/10/19	00:55	75-00.0427N	172-59.8574W	345	-0.851	27.771	19018692
82	X081	2020/10/19	06:32	74-47.7548W	171-06.0559W	264	-0.992	27.489	19018630
83	X082	2020/10/19	12:05	74-23.1225N	169-22.1402W	184	0.599	28.471	19018695
84	X083	2020/10/20	04:05	72-29.9865N	168-49.7155W	60	2.816	31.989	19018629
85	X084	2020/10/20	10:40	71-30.0312N	168-49.5562W	48	3.171	31.704	19018694
86	X085	2020/10/20	16:48	70-30.0230N	168-49.4990W	39	3.024	31.202	19018624
87	X086	2020/10/21	00:13	69-29.9970N	168-49.8354W	51	3.469	31.598	19018625
88	X087	2020/10/21	06:22	68-30.0250N	168-49.6974W	52	3.500	31.707	19018628
89	X088	2020/10/21	15:13	67-29.9964N	168-49.6093W	48	3.636	32.513	19018627
90	X089	2020/10/21	21:04	66-30.0041N	168-50.0369W	50	5.738	30.732	19018702
91	X090	2020/10/22	00:15	66-00.2831N	168-49.4823W	52	4.844	32.245	19018701
92	X091	2020/10/22	02:53	65-38.1218N	168-27.9668W	53	5.946	30.132	19018696

SST : Sea Surface Temperature [deg-C] measured by TSG (ThermoSalinoGraph).
SSS : Sea Surface Salinity [PSU] measured by TSG.

(6) Data archives

These data obtained in this cruise will be submitted to the Data Management Group (DMG) of JAMSTEC, and will be opened to the public via “Data Research System for Whole Cruise Information in JAMSTEC (DARWIN)” in JAMSTEC web site. <http://www.godac.jamstec.go.jp/darwin/e>

3.4. Shipboard ADCP

(1) Personnel

Shigeto Nishino (JAMSTEC) – Principal investigator
Ryo Oyama (Nippon Marine Enterprises, Ltd.; NME) – Operation leader
Souichiro Sueyoshi (NME)
Wataru Tokunaga (NME)
Masanori Murakami (NME)
Yoichi Inoue (MIRAI Crew)

(2) Objectives

To obtain continuous measurement data of the current profile along the ship's track.

(3) Parameters

Major parameters for the measurement, Direct Command, are shown in Table 3.4-1.

Table 3.4-1. Major parameters.

Bottom-Track Commands	
BP = 001	Pings per Ensemble (almost less than 1,300m depth)
Environmental Sensor Commands	
EA = 04500	Heading Alignment (1/100 deg)
ED = 00065	Transducer Depth (0 - 65535 dm)
EF = +001	Pitch/Roll Divisor/Multiplier (pos/neg) [1/99 - 99]
EH = 00000	Heading (1/100 deg)
ES = 35	Salinity (0-40 pp thousand)
EX = 00000	Coordinate Transform (Xform:Type; Tilts; 3Bm; Map)
EZ = 10200010	Sensor Source (C; D; H; P; R; S; T; U)
	C (1): Sound velocity calculates using ED, ES, ET (temp.)
	D (0): Manual ED
	H (2): External synchro
	P (0), R (0): Manual EP, ER (0 degree)
	S (0): Manual ES
	T (1): Internal transducer sensor
	U (0): Manual EU
EV = 0	Heading Bias(1/100 deg)
Timing Commands	
TE = 00:00:02.00	Time per Ensemble (hrs:min:sec.sec/100)
TP = 00:02.00	Time per Ping (min:sec.sec/100)
Water-Track Commands	
WA = 255	False Target Threshold (Max) (0-255 count)
WC = 120	Low Correlation Threshold (0-255)
WD = 111 100 000	Data Out (V; C; A; PG; St; Vsum; Vsum^2; #G; P0)
WE = 1000	Error Velocity Threshold (0-5000 mm/s)

WF = 0800	Blank After Transmit (cm)
WN = 100	Number of depth cells (1-128)
WP = 00001	Pings per Ensemble (0-16384)
WS = 800	Depth Cell Size (cm)
WV = 0390	Radial Ambiguity Velocity (cm/s)

(4) Instruments and methods

Upper ocean current measurements were made during this cruise, using the hull-mounted Acoustic Doppler Current Profiler (ADCP) system. For most of its operation, the instrument was configured for water-tracking mode. Bottom-tracking mode, interleaved bottom-ping with water-ping, was made to get the calibration data for evaluating transducer misalignment angle in the shallow water. The system consists of following components;

1. R/V MIRAI has installed the Ocean Surveyor for vessel-mount ADCP (frequency 76.8 kHz; Teledyne RD Instruments, USA). It has a phased-array transducer with single ceramic assembly and creates 4 acoustic beams electronically. We mounted the transducer head rotated to a ship-relative angle of 45 degrees azimuth from the keel.
2. For heading source, we use ship's gyro compass (Tokyo Keiki, Japan), continuously providing heading to the ADCP system directory. Additionally, we have Inertial Navigation Unit (Phins, Ixblue, France) which provide high-precision heading, attitude information, pitch and roll. They are stored in ".N2R" data files with a time stamp.
3. Differential GNSS system (StarPack-D, Fugro, Netherlands) providing precise ship's position.
4. We used VmDas software version 1.49 (TRDI) for data acquisition.
5. To synchronize time stamp of ping with Computer time, the clock of the logging computer is adjusted to GPS time server by using NTP (Network Time Protocol).
6. Fresh water is charged in the sea chest to prevent bio fouling at transducer face.
7. The sound speed at the transducer does affect the vertical bin mapping and vertical velocity measurement, and that is calculated from temperature, salinity (constant value; 35.0 PSU) and depth (6.5 m; transducer depth) by equation in Medwin (1975).

Data were configured for "8 m" layer intervals starting about 19m below sea surface. Data were recorded every ping as raw ensemble data (.ENR). Additionally, 15 seconds averaged data were recorded as short-term average (.STA). 300 seconds averaged data were long-term average (.LTA), respectively.

(5) Observation Period

19 Sep. 2020 - 01 Nov. 2020 (UTC)

(6) Data archives

These data obtained in this cruise will be submitted to the Data Management Group (DMG) of JAMSTEC, and will be opened to the public via "Data Research System for Whole Cruise Information in JAMSTEC (DARWIN)" in JAMSTEC web site.
<http://www.godac.jamstec.go.jp/darwin/e>

3.5. RINKO-Profiler

(1) Personnel

Shigeto Nishino (JAMSTEC) – Principal investigator

Keisuke Matsumoto (Marine Works Japan Ltd.; MWJ) – Operation leader

(2) Objective

RINKO-Profiler is a small and lightweight instrument to obtain vertical profiles of water temperature, salinity, turbidity, chlorophyll, and dissolved oxygen (DO). This instrument is able to acquire the data in a short time compared with CTD operations, and thus, suitable for the observations of sub-mesoscale phenomena such as ocean eddies, fronts, and filaments in marginal ice zones, where the observations are limited to the daytime in the case of R/V Mirai, an ice strengthened ship. This instrument may be also useful to acquire the data in a shallow shelf area (~50 m) instead of CTD operations, if the ship time is limited.

(3) Parameters

The ranges and accuracies of parameters measured by the RINKO-Profiler are as follows;

Parameter	Range	Accuracy
Conductivity	0.5 ~ 70 [mS/cm]	+/- 0.01 [mS/cm]
Temperature	-3 ~ 45 [deg-C]	+/- 0.01 [deg-C]
Depth	0 ~ 600 [m]	+/- 0.3 [%] FS
Turbidity	0 ~ 1000 [FTU]	+/- 0.3 [FTU] or +/- 2 [%]
Chlorophyll	0 ~ 400 [ppb]	+/- 1 [%] FS
DO	0 ~ 200 [%]	+/- 2 [%] FS

(4) Instruments and Methods

We observed vertical profiles of sea water temperature, salinity, turbidity, chlorophyll, and DO using a RINKO-Profiler, which was manufactured by JFE Advantech Co., Ltd. The profiler was lowered from the broadside with its lowering speed less than 0.5 m/sec (Photo 3.5-1). We obtained 13 profiles and the observation log is shown in Table 3.5-1.

Photo 3.5-1. RINKO-Profiler lowered from the broadside.

(5) Observation log

Table 3.5-1. RINKO-Profiler observation log.

No.	Data file name	Start time of observation	Latitude	Longitude
1	202009230259_ASTD152-ALC-R02_0659_025955	2020/09/23 03:00:00	32-59.52221N	146-59.76714E
2	202009232340_ASTD152-ALC-R02_0659_234031	2020/09/23 23:40:36	34-00.01152N	146-59.84047E
3	202010120148_ASTD152-ALC-R02_0659_014831	2020/10/12 01:48:36	74-59.01744N	159-18.97630W
4	202010120305_ASTD152-ALC-R02_0659_030526	2020/10/12 03:05:31	74-59.99886N	159-59.93229W
5	202010122055_ASTD152-ALC-R02_0659_205520	2020/10/12 20:55:25	75-11.26846N	157-05.59165W
6	202010122152_ASTD152-ALC-R02_0659_215227	2020/10/12 21:52:32	75-10.80992N	157-18.71016W
7	202010122259_ASTD152-ALC-R02_0659_225912	2020/10/12 22:59:17	75-10.79122N	157-36.70037W
8	202010130012_ASTD152-ALC-R02_0659_001203	2020/10/13 00:12:08	75-10.87960N	157-49.54071W
9	202010130134_ASTD152-ALC-R02_0659_013428	2020/10/13 01:34:33	75-10.95739N	158-19.90289W
10	202010130242_ASTD152-ALC-R02_0659_024223	2020/10/13 02:42:28	75-10.84359N	158-38.98558W
11	202010210914_ASTD152-ALC-R02_0659_091455	2020/10/21 09:15:00	67-59.98899N	168-49.98293W
12	202010212358_ASTD152-ALC-R02_0659_235841	2020/10/21 23:58:46	66-00.20467N	168-49.76980W
13	202010220237_ASTD152-ALC-R02_0659_023734	2020/10/22 02:37:39	65-38.11282N	168-28.02517W

(6) Data archives

These data obtained in this cruise will be submitted to the Data Management Group (DMG) of JAMSTEC, and will be opened to the public via “Data Research System for Whole Cruise Information in JAMSTEC (DARWIN)” in JAMSTEC web site. <http://www.godac.jamstec.go.jp/darwin/e>

3.6. TurboMap

(1) Personnel

Yusuke Kawaguchi (The University of Tokyo)
– Principal investigator, Not on board
Shigeto Nishino (JAMSTEC)
Eun Yae Son (The University of Tokyo)
Ryo Oyama (Nippon Marine Enterprises, Ltd.; NME) – Operation leader
Soichiro Sueyoshi (NME)
Wataru Tokunaga (NME)
Masanori Murakami (NME)
Yoichi Inoue (MIRAI Crew)

(2) Objectives

1. Investigate on turbulent mixing at the surface front in the marginal ice zone and under newly formed sea ice during MR20-05C.
2. Collect examples for verification of proper fine-scale parameterization in the Arctic Basin.

(3) Parameter

According to the manufacture's nominal specifications, the range, accuracy and sampling rates of acquisition parameters are shown in Table 3.6-1.

Table 3.6-1. Parameters and accuracy for each sensor.

Parameter	Sensor type	Measurable range	Accuracy	Sampling rate
$\partial u/\partial z$ (primary)	Shear probe	0~10 /s	5%	512Hz
$T+\partial T/\partial z$	FPO-7 thermistor	±0.01°C	±0.01°C	512Hz
T	Platinum wire thermometer	−5~45°C	±0.01°C	64 Hz
Conductivity	Inductive Cell	0~70 mS	±0.01 mS	64 Hz
Depth	Semiconductor strain gauge	0~1000 m	±0.2%	64Hz
x-acceleration	Solid-state fixed mass	±2 G	±1%	256 Hz
y-acceleration	Solid-state fixed mass	±2 G	±1%	256 Hz
z-acceleration	Solid-state fixed mass	±2 G	±1%	64Hz
Chlorophyll	Solid-state fixed mass	0~100 µg/Lm	0.5 µg/L or ±1%	256 Hz
Turbidity	Backscatter	0~100 ppm	1ppm or ±2%	256 Hz
$\partial u/\partial z$ (Secondary)	$\partial u/\partial z$ Shear	0~10 s^{-1}	5%	512 Hz

(4) Instruments and methodology

Turbulence Ocean Microstructure Acquisition Profiler (TurboMAP-L, manufactured by JFE Alec Co Ltd.) was used to measure turbulence-scale temperature and shear. TurboMap is a quasi-free-falling instrument that obtains turbulent mixing parameters ($\partial u/\partial z$ and $\partial T/\partial z$), bio-optical parameters (in vivo fluorescence and back scatter) and hydrographic parameters (conductivity, temperature, and pressure). The TurboMAP is a loosely tethered free-fall profiler that carries two airfoil shear probes, a fast-response thermistor (FP07), a light-emitting diode fluorescence/turbidity probe, and a CTD package (Wolk et al. 2002). The TurboMAP collects vertical profiles of microscale velocity shear, high- and low-resolution temperature, conductivity, and pressure, as the underwater device descends from the surface to maximum depth. The free-falling speed of the instrument is roughly at 0.5–0.6 m s−1. Operation of the ship's side thrusters is halted under operation of micro-data acquisition so that they may not create any artificial noise corruption or disturbance in the micro-scale data. The microscale data within 5 m depth are not recommended for the use in analysis as they may include potential noise due to the instrument's initial adjustment to free-falling.

(5) Station log

Each raw data has a format of MR2005C-No..BIN, where No. is written in Table 3.6-2, the data log. Data acquisition location is marked as yellow dots in Figure 3.6-1.

Table 3.6-2. Station lists.

No.	Date [YYYY/MM/DD]	Latitude [deg-min]	Longitude [deg-min]	Logging Time		Dep. [m]	Obs. Depth [m]
				Start	Stop		
01	2020/10/01	47-00.1696N	160-01.6932E	05:58	06:23	5230	818
02	2020/10/01	47-00.2515N	160-01.6114E	06:56	07:21	5230	852
03	2020/10/07	67-00.4876N	168-49.7005W	14:33	14:34	47	33
04	2020/10/07	67-00.4876N	168-49.7005W	14:35	14:36	47	32
05	2020/10/07	67-00.4876N	168-49.7005W	14:38	14:39	47	38
06	2020/10/08	69-00.5152N	168-49.6204W	06:54	06:55	51	50
07	2020/10/08	69-00.5152N	168-49.6204W	06:58	06:59	52	35
08	2020/10/08	69-00.5152N	168-49.6204W	06:59	07:00	53	36
09	2020/10/08	69-59.9632N	168-49.6626W	14:24	14:26	40	25
10	2020/10/08	69-59.9632N	168-49.6626W	14:27	14:29	40	28
11	2020/10/08	69-59.9632N	168-49.6626W	14:29	14:30	40	24
12	2020/10/10	74-31.6500N	161-54.8736W	19:21	19:41	1697	730
13	2020/10/10	74-31.9929N	161-53.9959W	19:56	20:15	1697	674
14	2020/10/12	74-59.2070N	159-18.3376W	00:53	01:11	1766	796
15	2020/10/12	74-59.1021N	159-18.6893W	01:28	01:37	1766	320
16	2020/10/12	74-59.9709N	159-59.6858W	03:16	03:37	1969	766
17	2020/10/12	75-11.0069N	159-59.9673W	07:18	07:40	1983	860

No.	Date [YYYY/MM/DD]	Latitude [deg-min]	Longitude [deg-min]	Logging Time		Dep. [m]	Obs. Depth [m]
				Start	Stop		
18	2020/10/12	75-11.0104N	159-59.6407W	07:53	08:00	1983	310
19	2020/10/12	75-11.0888N	157-06.3133W	20:32	20:43	1157	336
20	2020/10/12	75-10.8233N	157-18.7378W	22:01	22:12	1480	374
21							
22	2020/10/12	75-10.7513N	157-36.8042W	23:20	23:30	1540	440
23	2020/10/12	75-10.8707N	157-49.5427W	00:21	00:31	1441	450
24	2020/10/13	75-10.9431N	158-20.0285W	01:41	01:53	1151	186
25	2020/10/13	75-10.9431N	158-20.0285W	02:01	02:07	1151	370
26	2020/10/13	75-10.8169N	158-39.2490W	02:54	03:04	1054	318
27	2020/10/15	71-47.6874N	152-59.6609W	17:24	17:36	454	380
28	2020/10/15	71-58.4264N	153-59.6025W	22:22	22:41	736	622
29	2020/10/17	74-59.9850N	165-00.1741W	19:14	19:26	545	347
30	2020/10/17	75-00.3203N	164-59.3723W	19:36	19:47	546	376
31	2020/10/18	75-00.2964N	167-14.5324W	03:23	03:29	251	190
32	2020/10/18	75-00.4021N	167-14.4183W	03:33	03:41	251	218
33	2020/10/18	75-00.0082N	169-38.0693W	09:30	09:37	242	221
34	2020/10/18	75-00.0871N	169-37.9634W	09:42	09:48	242	220
35	2020/10/18	75-00.0650N	174-59.7933W	20:16	20:23	265	246
36	2020/10/18	75-00.1252N	174-59.7774W	20:27	20:34	265	215
37	2020/10/19	75-00.1852N	171-59.4618W	03:31	03:41	384	400
38	2020/10/19	75-00.3029N	171-59.1772W	03:49	03:54	384	230
39	2020/10/19	74-35.9957N	170-12.0274W	09:19	09:25	211	183
40	2020/10/19	74-36.0392N	170-12.0187W	09:28	09:29	211	169
41	2020/10/21	68-00.0768N	168-49.8928W	10:20	10:23	57	60
42	2020/10/21	68-00.0768N	168-49.8928W	10:24	10:26	57	60
43	2020/10/21	68-00.0768N	168-49.8928W	10:28	10:30	57	60

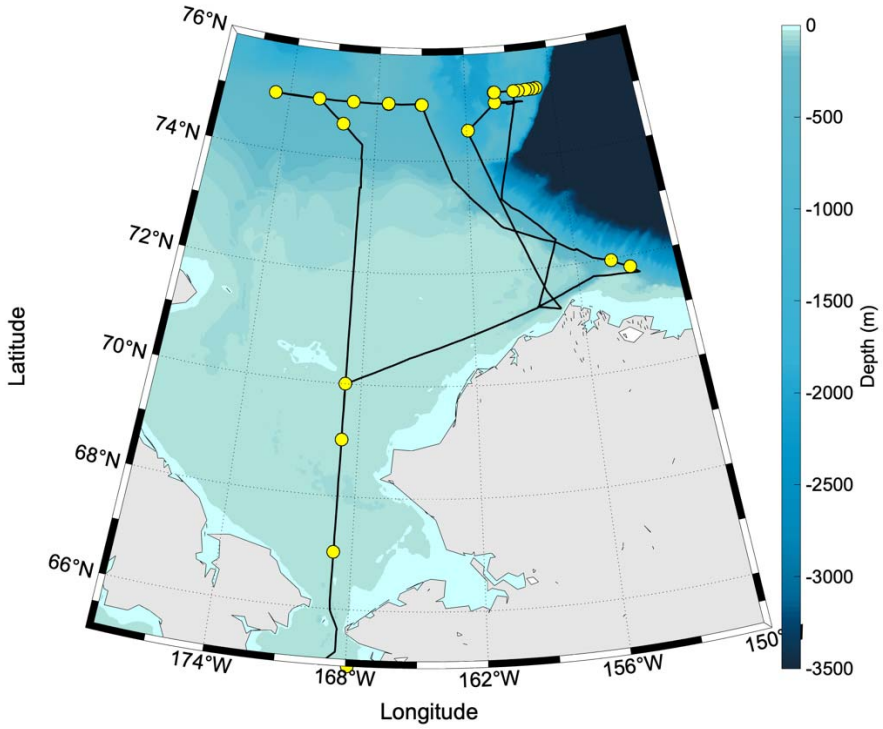

Figure 3.6-1. Observation location of TurboMap in MR20-05C cruise. Black solid line shows cruise track and yellow dots are operation site.

(6) Remarks

TurboMAP is designed to be used stand-alone without additional CTD observation. However, it is recommended to check incoming CTD data's quality by comparing SBE9plus (Sea Bird Electronics). TurboMAP cast was accomplished right after or before the CTD cast. Since the observation was conducted under cold air temperature (< 0°C), slow temperature sensor showed delayed response to the real-upper ocean temperature. It is recommended to use data acquired from second or third cast for the CTD, shear, and FP07 data.

TurboMAP consists 2 shear probes for checking shear data validity. It is able to be utilized with only one shear probe, however, a pair of shear sensor is recommended. Figure 3.6-2 is turbulence dissipation rate that obtained by each shear sensors to see the validation among sensors. During MR20-05C, we utilized one set of shear probe (shear1: S/N 1233, shear2: S/N 505). At the test cast station (No.1 and No.2), FP07 S/N 144 was broken.

Also, Table 3.6-3 shows notification profiles that should be considered when you use data.

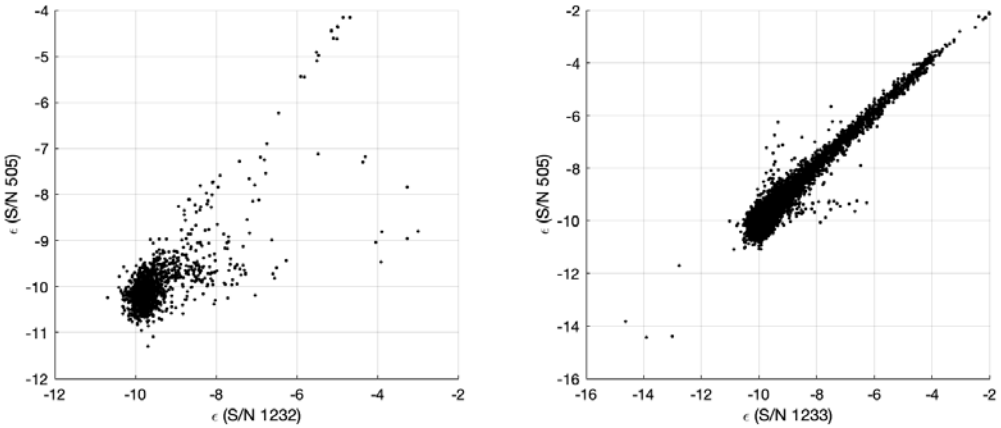

Figure 3.6-2. Correlation between the two shear sensors that used for MR20-05C.

Table 3.6-3. Denote for data utilization.

Cast No.	Denote
12	Sonar (MBES) is on
24	Shear probe 1 had noise
33	Shear probe 1 had noise at 100-150 m
35	Cable felt tension near 26 m
39	FP07 delayed in mixed layer
40	Shear1 had noise at 140 m
41	FP07 delayed in mixed layer

(7) Data archive

These data obtained in this cruise will be submitted to the Data Management Group (DMG) of JAMSTEC, and will be opened to the public via "Data Research System for Whole Cruise Information in JAMSTEC (DARWIN)" in JAMSTEC web site.

<http://www.godac.jamstec.go.jp/darwin/e>

3.7. Drifting buoys

3.7.1. Ice buoy

(1) Personnel

Yusuke Kawaguchi (The University of Tokyo)
– Principal investigator, Not on board
Eun Yae Son (The University of Tokyo)

(2) Objectives

To examine the upper ocean bulk-heat variation in the western Arctic during sea ice freezing season.

(3) Parameter

IceBTC60/40
GPS positions and air pressure of drifting buoy
Water temperature and hydrostatic pressure at certain depth

(4) Instruments and methodology

IceBTC60/40 is designed for utilization in the sea ice covered area which has a 60 m-long thermistor chain with the pressure sensors. It measures upper ocean temperature with the accuracy of +/-0.1°C (resolution of 0.04°C) and air pressure with the accuracy of +/-1 hPa (resolution of 0.1 hPa). IceBTC40/60 has thermistors at depths of 0, 2.5, 5, 7.5, 10, 12.5, 15, 17.5, 20, 25, 30, 35, 40, 45, 50, 55, and 60 m and especially, it consists hydrostatic pressure sensor at depths of 20, 40, and 60 m. We deployed IceBTC40/60 in the marginal ice zone in the Canada Basin, Arctic where covered with the grease ice.
When buoy deploy, the XCTD (X41) and TurboMap observations were accompanied.

Table 3.7.1-1. Deployment information.

Type	IMEI	Deploy time (UTC)	Deploy location [deg-min]	Data interval	denotes
IceBTC40/60	300234061160500	2020/10/12 21:15	75-11.42N, 157-06.41W	hourly	Deployed in the pancake ice zone

(5) Preliminary result

After the deployment, buoy collected near-surface temperature data. Until October 19, buoy kept drifting north-westward showing the inertial motion (Figure 3.7.1-1). Even during the strong wind event during October 17 to 18, inertial motion remained with tilted thermistor chain by the fast drift speed (Figure 3.7.1-2). During the period, near-surface temperature maximum located at depths of 20 m within the mixed layer where has temperature near -1.4°C. Even though the water surface is warmer than local freezing temperature, sea ice was fully covered with the sea surface.

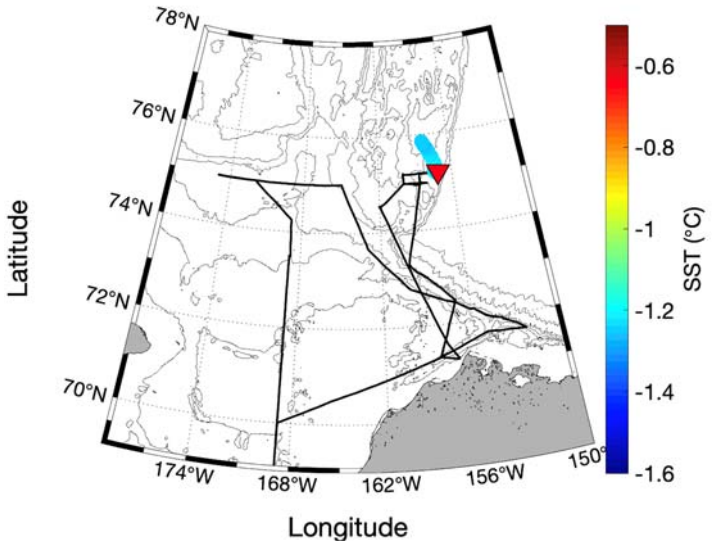

Figure 3.7.1-1. Buoy deploy location and drift with the sea surface temperature. Red reversed triangle shows deployed location and black solid line is MR20-05C ship track.

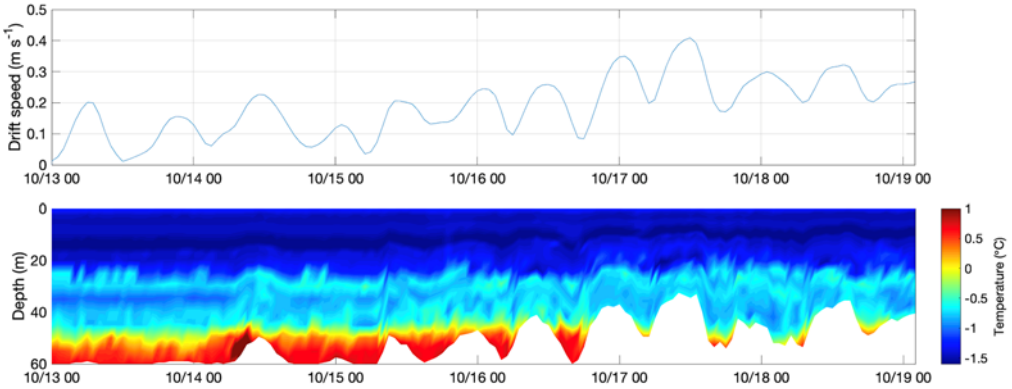

Figure 3.7.1-2. (Upper panel) Timeseries of sea ice drift speed that obtained from hourly GPS data. (Lower panel) Near-surface temperature along the time.

(6) Data archive

These data obtained in this cruise will be submitted to the Data Management Group (DMG) of JAMSTEC, and will be opened to the public via "Data Research System for Whole Cruise Information in JAMSTEC (DARWIN)" in JAMSTEC web site.

<http://www.godac.jamstec.go.jp/darwin/e>

3.7.2 Wave buoy

(1) Personnel

Takuji Waseda (The University of Tokyo) – Principal investigator, Not on board
Tsubasa Kodaira (The University of Tokyo) – Not on board
Takehiko Nose (The University of Tokyo) – Not on board
Yasushi Fujiwara (The University of Tokyo) – Not on board
Keita Nishizawa (The University of Tokyo)
Ryosuke Uchiyama (The University of Tokyo) – Not on board

(2) Objectives

According to recent studies, surface ocean waves are playing an important role in the mechanism of the freeze-up and break-up of sea ice. Our observation in the western Arctic was carried out to collect the surface ocean waves data in various ways.
This section describes the observation by Drifting-type wave buoy.

(3) Parameters

Significant wave height (Hm0), peak period (Tp), peak direction, peak directional spread, mean period (Tm01), mean direction, mean directional spread, power spectral density (PSD), sea surface temperature (SST), time and GPS coordinates.

(4) Instruments and methods

The type of drifting wave buoy used was a Spotter device manufactured by Sofar Ocean Technologies. The device is fully solar powered and has a two-way communication function via Iridium satellite communication.
The total number of wave buoys we brought is five. (SPOT-0752, SPOT-0753, SPOT-0754, SPOT-0758, and SPOT-0759) Two of the five buoys (SPOT-0752 and SPOT-0753) were deployed in Marginal Ice Zone (MIZ) covered with pancake ice. Other two buoys (SPOT-0754 and SPOT-0758) were deployed in an open-ocean area which was close to MIZ. The fifth buoy was deployed in another open-ocean area under relatively rough wave condition.

(5) Station list or Observation log

Wave buoys were deployed in numerical order. (SPOT-0752, 0753, 0754, 0758, 0759) Four wave buoys (SPOT-0752, 0753, 0754, and 0758) were deployed during the ice edge observation on 12 and 13 October 2020. The fifth buoy (SPOT-0759) was deployed on 17 October 2020 in open water. Table 3.7.2-1 shows the deployed time and position of each

buoy. As of 28 October 2020 (UTC), all five buoys stopped transmitting the data since the limited solar radiation at high latitudes in October did not allow the batteries to be charged sufficiently. Table 3.7.2-2 shows the time and location of final transmission from buoys. The locations of deployment and loss of transmission for all buoys are also plotted in Figure 3.7.2-1.

Table 3.7.2-1. The time and position five wave buoys were deployed in.

Name of buoy	Time (UTC)	Latitude N [deg]	Longitude W [deg]
SPOT-0752	2020/10/12 21:15	75.1902	157.1070
SPOT-0753	2020/10/12 23:45	75.1758	157.6332
SPOT-0754	2020/10/13 03:21	75.1772	158.6670
SPOT-0758	2020/10/13 05:50	74.9982	158.6717
SPOT-0759	2020/10/17 19:07	74.9983	165.0067

Table 3.7.2-2. Final transmitted time and position from five wave buoys.

Name of buoy	Time (UTC)	Latitude N [deg]	Longitude W [deg]
SPOT-0752	2020/10/25 05:58	76.2726	155.5664
SPOT-0753	2020/10/23 22:58	76.6374	157.5971
SPOT-0754	2020/10/19 16:58	76.2561	159.1742
SPOT-0758	2020/10/22 15:14	76.3712	159.5931
SPOT-0759	2020/10/26 16:27	75.9394	162.5987

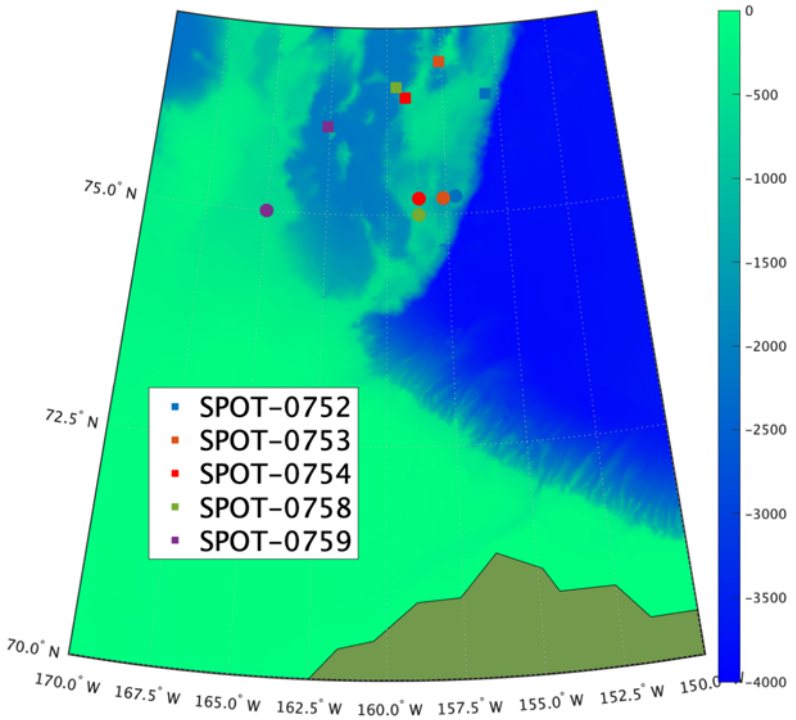

Figure 3.7.2-1. The map showing locations of buoys. Circles indicate deployment locations of the buoys. Squares indicate locations that buoy transmitted last. Colored shading represents bathymetry.

(6) Preliminary results

Figure 3.7.2-2 shows the wave statistics recorded by the drifting wave buoys. SPOT-0759 measured a maximum significant wave height of 3.70 m with peak period of 9.31 s at 21:27 UTC on 17 October 2020. Five buoys measured different wave heights when SPOT-0759 showed the maximum height. During this event, SPOT-0759, which was in the open ocean, measured the highest wave height of all. The second, third, fourth, and fifth highest wave heights of all were recorder by SPOT-0758, SPOT-0753, SPOT-0754, and SPOT-0752 respectively and those four buoys were expected to be in the ice-covered area. On the other hand, the mean period of the waves became smaller in reverse order of wave heights. The results indicate that the difference of the sea ice the buoys were surrounded by and geographical locations had the influence upon the feature of surface ocean waves attenuation.

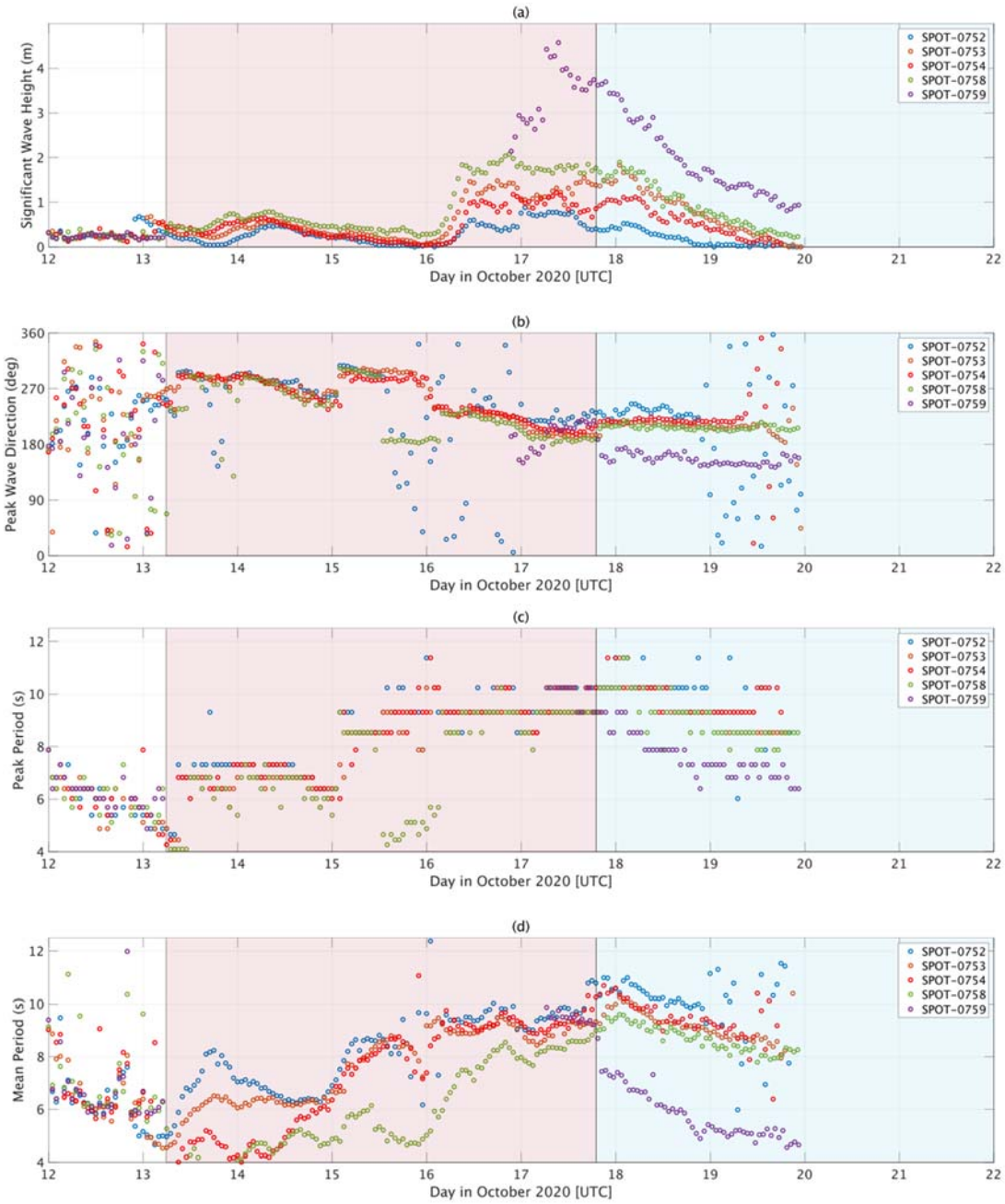

Figure 3.7.2-2. Wave statistics recorded by five wave buoys. Duration in red represents that four buoys (SPOT-0752, 0753, 0754, and 0758) transmitted surface ocean waves data. Duration in blue represents that all buoys transmitted surface ocean waves data. (a) Significant wave heights (b) Peak Wave direction (c) Peak Period (d) Mean Period.

(7) Data archives

These data obtained in this cruise will be submitted to the Data Management Group

(DMG) of JAMSTEC, and will be opened to the public via “Data Research System for Whole Cruise Information in JAMSTEC (DARWIN)” in JAMSTEC web site.
<http://www.godac.jamstec.go.jp/darwin/e>

3.8. Stereo camera system

(1) Personnel

Takuji Waseda (The University of Tokyo) – Principal investigator, Not on board
Tsubasa Kodaira (The University of Tokyo) – Not on board
Takehiko Nose (The University of Tokyo) – Not on board
Yasushi Fujiwara (The University of Tokyo) – Not on board
Keita Nishizawa (The University of Tokyo)
Ryosuke Uchiyama (The University of Tokyo) – Not on board

(2) Objectives

According to recent studies, surface ocean waves are playing an important role in the mechanism of the freeze-up and break-up of sea ice. Our observation in the western Arctic was carried out to collect the surface ocean waves data in various ways.
This section describes the observation by Stereo Camera System.

(3) Parameters

Monochrome images (4064 × 4064 pixels), acceleration (3-axis), gyro (3-axis) and geomagnetism (3-axis).

(4) Instruments and methods

The two cameras, mounted in separate housing on the compass deck of the R/V Mirai, were synchronized to allow stereo reconstruction of the captured images of surface ocean waves. (Figure 3.8-1) Both cameras were connected via USB cables to a laptop computer placed in a watertight black plastic box (Figure 3.8-1). A 5-bay HDD storage device whose capacity was 50TB in total were also installed in the box. The system was directly connected to the environmental research lab with ethernet cables, which enable us to access the system from inside the vessel. A 9-axis inertial moment unit (ZMP-IMUZ) was also placed in the box to measure the motion of the cameras.

Figure 3.8-1. Stereo Camera System on the compass deck (Left: Left camera, Center: housing box, Right: Right camera).

(5) Observation log

The stereo camera system was used hourly and sometimes half-hourly when the track of the R/V Mirai cruise approached the area covered with sea ice.

(6) Preliminary results

Figure 3.8-2. Sample images obtained by the stereo camera system.

(7) Data archives

These data obtained in this cruise will be submitted to the Data Management Group (DMG) of JAMSTEC, and will be opened to the public via "Data Research System for Whole Cruise Information in JAMSTEC (DARWIN)" in JAMSTEC web site.
<http://www.godac.jamstec.go.jp/darwin/e>

3.9. Radar

3.9.1. Sea ice radar

(1) Personnel

Shigeto Nishino (JAMSTEC) – Principal investigator
Ryo Oyama (Nippon Marine Enterprises, Ltd.; NME) – Operation leader
Souichiro Sueyoshi (NME)
Wataru Tokunaga (NME)
Masanori Murakami (NME)
Yoichi Inoue (MIRAI Crew)

(2) Objectives

In the sea ice areas, marine radar provides an important tool for the detection of sea ice and icebergs. It is importance to monitor the sea ice daily and produce ice forecasts to assist ship traffic and other marine operations. In order to select route optimally, ice condition prediction technology is necessary, and image information of ice-sea radar is used for constructing a route selection algorithm.

(3) Parameters

Capture format: JPEG
Capture interval: 60 seconds
Resolution: 1,024×768 pixel
Color tone: 256 gradation

(4) Instruments and methods

R/V MIRAI is equipped with an Ice Navigation Radar, "sigma S6 Ice Navigator (Rutter Inc.)". The ice navigation radar, the analog signal from the x-band radar is converted by a modular radar interface and displayed as a digital video image (Figure 3.9.1-1). The sea ice radar is equipped with a screen capture function and saves at arbitrary time intervals.

(5) Observation Period

08 Oct. 2020 - 21 Oct. 2020

(6) Data archives

These data obtained in this cruise will be submitted to the Data Management Group (DMG) of JAMSTEC, and will be opened to the public via "Data Research System for Whole Cruise Information in JAMSTEC (DARWIN)" in JAMSTEC web site.
<http://www.godac.jamstec.go.jp/darwin/e>

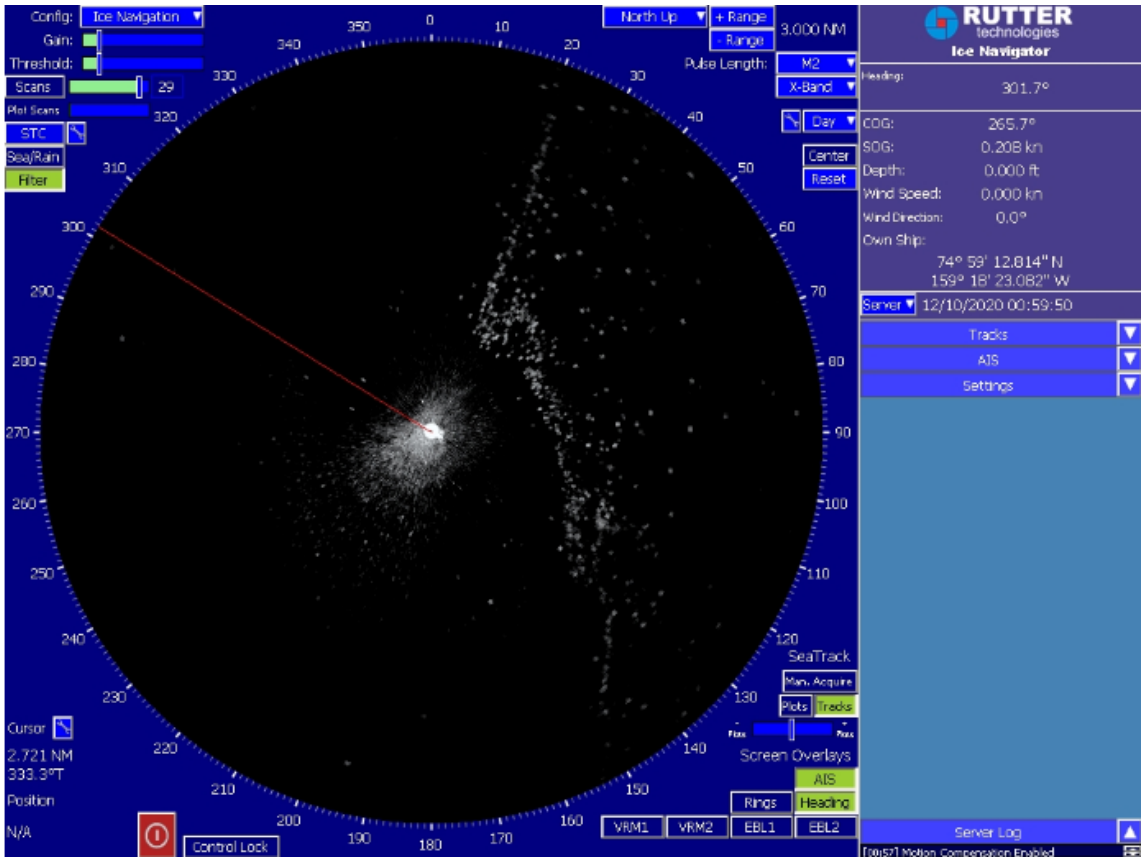

Figure 3.9.1-1. Image of sea ice from Sea ice radar.

3.9.2 Wave radar

(1) Personnel

Takuji Waseda (The University of Tokyo) – Principal investigator, Not on board
Tsubasa Kodaira (The University of Tokyo) – Not on board
Takehiko Nose (The University of Tokyo) – Not on board
Yasushi Fujiwara (The University of Tokyo) – Not on board
Keita Nishizawa (The University of Tokyo)
Ryosuke Uchiyama (The University of Tokyo) – Not on board

(2) Objectives

According to recent studies, surface ocean waves are playing an important role in the mechanism of the freeze-up and break-up of sea ice. Our observation in the western Arctic was carried out to collect the surface ocean waves data in various ways.
This section describes the observation by Wave Radar.

(3) Parameters

OBW file (bulk parameters, e.g. significant wave height), csv file (2-D wave spectrum), and raw Radar image

(4) Instruments and methods

The analysis unit was installed on the bridge and provided the signal from shipborne nautical X-band RADAR to calculate the wave bulk parameters. Range and pulse length of the RADAR should be set to 1.5 NM and Short Pulse (SP) respectively in order to conduct the analysis. The analyzed domain was limited by the range from 300 m to 2400 m and the relative azimuthal angle from -100 deg to 100 deg as heading of the vessel is 0 deg.

Calibration experiments were needed to adjust the significant wave height analyzed by Wave Radar unit to observed wave height in another way. In this cruise, wave buoy, which is described in 3.7.2, was used for the calibration. Wave buoy was deployed and collected twice for the purpose of calibration. Time for the calibration was shown in Table 3.9.2-1.

Table 3.9.2-1. Time for calibration.

Order	Start (UTC)	End (UTC)
1st calibration	2020/9/20 22:07	2020/9/20 03:00
2nd calibration	2020/10/02 21:10	2020/10/03 00:15

(5) Observation log

This unit aimed to conduct a consecutive observation of sea surface wave during the whole cruise. In fact, the period of the observation was restricted because the navigation purpose had the priority in operating the shipboard X-band Radar. Table 3.9.2-2 show the duration that X-band RADAR was used for the wave analysis purpose.

Table 3.9.2-2. Wave Radar analysis unit operation time.

Order	Start time (UTC)	End time (UTC)
1st	2020/9/19 22:35	2020/9/25 17:34
2nd	2020/9/26 14:25	2020/9/28 13:30
3rd	2020/9/28 22:10	2020/9/30 08:05
4th	2020/10/1 14:15	2020/10/7 03:17
5th	2020/10/7 13:54	2020/10/7 15:14
6th	2020/10/8 22:18	2020/10/8 23:46
7th	2020/10/9 23:35	2020/10/10 02:45
8th	2020/10/10 16:25	2020/10/11 02:58
9th	2020/10/12 23:43	2020/10/13 00:13
10th	2020/10/15 00:11	2020/10/15 07:30
11th	2020/10/15 19:05	2020/10/16 00:00
12th	2020/10/17 06:45	2020/10/18 00:00
13th	2020/10/18 19:00	2020/10/28 24:00

(6) Preliminary results

Figure 3.9.2-1 shows time series of significant wave height analyzed by Wave Radar unit on 23 October, 2020.

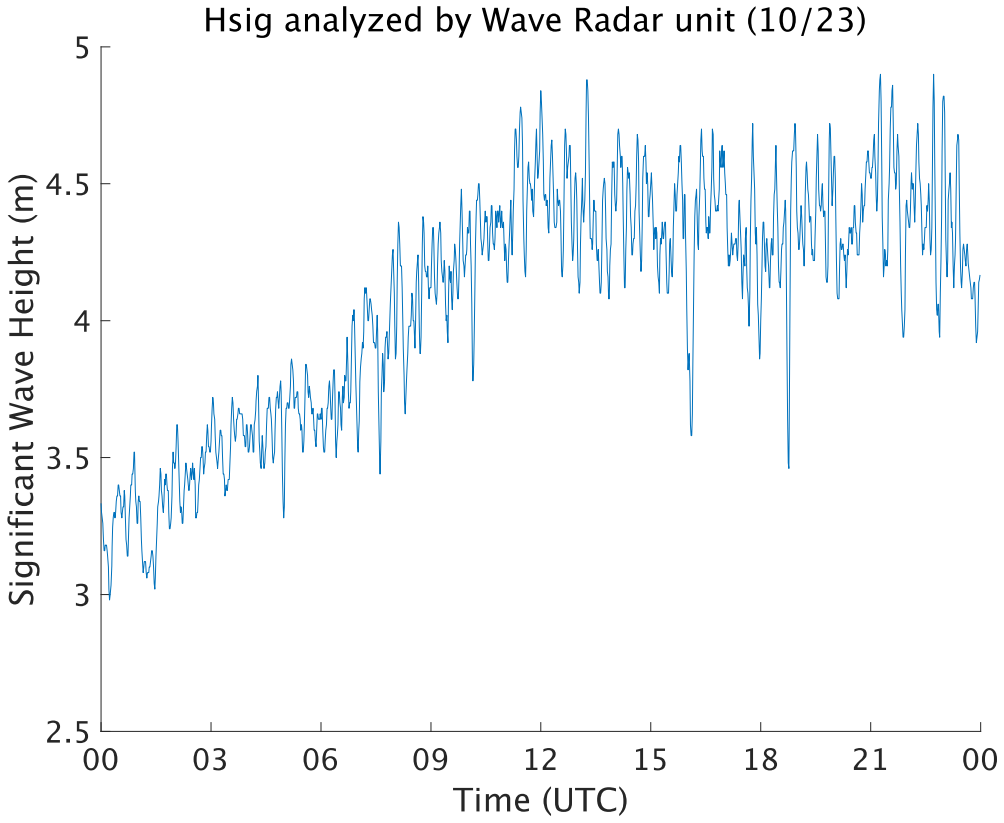

Figure 3.9.2-1. Time series of significant wave height analyzed by Wave Radar unit. Data was obtained on 23 October 2020.

(7) Data archives

These data obtained in this cruise will be submitted to the Data Management Group (DMG) of JAMSTEC, and will be opened to the public via "Data Research System for Whole Cruise Information in JAMSTEC (DARWIN)" in JAMSTEC web site.
<http://www.godac.jamstec.go.jp/darwin/e>

3.10. Drone

(1) Personnel

Takuji Waseda (The University of Tokyo) – Principal investigator, Not on board
Tsubasa Kodaira (The University of Tokyo) – Not on board
Takehiko Nose (The University of Tokyo) – Not on board
Yasushi Fujiwara (The University of Tokyo) – Not on board
Keita Nishizawa (The University of Tokyo)
Ryosuke Uchiyama (The University of Tokyo) – Not on board

(2) Objectives

According to recent studies, surface ocean waves are playing an important role in the mechanism of the freeze-up and break-up of sea ice. Our observation in the western Arctic was carried out to collect the surface ocean waves data in various ways. To verify the feasibility, test flights were carried out in the Pacific.

(3) Parameters

Video

(4) Instruments and methods

The Drone used for the observation is Mavic2 Pro manufactured by DJI. It flighted over the ocean to capture the sea surface displacement from a bird's-eye view.

(5) Station list

The Drone flight was carried out twice at the different observation points. Table 3.10-1 shows the locations and times of the flights.

Table 3.10-1. List of drone flight.

Station	Time (UTC)	Latitude	Longitude
Station 001	2020/09/21 05:00	$32°00'N$	$147°00'E$
Station 002	2020/09/23 07:00	$33°00'N$	$147°00'E$

(6) Preliminary results

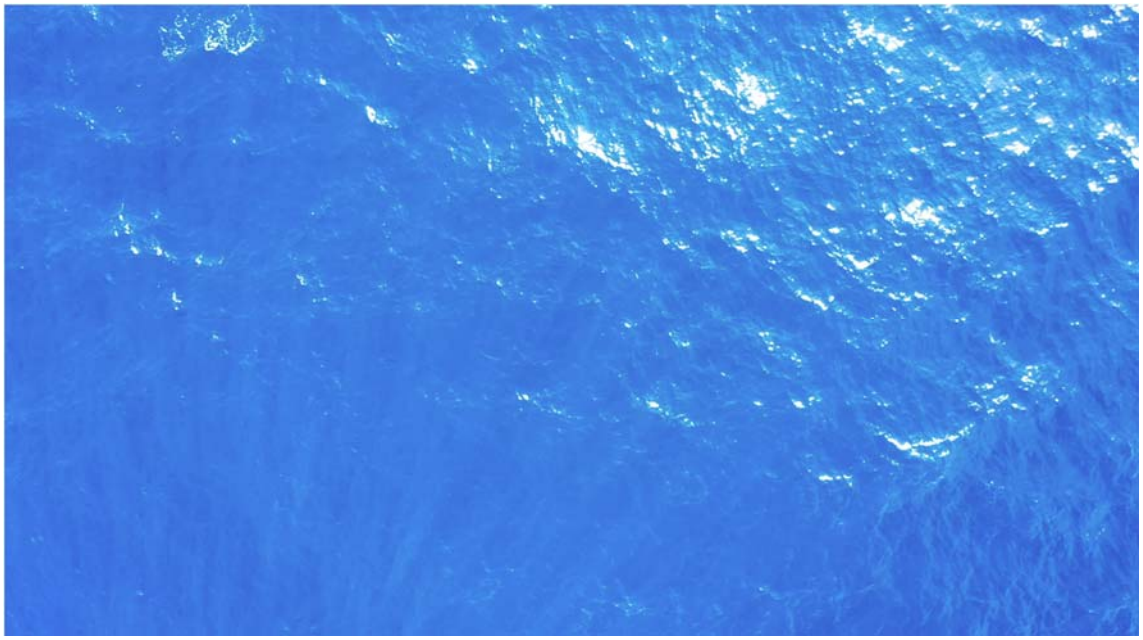

Figure 3.10-1. Sample image obtained by Drone.

(7) Data archives

These data obtained in this cruise will be submitted to the Data Management Group (DMG) of JAMSTEC, and will be opened to the public via "Data Research System for Whole Cruise Information in JAMSTEC (DARWIN)" in JAMSTEC web site.
<http://www.godac.jamstec.go.jp/darwin/e>

3.11. Moorings

3.11.1. B4

(1) Personnel

Daisuke Hirano (Hokkaido University) – Principal investigator, Not on board
Shigeto Nishino (JAMSTEC)
Amane Fujiwara (JAMSTEC)
Motoyo Itoh (JAMSTEC) – Not on board
Takashi Kikuchi (JAMSTEC) – Not on board
Masato Ito (JAMSTEC) – Not on board
Yasushi Fukamachi (Hokkaido University) – Not on board
Kay. I. Ohshima (Hokkaido University) – Not on board
Keisuke Matsumoto (Marine Works Japan Ltd.; MWJ) – Operation leader

(2) Objectives

In August 2019, we tried to recover B4 mooring deployed in August 2017 in the northeastern Chukchi Sea (Barrow Coastal Polynya area). Because the acoustic release in the water responded to enable command but not release command, B4 mooring was not recovered acoustically in 2019.

During the MR20-05c cruise in 2020, we tried again to recover B4 mooring from R/V *Mirai* with the dragging method. On 9 October, we successfully confirmed the exact position of B4 mooring with acoustic measurements, but we abandoned the dragging operation due to bad weather. On 14 October, nice weather and ocean conditions allowed us to try recovering B4 mooring by dragging. The dragging operations were done two times in the morning and afternoon, but unfortunately, we could not recover the B4 mooring. After the second operation, we acoustically confirmed that B4 mooring has stayed in the initial deployed position, then R/V *Mirai* left there.

The purpose of the B4 mooring measurement is to obtain long-term time-series data for ocean conditions such as temperature, salinity, and currents for understanding the variability in the ocean and sea ice in the Pacific Arctic under climate change. Components of the mooring are depicted in Figures 3.11.1-1.

(3) Parameters

- Pressure, temperature, and conductivity
- Ocean velocity

(4) Instruments and methods

- CT, T, and P sensors
  SBE37-SM (Sea-Bird Electronics Inc.)
  SBE56 temperature logger (Sea-Bird Electronics Inc.)
  DEFI2-D50HG (JFE Advantech)

- Current meter
  Aquadopp Current Meter (NORTEK AS)

- Acoustic transponder
  Universal Deck Unit UDB-9400 (Teledyne Benthos)
  Universal Deck Unit DS-7000 (Teledyne Benthos)

- Acoustic Release
  866A (Teledyne Benthos)

(5) Station list

Table 3.11.1-1. Information for B4 mooring.

Mooring ID	Latitude [N]	Longitude [W]	Bottom depth [m]
B4	71-19.28	158-24.20	114.9

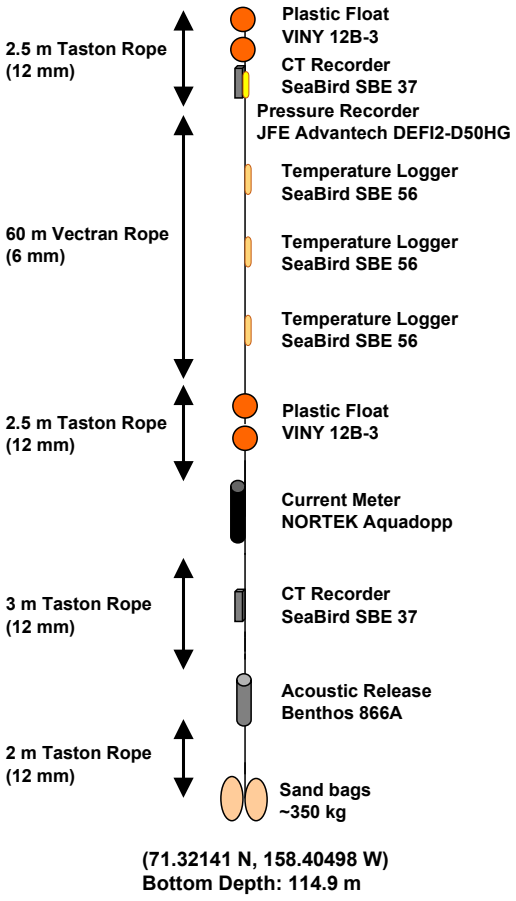

Figure 3.11.1-1. Diagram of B4 mooring.

3.11.2. Sediment trap

(1) Personnel

Naomi Harada (JAMSTEC) – Principal investigator, Not on board
Jonaotaro Onodera (JAMSTEC) – Not on board
Atsushi Suzuki (National Institute of Advanced Industrial Science and Technology; AIST) – Not on board
Motoyo Itoh (JAMSTEC) – Not on board
Katsunori Kimoto (JAMSTEC) – Not on board
Eiji Watanabe (JAMSTEC) – Not on board
Takuhei Shiozaki (JAMSTEC/The University of Tokyo)
Koki Tokuhiro (Hokkaido University)
Keisuke Matsumoto (Marine Works Japan Ltd., MWJ) – Operation leader (for mooring operation)
Ryo Ohyama (Nippon Marine Enterprises, Ltd.; NME) – Operation leader (for SSBL acoustic survey)

(2) Objectives

For the below objectives, one sediment trap mooring have been deployed at Station NAP in the North Abyssal Plain.

- To monitor hydrographic condition regarding to ocean acidification and warming.
- To understand lateral transportation of shelf materials to basin with physical oceanographic condition.
- To investigate biodiversity in the study region.

(3) Parameters

Settling particles, temperature, salinity, current, pH, dissolved oxygen, turbidity, chlorophyll-a, PAR, ice profiling (sea ice thickness).

(4) Instruments and methods

<Instruments>

All instruments on deployed mooring are listed in Table 3.11.2-1.

<Methods>

All equipment has passed export at the Shimizu Custom. The all required procedure at the custom was performed by the Suzuyo, Co. Ltd. Acoustic communication of all releasers to be deployed in this cruise were examined between this ship and 1000 m deep in the northeastern Aleutian Basin. The battery of acoustic releasers is for continuous two-years deployment. For the deployment sensors, log file or photograph of configuration process were taken. Sample cup of sediment bottles were filled-with filtered sea water taken at 1000 m depth in the southwestern Canada Basin in MR16-

06 cruise. The water contains formalin (4v/v%) and sodium hydroborate as pH adjustment (pH ~8.2).

(5) Table of sediment trap mooring operation.

Table 3.11.2-1. Deployment of NAP20t on October 11th, 2020.

NAP20t deployment (74°31.36' N 161°55.59' W, 1,680 m water depth)			
Frame#	**Type**	**Model**	**Serial Number**
1	Float Ice profiler CT DO Multi-Exciter PAR Iridium Beacon LED Flasher	MN-IP123 IPS-5 A7CT2-USB ARO-USB MFL50W-USB DEF12-L iBCN-7	ASL-SFFC-001 51032 613 136 44 0BKB022 H01-001 J01-055
-	Transponder Floats	XT6001-17" Benthos 17" x4	75683 -
2	CT	SBE37SM	13678
3	CT	SBE37SM	13677
4	CT DO pH	SBE37SM ARO-USB SPS-14	15456 131 40306166001
5	ADCP	WHS-300	24534
-	Floats	Benthos 17" x5	-
-	Trap CT	SMD26S-6000 A7CT-USB	98063 691
6	ADCP	Aquadopp DW	AQD15193
-	Floats	Benthos 17" x5	-
-	Trap	SMD26S-6000	98057
-	Floats	Benthos 17" x5	-
-	Releaser Releaser	Nichiyu LGC Nichiyu LGC	0078 0079

(towing with 0.6~1.6 knot to planned mooring position)

-	Anchor	Rail 1,000kg in air	-
Releaser ranging at 1,000m away from anchor position (distance = 2,016 m, 2,018 m) (distance = 2,045 m, 2,048 m)			 0078 0079
SSBL transponder survey position water depth depth of transponder		 74°31.37' N 161°55.88' W 1,685 m -	

All serial numbers of deploying equipment and connection of all parts were checked by Dr. Nishino, S. as a third-party inspector, just before the deployment and/or during the deployment operation. Mooring deployment starts from the throw-in of top buoy into water. The ships go forward with slow speed (~1.0knot). Before the dropping sinker, the slow towing of mooring continued until the ship reaches at the planned target position of the mooring. Deepening and vanish of top buoy from sea surface was confirmed, and then acoustic ranging and determination of mooring position was conducted using SSBL and transducer for Nichiyu releaser. The position, water depth, top depth, and recovery plan (season and ship) of the newly deployed mooring were noticed by Dr. Itoh, M. to AOOS and related persons in the world during the cruise.

(6) Data archives

These data obtained in this cruise will be submitted to the Data Management Group (DMG) of JAMSTEC, and will be opened to the public via "Data Research System for Whole Cruise Information in JAMSTEC (DARWIN)" in JAMSTEC web site.
<http://www.godac.jamstec.go.jp/darwin/e>

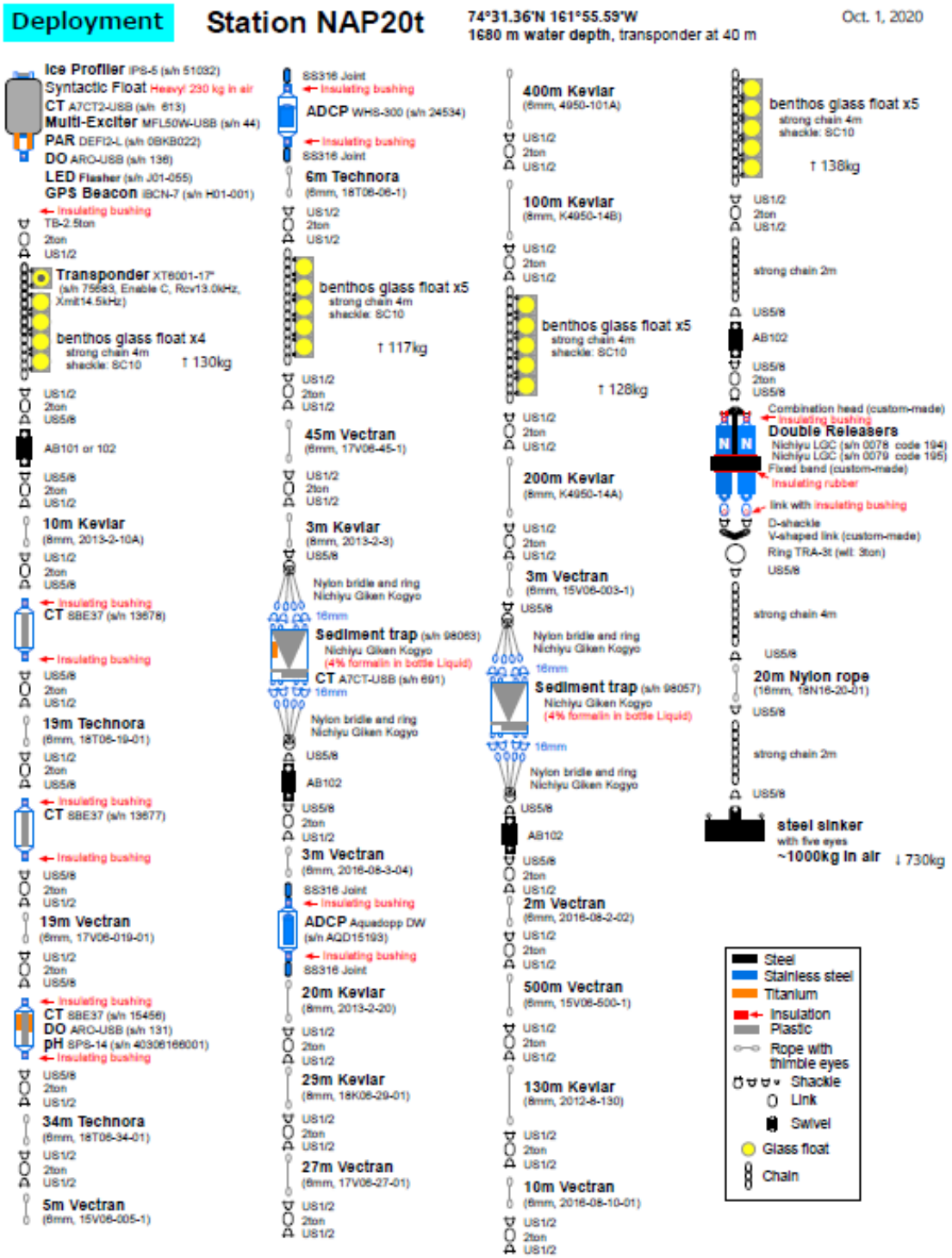

Figure 3.11.2-1. Design of deployed sediment trap mooing NAP20t.

3.12. Salinity measurements

(1) Personnel

Shigeto Nishino (JAMSTEC) – Principal investigator

Yuya Hitomi (Marine Works Japan Ltd.; MWJ) – Operation leader

(2) Objective

To provide calibrations for the measurements of salinity collected from CTD casts, bucket sampling, and underway surface water monitoring system.

(3) Parameters

Salinity

(4) Instruments and methods

a. Sampling

Seawater samples were collected with 12 liter water sampling bottles and underway surface water monitoring system. The salinity sample bottle of the 250ml brown glass bottle with screw cap was used for collecting the sample water. Each bottle was rinsed 3 times with the sample water, and was filled with sample water to the bottle shoulder. The salinity sample bottles for underway surface water monitoring system were sealed with a plastic septum and screw cap because we took into consideration the possibility of storage for about one month. The caps was rinsed 3 times with the sample seawater before its use. Each bottle was stored for more than 24 hours in the laboratory before the salinity measurement.

The kind and number of samples taken are shown as follows ;

Table 3.12-1. Kind and number of samples.

Kind of Samples	Number of Samples
Samples for CTD	436
Samples for Bucket	23
Samples for underway surface water monitoring system	37
Total	496

b. Instruments and Method

The salinity analysis was carried out on R/V MIRAI during the cruise of MR20-05C using the salinometer (Model 8400B "AUTOSAL" ; Guildline Instruments Ltd.: S/N 62827) with an additional peristaltic-type intake pump (Ocean Scientific International, Ltd.). A pair of precision digital thermometers (1502A; FLUKE: S/N B78466 and B81550) were used for monitoring the ambient temperature and the bath temperature of the salinometer.

The specifications of the AUTOSAL salinometer and thermometer are shown as follows ;

Salinometer (Model 8400B "AUTOSAL" ; Guildline Instruments Ltd.)

Measurement Range	:	0.005 to 42 (PSU)
Accuracy	:	Better than ±0.002 (PSU) over 24 hours
Maximum Resolution	:	Better than ±0.0002 (PSU) at 35 (PSU)

Thermometer (1502A: FLUKE)

Measurement Range	:	16 to 30 deg C (Full accuracy)
Resolution	:	0.001 deg C
Accuracy	:	0.006 deg C (@ 0 deg C)

The measurement system was almost the same as Aoyama *et al.* (2002). The salinometer was operated in the air-conditioned ship's laboratory at a bath temperature of 24 deg C. The ambient temperature varied from approximately 22 deg C to 24 deg C, while the bath temperature was very stable and varied within +/- 0.002 deg C on rare occasion. The measurement for each sample was done with a double conductivity ratio and defined as the median of 33 readings of the salinometer. Data were taken after rinsed 5 times with the sample water. The double conductivity ratio of sample was calculated from average value of two measurements. And it was used to calculate the bottle salinity with the algorithm for the practical salinity scale, 1978 (UNESCO, 1981). In the case of the difference between the double conductivity ratio of these two measurements being greater than or equal to 0.00003, continue to be measured up to 3 times. The difference between the double conductivity ratio of these two measurements being smaller than 0.00002 were selected. The measurement was conducted in about 8 hours per day and the cell was cleaned with neutral detergent after the measurement of the day.

(5) Station list

Table 3.12-2 shows the sampling locations for the salinity analysis in this cruise.

Table 3.12-2. List of sampling locations of the salinity samples collected from CTD.

Station	Cast	Date (UTC)	Bottom position		Depth (m)
		(mmddyy)	Latitude	Longitude	
001	2	092220	32-00.00N	147-00.04W	5969.0
002	1	092220	32-59.83N	146-59.92W	5997.0
003	1	092320	34-00.13N	146-59.69W	5825.0
004	1	100120	47-00.03N	160-01.95W	5230.0
007	1	100820	69-00.83N	168-49.77W	51.3
009	1	100820	70-30.02N	165-29.73W	43.9
010	2	101020	74-33.03N	161-53.06W	1721.0
011	1	101120	74-58.81N	158-07.55W	841.0
012	1	101220	75-10.95N	160-00.17W	1985.0
013	1	101320	73-17.32N	160-00.66W	1212.0
015	1	101420	72-47.32N	157-59.98W	773.0
017	1	101520	71-19.18N	158-26.24W	114.8
020	1	101520	71-58.34N	153-59.67W	740.0
022	1	101720	75-00.87N	164-57.48W	552.0

Station	Cast	Date (UTC)	Bottom position		Depth (m)
		(mmddyy)	Latitude	Longitude	
023	1	101820	75-00.17N	167-14.30W	262.0
024	1	102020	75-00.04N	169-38.22W	236.0
025	1	102020	75-00.21N	174-59.64W	266.0
026	1	102020	75-00.05N	172-00.23W	383.0
027	1	102220	74-36.00N	170-11.94W	208.0
029	1	102220	73-29.97N	168-48.83W	115.6
030	1	102220	73-00.08N	168-49.55W	64.2
031	1	102320	72-00.00N	168-49.98W	50.4
033	1	102320	69-59.98N	168-48.79W	39.4
034	1	102320	69-00.22N	168-49.64W	51.7
035	1	102320	68-00.00N	168-49.98W	57.5

(6) Preliminary results

a. Standard Seawater

Standardization control of the salinometer was set to 474 and all measurements were done at this setting. The value of STANDBY was between 24+5452 and 24+5455 and that of ZERO was 0.0+0000. The IAPSO Standard Seawater (SSW) batch P162 was used as the standard for salinity. 24 bottles of P162 were measured.

Figure 3.12-1 shows the time series of the double conductivity ratio of the Standard Seawater batch P162. The average of the double conductivity ratio was 1.99963 and the standard deviation was 0.00002 which is equivalent to 0.0003 in salinity.

Figure 3.12-2 shows the time series of the double conductivity ratio of the Standard Seawater batch P162 after correction. The average of the double conductivity ratio after correction was 1.99966 and the standard deviation was 0.00001, which is equivalent to 0.0001 in salinity.

The specifications of SSW batch P162 used in this cruise are shown as follows ;

Batch	:	P162
Conductivity ratio	:	0.99983
Salinity	:	34.993
Use by	:	16th April. 2021

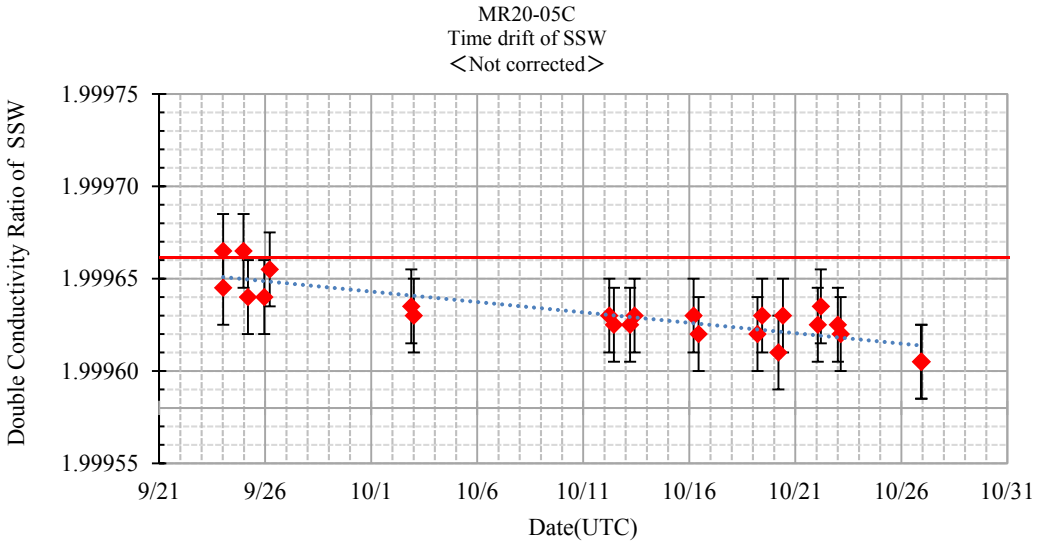

Figure 3.12-1. Time series of double conductivity ratio for the Standard Seawater. (before correction)

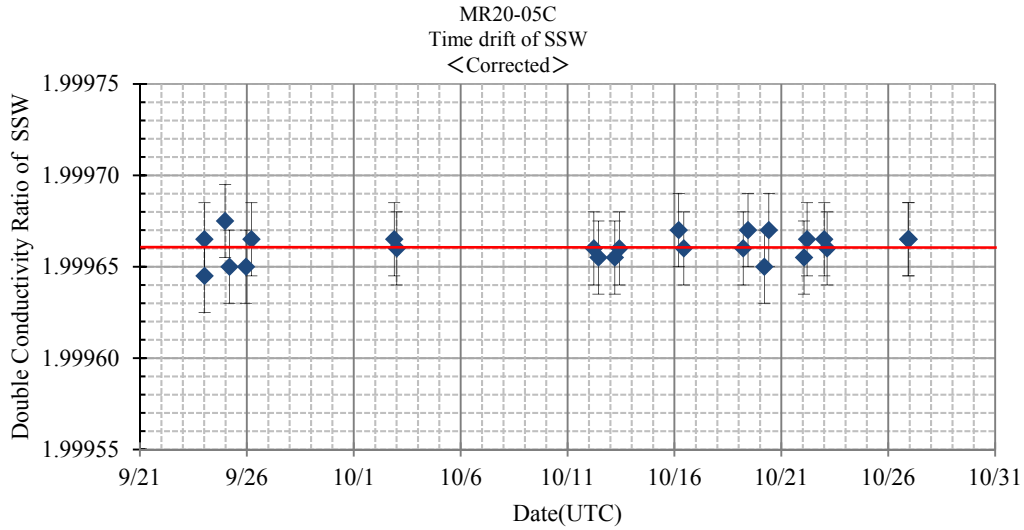

Figure 3.12-2. Time series of double conductivity ratio for the Standard Seawater. (after correction)

b. Sub-Standard Seawater

Sub-standard seawater was made from surface sea water filtered by a pore size of 0.2 micrometer and stored in a 20 liter container made of polyethylene and stirred for at least 24 hours before measuring. It was measured about every 6 samples in order to check for the possible sudden drifts of the salinometer.

c. Replicate Samples

We estimated the precision of this method using 58 pairs of replicate samples taken from the same water sampling bottle. Figure 3.12-3 shows the histogram of the

absolute difference between each pair of the replicate samples. The average and the standard deviation of absolute difference among 58 pairs of replicate samples were 0.0005 and 0.0006 in salinity, respectively.

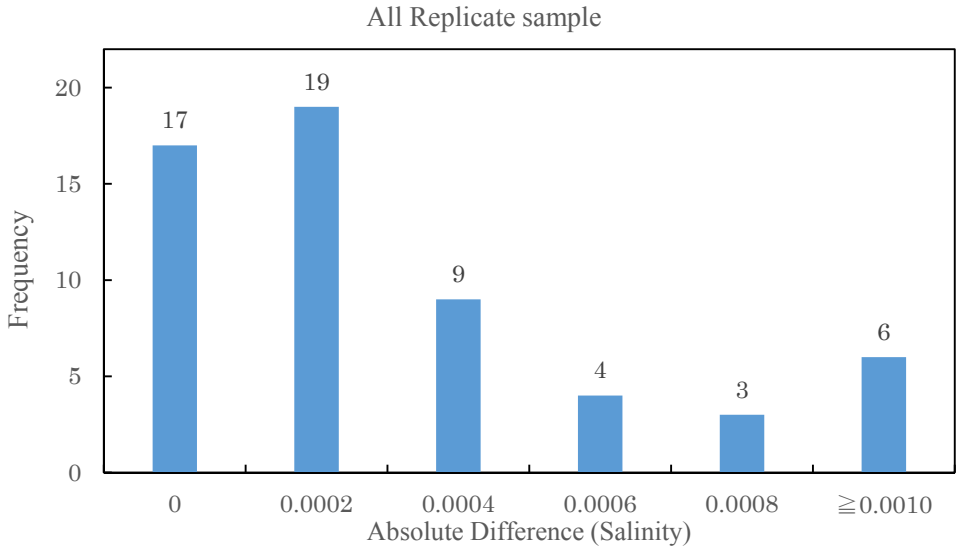

Figure 3.12-3. The histogram of the salinity for the absolute difference of all replicate samples.

32 pairs of replicate samples were to estimate the precision of shallow (<200dbar) samples. Figure 3.12-4 shows the histogram of the absolute difference between each pair of shallow (<200dbar) replicate samples. The average and the standard deviation of absolute difference among 32 pairs were 0.0005 and 0.0007 in salinity, respectively.

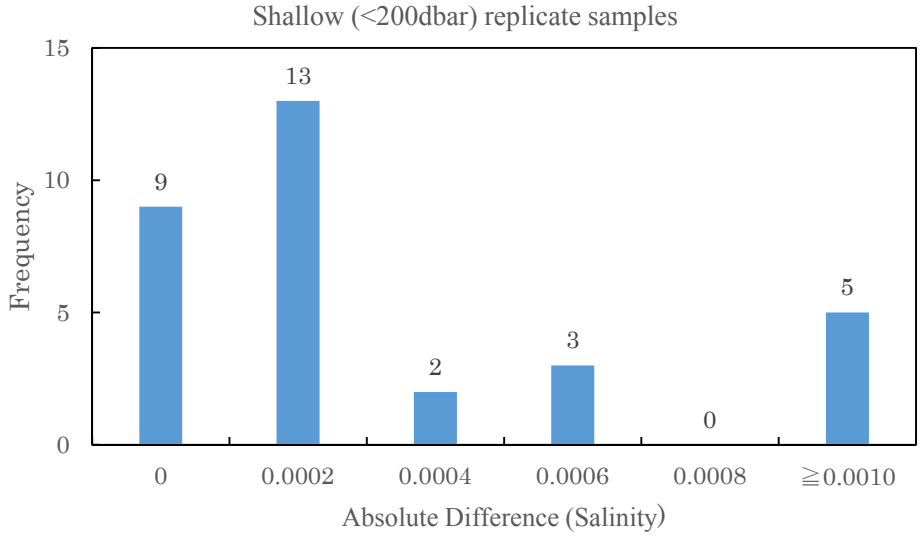

Figure 3.12-4. The histogram of the absolute difference between shallow (<200dbar) replicate samples.

26 pairs of replicate samples were to estimate the precision of deep (>=200dbar) samples. Figure 3.12-5 shows the histogram of the absolute difference between each pair of deep (>=200dbar) replicate samples. The average and the standard deviation of absolute difference among 26 pairs were 0.0004 and 0.0005 in salinity, respectively.

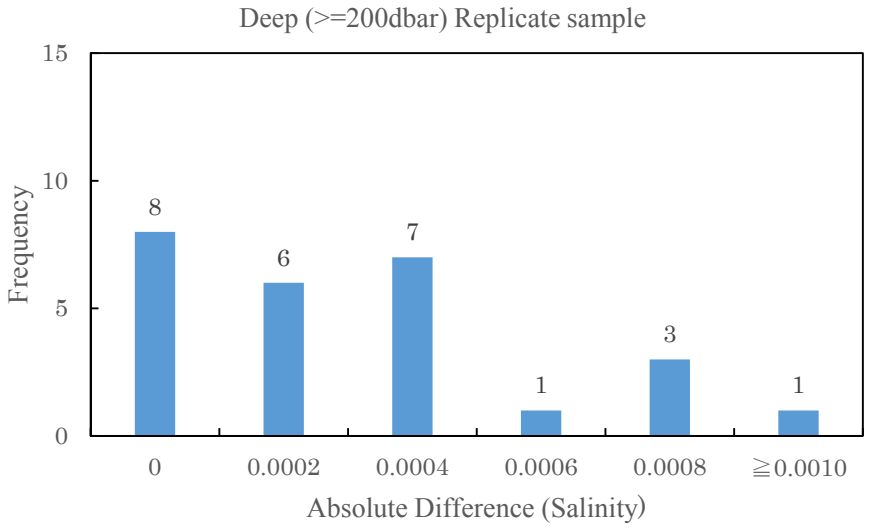

Figure 3.12-5. The histogram of the absolute difference between deep (>=200dbar) replicate samples.

(7) Data archive

These data obtained in this cruise will be submitted to the Data Management Group (DMG) of JAMSTEC, and will be opened to the public via "Data Research System for Whole Cruise Information in JAMSTEC (DARWIN)" in JAMSTEC web site. <http://www.godac.jamstec.go.jp/darwin/e>

(8) References

Aoyama, M., T. Joyce, T. Kawano and Y. Takatsuki : Standard seawater comparison up to P129. Deep-Sea Research, I, Vol. 49, 1103-1114, 2002.

UNESCO : Tenth report of the Joint Panel on Oceanographic Tables and Standards. UNESCO Tech. Papers in Mar. Sci., 36, 25 pp., 1981.

4. Chemical and Biological Oceanography

4.1. Dissolved oxygen

(1) Personnel

Amane Fujiwara (JAMSTEC) – Principal investigator
Misato Kuwahara (Marine Works Japan Ltd.; MWJ) – Operation leader
Masahiro Orui (MWJ)
Haruka Sato (MWJ)

(2) Objective

Determination of dissolved oxygen in seawater by Winkler titration.

(3) Parameters

Dissolved Oxygen

(4) Instruments and Methods

Following procedure is based on winkler method (Dickson, 1996; Culberson, 1991).

a. Instruments

Burette for sodium thiosulfate and potassium iodate;
Automatic piston burette (APB-610 / APB-620) manufactured by Kyoto Electronics Manufacturing Co., Ltd. / 10 cm^3 of titration vessel

Detector;
Automatic photometric titrator (DOT-15X) manufactured by Kimoto Electric Co., Ltd.

Software;
DOT_Terminal Ver. 1.3.1

b. Reagents

Pickling Reagent I:
Manganese(II) chloride solution (3 mol dm^{-3})

Pickling Reagent II:
Sodium hydroxide (8 mol dm^{-3}) / Sodium iodide solution (4 mol dm^{-3})

Sulfuric acid solution (5 mol dm^{-3})
Sodium thiosulfate (0.025 mol dm^{-3})
Potassium iodate (0.001667 mol dm^{-3})

c. Sampling

Seawater samples were collected with Niskin bottle attached to the CTD/Carousel Water Sampling System (CTD system). Seawater for oxygen measurement was transferred from the bottle to a volume calibrated flask (ca. 100

cm^3), and three times volume of the flask was overflowed. Temperature was simulteneously measured by digital thermometer during the overflowing. After transfering the sample, two reagent solutions (Reagent I and II) of 1 cm^3 each were added immediately and the stopper was inserted carefully into the flask. The sample flask was then shaken vigorously to mix the contents and to disperse the precipitate finely throughout. After the precipitate has settled at least halfway down the flask, the flask was shaken again vigorously to disperse the precipitate. The sample flasks containing pickled samples were stored in a laboratory until they were titrated.

d. Sample measurement

For over two hours after the re-shaking, the pickled samples were measured on board. Sulfuric acid solution with its volume of 1 cm^3 and a magnetic stirrer bar were put into the sample flask and the sample was stirred. The samples were titrated by sodium thiosulfate solution whose morality was determined by potassium iodate solution. Temperature of sodium thiosulfate during titration was recorded by a digital thermometer. Dissolved oxygen concentration ($\mu mol\ kg^{-1}$) was calculated by sample temperature during seawater sampling, salinity of the sensor on CTD system, flask volume, and titrated volume of sodium thiosulfate solution without the blank. During this cruise, 2 sets of the titration apparatus were used.

e. Standardization and determination of the blank

Concentration of sodium thiosulfate titrant was determined by potassium iodate solution. Pure potassium iodate was dried in an oven at 130 ºC, and 1.7835 g of it was dissolved in deionized water and diluted to final weight of 5 kg in a flask. After 10 cm^3 of the standard potassium iodate solution was added to an another flask using a volume-calibrated dispenser, 90 cm^3 of deionized water, 1 cm^3 of sulfuric acid solution, and 1 cm^3 of pickling reagent solution II and I were added in order. Amount of titrated volume of sodium thiosulfate for this diluted standard potassium iodate solution (usually 5 times measurements average) gave the morality of sodium thiosulfate titrant.

The oxygen in the pickling reagents I (1 cm^3) and II (1 cm^3) was assumed to be 7.6×10^{-8} mol (Murray et al., 1968). The blank due to other than oxygen was determined as follows. First, 1 and 2 cm^3 of the standard potassium iodate solution were added to each flask using a calibrated dispenser. Then 100 cm^3 of deionized water, 1 cm^3 of sulfuric acid solution, 1 cm^3 of pickling II reagent solution, and same volume of pickling I reagent solution were added into the flask in order. The blank was determined by difference between the first (1 cm^3 of potassium iodate) titrated volume of the sodium thiosulfate and the second (2 cm^3 of potassium iodate) one. The titrations were conducted for 3 times and their average was used as the blank value.

(5) Observation log

a. Standardization and determination of the blank

Table 4.1-1 shows results of the standardization and the blank determination during this cruise.

Table 4.1-1. Results of the standardization and the blank determinations during cruise.

Date (yyyy/mm/dd)	Potassium iodate ID	Sodium thiosulfate ID	DOT-15X (No.9)		DOT-15X (No.10)		Station
			E.P. (cm3)	Blank (cm3)	E.P. (cm3)	Blank (cm3)	
2020/09/21	K20B01	T-19W	3.960	0.003	3.956	-0.005	001, 003
2020/09/25	K20B02	T-19W	3.962	0.003	3.955	-0.005	
2020/09/30	K20B03	T-19W	3.966	0.005	3.958	-0.006	004
2020/10/05	K20B04	T-19W	3.962	0.002	3.957	-0.006	
2020/10/07	K20B05	T-19W	3.961	0.006	3.955	-0.003	007, 009
2020/10/11	K20B06	T-19W	3.967	0.002	3.958	-0.003	
2020/10/11	K20B07	T-19W	3.965	0.002	3.959	-0.005	010, 011, 012, 013, 015, 017
2020/10/15	K20B08	T-19W	3.962	0.002	3.956	-0.004	
2020/10/15	K20B08	T-19X	3.960	-0.001	3.955	-0.006	020, 022, 023, 024, 025, 026, 027, 029, 030
2020/10/20	K20B09	T-19X	3.963	0.003	3.957	-0.005	031, 033, 034, 035
2020/10/24	K20B10	T-19X	3.961	0.001	3.957	-0.005	
2020/10/26	K20C01	T-19X	3.962	0.001	3.958	-0.005	

b. Repeatability of sample measurement

Replicate samples were taken at every CTD casts. The standard deviation of the replicate measurement (Dickson et al., 2007) was 0.17 μmol kg^{-1} (n= 55). Results of replicate samples were shown in Table 4.1-2 and this diagram shown in Figure 4.1-1. These data use the preliminary data. The standard deviation (s) is given by the expression

$$s = \sqrt{\frac{\sum_{i=1} {d_i}^2}{2k}}$$

where d and k are the difference of replicate measurements and the number of replicate samples respectively

Table 4.1-2. Results of the replicate sample measurements.

Layer	Number of replicate sample pairs	Oxygen concentration (μmol kg^{-1}) Standard Deviation
200m>	32	0.21
>=200m	23	0.12
All	55	0.17

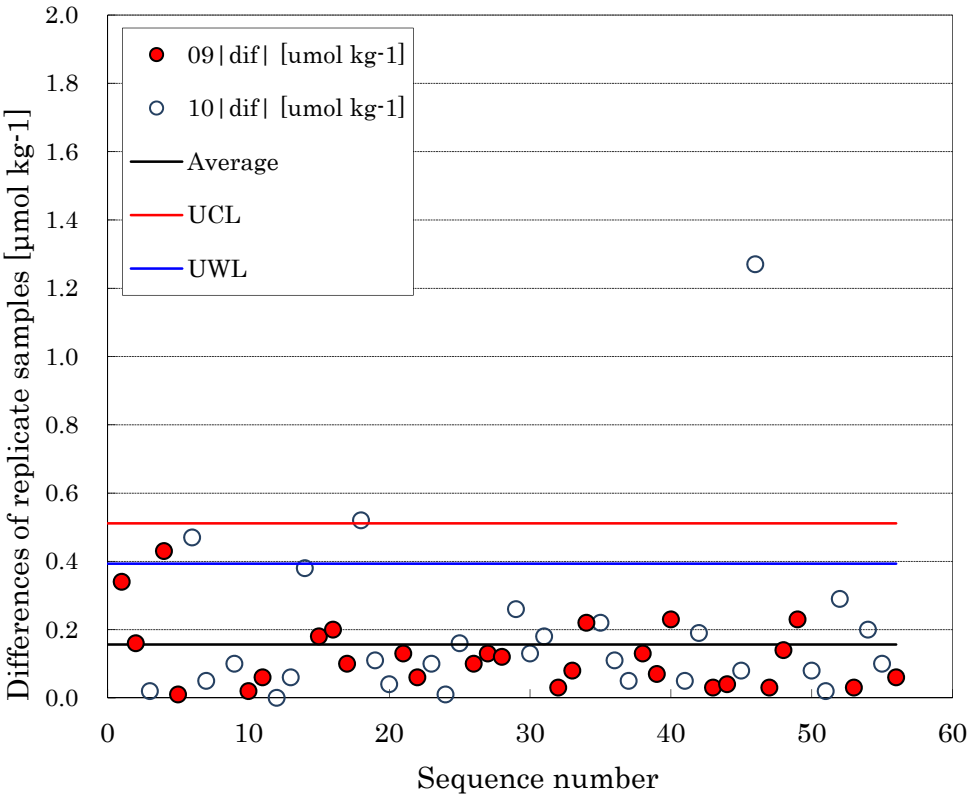

Figure 4.1-1. Difference of replicate samples against sequence number.

(6) Data archives

These data obtained in this cruise will be submitted to the Data Management Group (DMG) of JAMSTEC, and will opened to the public via "Data Research System for Whole Cruise Information in JAMSTEC (DARWIN)" in JAMSTEC web site.

<http://www.godac.jamstec.go.jp/darwin/e>

(7) References

Culberson, C. H. (1991). *Dissolved Oxygen.* WHPO Publication 91-1.

Dickson, A. G. (1996). Determination of dissolved oxygen in sea water by Winkler titration. In *WOCE Operations Manual*, Part 3.1.3 Operations & Methods, WHP

Office Report WHPO 91-1.

Dickson, A. G., Sabine, C. L., & Christian, J. R.(Eds.), (2007). *Guide to best practices for ocean CO_2 measurements, PICES Special Publication 3*: North Pacific Marine Science Organization.

Murray, C. N., Riley, J. P., & Wilson, T. R. S. (1968). The solubility of oxygen in Winklerreagents used for the determination of dissolved oxygen. *Deep Sea Res.*, 15, 237-238.

4.2. Nutrients

as of 26 November 2020 ver4.8

(1) Personnel

Michio Aoyama (JAMSTEC/University of Tsukuba)
– Principal investigator, Not on board
Shigeto Nishino (JAMSTEC)
Tomomi Sone (Marine Works Japan Ltd.; MWJ) – Operation leader
Jun Matsuoka (MWJ)
Yuko Miyoshi (MWJ)
Shintaro Amikura (MWJ)

(2) Objectives

The objective of this document is to show the present status of the nutrient concentrations during the R/V Mirai MR20-05C cruise (EXPOCODE: 49NZ20200919) in the Pacific Ocean and the Arctic Ocean, and then evaluate the comparability of this obtained data set during this cruise using the certified reference materials of the nutrients in seawater.

(3) Parameters

The parameters are nitrate, nitrite, silicate, phosphate and ammonia in seawater.

(4) Instruments and methods

(4.1) Analytical detail using QuAAtro 2-HR systems (BL TEC K.K.)

Nitrate + nitrite and nitrite were analyzed by the following methodology that was modified from the original method of Grasshoff (1976). The flow diagrams were shown in Figure 4.2-1 for nitrate + nitrite and Figure 4.2-2 for nitrite. For the nitrate + nitrite analysis, the sample were mixed with the alkaline buffer (Imidazole) and then the mixture was pushed through a cadmium coil which was coated with a metallic copper. This step was conducted due to reduce from nitrate to nitrite in the sample, which allowed us to determine nitrate + nitrite in the seawater sample. For the nitrite analysis, the sample was mixed with reagents without this reduction step. In the flow system, seawater sample with or without the reduction step was mixed with an acidic sulfanilamide reagent through a mixing coil to produce a diazonium ion. And then, the mixture was mixed with the N-1-naphthylethylenediamine dihydrochloride (NED) to produce a red azo dye. The azo dye compound was injected into the spectrophotometric detection to monitor the signal at 545 nm. Thus, for the nitrite analysis, sample was determined without passing thought the Cd coil. Nitrate was computed by the difference between nitrate+nitrite concentration and nitrite concentration.

The silicate method is analogous to that described for phosphate (see below). The method is essentially that of Grasshoff et al. (1999). The flow diagrams were shown in Figure 4.2-3. Silicomolybdic acid compound was first formed by mixing silicate in the

sample with the molybdic acid. The silicomolybdic acid compound was then reduced to silicomolybdous acid, "molybdenum blue," using L-ascorbic acid as the reductant. And then the signal was monitored at 630nm.

The methodology for the phosphate analysis is a modified procedure of Murphy and Riley (1962). The flow diagrams were shown in Figure 4.2-4. Molybdic acid was added to the seawater sample to form the phosphomolybdic acid compound, and then it was reduced to phosphomolybdous acid compound using L-ascorbic acid as the reductant. And then the signal was monitored at 880nm.

The ammonia in seawater was determined using the flow diagrams shown in Figure 4.2-5. Sample was mixed with an alkaline solution containing EDTA, which ammonia as gas state was formed from seawater. The ammonia (gas) is absorbed in a sulfuric acid by way of 0.5 μm pore size membrane filter (ADVANTEC PTFE) at the dialyzer attached to the analytical system. And then the ammonia absorbed in sulfuric acid was determined by coupling with phenol and hypochlorite to form indophenols blue, and the signal was determined at 630nm.

The details of a modification of analytical methods for four parameters, nitrate, nitrite, silicate and phosphate, are also compatible with the methods described in nutrients section in the new GO-SHIP repeat hydrography nutrients manual (Becker et al., 2019). This manual is a revised version of the GO-SHIP repeat hydrography nutrients manual (Hydes et al., 2019). Theanalytical method of ammonium is compatible with the determination of ammonia in seawater using a vaporization membrane permeability method (Kimura, 2000).

(4.2) Nitrate + Nitrite reagents

50 % Triton solution

50 mL of Triton™ X-100 provided by Sigma-Ardrich Japan G. K. (CAS No. 9002-93-1) were mixed with 50 mL of ethanol (99.5 %).

Imidazole (buffer), 0.06 M (0.4 % w/v)

Dissolved 4 g of the imidazole (CAS No. 288-32-4) in 1000 mL ultra-pure water, and then added 2 mL of the hydrogen chloride (CAS No. 7647-01-0). After mixing, 1 mL of the 50 % triton solution was added.

Sulfanilamide, 0.06 M (1 % w/v) in 1.2 M HCl

Dissolved 10 g of 4-aminobenzenesulfonamide (CAS No. 63-74-1) in 900 mL of ultra-pure water, and then add 100 mL of the hydrogen chloride (CAS No. 7647-01-0). After mixing, 2 mL of the 50 % triton solution was added.

NED, 0.004 M (0.1 % w/v)

Dissolved 1 g of N-(1-naphthalenyl)-1,2-ethanediamine dihydrochloride (CAS No. 1465-25-4) in 1000 mL of ultra-pure water and then added 10 mL of hydrogen chloride (CAS No. 7647-01-0). After mixing, 1 mL 50 % of the Triton solution was added. This

reagent was stored in a dark bottle.

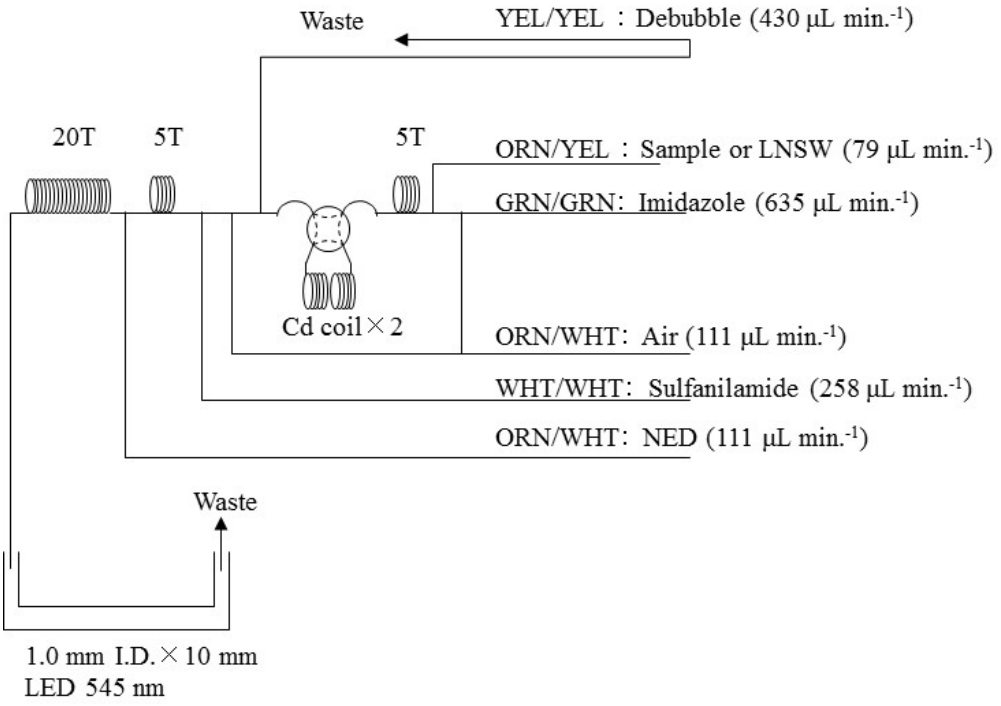

Figure 4.2-1. NO_3+NO_2 (1ch.) flow diagram.

(4.3) Nitrite reagents

50 % Triton solution

50 mL of the Triton™ X-100 provided by Sigma-Ardrich Japan G. K. (CAS No. 9002-93-1) were mixed with 50 mL ethanol (99.5 %).

Sulfanilamide, 0.06 M (1 % w/v) in 1.2 M HCl

Dissolved 10 g of 4-aminobenzenesulfonamide (CAS No. 63-74-1) in 900 mL of ultra-pure water, and then added 100 mL of hydrogen chloride (CAS No. 7647-01-0). After mixing, 2 mL of the 50 % triton solution were added.

NED, 0.004 M (0.1 % w/v)

Dissolved 1 g of N-(1-naphthalenyl)-1,2-ethanediamine dihydrochloride (CAS No. 1465-25-4) in 1000 mL of ultra-pure water and then added 10 mL of hydrogen chloride (CAS No. 7647-01-0). After mixing, 1 mL of the 50 % triton solution was added. This reagent was stored in a dark bottle.

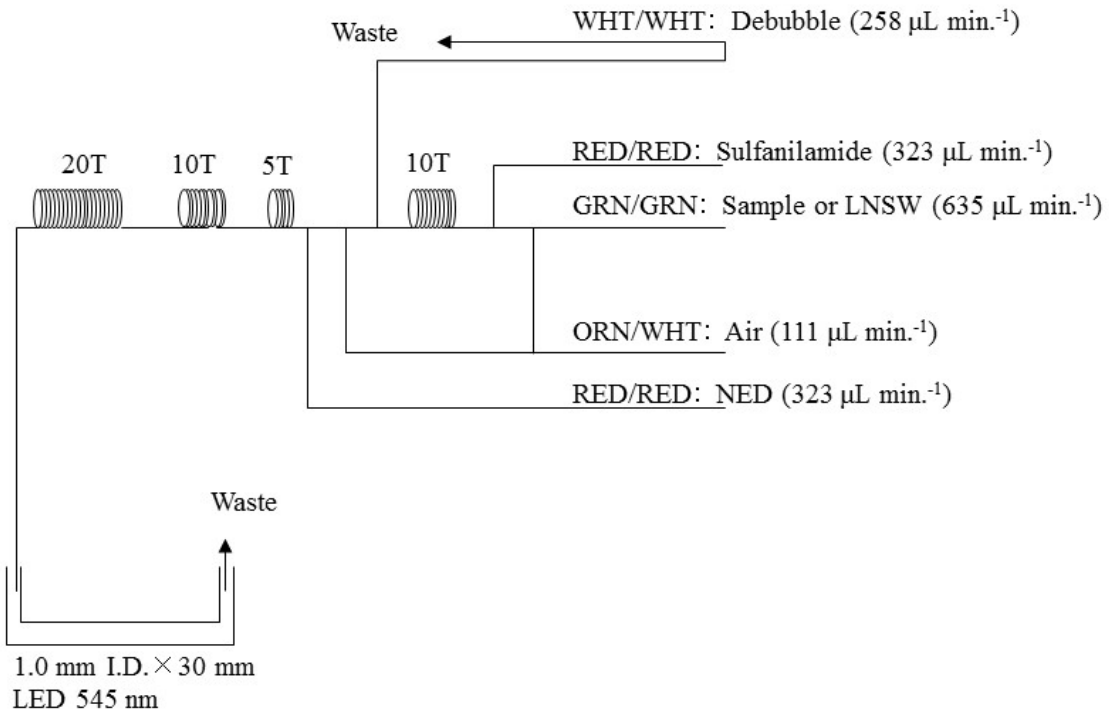

Figure 4.2 -2. NO_2 (2ch.) flow diagram.

(4.4) Silicate reagents

15 % Sodium dodecyl sulfate solution

75 g of sodium dodecyl sulfate (CAS No. 151-21-3) was mixed with 425 mL ultra-pure water.

Molybdic acid, 0.03 M (1 % w/v)

Dissolved 7.5 g of sodium molybdate dihydrate (CAS No. 10102-40-6) in 980 mL ultra-pure water, and then added 12 mL of a 4.5M sulfuric acid. After mixing, 20 mL of the 15 % sodium dodecyl sulfate solution was added. Note that the amount of sulfuric acid was reduced from the previous report (MR19-03C) since we have modified the method of Grasshoff et al. (1999).

Oxalic acid, 0.6 M (5 % w/v)

Dissolved 50 g of oxalic acid (CAS No. 144-62-7) in 950 mL of ultra-pure water.

Ascorbic acid, 0.01 M (3 % w/v)

Dissolved 2.5 g of L-ascorbic acid (CAS No. 50-81-7) in 100 mL of ultra-pure water. This reagent was freshly prepared every day.

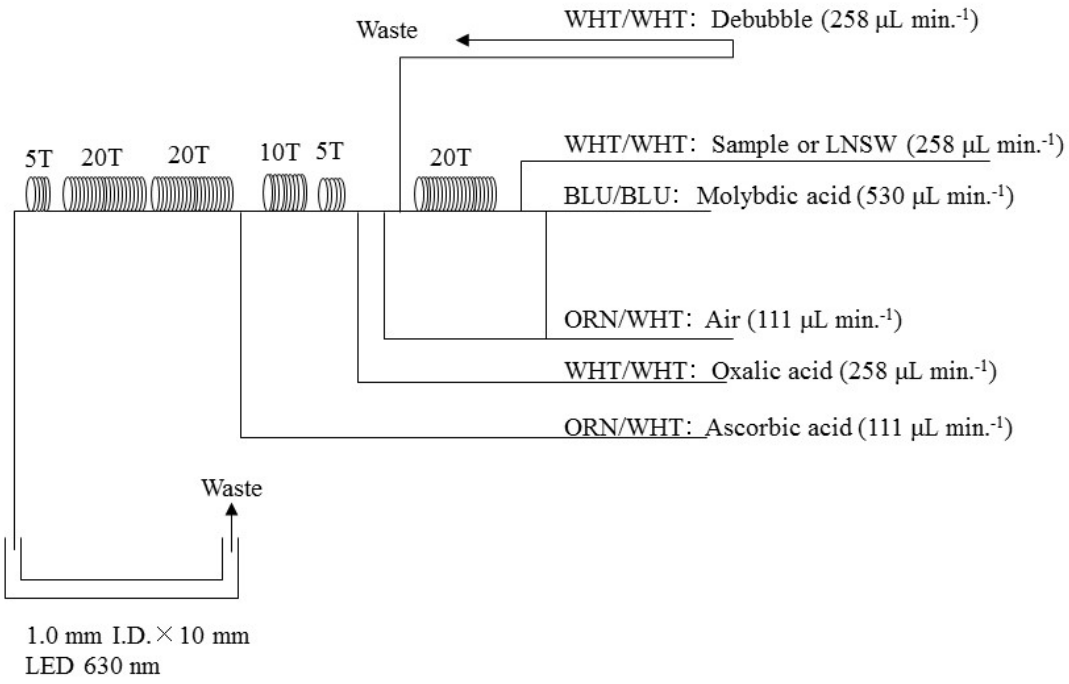

Figure 4.2-3. SiO_2 (3ch.) flow diagram.

(4.5) Phosphate reagents

15 % Sodium dodecyl sulfate solution

75 g of sodium dodecyl sulfate (CAS No. 151-21-3) were mixed with 425 mL of ultra-pure water.

Stock molybdate solution, 0.03 M (0.8 % w/v)

Dissolved 8 g of sodium molybdate dihydrate (CAS No. 10102-40-6) and 0.17 g of antimony potassium tartrate trihydrate (CAS No. 28300-74-5) in 950 mL of ultra-pure water, and then added 50 mL of sulfuric acid (CAS No. 7664-93-9).

PO_4 color reagent

Dissolved 1.2 g of L-ascorbic acid (CAS No. 50-81-7) in 150 mL of the stock molybdate solution. After mixing, 3 mL of the 15 % sodium dodecyl sulfate solution was added. This reagent was freshly prepared before every measurement.

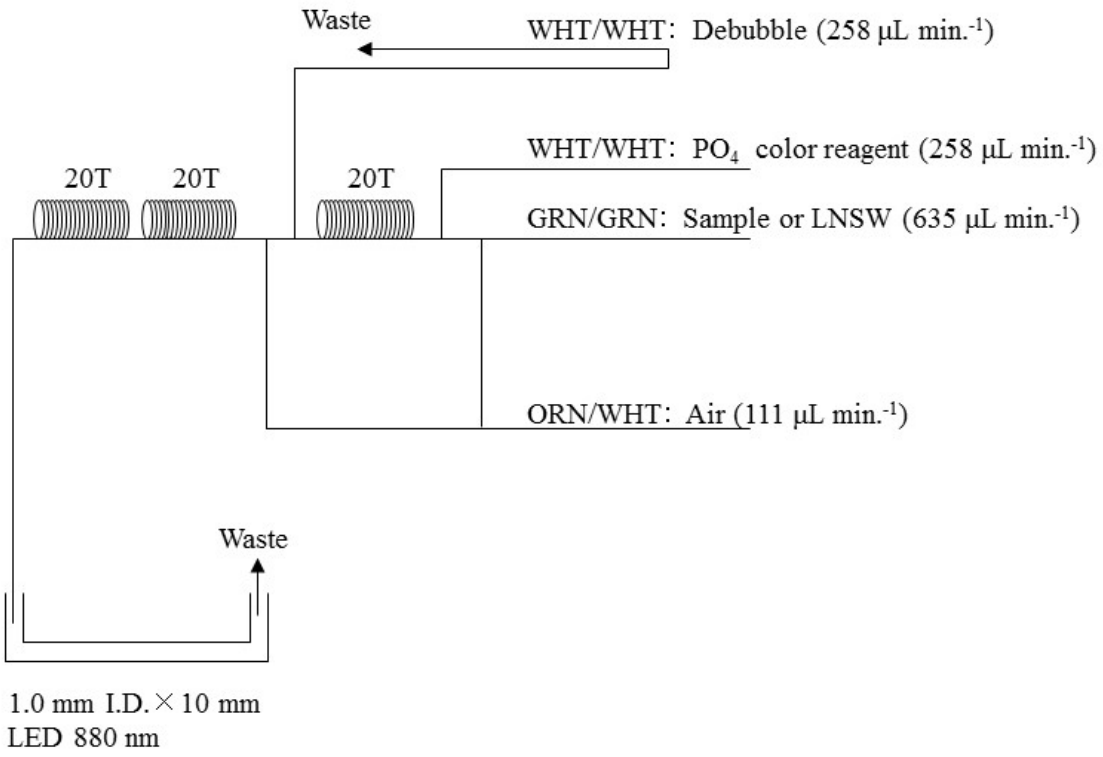

Figure 4.2-4. PO_4 (4ch.) flow diagram.

(4.6) Ammonia reagents

30 % Triton solution

30 mL of a Triton™ X-100 provided by Sigma-Ardrich Japan G. K. (CAS No. 9002-93-1) were mixed with 70 mL ultra-pure water.

EDTA

Dissolved 41 g of a tetrasodium; 2-[2-[bis(carboxylatomethyl)amino]ethyl-(carboxylatemethyl)amino]acetate;tetrahydrate (CAS No. 13235-36-4) and 2 g of a boric acid (CAS No. 10043-35-3) in 200 mL of ultra-pure water. After mixing, a 1 mL of the 30 % triton solution was added. This reagent is prepared every week.

NaOH liquid

Dissolved 1.5 g of a sodium hydroxide (CAS No. 1310-73-2) and 16 g of a tetrasodium; 2-[2-[bis(carboxylatomethyl)amino]ethyl-(carboxylatomethyl)amino]acetate; tetrahydrate (CAS No. 13235-36-4) in 100 mL of ultra-pure water. This reagent was prepared every week. Note that we reduced the amount of a sodium hydroxide from 5 g to 1.5 g because pH of C standard solutions has been lowered 1 pH unit due to the change of recipe of B standards solution (the detailed of those standard solution, see 7.2.4).

Stock nitroprusside

Dissolved 0.25 g of a sodium nitroferricyanide dihydrate (CAS No. 13755-38-9) in 100 mL of ultra-pure water, and then added 0.2 mL of a 1M sulfuric acid. Stored in a dark bottle and prepared every month.

Nitroprusside solution

Added 4 mL of the stock nitroprusside and 4 mL of a 1M sulfuric acid in 500 mL of ultra-pure water. After mixing, 2 mL of the 30 % triton solution was added. This reagent was stored in a dark bottle and prepared every 2 or 3 days.

Alkaline phenol

Dissolved 10 g of a phenol (CAS No. 108-95-2), 5 g of a sodium hydroxide (CAS No. 1310-73-2) and 2 g of a sodium citrate dihydrate (CAS No. 6132-04-3) in 200 mL of ultra-pure water. Stored in a dark bottle and prepared every week.

NaClO solution

Mixed 3 mL of a sodium hypochlorite (CAS No. 7681-52-9) in 47 mL of ultra-pure water. Stored in a dark bottle and fleshly prepared before every measurement. This reagent need be 0.3 % available chlorine.

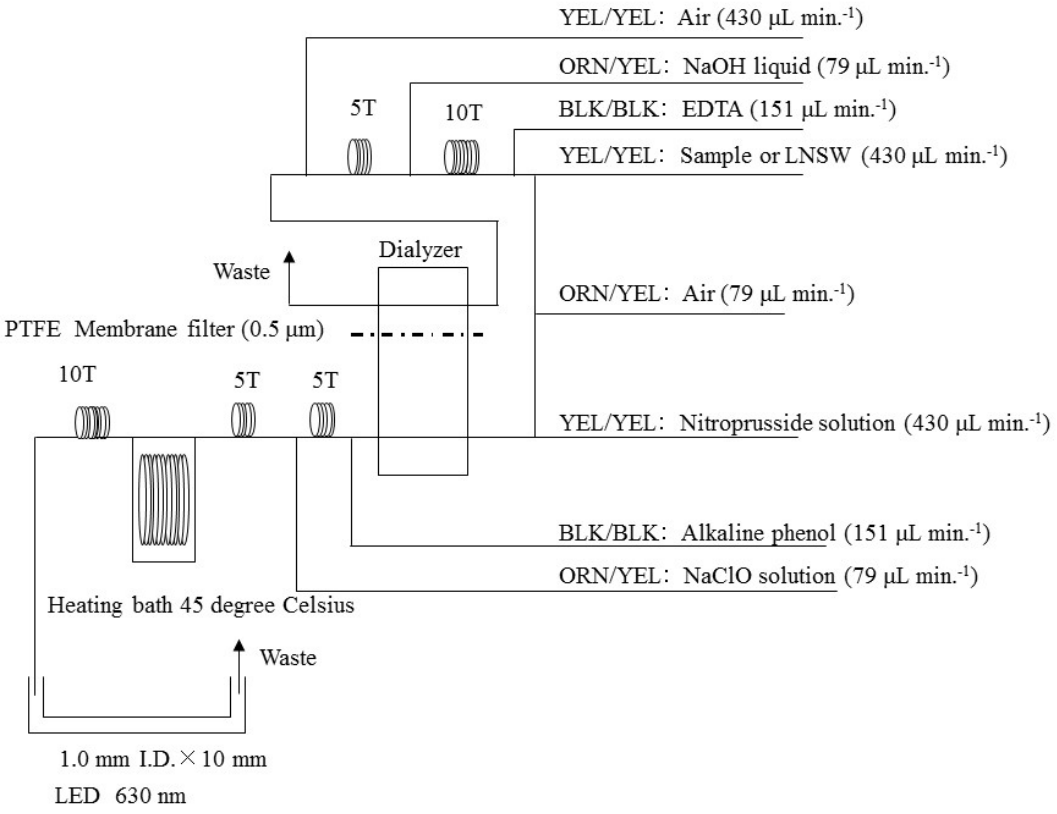

Figure 4.2-5. NH_4 (5ch.) flow diagram.

(4.7) Sampling procedures

Sampling for nutrient samples was conducted right after the sampling for other parameters (oxygen, salinity, trace gases and chlorophyll). We rinsed latex globes with the low nutrients seawater (LNSW) before sampling to avoid nitrate contamination. Samples were collected into two new 10 mL polyacrylates vials without any sample drawing tube that usually used for the oxygen samples. All samples at each station were collected by a dedicated person. Each vial was rinsed three times before filling and then was sealed without any head-space immediately after the collection. The vials were put into a water bath that was adjusted to the ambient temperature at 22.1 ± 0.5 degree Celsius, for more than 30 minutes to keep the constant temperature of samples. When the transmissometer signal (Xmiss) of the sample was less than 95 % or comfirmed the presence of particles in the vial, we carried out centrifuging the sample by using a centrifuge (type: CN-820, Hsiang Tai). The conditions of centrifuging were set about 3400 rpm for 2.5 minute. The treated samples were listed in Table 4.2-1.

No transfer from the vial to another container was made and the vials were set an autosampler tray directly. Samples were analyzed after collection within 24 hours.

(4.8) Data processing

Raw data from QuAAtro 2-HR were treated as follows:

- Checked if there were any baseline shift.
- Checked the shape of each peak and positions of peak values. If necessary, a change was made for the positions of peak values.
- Conducted carry-over correction and baseline drift correction to apply to the peak height of each sample followed by sensitivity correction.
- Conducted baseline correction and sensitivity correction using the linear regression.
- Using the pressure from uncalibrated CTD data, the salinity (determined on the ship) and the laboratory room temperature (20 degree Celsius), the density of each sample had been calculated tentatively. The obtained density was used to calculate the final nutrient concentration with the unit of umol kg^{-1}.
- Calibration curves to obtain the nutrients concentrations were assumed second order equations.

(4.9) Summary of nutrients analysis

During this cruise, 19 runs were conducted to obtain the values for the samples collected by 24 casts at 24 stations shown in Table 4.2-2. The total number of the seawater samples were 371. Each sample depth, we collected duplicate samples, and then determined all of the samples. The sampling locations for the nutrients was shown in Table 4.2-2. and Figure 4.2-6.

Table 4.2-1. Centrifuged samples.

Station	Cast	Bottle	Depth (dbar)	Trans (%)
7	1	13	46.4	52.4
9	1	0	0.0	-
9	1	34	4.6	94.9
9	1	33	9.5	94.9
9	1	35	11.3	95.1
9	1	32	19.9	95.1
9	1	31	29.7	88.0
9	1	13	37.8	39.3
13	1	27	125.5	92.6
15	1	33	9.5	89.0
15	1	30	49.6	91.3
15	1	29	74.6	90.8
15	1	28	99.6	92.8
15	1	27	124.6	93.4
17	1	30	50.1	85.0
17	1	29	74.8	84.6
17	1	28	99.9	83.6
17	1	13	110.9	83.5
20	1	0	0.0	-
20	1	34	4.9	86.2
20	1	33	9.8	73.9
20	1	35	15.2	66.5
20	1	32	20.3	63.1
20	1	31	30.2	73.1
20	1	30	50.0	83.8
20	1	29	75.3	87.3
20	1	28	100.4	84.6
20	1	27	125.1	84.9
20	1	26	150.2	86.3
20	1	25	174.8	93.1
20	1	20	400.3	94.6
24	1	23	227.8	91.9
24	1	13	228.2	92.0
25	1	13	268.0	94.4
26	1	13	373.9	94.8
27	1	25	175.2	93.8
27	1	24	199.4	87.9

Station	Cast	Bottle	Depth (dbar)	Trans (%)
29	1	28	99.9	50.3
29	1	13	110.1	4.6
30	1	0	0.0	-
30	1	34	5.0	94.7
30	1	33	10.4	94.5
30	1	35	14.4	94.7
30	1	32	20.8	94.3
30	1	31	30.8	93.5
30	1	30	50.7	84.1
30	1	13	58.3	31.8
31	1	0	0.0	-
31	1	34	4.6	93.3
31	1	33	9.6	93.3
31	1	35	12.5	93.3
31	1	32	19.8	93.3
31	1	31	29.9	94.0
31	1	13	45.3	29.8
33	1	0	0.0	-
33	1	34	4.9	65.3
33	1	33	9.9	64.9
33	1	35	14.9	63.9
33	1	32	20.1	62.7
33	1	31	30.0	49.0
33	1	13	33.8	48.0
34	1	0	0.0	-
34	1	34	5.4	93.8
34	1	33	10.1	93.9
34	1	35	16.1	92.5
34	1	32	20.1	90.2
34	1	31	30.1	69.1
34	1	13	46.3	41.8
35	1	0	0.0	-
35	1	34	4.7	83.8
35	1	33	9.8	83.0
35	1	32	19.9	74.2
35	1	35	25.8	67.8
35	1	31	29.8	68.8
35	1	30	49.7	41.0
35	1	13	52.5	39.6

(5) Station list

The sampling stations were listed as shown in Table 4.2-2.

Table 4.2-2. List of stations.

Station	Cast	Date (UTC)	Position*		Depth (m)
		(mmddyy)	Latitude	Longitude	
002	1	200922	32-59.83N	146-59.92E	5997
003	1	200923	34-00.13N	146-59.69E	5825
004	1	201001	47-00.03N	160-01.96E	5230
007	1	201008	69-00.83N	168-49.77W	51
009	1	201008	70-30.02N	165-29.73W	44
010	2	201010	74-33.03N	161-53.06W	1721
011	1	201011	74-58.81N	158-07.55W	841
012	1	201012	75-10.95N	160-00.17W	1985
013	1	201013	73-17.32N	160-00.00W	1212
015	1	201014	72-47.32N	157-59.98W	773
017	1	201015	71-19.18N	158-26.24W	115
020	1	201015	71-58.34N	153-59.67W	740
022	1	201017	75-00.88N	195-00.00W	552
023	1	201018	75-00.17N	192-45.70W	262
024	1	201018	75-00.04N	190-00.00W	236
025	1	201018	75-00.20N	185-00.35W	266
026	1	201019	75-00.05N	187-59.77W	383
027	1	201019	74-00.45N	189-00.00W	208
029	1	201019	73-29.97N	191-11.17W	116
030	1	201020	73-00.08N	191-10.45W	64
031	1	201020	72-00.43N	191-00.00W	50
033	1	201020	69-59.98N	191-11.21W	39
034	1	201021	69-00.22N	191-10.36W	52
035	1	201021	68-00.41N	191-10.01W	58

* Position indicates latitude and longitude where CTD reached maximum depth at the cast.

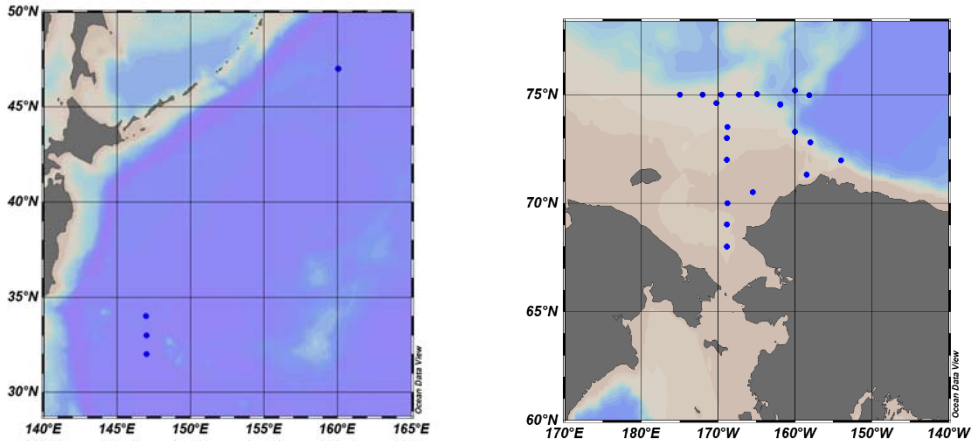

Figure 4.2-6. Sampling positions of nutrients sample.

(6) Certified Reference Material of nutrients in seawater

KANSO certified reference materials (CRMs, Lot: CE, CL, CO, CG) were used to ensure the comparability and traceability of nutrient measurements during this cruise. The details of CRMs are shown below.

Production

KANSO CRMs for inorganic nutrients in seawater were produced by KANSO Co.,Ltd. This CRM has been produced using autoclaved natural seawater based on the quality control system under ISO Guide 34 (JIS Q 0034).

KANSO Co.,Ltd. has been accredited under the Accreditation System of National Institute of Technology and Evaluation (ASNITE) as a CRM producer since 2011. (Accreditation No.: ASNITE 0052 R)

Property value assignment

The certified values were the arithmetic means of the results of 30 bottles from each batch (measured in duplicates) analyzed by both KANSO Co.,Ltd. and Japan Agency for Marine-Earth Science and Technology (JAMSTEC) using the colorimetric method (continuous flow analysis, CFA, method). The salinity of the calibration standards solution to obtain each calibration curve was adjusted to the salinity of the used CRMs within ± 0.5.

Metrological Traceability

Each certified value of nitrate, nitrite, and phosphate of KANSO CRMs were calibrated using one of Japan Calibration Service System (JCSS) standard solutions for each nitrate ions, nitrite ions, and phosphate ions. JCSS standard solutions were calibrated using the secondary solution of JCSS for each of these ions. The secondary solution of JCSS was calibrated using the specified primary solution produced by

Chemicals Evaluation and Research Institute (CERI), Japan. CERI specified primary solutions were calibrated using the National Metrology Institute of Japan (NMIJ) primary standards solution of nitrate ions, nitrite ions and phosphate ions, respectively.

For the certified value of silicate of KANSO CRM was calibrated using a newly established silicon standards solution named "exp64" produced by JAMSTEC and KANSO. This silicon standard solution was produced by a dissolution technique with an alkaline solution. The mass fraction of Si in the produced solution was calibrated based on NMIJ CRM 3645-a Si standard solution by a technology consulting system of National Institute of Advanced Industrial Science and Technology (AIST), and this value is traceable to the International System of Units (SI).

The certified values of nitrate, nitrite, and phosphate of KASNO CRM are thus traceable to the SI through the unbroken chain of calibrations, JCSS, CERI and NMIJ solutions as stated above, each having stated uncertainties. The certified values of silicate of KANSO CRM are traceable to the SI through the unbroken chain of calibrations, NMIJ CRM 3645-a02 Si standard solution, having stated uncertainties.

As stated in the certificate of NMIJ CRMs, each certified value of dissolved silica, nitrate ions, and nitrite ions was determined by more than one method using one of NIST SRM of silicon standard solution and NMIJ primary standards solution of nitrate ions and nitrite ions. The concentration of phosphate ions as stated information value in the certificate was determined NMIJ primary standards solution of phosphate ions. Those values in the certificate of NMIJ CRMs are traceable to the SI.

One of the analytical methods used for certification of NMIJ CRM for nitrate ions, nitrite ions, phosphate ions and dissolved silica was a colorimetric method (continuous mode and batch mode). The colorimetric method is the same as the analytical method (continuous mode only) used for certification of KANSO CRM. For certification of dissolved silica, exclusion chromatography/isotope dilution-inductively coupled plasma mass spectrometry and ion exclusion chromatography with post-column detection was used. For certification of nitrate ions, ion chromatography by direct analysis and ion chromatography after halogen-ion separation was used. For certification of nitrite ions, ion chromatography by direct analysis was used.

NMIJ CRMs were analyzed at the time of certification process for CRM and the results were confirmed within expanded uncertainty stated in the certificate of NMIJ CRMs.

(6.1) CRM for this cruise

15 sets of CRM lots CE, CL, CO and CG were used, which almost cover a range of nutrients concentrations in the Pacific Ocean and the Arctic Ocean.

Each CRM's serial number was randomly selected. The CRM bottles were stored at a room named "BIOCHEMICAL LABORATORY" on the ship, where the temperature was maintained around 19.78 degree Celsius – 23.78 degree Celsius.

(6.2) CRM concentration

Nutrients concentrations for the CRM lots CE, CL, CO and CG were shown in Table 4.2-3.

Table 4.2-3. Certified concentration and the uncertainty (k=2) of CRMs.

unit: μmol kg^{-1}

Lot	Nitrate	Nitrite*	Silicate	Phosphate	Ammonia***
CE**	0.01 ± 0.03	0.016 ± 0.01	0.06 ± 0.09	0.012 ± 0.006	0.69
CL	5.47 ± 0.15	0.015 ± 0.01	13.80 ± 0.30	0.425 ± 0.019	1.68
CO	15.86± 0.15	0.04 ± 0.04	34.72 ± 0.16	1.177 ± 0.014	0.54
CG	23.70 ± 0.20	0.06 ± 0.03	56.40 ± 0.50	1.700 ± 0.020	0.61

*Nitrite value will be changed. We need to check.

**Nitrate, silicate and phosphate values of CRM lot CE are not certified and shown as only reference values.

***Ammonia values are not certified and shown as only reference values.

(7) Nutrients standards

(7.1) Volumetric laboratory-ware of in-house standards

All volumetric glassware and polymethylpentene (PMP)-ware used were gravimetrically calibrated. Plastic volumetric flasks were gravimetrically calibrated at the temperature of use within 4 K at around 22 degree Celsius.

(7.1.1) Volumetric flasks

Volumetric flasks of Class quality (Class A) are used because their nominal tolerances are 0.05 % or less over the size ranges likely to be used in this work. Since Class A flasks are made of borosilicate glass, the standard solutions were transferred to plastic bottles as quickly as possible after the solutions were made up to volume and well mixed in order to prevent the excessive dissolution of silicate from the glass. PMP volumetric flasks was gravimetrically calibrated and used only within 4 K of the calibration temperature.

The computation of volume contained by the glass flasks at various temperatures other than the calibration temperatures were conducted by using the coefficient of linear expansion of borosilicate crown glass.

Because of their larger temperature coefficients of cubical expansion and lack of tables constructed for these materials, the plastic volumetric flasks were gravimetrically calibrated over the temperature range of the intended use and used at the temperature of calibration within 4 K. The weights obtained in the calibration weightings were corrected for the density of water and air buoyancy.

(7.1.2) Pipettes

All glass pipettes have nominal calibration tolerances of 0.1 % or better. These were gravimetrically calibrated to verify and improve upon this nominal tolerance.

(7.2) Reagents, general considerations

(7.2.1) Specifications

For nitrate standard, "potassium nitrate 99.995 suprapur®" provided by Merck, Batch B1452165, CAS No. 7757-79-1, was used.

For nitrite standard solution, we used a nitrite ion standard solution (NO_2^- 1000) provided by Wako, Lot ESQ6029, Code. No. 146-06453. This standard solution was certified by Wako using the ion chromatography method. Calibration result is 1001 mg L^{-1} at 20 degree Celsius. Expanded uncertainty of calibration (k=2) is 0.8 % for the calibration result.

For the silicate standard solution, we used our in-house Si standard solution "exp64" which was produced by alkali fusion technique from 5N SiO_2 powder produced jointly by JAMSTEC and KANSO. The mass fraction of Si in the "exp64" solution was calibrated based on NMIJ CRM 3645-a02 Si standard solution.

For phosphate standard, we used a potassium dihydrogen phosphate anhydrous 99.995 suprapur®" provided by Merck, Batch B1642908, CAS No.: 7778-77-0, was used.

For ammonia standard, ammonium chloride (CRM 3011-a) provided by NMIJ, CAS No. 12125-02-9 was used. The purity of this standard was reported as >99.9 % by the manufacture. Expanded uncertainty of calibration (k=2) was 0.022 %.

(7.2.2) Ultra-pure water

Ultra-pure water (Milli-Q water) freshly drawn was used for the preparation of reagents, standard solutions and for measurements of the reagent and the system blanks.

(7.2.3) Low nutrients seawater (LNSW)

Surface water having low nutrient concentration was taken and filtered using 0.20 μm pore capsule cartridge filter around 17S and 100E during MR19-04 cruise in February 2020. This water was drained into 20 L cubitainers and stored in a cardboard box.

Nutrients concentrations in LNSW were measured on August 2020. The averaged nutrient concentrations in the LNSW were 0.00 μmol L^{-1} for nitrite, 0.00 μmol L^{-1} for nitrate, 1.93 μmol L^{-1} for silicate, 0.081 μmol L^{-1} for phosphate and 0.00 μmol L^{-1} for ammonia. The concentrations of nitrate, nitrite and ammonia were lower than detection limit as stated in chapter (8.5).

(7.2.4) Concentrations of nutrients for A, D, B and C standards

Concentrations of nutrients for A, D, B and C standards were adjusted as shown in Tables 4.2-4(a) and (b). We analyzed samples at stations 002, 003 and 004 using the

standard solution set 4.2-4(a), and the samples at the rest of the stations were used the standard solution set 4.2-4(b).

We used JAMSTEC-KANSO in-house Si standard solution for A standard of silicate, which doesn't need to neutralize by the hydrochloric acid. B standard was diluted from A standard with the following recipes shown in Tables 4.2-5(a) and (b). In order to match the salinity and the density of the stock solution (B standard) to the LNSW, during this dilution step, B standard was added the solution that 14.950 g of a sodium chloride powder was dissolved in pure water, and then the final volume was adjusted to 500 mL.

The C standard solution was prepared in the LNSW following the recipes shown in Table 4.2-5(c). All volumetric laboratory tools were calibrated prior the cruise as stated in chapter (7.1). Then the actual concentrations of nutrients in each fresh standard solution were calculated based on the ambient and the solution temperature, together with the determined factors of volumetric laboratory wares.

The calibration curves for each run were obtained using 5 levels, C-1 (LNSW), C-2, C-3, C-4 and C-5 that were diluting using the B standard solution.

The D standard solutions were made to calculate the reduction rate of Cd coil. The D standard was diluted from the A standard solution into the pure water, final concentrations were shown in Tables 4.2-4 (a) and (b).

Table 4.2-4(a). Nominal concentrations of nutrients for A, D, B and C standards for station 002, 003 and 004.

Unit: μmol kg^{-1}

	A	B	D	C-1	C-2	C-3	C-4	C-5
NO_3	45100	898	900	LNSW	9.0	18	37	54
NO_2	21800	26	870	LNSW	0.3	0.5	1.0	1.6
SiO_2	35600	2850		LNSW	30	59	116	172
PO_4	6000	60		LNSW	0.7	1.3	2.5	3.7
NH_4	4000	160		LNSW	1.6	3.2	6.4	9.6

Table 4.2-4(b). Nominal concentrations of nutrients for A, D, B and C standards for the other stations.

Unit: μmol kg^{-1}

	A	B	D	C-1	C-2	C-3	C-4	C-5
NO_3	45100	898	900	LNSW	9.0	18	37	54
NO_2	21800	26	870	LNSW	0.3	0.5	1.0	1.6
SiO_2	35600	1425		LNSW	16	30	59	87
PO_4	6000	60		LNSW	0.7	1.3	2.5	3.7
NH_4	4000	160		LNSW	1.6	3.2	6.4	9.6

Table 4.2-5(a). B standard recipes for Stations 002, 003 and 004. Final volume was 500 mL.

	A Std.
NO_3	10 mL
NO_2	15 mL
SiO_2	40 mL
PO_4	5 mL
NH_4	20 mL

Table 4.2-5(b). B standard recipes for the other stations. Final volume was 500 mL.

	A Std.
NO_3	10 mL
NO_2	15 mL
SiO_2	20 mL
PO_4	5 mL
NH_4	20 mL

Table 4.2-5(c). Working calibration standard recipes. Final volume was 500 mL.

C Std.	B Std.
C-2	5 mL
C-3	10 mL
C-4	20 mL
C-5	30 mL

(7.2.5) Renewal of in-house standard solutions

In-house standard solutions as stated in paragraph (7.2.4) were remade by each "renewal time" shown in Tables 4.2-6(a) to (c).

Table 4.2-6(a). Timing of renewal of in-house standards.

NO_3, NO_2, SiO_2, PO_4, NH_4	Renewal time
A-1 Std. (NO_3)	maximum a month
A-2 Std. (NO_2)	commercial prepared solution
A-3 Std. (SiO_2)	JAMSTEC-KANSO Si standard solution
A-4 Std. (PO_4)	maximum a month
A-5 Std. (NH_4)	maximum a month
D-1 Std.	maximum 8 days
D-2 Std.	maximum 8 days
B Std. (mixture of A-1, D-2, A-3, A-4 and A-5 std.)	maximum 8 days

Table 4.2-6(b). Timing of renewal of working calibration standards.

Working standards	Renewal time
C Std. (diluted from B Std.)	every 24 hours

Table 4.2-6(c). Timing of renewal of in-house standards for reduction estimation.

Reduction estimation	Renewal time
36 μM NO_3 (diluted D-1 Std.)	when C Std. renewed
35 μM NO_2 (diluted D-2 Std.)	when C Std. renewed

(8) Quality control

(8.1) The precision of the nutrient analyses during the cruise

The highest standard solution (C-5) was repeatedly determined every 8 to 15 samples to obtain the analytical precision of the nutrient analyses during this cruise. During each run, the total number of the C-5 determination was 7-15 times depending on the run. Each run, we obtained the analytical precision based on this C-5 results, shown in Figures 4.2-7 to 4.2-11. In this cruise, there was total 19 runs. Except for a few runs, the analytical precisions were less than 0.2% for nitrate (Figure 4.2-7), silicate (Figure 4.2-9), and phosphate (Figure 4.2-10).

The overall precisions throughout this cruise were calculated based on the analytical precisions obtained from all of the runs, and shown in Table 4.2-7. During this cruise, overall median precisions were 0.13 % for nitrate, 0.16 % for nitrite, 0.10 % for silicate, 0.14 % for phosphate and 0.29 % for ammonia, respectively. The overall median precision for each parameter during this cruise was comparable to the previously published the precisions during the R/V Mirai cruises conducted in 2009 - 2019.

Table 4.2-7. Summary of overall precision based on the replicate analyses (k=1).

	Nitrate CV %	Nitrite CV %	Silicate CV %	Phosphate CV %	Ammonia CV %
Median	0.13	0.16	0.10	0.14	0.29
Mean	0.13	0.18	0.11	0.14	0.29
Maximum	0.24	0.34	0.16	0.18	0.47
Minimum	0.06	0.09	0.05	0.10	0.12
N	19	19	19	19	19

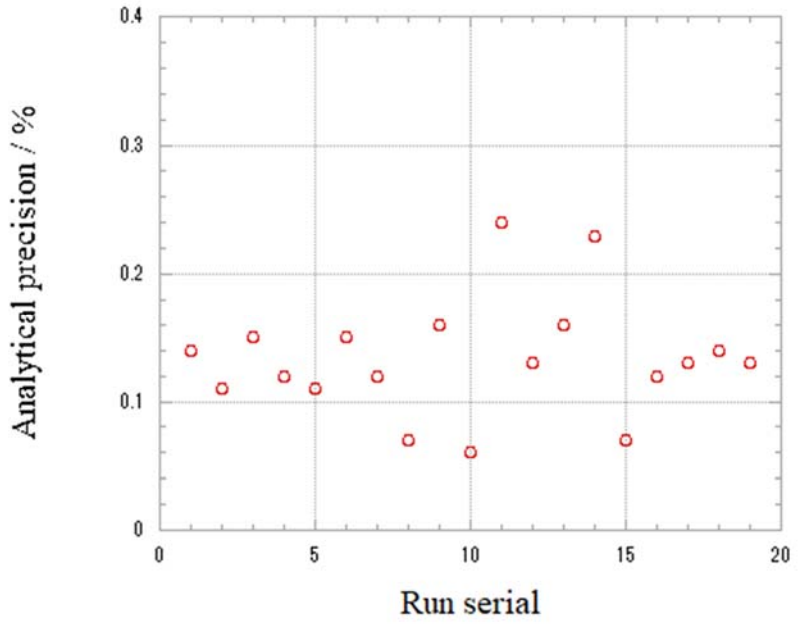

Figure 4.2-7. Time series of precision of nitrate in MR20-05C.

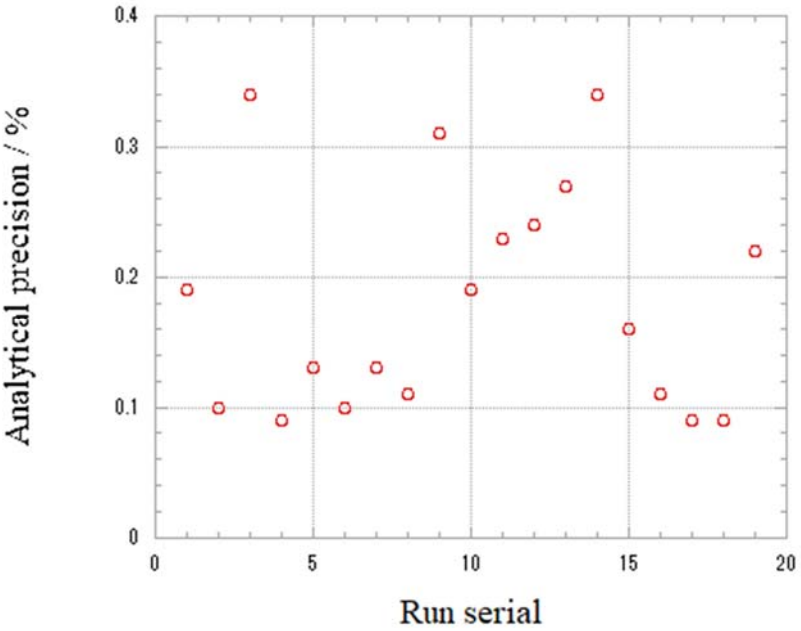

Figure 4.2-8. Same as Figure 4.2-7, but for nitrite.

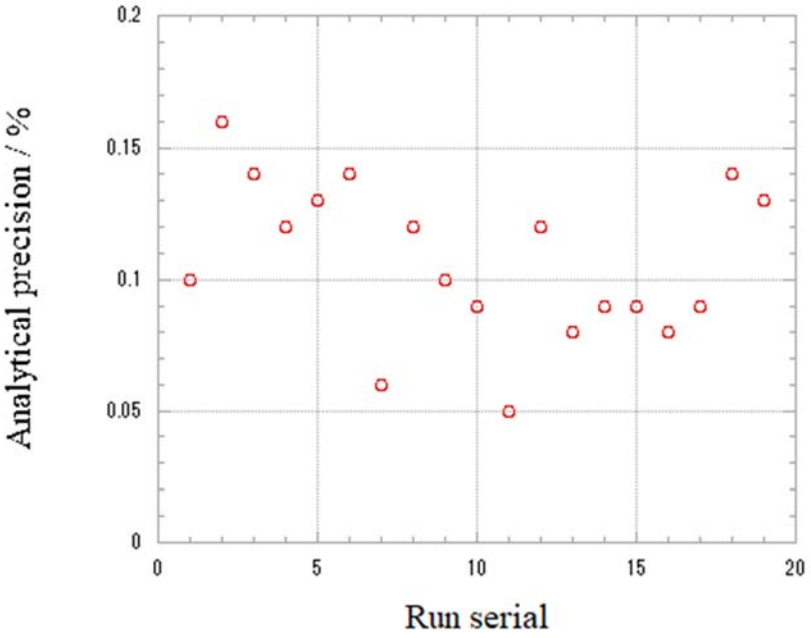

Figure 4.2-9. Same as Figure 4.2-7, but for silicate.

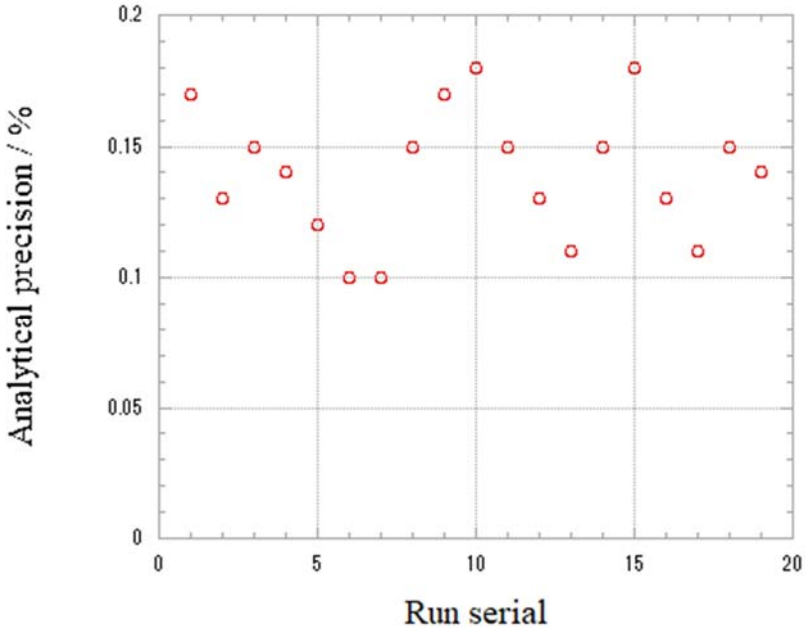

Figure 4.2-10. Same as Figure 4.2-7, but for phosphate.

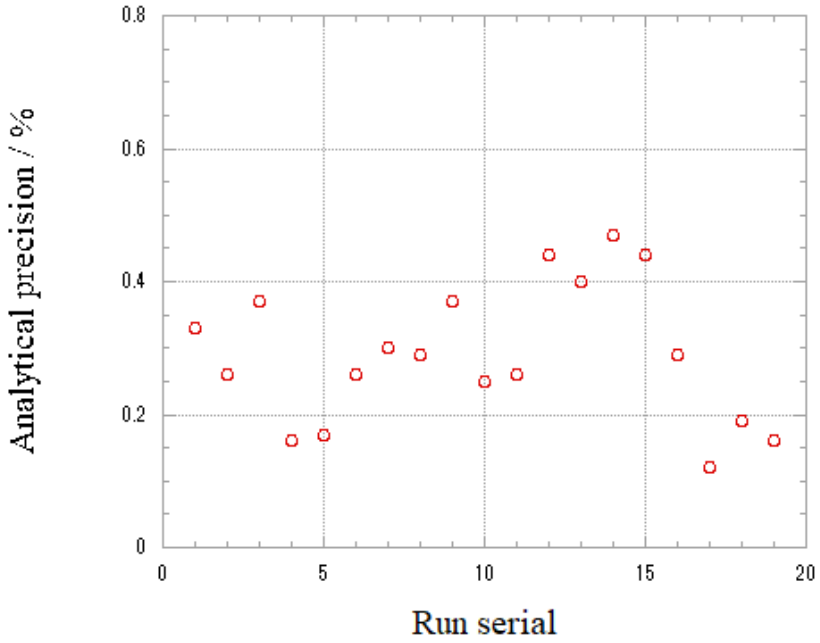

Figure 4.2-11. Same as Figure 4.2-7, but for ammonia.

(8.2) CRM lot. CG measurement during this cruise

CRM lot. CG was measured every run to evaluate the comparability throughout the cruise. The all of the results of lot. CG during this cruise were shown as Figures 4.2-12 to 4.2-16. All of the measured concentrations of CRM lot. CG was within the uncertainty of certified values for nitrate, nitrite, silicate and phosphate. The reported CRM values were shown in Table 4.2-3.

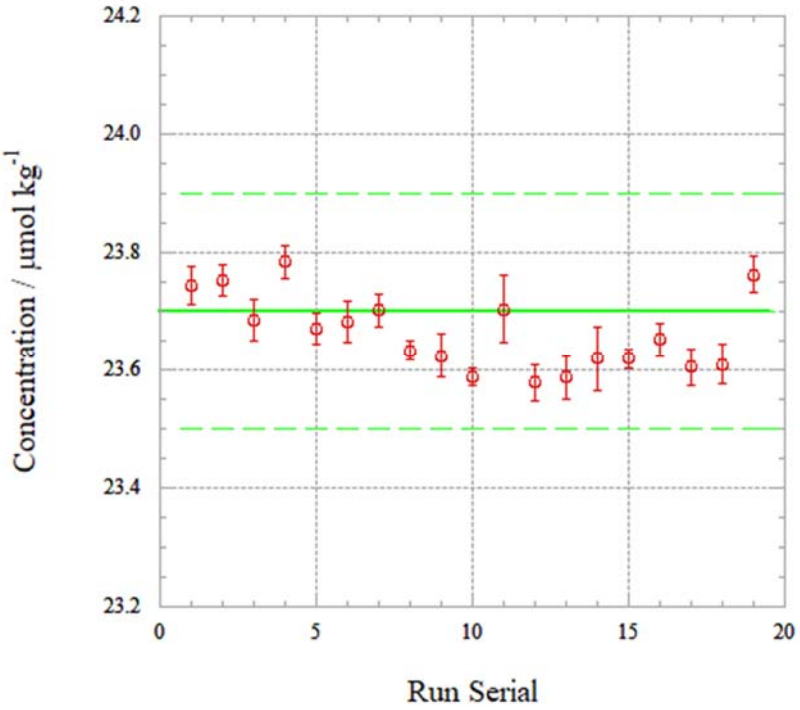

Figure 4.2-12. Time series of CRM-CG of nitrate in MR20-05C. Solid green line is certified nitrate concentration of CRM and dotted green line show uncertainty of certified value at k=2.

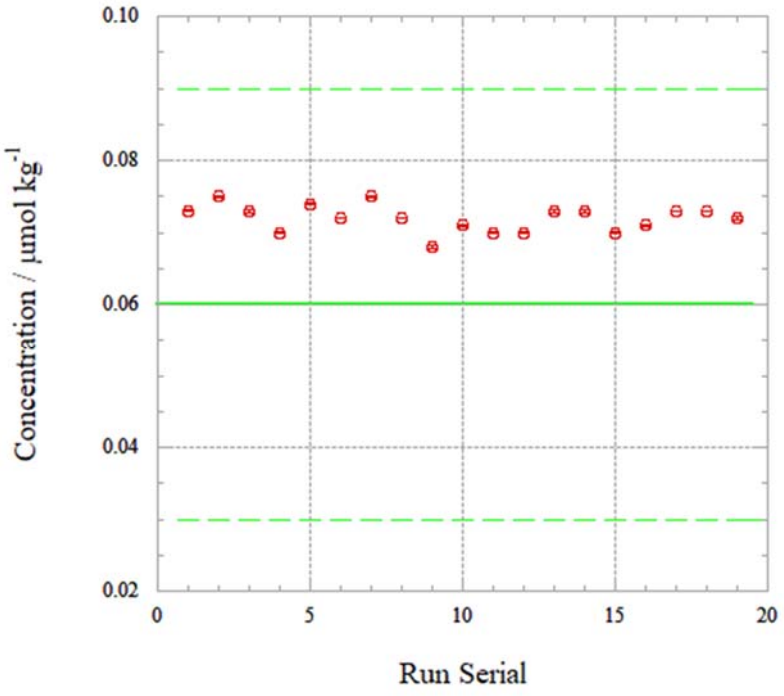

Figure 4.2-13. Same as Figure 4.2-12, but for nitrite.

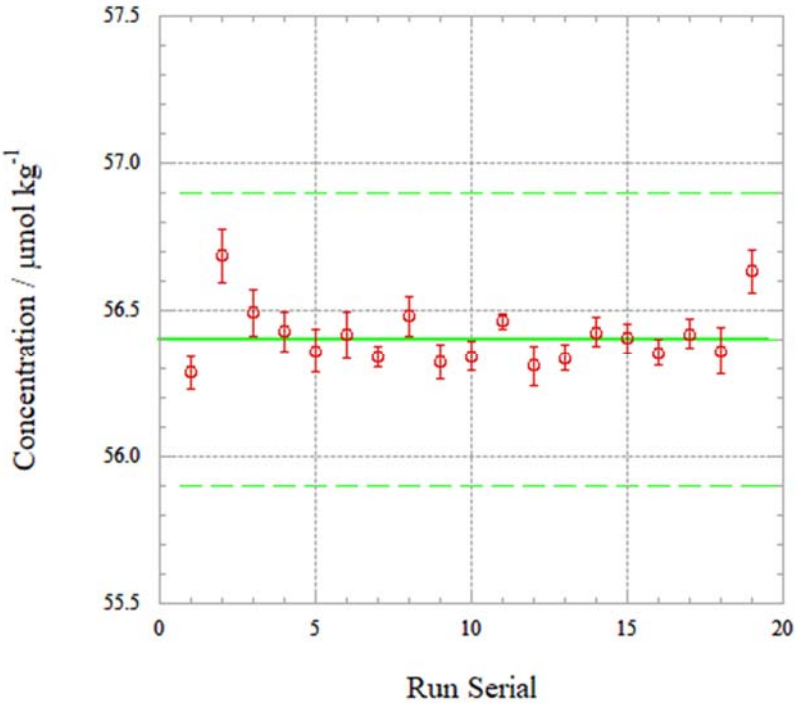

Figure 4.2-14. Same as Figure 4.2-12, but for silicate.

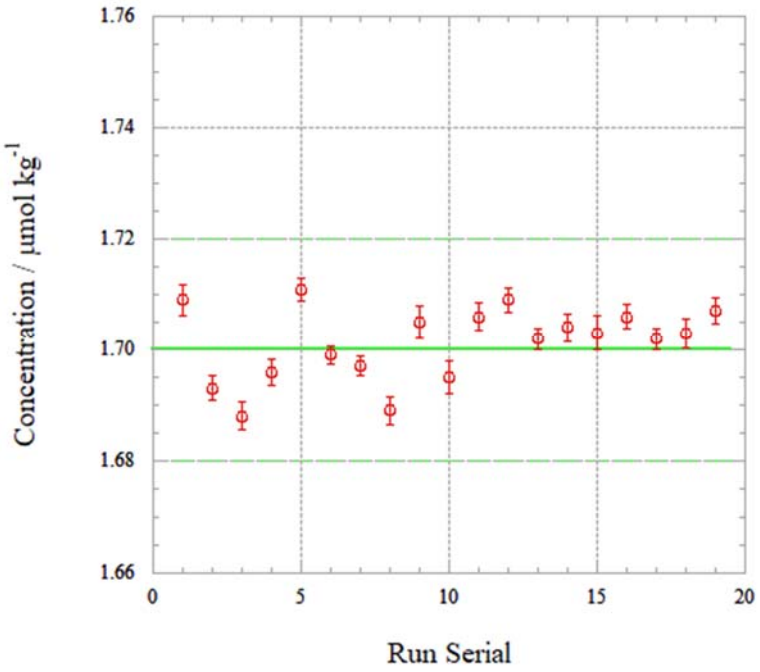

Figure 4.2-15. Same as Figure 4.2-12, but for phosphate.

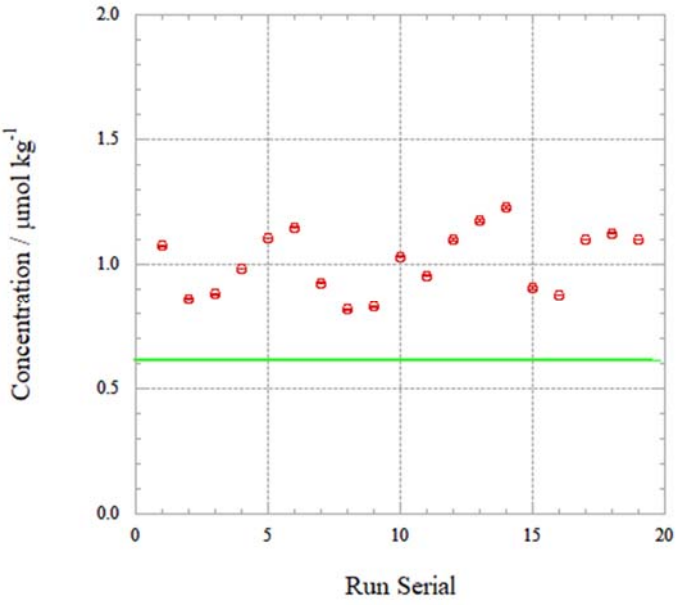

Figure 4.2-16. Time series of CRM-CG of ammonia in MR20-05C. Green line is reference value for ammonia concentration of CRM-CG.

(8.3) Carryover

We also summarized the magnitudes of carry over throughout the cruise. In order to evaluate carryover in each run, we conducted determinations C-5 followed by determination of LNSW twice. The difference from LNSW-1 to LNSW-2 was obtained and used for this "carryover" evaluation. The Carryover (%) was obtained from the following equation.

Carryover (%) = (LNSW-1 – LNSW-2) / (C-5 – LNSW-2) * 100 (%)

The summary of the carryover (%) was shown in Table 4.2-8. The results were low % (~0.1 % for nitrate and nitrite; ~0.2% for silicate and phosphate; <1% for ammonia). The low % indicates that there is no significant issue during this cruise.

Table 4.2-8. Summary of carryover throughout MR20-05C.

	Nitrate %	Nitrite %	Silicate %	Phosphate %	Ammonia %
Median	0.13	0.07	0.21	0.24	0.74
Mean	0.14	0.09	0.20	0.24	0.75
Maximum	0.22	0.34	0.25	0.33	1.18
Minimum	0.10	0.00	0.14	0.16	0.38
N	19	19	19	19	19

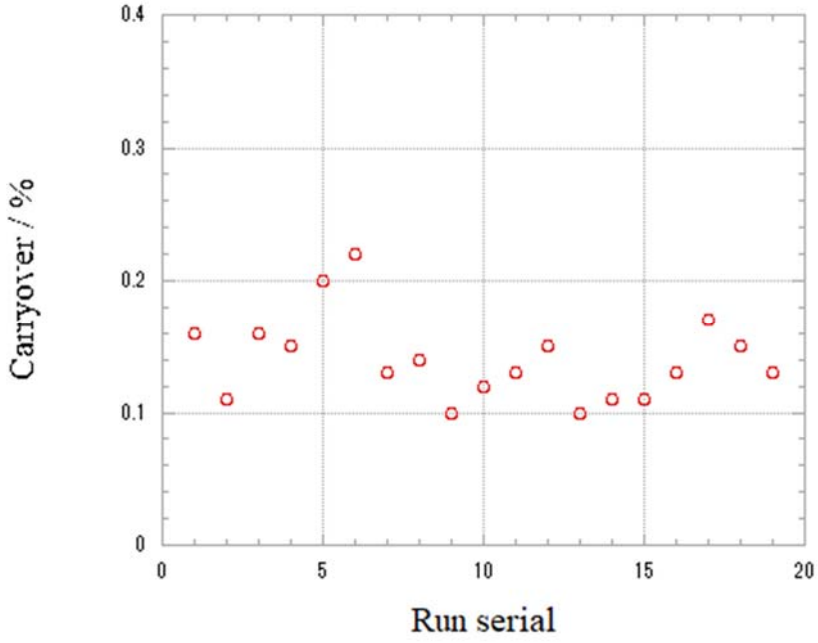

Figure 4.2-17. Time series of carry over of nitrate in MR20-05C.

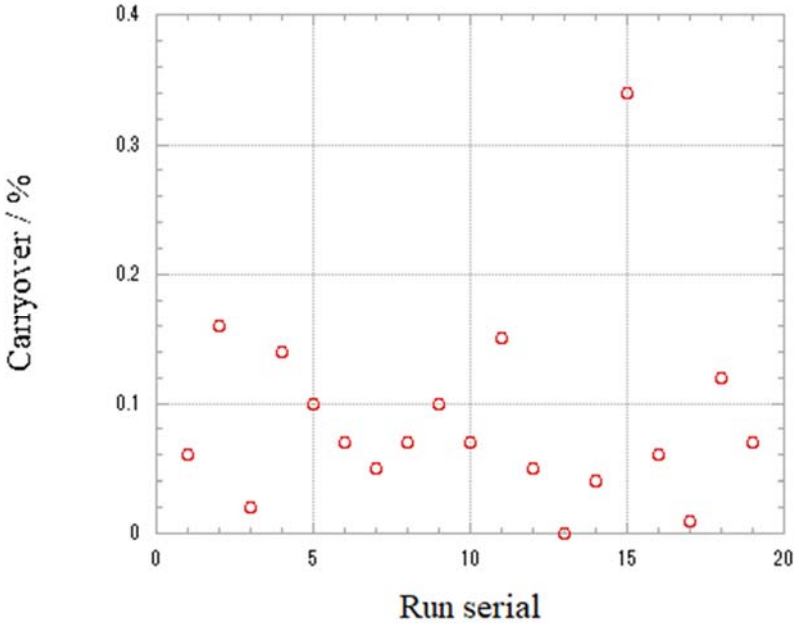

Figure 4.2-18. Same as Figure 4.2-17, but for nitrite.

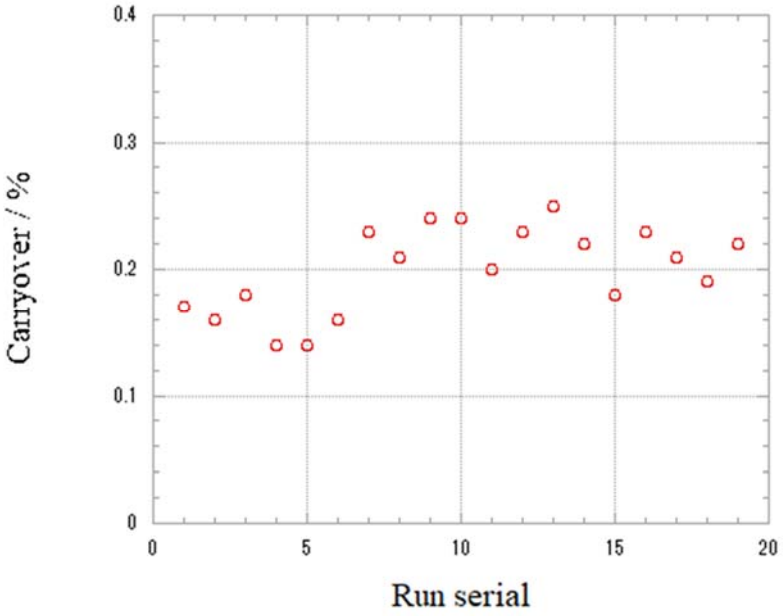

Figure 4.2-19. Same as Figure 4.2-17, but for silicate.

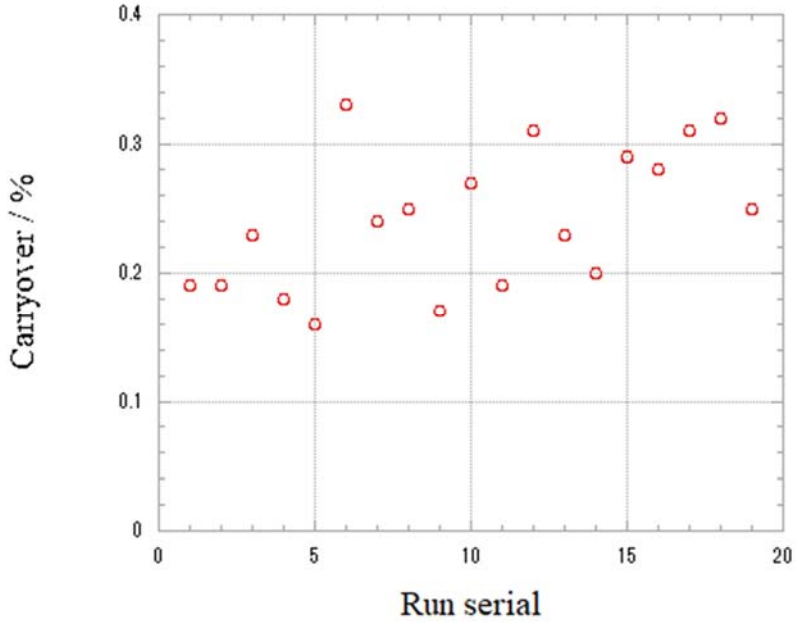

Figure 4.2-20. Same as Figure 4.2-17, but for phosphate.

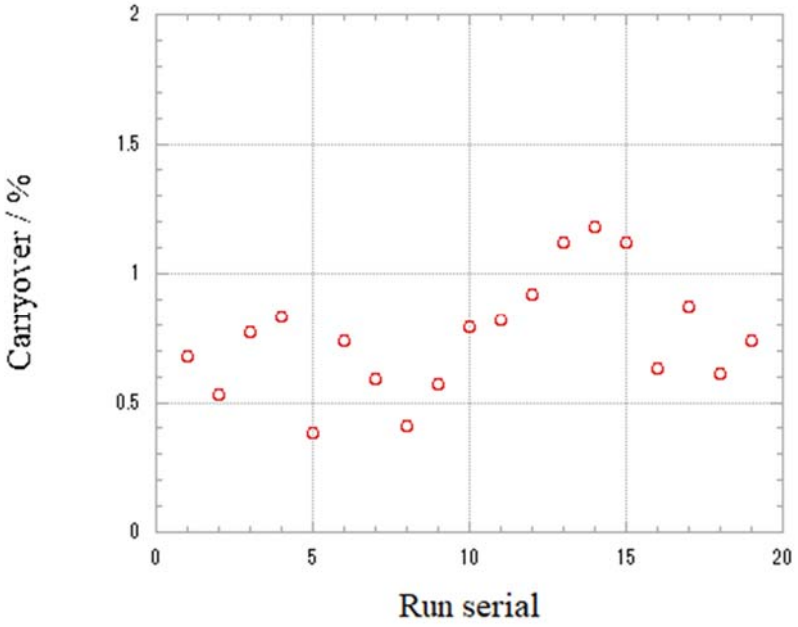

Figure 4.2-21. Same as Figure 4.2-17, but for ammonia.

(8.4) Estimation of uncertainty of nitrate, silicate, phosphate, nitrite and ammonia concentrations

Empirical equations, eq. (1), (2) and (3) to estimate the uncertainty of measurement of nitrate, silicate and phosphate were obtained based on 19 measurements of 15 sets of CRMs (Table 4.2-3). These empirical equations are as follows, respectively.

Nitrate Concentration C_{NO3} in µmol kg^{-1}:
Uncertainty of measurement of nitrate (%) = 0.26588 + 0.69976 * (1 / C_{NO3}) -- (1)
where C_{NO3} is nitrate concentration of sample.

Silicate Concentration C_{SiO2} in µmol kg^{-1}:
Uncertainty of measurement of silicate (%) = 0.15872 + 3.219 * (1 / C_{SiO2}) --- (2)
where C_{SiO2} is silicate concentration of sample.

Phosphate Concentration C_{PO4} in µmol kg^{-1}:
Uncertainty of measurement of phosphate (%) = 0.14647 + 0.321 * (1 / C_{PO4}) --- (3)
where C_{PO4} is phosphate concentration of sample.

Empirical equations, eq. (4) and (5) to estimate the uncertainty of measurement of nitrite and ammonia were obtained based on duplicate measurements of the samples.

Nitrite Concentration C_{NO2} in µmol kg^{-1}:
Uncertainty of measurement of nitrite (%) =
– 0.2323 + 0.25252 * (1 / C_{NO2}) – 0.00054968 * (1 / C_{NO2}) * (1 / C_{NO2}) --- (4)
where C_{NO2} is nitrite concentration of sample.

Ammonia Concentration C_{NH4} in µmol kg^{-1}:
Uncertainty of measurement of ammonia (%) =
0.64627 + 1.4308 * (1 / C_{NH4}) --- (5)
where C_{NH4} is ammonia concentration of sample.

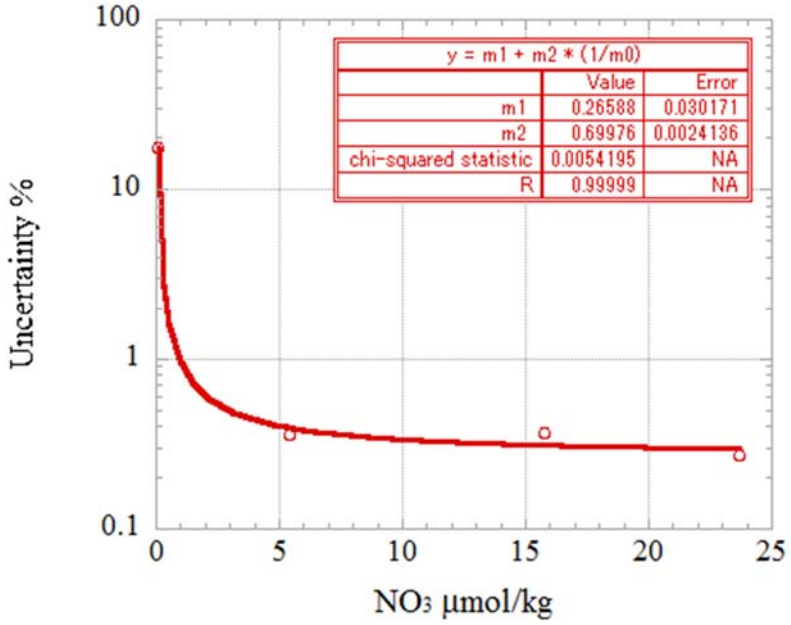

Figure 4.2-22. Estimation of uncertainty for nitrate.

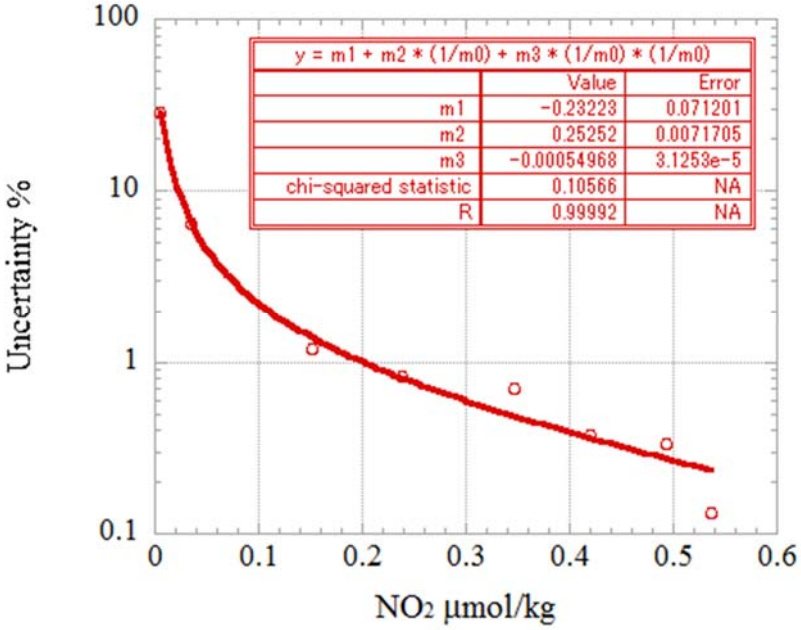

Figure 4.2-23. Estimation of uncertainty for nitrite.

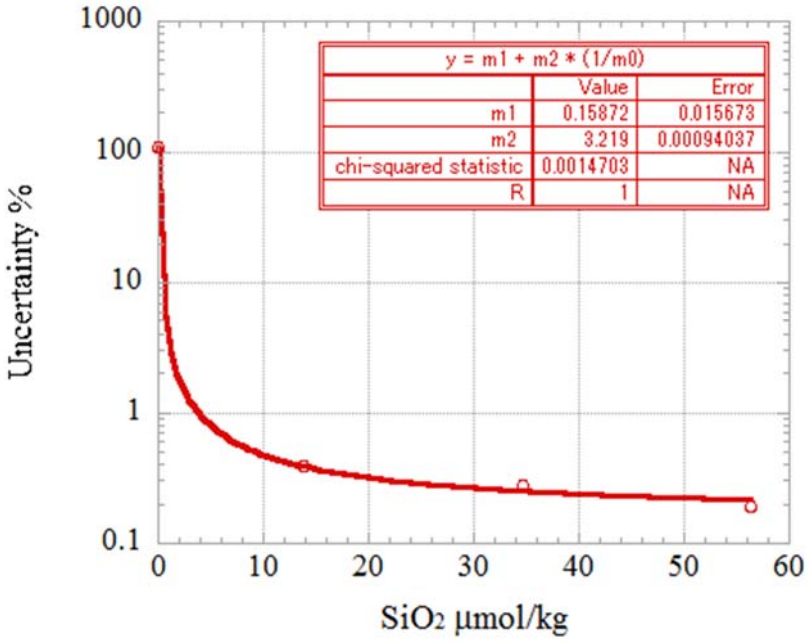

Figure 4.2-24. Estimation of uncertainty for silicate.

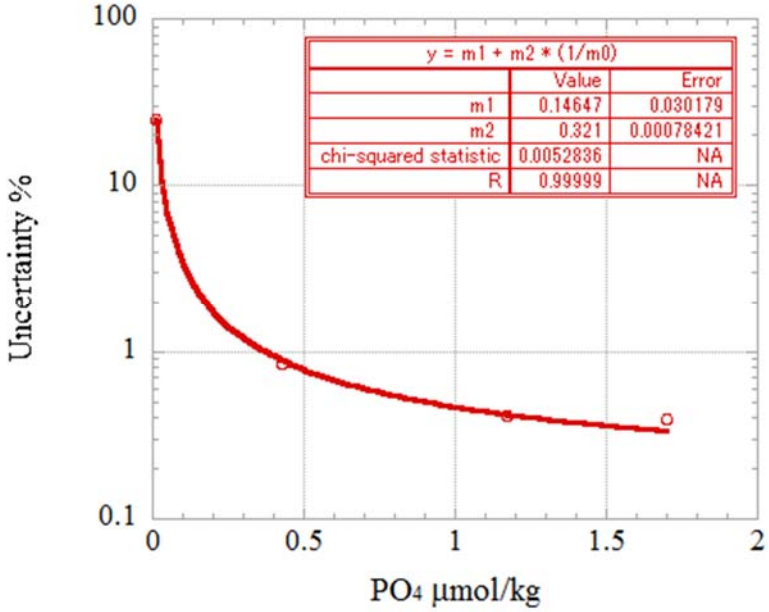

Figure 4.2-25. Estimation of uncertainty for phosphate.

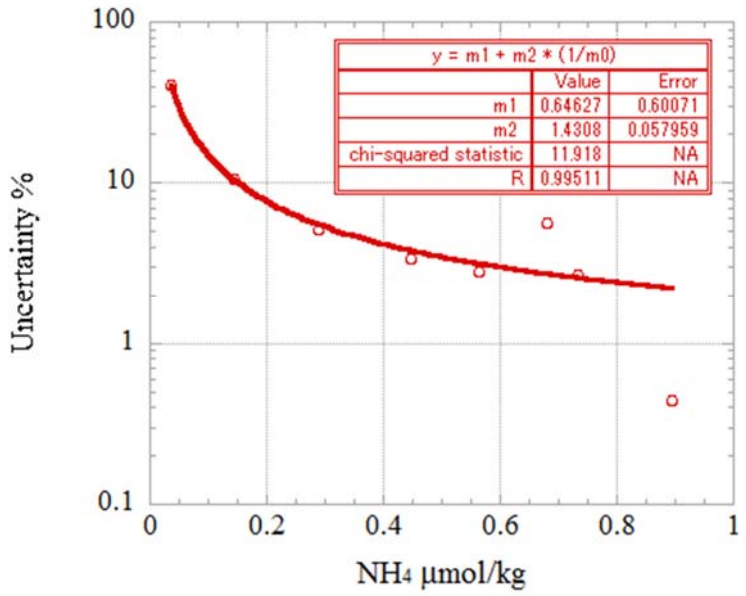

Figure 4.2-26. Estimation of uncertainty for ammonia.

(8.5) Detection limit and quantitative determination of nutrients analyses during the cruise

The LNSW was determined every 8 to 15 samples to obtain detection limit of the nutrient analyses during this cruise. During each run, the total number of the LNSW determination was 7-15 times depending on the run. The detection limit was calculated based on the LNSW results obtained from all the runs by the following equation.

Detection limit = 3 * standard deviation of repeated measurement of LNSW

The summary of detection limit are shown in Table 4.2-9. During in this cruise, detection limit were 0.03 µmol kg^{-1} for nitrate, 0.00 µmol kg^{-1} for nitrite, 0.07 µmol kg^{-1} for silicate, 0.005 µmol kg^{-1} for phosphate and 0.05 µmol kg^{-1} for ammonia, respectively.

The quantitative determination of nutrient analyses is the concentration of which uncertainty is 33 % in the empirical equations, eq. (1) to (5) in chapter (8.4). The summary of quantitative determination are shown in Table 4.2-9. During in this cruise, the quantitative determination were 0.02 µmol kg^{-1} for nitrate, 0.01 µmol kg^{-1} for nitrite, 0.10 µmol kg^{-1} for silicate, 0.010 µmol kg^{-1} for phosphate and 0.04 µmol kg^{-1} for ammonia, respectively.

Table 4.2-9. Summary of detection limit and quantitative determination.

	Nitrate µmol kg^{-1}	Nitrite µmol kg^{-1}	Silicate µmol kg^{-1}	Phosphate µmol kg^{-1}	Ammonia µmol kg^{-1}
Detection limit	0.03	0.00	0.07	0.005	0.05
Quantitative determination	0.02	0.01	0.10	0.010	0.04

(9) Problems and our actions/solutions

There is no significant issue of this data set during this cruise.

(10) List of reagents

List of reagents is shown in Table 4.2-10.

Table 4.2-10. List of reagent in MR20-05C.

IUPAC name	CAS Number	Formula	Compound Name	Manufacture	Grade
4-Aminobenzenesulfonamide	63-74-1	$C_6H_8N_2O_2S$	Sulfanilamide	FUJIFILM Wako Pure Chemical Corporation	JIS Special Grade
Ammonium sulfate	7783-20-2	$(NH_4)_2SO_4$	Ammonium Sulfate	National Metrology Institute of Japan	Certified Reference Material
Antimony potassium tartrate trihydrate	28300-74-5	$K_2(SbC_4H_2O_6)_2 \cdot 3H_2O$	Bis[(+)-tartrato]diantimonate(III) Dipotassium Trihydrate	FUJIFILM Wako Pure Chemical Corporation	JIS Special Grade
Boric acid	10043-35-3	H_3BO_3	Boric Acid	FUJIFILM Wako Pure Chemical Corporation	JIS Special Grade
Hydrogen chloride	7647-01-0	HCl	Hydrochloric Acid	FUJIFILM Wako Pure Chemical Corporation	JIS Special Grade
Imidazole	288-32-4	$C_3H_4N_2$	Imidazole	FUJIFILM Wako Pure Chemical Corporation	JIS Special Grade
L-Ascorbic acid	50-81-7	$C_6H_8O_6$	L-Ascorbic Acid	FUJIFILM Wako Pure Chemical Corporation	JIS Special Grade
N-(1-Naphthalenyl)-1,2-ethanediamine, dihydrochloride	1465-25-4	$C_{12}H_{16}Cl_2N_2$	N-1-Naphthylethylenediamine Dihydrochloride	FUJIFILM Wako Pure Chemical Corporation	for Nitrogen Oxides Analysis
Oxalic acid	144-62-7	$C_2H_2O_4$	Oxalic Acid	FUJIFILM Wako Pure Chemical Corporation	Wako Special Grade
Phenol	108-95-2	C_6H_6O	Phenol	FUJIFILM Wako Pure Chemical Corporation	JIS Special Grade
Potassium nitrate	7757-79-1	KNO_3	Potassium Nitrate	Merck KGaA	Suprapur®
Potassium dihydrogen phosphate	7778-77-0	KH_2PO_4	Potassium dihydrogen phosphate anhydrous	Merck KGaA	Suprapur®
Sodium chloride	7647-14-5	NaCl	Sodium Chloride	FUJIFILM Wako Pure Chemical Corporation	TraceSure®
Sodium citrate dihydrate	6132-04-3	$Na_3C_6H_5O_7 \cdot 2H_2O$	Trisodium Citrate Dihydrate	FUJIFILM Wako Pure Chemical Corporation	JIS Special Grade
Sodium dodecyl sulfate	151-21-3	$C_{12}H_{25}NaO_4S$	Sodium Dodecyl Sulfate	FUJIFILM Wako Pure Chemical Corporation	for Biochemistry
Sodium hydroxide	1310-73-2	NaOH	Sodium Hydroxide for Nitrogen Compounds Analysis	FUJIFILM Wako Pure Chemical Corporation	for Nitrogen Analysis
Sodium hypochlorite	7681-52-9	NaClO	Sodium Hypochlorite Solution	Kanto Chemical co., Inc.	Extra pure
Sodium molybdate dihydrate	10102-40-6	$Na_2MoO_4 \cdot 2H_2O$	Disodium Molybdate(VI) Dihydrate	FUJIFILM Wako Pure Chemical Corporation	JIS Special Grade
Sodium nitroferricyanide dihydrate	13755-38-9	$Na_2[Fe(CN)_5NO] \cdot 2H_2O$	Sodium Pentacyanonitrosylferrate(III) Dihydrate	FUJIFILM Wako Pure Chemical Corporation	JIS Special Grade
Sulfuric acid	7664-93-9	H_2SO_4	Sulfuric Acid	FUJIFILM Wako Pure Chemical Corporation	JIS Special Grade
tetrasodium;2-[2-[bis(carboxylatomethyl)amino]ethyl-(carboxylatomethyl)amino]acetate;tetrahydrate	13235-36-4	$C_{10}H_{12}N_2Na_4O_8 \cdot 4H_2O$	Ethylenediamine-N,N,N',N'-tetraacetic Acid Tetrasodium Salt Tetrahydrate (4NA)	Dojindo Molecular Technologies, Inc.	-
Synonyms: t-Octylphenoxypolyethoxyethanol 4-(1,1,3,3-Tetramethylbutyl)phenyl-polyethylene glycol Polyethylene glycol tert-octylphenyl ether	9002-93-1	$(C_2H_4O)_nC_{14}H_{22}O$	Triton™ X-100	Sigma-Aldrich Japan G.K.	-

(11) Data archives

These data obtained in this cruise will be submitted to the Data Management Group (DMG) of JAMSTEC, and will be opened to the public via "Data Research System for Whole Cruise Information in JAMSTEC (DARWIN)" in JAMSTEC web site. <http://www.godac.jamstec.go.jp/darwin/e>

(12) References

Susan Becker, Michio Aoyama E. Malcolm S. Woodward, Karel Bakker, Stephen Coverly, Claire Mahaffey, Toste Tanhua, (2019) The precise and accurate determination of dissolved inorganic nutrients in seawater, using Continuous Flow Analysis methods, n: The GO-SHIP Repeat Hydrography Manual: A Collection of Expert Reports and Guidelines. Available online at: http://www.go-ship.org/HydroMan.html. DOI: http://dx.doi.org/10.25607/OBP-555

Grasshoff, K. 1976. Automated chemical analysis (Chapter 13) in Methods of Seawater Analysis. With contribution by Almgreen T., Dawson R., Ehrhardt M., Fonselius S. H., Josefsson B., Koroleff F., Kremling K. Weinheim, New York: Verlag Chemie.

Grasshoff, K., Kremling K., Ehrhardt, M. et al. 1999. Methods of Seawater Analysis. Third, Completely Revised and Extended Edition. WILEY-VCH Verlag GmbH, D-69469 Weinheim (Federal Republic of Germany).

Hydes, D.J., Aoyama, M., Aminot, A., Bakker, K., Becker, S., Coverly, S., Daniel, A., Dickson, A.G., Grosso, O., Kerouel, R., Ooijen, J. van, Sato, K., Tanhua, T., Woodward, E.M.S., Zhang, J.Z., 2010. Determination of Dissolved Nutrients (N, P, Si) in Seawater with High Precision and Inter-Comparability Using Gas-Segmented Continuous Flow Analysers, In: GO-SHIP Repeat Hydrography Manual: A Collection of Expert Reports and Guidelines. IOCCP Report No. 14, ICPO Publication Series No 134.

Kimura, 2000. Determination of ammonia in seawater using a vaporization membrane permeability method. 7th auto analyzer Study Group, 39-41.

Murphy, J., and Riley, J.P. 1962. Analytica Chimica Acta 27, 31-36.

4.3. Dissolved inorganic carbon

4.3.1. Bottled-water analysis

(1) Personnel

Akihiko Murata (JAMSTEC) – Principal investigator, Not on board
Nagisa Fujiki (Marine Works Japan Ltd.; MWJ) – Operation leader
Yuta Oda (MWJ)
Hiroshi Hoshino (MWJ)

(2) Objective

To clarify vertical distributions of total dissolved inorganic carbon (DIC) in water columns.

(3) Parameter

Total dissolved Inorganic Carbon (DIC)

(4) Instruments and Methods

a. Seawater sampling

Seawater samples were collected by 12 liter Niskin bottles mounted on the CTD/Carousel Water Sampling System and a bucket at 96 stations. Seawater was sampled in a 250 mL glass bottle (SHOTT DURAN) that was previously soaked in 5 % alkaline detergent solution at least 3 hours and was cleaned by fresh water for 5 times and Milli-Q ultrapure water for 3 times. A sampling silicone rubber tube with PFA tip was connected to the outlet of Niskin bottle for water sampling. The glass bottles were filled from its bottom gently, without rinsing, and were overflowed for 20 seconds. They were sealed using the polyethylene inner lids with its diameter of 29 mm with care not to leave any bubbles in the bottle. Immediately after the water sampling on the deck, the glass bottles were carried to the laboratory for the addition of saturated solution of mercury (II) chloride ($HgCl_2$). Small volume (3 mL) of the sample (1 % of the bottle volume) was removed from the bottle and 100 μL of $HgCl_2$ was added. Then the samples were sealed by the polyethylene inner lids with its diameter of 31.9 mm and stored in a refrigerator at approximately 5 °C. About one hour before the analysis, the samples were taken from refrigerator and put in the water bath kept ~20 °C.

b. Seawater analysis

Measurements of DIC were made with total CO_2 measuring system (Nihon ANS Inc.). The system comprises of seawater dispensing unit, a CO_2 extraction unit, and a coulometer (Model 3000, Nihon ANS Inc.) The seawater dispensing unit has an auto-sampler (6 ports), which dispenses the seawater from a glass bottle to a pipette of nominal 15 mL volume. The pipette was kept at 20.00 °C ± 0.05 °C by a water jacket, in which water circulated through a thermostatic water bath. The CO_2 dissolved in a seawater sample is extracted in a stripping chamber of the CO_2 extraction unit by adding

10 % phosphoric acid solution. The stripping chamber is made approx. 25 cm long and has a fine frit at the bottom. First, a constant volume of acid is added to the stripping chamber from its bottom by pressurizing an acid bottle with nitrogen gas (99.9999 %). Second, a seawater sample kept in a pipette is introduced to the stripping chamber by the same method. The seawater and phosphoric acid are stirred by the nitrogen bubbles through a fine frit at the bottom of the stripping chamber. The stripped CO_2 is carried to the coulometer through two electric dehumidifiers (kept at 2 °C) and a chemical desiccant (magnesium perchlorate) by the nitrogen gas (flow rate of 140 mL min-1). Measurements of system blank (phosphoric acid blank), 1.5 % CO_2 standard gas in a nitrogen base, and seawater samples (6 samples) were programmed to repeat. The variation of our own made JAMSTEC DIC reference material was used to correct the signal drift results from chemical alternation of coulometer solutions. The values of DIC were set to the certified values of CRM (Batch 190) provided by Prof. Dickson, Scripps Institution of Oceanography, Univ. of California.

(5) Observation log

Seawater samples were collected at 24 stations.

(6) Preliminary results

A few replicate samples were taken at most of the stations and difference between each pair of analyses was plotted on a range control chart (Figure 4.3.1-1). The repeatability was estimated to be provisionally 0.63 μmol kg^{-1} (n=49).

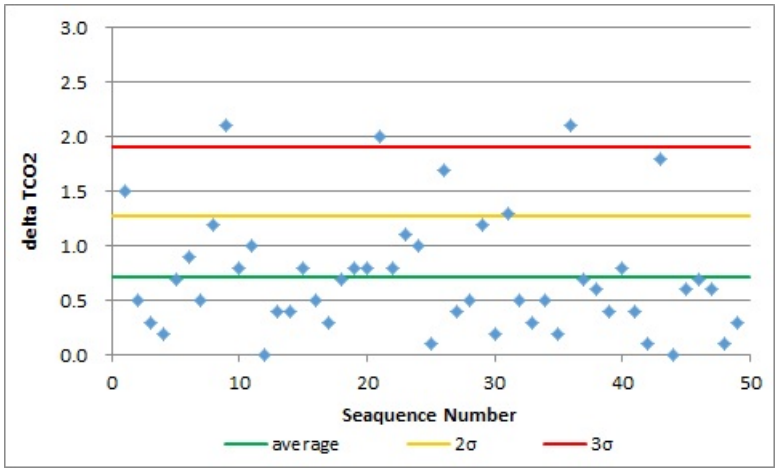

Figure 4.3.1-1. Range control chart of the absolute differences of replicate measurements of DIC carried out during this cruise. The 2σ and 3σ indicate the upper control limits of standard deviation (σ) × 2 and σ × 3, respectively.

(7) Data archives

These data obtained in this cruise will be submitted to the Data Management Group (DMG) of JAMSTEC, and will be opened to the public via "Data Research System for Whole Cruise Information in JAMSTEC (DARWIN)" in JAMSTEC web site.

<http://www.godac.jamstec.go.jp/darwin/e>

4.3.2. Underway DIC

(1) Personnel

Akihiko Murata (JAMSTEC) – Principal investigator, Not on board
Nagisa Fujiki (Marine Works Japan Ltd.; MWJ) – Operation leader
Yuta Oda (MWJ)
Hiroshi Hoshino (MWJ)

(2) Objective

To elucidate spatial variations of total dissolved inorganic carbon (DIC) concentration in sea surface water.

(3) Parameter

Total Dissolved Inorganic Carbon (DIC)

(4) Instruments and Methods

Surface seawater was continuously collected from 3rd to 25th, October 2020 (UTC) during this cruise. Surface seawater was taken from an intake placed at the approximately 4.5 m below the sea surface by a pump, and was filled in a 250 mL glass bottle (SCHOTT DURAN) from the bottom, without rinsing, and overflowed for more than 2 times the amount. Before the analysis, the samples were put in the water bath kept about 20°C for one hour. Measurements of DIC were made with total CO_2 measuring system (Nihon ANS Inc.). The system was comprised of seawater dispensing unit, a CO_2 extraction unit, and a coulometer (Model 3000A, Nihon ANS Inc.). The seawater dispensing unit has an auto-sampler (6 ports), which dispenses the seawater from a glass bottle to a pipette of nominal 15 mL volume. The pipette was kept at 20.00 °C ± 0.05 °C by a water jacket, in which water circulated through a thermostatic water bath. The CO_2 dissolved in a seawater sample is extracted in a stripping chamber of the CO_2 extraction unit by adding 10 % phosphoric acid solution. The stripping chamber is made approx. 25 cm long and has a fine frit at the bottom. First, the certain amount of acid is taken to the constant volume tube from an acid bottle and transferred to the stripping chamber from its bottom by nitrogen gas (99.9999 %). Second, a seawater sample kept in a pipette is introduced to the stripping chamber by the same method as that for an acid. The seawater and phosphoric acid are stirred by the nitrogen bubbles through a fine frit at the bottom of the stripping chamber. The stripped CO_2 is carried to the coulometer through two electric dehumidifiers (kept at 2 °C) and a chemical desiccant (Magnesium perchlorate) by the nitrogen gas (flow rate of 140 mL min-1). Measurements of approx.1.5 % CO_2 standard gas in a nitrogen base, system blank (phosphoric acid blank), and seawater samples (6 samples) were programmed to repeat. Both CO_2 standard gas and blank signals were used to correct the signal drift results from chemical alternation of coulometer solutions. The coulometer solutions were renewed every about 2 days, and a certified reference material (CRM: batch 190) was measured to correct systematic

difference between measurements.

(5) Observation log

The cruise track during underway DIC observation is shown in Figure 4.3.2-1.

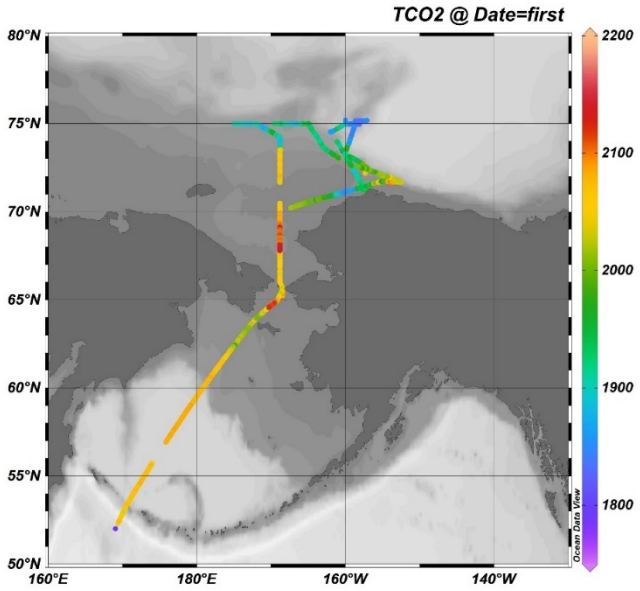

Figure 4.3.2-1. Cruise track where underway DIC was measured during the cruise. Concentrations of DIC were shown in color.

(6) Results

Temporal variations of DIC in surface sweater are shown in Figure 4.3.2-2, together with those of salinity.

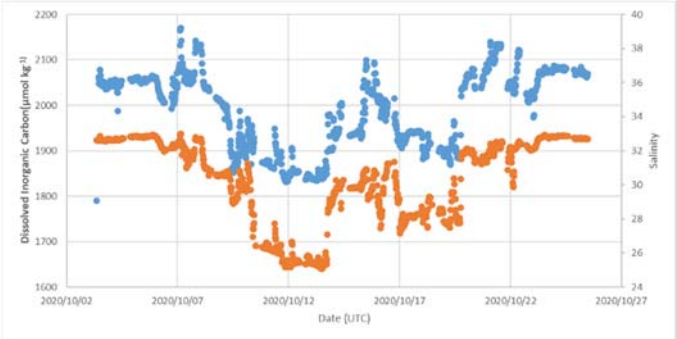

Figure 4.3.2-2. Temporal variations of DIC in surface seawater (blue) and sea surface salinity (red).

(7) Date archives

These data obtained in this cruise will be submitted to the Data Management Group (DMG) of JAMSTEC, and will be opened to the public via "Data Research System for Whole Cruise Information in JAMSTEC (DARWIN)" in JAMSTEC web site.
<http://www.godac.jamstec.go.jp/darwin/e>

4.4. δ^{13}C-DIC

(1) Personnel

Wei-Jun Cai (University of Delaware) – Principal investigator, Not on board
Zhangxian Ouyang (University of Delaware) – Not on board
Akihiko Murata (JAMSTEC) – Not on board
Shigeto Nishino (JAMSTEC)

(2) Objectives

Based on the data collected in previous cruises, we identified the substantial expansion of the subsurface acidified water (Qi et al., 2017). From 1994 to 2010, the aragonite undersaturated water became deeper in the Canada Basin and extended into higher latitude. Our analysis confirms that the atmospheric CO_2 intrusion and sea-ice melt are two dominant drivers for acidification in the stratified and freshened surface waters. Meanwhile, we attributed increased Pacific Winter Water inflow as the main cause for intensified acidification in the subsurface Canada Basin as it has an original low Ω_{ar} and as it is further modified by receiving extra respiratory CO_2 addition in the Chukchi Sea Shelf.

However, it is challenge to separate and quantify the contributions of Pacific corrosive water, terrestrial organic carbon remineralization and local organic matter respiration to ocean acidification. Therefore, our proposed data sampling of δ^{13}C-DIC is designed to collect relevant observations of geochemical tracers and will help to decipher carbon source in different water masses and improve our understanding of mechanisms affecting the western Arctic Ocean acidification.

δ^{13}C-DIC analysis provides us with a useful tool for identifying the carbon source adding into DIC pool. The effects of degradation of organic carbon to DIC, drawdown of DIC by primary production and air-sea CO_2 exchange could be distinguished from one another by analyzing DIC and δ^{13}C-DIC. In the water column, loss of DIC generally leaves isotopically heavy C, whereas addition of DIC by degradation of organic carbon matters adds isotopically light C. As a result, the relative changes in DIC leaves unique carbon isotopic fingerprints in water. Combined with water mixing model, the deviations between observed δ^{13}C-DIC and conservative mixed δ^{13}C-DIC ($\Delta\delta^{13}$C-DIC) associated with the deviation in DIC (ΔDIC) become a useful and powerful tool to quantify the contributions of degradation of terrestrial and local organic carbon at the background of corrosive PWW.

Therefore, we propose to collect δ^{13}C-DIC samples in 2020 JAMSTEC cruises, extending our study scope in carbon isotopic perspective to a more comprehensive area covering from the Chukchi shelf to the Canada Basin. This approach will provide us with a better understanding of Arctic carbon dynamics, in particular, the carbon flows, exports, and degradation from highly productive shelves to oligotrophic basins, and thus a better ability to predict future changes in the Arctic carbon system, as well as other geophysical and biogeochemical components.

(3) Parameters

δ^{13}C-DIC

(4) Instruments and methods

I. Sampling

δ^{13}C-DIC sampling procedure is basically following the procedure of DIC sampling, described in the book *Guide to Best Practices for Ocean CO_2 Measurements (Dickson et al. 2007).* First, rinse the sample bottle twice with 30–40 ml of sample seawater from Niskin bottle to remove any dust and particles. Second, fill the bottle smoothly from the bottom using a drawing tube which extends from the Niskin drain to the bottom of the glass sample bottle. It is critical to remove any bubbles from the draw tube before filling. Overflow the water by at least a half, and preferably by a full, bottle volume. Insert the stopper and transport the samples from to the lab. Then, a headspace of ~1% of the bottle volume is left to allow for water expansion (i.e., 1 ml for a 125 ml bottle). This can be achieved by pulling out the stopper and using a pipette to remove excess water (1 ml). Mercuric chloride is added to poison the sample using a pipette (to poison a 125 ml sample requires 50 µl of saturated mercuric chloride solution). Next, seal the bottle carefully to ensure that it remains gas-tight. Wipe the excess water from the ground glass in the bottle neck and apply some grease (not too much) around the ground glass stopper, insert the stopper completely, and twist the stopper to squeeze the air out of the grease to make a good seal. Finally, use a rubber band and a clamp to positively reinforce closure and invert the bottle several times to disperse the mercuric chloride solution thoroughly. The samples should be stored in a cool, dark, location.

II. Sample Analysis

Analysis of δ^{13}C-DIC samples are conducted using a DIC- δ^{13}C analyzer (Apollo SciTech, USA). Briefly, a CO_2 extraction device and Cavity Ring-Down Spectrometer (CRDS) isotopic detector (G2131-i, Picarro, USA) were coupled to simultaneously measure DIC and δ^{13}C in a 3–4 mL sample over an ~11 min interval, with average precision of 1.5 ± 0.6 µmol kg^{-1} for DIC and 0.07 ± 0.05‰ for δ^{13}C-DIC. The instrumentation principles and sample analysis procedure are described in detail in Su et al., (2019).

(5) Station list

Table 4.4-1. List of water sampling for δ^{13}C-DIC analysis.

No.	Station	Date Collected (UTC)				Latitude			Longitude			Depth
		YYYY	MM	DD	hh:mm:ss	Deg.	Min.	N/S	Deg.	Min.	E/W	[m]
1	St.07	2020	10	08	8:45	69	0.83	N	168	49.77	W	0
2	St.07	2020	10	08	8:45	69	0.83	N	168	49.77	W	Chl-aMax
3	St.07	2020	10	08	8:45	69	0.83	N	168	49.77	W	5
4	St.07	2020	10	08	8:45	69	0.83	N	168	49.77	W	10
5	St.07	2020	10	08	8:45	69	0.83	N	168	49.77	W	20
6	St.07	2020	10	08	8:45	69	0.83	N	168	49.77	W	30
7	St.07	2020	10	08	8:45	69	0.83	N	168	49.77	W	B-5
8	St.09	2020	10	08	23:53	70	30.02	N	165	29.73	W	0
9	St.09	2020	10	08	23:53	70	30.02	N	165	29.73	W	Chl-aMax
10	St.09	2020	10	08	23:53	70	30.02	N	165	29.73	W	5
11	St.09	2020	10	08	23:53	70	30.02	N	165	29.73	W	10
12	St.09	2020	10	08	23:53	70	30.02	N	165	29.73	W	20
13	St.09	2020	10	08	23:53	70	30.02	N	165	29.73	W	30
14	St.09	2020	10	08	23:53	70	30.02	N	165	29.73	W	B-10
15	St.10	2020	10	11	1:05	74	33.03	N	161	53.06	W	0
16	St.10	2020	10	11	1:05	74	33.03	N	161	53.06	W	Chl-aMax
17	St.10	2020	10	11	1:05	74	33.03	N	161	53.06	W	5
18	St.10	2020	10	11	1:05	74	33.03	N	161	53.06	W	10
19	St.10	2020	10	11	1:05	74	33.03	N	161	53.06	W	20
20	St.10	2020	10	11	1:05	74	33.03	N	161	53.06	W	30
21	St.10	2020	10	11	1:05	74	33.03	N	161	53.06	W	50
22	St.10	2020	10	11	1:05	74	33.03	N	161	53.06	W	75
23	St.10	2020	10	11	1:05	74	33.03	N	161	53.06	W	100
24	St.10	2020	10	11	1:05	74	33.03	N	161	53.06	W	125
25	St.10	2020	10	11	1:05	74	33.03	N	161	53.06	W	150
26	St.10	2020	10	11	1:05	74	33.03	N	161	53.06	W	175
27	St.10	2020	10	11	1:05	74	33.03	N	161	53.06	W	200
28	St.10	2020	10	11	1:05	74	33.03	N	161	53.06	W	225
29	St.10	2020	10	11	1:05	74	33.03	N	161	53.06	W	250
30	St.10	2020	10	11	1:05	74	33.03	N	161	53.06	W	300
31	St.10	2020	10	11	1:05	74	33.03	N	161	53.06	W	400
32	St.10	2020	10	11	1:05	74	33.03	N	161	53.06	W	500
33	St.10	2020	10	11	1:05	74	33.03	N	161	53.06	W	600
34	St.10	2020	10	11	1:05	74	33.03	N	161	53.06	W	800
35	St.10	2020	10	11	1:05	74	33.03	N	161	53.06	W	1000
36	St.10	2020	10	11	1:05	74	33.03	N	161	53.06	W	1500
37	St.10	2020	10	11	1:05	74	33.03	N	161	53.06	W	B-10
38	St.11	2020	10	11	23:35	74	58.81	N	158	7.55	W	0

No.	Station	Date Collected (UTC)				Latitude			Longitude			Depth
		YYYY	MM	DD	hh:mm:ss	Deg.	Min.	N/S	Deg.	Min.	E/W	[m]
39	St.11	2020	10	11	23:35	74	58.81	N	158	7.55	W	Chl-aMax
40	St.11	2020	10	11	23:35	74	58.81	N	158	7.55	W	5
41	St.11	2020	10	11	23:35	74	58.81	N	158	7.55	W	10
42	St.11	2020	10	11	23:35	74	58.81	N	158	7.55	W	20
43	St.11	2020	10	11	23:35	74	58.81	N	158	7.55	W	30
44	St.11	2020	10	11	23:35	74	58.81	N	158	7.55	W	50
45	St.11	2020	10	11	23:35	74	58.81	N	158	7.55	W	75
46	St.11	2020	10	11	23:35	74	58.81	N	158	7.55	W	100
47	St.11	2020	10	11	23:35	74	58.81	N	158	7.55	W	125
48	St.11	2020	10	11	23:35	74	58.81	N	158	7.55	W	150
49	St.11	2020	10	11	23:35	74	58.81	N	158	7.55	W	175
50	St.11	2020	10	11	23:35	74	58.81	N	158	7.55	W	200
51	St.11	2020	10	11	23:35	74	58.81	N	158	7.55	W	225
52	St.11	2020	10	11	23:35	74	58.81	N	158	7.55	W	250
53	St.11	2020	10	11	23:35	74	58.81	N	158	7.55	W	300
54	St.11	2020	10	11	23:35	74	58.81	N	158	7.55	W	400
55	St.11	2020	10	11	23:35	74	58.81	N	158	7.55	W	500
56	St.11	2020	10	11	23:35	74	58.81	N	158	7.55	W	600
57	St.11	2020	10	11	23:35	74	58.81	N	158	7.55	W	800
58	St.11	2020	10	11	23:35	74	58.81	N	158	7.55	W	Bottom
59	St.12	2020	10	12	8:53	75	10.95	N	160	0.17	W	0
60	St.12	2020	10	12	8:53	75	10.95	N	160	0.17	W	Chl-aMax
61	St.12	2020	10	12	8:53	75	10.95	N	160	0.17	W	5
62	St.12	2020	10	12	8:53	75	10.95	N	160	0.17	W	10
63	St.12	2020	10	12	8:53	75	10.95	N	160	0.17	W	20
64	St.12	2020	10	12	8:53	75	10.95	N	160	0.17	W	30
65	St.12	2020	10	12	8:53	75	10.95	N	160	0.17	W	50
66	St.12	2020	10	12	8:53	75	10.95	N	160	0.17	W	75
67	St.12	2020	10	12	8:53	75	10.95	N	160	0.17	W	100
68	St.12	2020	10	12	8:53	75	10.95	N	160	0.17	W	125
69	St.12	2020	10	12	8:53	75	10.95	N	160	0.17	W	150
70	St.12	2020	10	12	8:53	75	10.95	N	160	0.17	W	175
71	St.12	2020	10	12	8:53	75	10.95	N	160	0.17	W	200
72	St.12	2020	10	12	8:53	75	10.95	N	160	0.17	W	225
73	St.12	2020	10	12	8:53	75	10.95	N	160	0.17	W	250
74	St.12	2020	10	12	8:53	75	10.95	N	160	0.17	W	300
75	St.12	2020	10	12	8:53	75	10.95	N	160	0.17	W	400
76	St.12	2020	10	12	8:53	75	10.95	N	160	0.17	W	500
77	St.12	2020	10	12	8:53	75	10.95	N	160	0.17	W	600
78	St.12	2020	10	12	8:53	75	10.95	N	160	0.17	W	800
79	St.12	2020	10	12	8:53	75	10.95	N	160	0.17	W	1000

No.	Station	Date Collected (UTC)				Latitude			Longitude			Depth
		YYYY	MM	DD	hh:mm:ss	Deg.	Min.	N/S	Deg.	Min.	E/W	[m]
80	St.12	2020	10	12	8:53	75	10.95	N	160	0.17	W	1500
81	St.12	2020	10	12	8:53	75	10.95	N	160	0.17	W	B-10
82	St.13	2020	10	14	0:09	73	17.32	N	160	54.07	W	0
83	St.13	2020	10	14	0:09	73	17.32	N	160	54.07	W	Chl-aMax
84	St.13	2020	10	14	0:09	73	17.32	N	160	54.07	W	5
85	St.13	2020	10	14	0:09	73	17.32	N	160	54.07	W	10
86	St.13	2020	10	14	0:09	73	17.32	N	160	54.07	W	20
87	St.13	2020	10	14	0:09	73	17.32	N	160	54.07	W	30
88	St.13	2020	10	14	0:09	73	17.32	N	160	54.07	W	50
89	St.13	2020	10	14	0:09	73	17.32	N	160	54.07	W	75
90	St.13	2020	10	14	0:09	73	17.32	N	160	54.07	W	100
91	St.13	2020	10	14	0:09	73	17.32	N	160	54.07	W	125
92	St.13	2020	10	14	0:09	73	17.32	N	160	54.07	W	150
93	St.13	2020	10	14	0:09	73	17.32	N	160	54.07	W	175
94	St.13	2020	10	14	0:09	73	17.32	N	160	54.07	W	200
95	St.13	2020	10	14	0:09	73	17.32	N	160	54.07	W	225
96	St.13	2020	10	14	0:09	73	17.32	N	160	54.07	W	250
97	St.13	2020	10	14	0:09	73	17.32	N	160	54.07	W	300
98	St.13	2020	10	14	0:09	73	17.32	N	160	54.07	W	400
99	St.13	2020	10	14	0:09	73	17.32	N	160	54.07	W	500
100	St.13	2020	10	14	0:09	73	17.32	N	160	54.07	W	750
101	St.13	2020	10	14	0:09	73	17.32	N	160	54.07	W	1000
102	St.13	2020	10	14	0:09	73	17.32	N	160	54.07	W	B-10
103	St.15	2020	10	14	6:30	72	47.32	N	157	59.98	W	0
104	St.15	2020	10	14	6:30	72	47.32	N	157	59.98	W	Chl-aMax
105	St.15	2020	10	14	6:30	72	47.32	N	157	59.98	W	5
106	St.15	2020	10	14	6:30	72	47.32	N	157	59.98	W	10
107	St.15	2020	10	14	6:30	72	47.32	N	157	59.98	W	20
108	St.15	2020	10	14	6:30	72	47.32	N	157	59.98	W	30
109	St.15	2020	10	14	6:30	72	47.32	N	157	59.98	W	50
110	St.15	2020	10	14	6:30	72	47.32	N	157	59.98	W	75
111	St.15	2020	10	14	6:30	72	47.32	N	157	59.98	W	100
112	St.15	2020	10	14	6:30	72	47.32	N	157	59.98	W	125
113	St.15	2020	10	14	6:30	72	47.32	N	157	59.98	W	150
114	St.15	2020	10	14	6:30	72	47.32	N	157	59.98	W	175
115	St.15	2020	10	14	6:30	72	47.32	N	157	59.98	W	200
116	St.15	2020	10	14	6:30	72	47.32	N	157	59.98	W	225
117	St.15	2020	10	14	6:30	72	47.32	N	157	59.98	W	250
118	St.15	2020	10	14	6:30	72	47.32	N	157	59.98	W	300
119	St.15	2020	10	14	6:30	72	47.32	N	157	59.98	W	400
120	St.15	2020	10	14	6:30	72	47.32	N	157	59.98	W	500

No.	Station	Date Collected (UTC)				Latitude			Longitude			Depth
		YYYY	MM	DD	hh:mm:ss	Deg.	Min.	N/S	Deg.	Min.	E/W	[m]
121	St.15	2020	10	14	6:30	72	47.32	N	157	59.98	W	600
122	St.15	2020	10	14	6:30	72	47.32	N	157	59.98	W	B-10
123	St.17	2020	10	15	5:26	71	19.18	N	158	26.24	W	0
124	St.17	2020	10	15	5:26	71	19.18	N	158	26.24	W	Chl-aMax
125	St.17	2020	10	15	5:26	71	19.18	N	158	26.24	W	5
126	St.17	2020	10	15	5:26	71	19.18	N	158	26.24	W	10
127	St.17	2020	10	15	5:26	71	19.18	N	158	26.24	W	20
128	St.17	2020	10	15	5:26	71	19.18	N	158	26.24	W	30
129	St.17	2020	10	15	5:26	71	19.18	N	158	26.24	W	50
130	St.17	2020	10	15	5:26	71	19.18	N	158	26.24	W	75
131	St.17	2020	10	15	5:26	71	19.18	N	158	26.24	W	100
132	St.17	2020	10	15	5:26	71	19.18	N	158	26.24	W	B-5
133	St.20	2020	10	15	23:23	71	58.34	N	153	59.67	W	0
134	St.20	2020	10	15	23:23	71	58.34	N	153	59.67	W	Chl-aMax
135	St.20	2020	10	15	23:23	71	58.34	N	153	59.67	W	5
136	St.20	2020	10	15	23:23	71	58.34	N	153	59.67	W	10
137	St.20	2020	10	15	23:23	71	58.34	N	153	59.67	W	20
138	St.20	2020	10	15	23:23	71	58.34	N	153	59.67	W	30
139	St.20	2020	10	15	23:23	71	58.34	N	153	59.67	W	50
140	St.20	2020	10	15	23:23	71	58.34	N	153	59.67	W	75
141	St.20	2020	10	15	23:23	71	58.34	N	153	59.67	W	100
142	St.20	2020	10	15	23:23	71	58.34	N	153	59.67	W	125
143	St.20	2020	10	15	23:23	71	58.34	N	153	59.67	W	150
144	St.20	2020	10	15	23:23	71	58.34	N	153	59.67	W	175
145	St.20	2020	10	15	23:23	71	58.34	N	153	59.67	W	200
146	St.20	2020	10	15	23:23	71	58.34	N	153	59.67	W	225
147	St.20	2020	10	15	23:23	71	58.34	N	153	59.67	W	250
148	St.20	2020	10	15	23:23	71	58.34	N	153	59.67	W	300
149	St.20	2020	10	15	23:23	71	58.34	N	153	59.67	W	400
150	St.20	2020	10	15	23:23	71	58.34	N	153	59.67	W	500
151	St.20	2020	10	15	23:23	71	58.34	N	153	59.67	W	600
152	St.20	2020	10	15	23:23	71	58.34	N	153	59.67	W	B-10
153	St.22	2020	10	18	0:09	75	0.88	N	164	59.75	W	0
154	St.22	2020	10	18	0:09	75	0.88	N	164	59.75	W	Chl-aMax
155	St.22	2020	10	18	0:09	75	0.88	N	164	59.75	W	5
156	St.22	2020	10	18	0:09	75	0.88	N	164	59.75	W	10
157	St.22	2020	10	18	0:09	75	0.88	N	164	59.75	W	20
158	St.22	2020	10	18	0:09	75	0.88	N	164	59.75	W	30
159	St.22	2020	10	18	0:09	75	0.88	N	164	59.75	W	50
160	St.22	2020	10	18	0:09	75	0.88	N	164	59.75	W	75
161	St.22	2020	10	18	0:09	75	0.88	N	164	59.75	W	100

No.	Station	Date Collected (UTC)				Latitude			Longitude			Depth
		YYYY	MM	DD	hh:mm:ss	Deg.	Min.	N/S	Deg.	Min.	E/W	[m]
162	St.22	2020	10	18	0:09	75	0.88	N	164	59.75	W	125
163	St.22	2020	10	18	0:09	75	0.88	N	164	59.75	W	150
164	St.22	2020	10	18	0:09	75	0.88	N	164	59.75	W	175
165	St.22	2020	10	18	0:09	75	0.88	N	164	59.75	W	200
166	St.22	2020	10	18	0:09	75	0.88	N	164	59.75	W	225
167	St.22	2020	10	18	0:09	75	0.88	N	164	59.75	W	250
168	St.22	2020	10	18	0:09	75	0.88	N	164	59.75	W	300
169	St.22	2020	10	18	0:09	75	0.88	N	164	59.75	W	400
170	St.22	2020	10	18	0:09	75	0.88	N	164	59.75	W	500
171	St.22	2020	10	18	0:09	75	0.88	N	164	59.75	W	B-10
172	St.23	2020	10	18	4:03	75	0.17	N	167	14.3	W	0
173	St.23	2020	10	18	4:03	75	0.17	N	167	14.3	W	Chl-aMax
174	St.23	2020	10	18	4:03	75	0.17	N	167	14.3	W	5
175	St.23	2020	10	18	4:03	75	0.17	N	167	14.3	W	10
176	St.23	2020	10	18	4:03	75	0.17	N	167	14.3	W	20
177	St.23	2020	10	18	4:03	75	0.17	N	167	14.3	W	30
178	St.23	2020	10	18	4:03	75	0.17	N	167	14.3	W	50
179	St.23	2020	10	18	4:03	75	0.17	N	167	14.3	W	75
180	St.23	2020	10	18	4:03	75	0.17	N	167	14.3	W	100
181	St.23	2020	10	18	4:03	75	0.17	N	167	14.3	W	125
182	St.23	2020	10	18	4:03	75	0.17	N	167	14.3	W	150
183	St.23	2020	10	18	4:03	75	0.17	N	167	14.3	W	175
184	St.23	2020	10	18	4:03	75	0.17	N	167	14.3	W	200
185	St.23	2020	10	18	4:03	75	0.17	N	167	14.3	W	225
186	St.23	2020	10	18	4:03	75	0.17	N	167	14.3	W	B-10
187	St.24	2020	10	18	10:12	75	0.04	N	169	57.82	W	0
188	St.24	2020	10	18	10:12	75	0.04	N	169	57.82	W	Chl-aMax
189	St.24	2020	10	18	10:12	75	0.04	N	169	57.82	W	5
190	St.24	2020	10	18	10:12	75	0.04	N	169	57.82	W	10
191	St.24	2020	10	18	10:12	75	0.04	N	169	57.82	W	20
192	St.24	2020	10	18	10:12	75	0.04	N	169	57.82	W	30
193	St.24	2020	10	18	10:12	75	0.04	N	169	57.82	W	50
194	St.24	2020	10	18	10:12	75	0.04	N	169	57.82	W	75
195	St.24	2020	10	18	10:12	75	0.04	N	169	57.82	W	100
196	St.24	2020	10	18	10:12	75	0.04	N	169	57.82	W	125
197	St.24	2020	10	18	10:12	75	0.04	N	169	57.82	W	150
198	St.24	2020	10	18	10:12	75	0.04	N	169	57.82	W	175
199	St.24	2020	10	18	10:12	75	0.04	N	169	57.82	W	200
200	St.24	2020	10	18	10:12	75	0.04	N	169	57.82	W	225
201	St.24	2020	10	18	10:12	75	0.04	N	169	57.82	W	B-10
202	St.25	2020	10	18	23:09	75	0.20	N	174	59.65	W	0

No.	Station	Date Collected (UTC)				Latitude			Longitude			Depth
		YYYY	MM	DD	hh:mm:ss	Deg.	Min.	N/S	Deg.	Min.	E/W	[m]
203	St.25	2020	10	18	23:09	75	0.20	N	174	59.65	W	Chl-aMax
204	St.25	2020	10	18	23:09	75	0.20	N	174	59.65	W	5
205	St.25	2020	10	18	23:09	75	0.20	N	174	59.65	W	10
206	St.25	2020	10	18	23:09	75	0.20	N	174	59.65	W	20
207	St.25	2020	10	18	23:09	75	0.20	N	174	59.65	W	30
208	St.25	2020	10	18	23:09	75	0.20	N	174	59.65	W	50
209	St.25	2020	10	18	23:09	75	0.20	N	174	59.65	W	75
210	St.25	2020	10	18	23:09	75	0.20	N	174	59.65	W	100
211	St.25	2020	10	18	23:09	75	0.20	N	174	59.65	W	125
212	St.25	2020	10	18	23:09	75	0.20	N	174	59.65	W	150
213	St.25	2020	10	18	23:09	75	0.20	N	174	59.65	W	175
214	St.25	2020	10	18	23:09	75	0.20	N	174	59.65	W	200
215	St.25	2020	10	18	23:09	75	0.20	N	174	59.65	W	225
216	St.25	2020	10	18	23:09	75	0.20	N	174	59.65	W	250
217	St.25	2020	10	18	23:09	75	0.20	N	174	59.65	W	B-10
218	St.26	2020	10	19	4:16	75	0.05	N	172	0.23	W	0
219	St.26	2020	10	19	4:16	75	0.05	N	172	0.23	W	Chl-aMax
220	St.26	2020	10	19	4:16	75	0.05	N	172	0.23	W	5
221	St.26	2020	10	19	4:16	75	0.05	N	172	0.23	W	10
222	St.26	2020	10	19	4:16	75	0.05	N	172	0.23	W	20
223	St.26	2020	10	19	4:16	75	0.05	N	172	0.23	W	30
224	St.26	2020	10	19	4:16	75	0.05	N	172	0.23	W	50
225	St.26	2020	10	19	4:16	75	0.05	N	172	0.23	W	75
226	St.26	2020	10	19	4:16	75	0.05	N	172	0.23	W	100
227	St.26	2020	10	19	4:16	75	0.05	N	172	0.23	W	125
228	St.26	2020	10	19	4:16	75	0.05	N	172	0.23	W	150
229	St.26	2020	10	19	4:16	75	0.05	N	172	0.23	W	175
230	St.26	2020	10	19	4:16	75	0.05	N	172	0.23	W	200
231	St.26	2020	10	19	4:16	75	0.05	N	172	0.23	W	225
232	St.26	2020	10	19	4:16	75	0.05	N	172	0.23	W	250
233	St.26	2020	10	19	4:16	75	0.05	N	172	0.23	W	300
234	St.26	2020	10	19	4:16	75	0.05	N	172	0.23	W	B-5
235	St.27	2020	10	19	10:00	74	0.04	N	170	55.19	W	0
236	St.27	2020	10	19	10:00	74	0.04	N	170	55.19	W	Chl-aMax
237	St.27	2020	10	19	10:00	74	0.04	N	170	55.19	W	5
238	St.27	2020	10	19	10:00	74	0.04	N	170	55.19	W	10
239	St.27	2020	10	19	10:00	74	0.04	N	170	55.19	W	20
240	St.27	2020	10	19	10:00	74	0.04	N	170	55.19	W	30
241	St.27	2020	10	19	10:00	74	0.04	N	170	55.19	W	50
242	St.27	2020	10	19	10:00	74	0.04	N	170	55.19	W	75
243	St.27	2020	10	19	10:00	74	0.04	N	170	55.19	W	100

No.	Station	Date Collected (UTC)				Latitude			Longitude			Depth
		YYYY	MM	DD	hh:mm:ss	Deg.	Min.	N/S	Deg.	Min.	E/W	[m]
244	St.27	2020	10	19	10:00	74	0.04	N	170	55.19	W	125
245	St.27	2020	10	19	10:00	74	0.04	N	170	55.19	W	150
246	St.27	2020	10	19	10:00	74	0.04	N	170	55.19	W	175
247	St.27	2020	10	19	10:00	74	0.04	N	170	55.19	W	200
248	St.27	2020	10	19	10:00	74	0.04	N	170	55.19	W	B-5
249	St.29	2020	10	19	22:24	73	29.97	N	168	48.83	W	0
250	St.29	2020	10	19	22:24	73	29.97	N	168	48.83	W	Chl-aMax
251	St.29	2020	10	19	22:24	73	29.97	N	168	48.83	W	5
252	St.29	2020	10	19	22:24	73	29.97	N	168	48.83	W	10
253	St.29	2020	10	19	22:24	73	29.97	N	168	48.83	W	20
254	St.29	2020	10	19	22:24	73	29.97	N	168	48.83	W	30
255	St.29	2020	10	19	22:24	73	29.97	N	168	48.83	W	50
256	St.29	2020	10	19	22:24	73	29.97	N	168	48.83	W	75
257	St.29	2020	10	19	22:24	73	29.97	N	168	48.83	W	100
258	St.29	2020	10	19	22:24	73	29.97	N	168	48.83	W	B-5
259	St.30	2020	10	20	1:22	73	0.08	N	168	49.55	W	0
260	St.30	2020	10	20	1:22	73	0.08	N	168	49.55	W	Chl-aMax
261	St.30	2020	10	20	1:22	73	0.08	N	168	49.55	W	5
262	St.30	2020	10	20	1:22	73	0.08	N	168	49.55	W	10
263	St.30	2020	10	20	1:22	73	0.08	N	168	49.55	W	20
264	St.30	2020	10	20	1:22	73	0.08	N	168	49.55	W	30
265	St.30	2020	10	20	1:22	73	0.08	N	168	49.55	W	50
266	St.30	2020	10	20	1:22	73	0.08	N	168	49.55	W	B-5
267	St.31	2020	10	20	8:35	72	0	N	168	59.00	W	0
268	St.31	2020	10	20	8:35	72	0	N	168	59.00	W	Chl-aMax
269	St.31	2020	10	20	8:35	72	0	N	168	59.00	W	5
270	St.31	2020	10	20	8:35	72	0	N	168	59.00	W	10
271	St.31	2020	10	20	8:35	72	0	N	168	59.00	W	20
272	St.31	2020	10	20	8:35	72	0	N	168	59.00	W	30
273	St.31	2020	10	20	8:35	72	0	N	168	59.00	W	B-5
274	St.33	2020	10	20	22:13	69	59.98	N	168	48.79	W	0
275	St.33	2020	10	20	22:13	69	59.98	N	168	48.79	W	Chl-aMax
276	St.33	2020	10	20	22:13	69	59.98	N	168	48.79	W	5
277	St.33	2020	10	20	22:13	69	59.98	N	168	48.79	W	10
278	St.33	2020	10	20	22:13	69	59.98	N	168	48.79	W	20
279	St.33	2020	10	20	22:13	69	59.98	N	168	48.79	W	30
280	St.33	2020	10	20	22:13	69	59.98	N	168	48.79	W	B-5
281	St.34	2020	10	20	4:08	69	0.22	N	168	49.64	W	0
282	St.34	2020	10	20	4:08	69	0.22	N	168	49.64	W	Chl-aMax
283	St.34	2020	10	20	4:08	69	0.22	N	168	49.64	W	5
284	St.34	2020	10	20	4:08	69	0.22	N	168	49.64	W	10

No.	Station	Date Collected (UTC)				Latitude			Longitude			Depth
		YYYY	MM	DD	hh:mm:ss	Deg.	Min.	N/S	Deg.	Min.	E/W	[m]
285	St.34	2020	10	20	4:08	69	0.22	N	168	49.64	W	20
286	St.34	2020	10	20	4:08	69	0.22	N	168	49.64	W	30
287	St.34	2020	10	20	4:08	69	0.22	N	168	49.64	W	B-5
288	St.35	2020	10	21	10:36	68	0	N	168	49.99	W	0
289	St.35	2020	10	21	10:36	68	0	N	168	49.99	W	Chl-aMax
290	St.35	2020	10	21	10:36	68	0	N	168	49.99	W	5
291	St.35	2020	10	21	10:36	68	0	N	168	49.99	W	10
292	St.35	2020	10	21	10:36	68	0	N	168	49.99	W	20
293	St.35	2020	10	21	10:36	68	0	N	168	49.99	W	30
294	St.35	2020	10	21	10:36	68	0	N	168	49.99	W	50
295	St.35	2020	10	21	10:36	68	0	N	168	49.99	W	B-5

(6) Data archives

These data obtained in this cruise will be submitted to the Data Management Group (DMG) of JAMSTEC, and will be opened to the public via "Data Research System for Whole Cruise Information in JAMSTEC (DARWIN)" in JAMSTEC web site. <http://www.godac.jamstec.go.jp/darwin/e>

(7) References

Qi, D., Chen, L., Chen, B., Gao, Z., Zhong, W., Feely, R. A., ... & Zhan, L. (2017). Increase in acidifying water in the western Arctic Ocean. *Nature Climate Change*, *7*(3), 195-199.

Dickson, A. G., Sabine, C. L., & Christian, J. R. (2007). *Guide to best practices for ocean CO2 measurements*. North Pacific Marine Science Organization.

Su, J., Cai, W. J., Hussain, N., Brodeur, J., Chen, B., & Huang, K. (2019). Simultaneous determination of dissolved inorganic carbon (DIC) concentration and stable isotope (δ13C-DIC) by Cavity Ring-Down Spectroscopy: Application to study carbonate dynamics in the Chesapeake Bay. *Marine Chemistry*, *215*, 103689.

4.5. Total Alkalinity

(1) Personnel

Akihiko Murata (JAMSTEC) – Principal investigator, Not on board
Nagisa Fujiki (Marine Works Japan Ltd.; MWJ) – Operation leader
Yuta Oda (MWJ)
Hiroshi Hoshino (MWJ)

(2) Objective

To survey influences of sea ice melting water and river input on carbonate system properties.

(3) Parameters

Total alkalinity (TA)

(4) Instruments and Methods

a. Seawater sampling

Seawater samples were collected by 12 L Niskin bottles mounted on the CTD/Carousel Water Sampling System and a bucket at 24 stations. The seawater from the Niskin bottle was filled into the 125 mL borosilicate glass bottles (SHOTT DURAN) using a sampling silicone rubber tube with PFA tip. The water was filled into the bottle from the bottom smoothly, without rinsing, and overflowed for 2 times bottle volume (10 seconds). These bottles were pre-washed in advance by soaking in 5 % alkaline detergent for more than 3 hours, and then rinsed 5 times with tap water and 3 times with Milli-Q deionized water. The samples were stored in a refrigerator at approximately 5 °C before the analysis, and were put in the water bath with its temperature of about 25 °C for one hour before analysis.

b. Seawater analysis

The total alkalinity was measured using a spectrophotometric system (Nihon ANS, Inc.) using a scheme of Yao and Byrne (1998). The calibrated volume of sample seawater (ca. 42 mL) was transferred from a sample bottle into the titration cell with its light path length of 4 cm long via dispensing unit. The TA is calculated by measuring two sets of absorbance at three wavelengths (730, 616 and 444) nm with the spectrometer (TM-UV/VIS C10082CAH, HAMAMATSU). One is the absorbance of seawater sample before injecting an acid with indicator solution (bromocresol green sodium) and another is the one after the injection. To mix the acidified-indicator solution with seawater sufficiently, the mixed solution is circulated in a circulation line by a peristaltic pump for 5 minutes. Nitrogen bubble were introduced into the titration cell for degassing CO_2 from the mixed solution sufficiently. The TA is calculated based on the following equation:

$$TA = (-[H^+]_T V_{SA} + M_A V_A)/V_S,$$

where M_A is the molarity of the acid titrant added to the seawater sample, $[H^+]_T$ is the total excess hydrogen ion concentration in the seawater, and V_S, V_A and V_{SA} are the initial seawater volume, the added acid titrant volume, and the combined seawater plus acid titrant volume, respectively. $[H^+]_T$ is calculated from the measured absorbances based on the following equation (Yao and Byrne, 1998):

$$pH_T = -\log[H^+]_T = 4.2699 + 0.002578(35 - S) + \log((R - 0.00131)/(2.3148 - 0.1299R)) - \log(1 - 0.001005S),$$

where S is the sample salinity, and R is the absorbance ratio calculated as:

$$R = (A_{616} - A_{730})/(A_{444} - A_{730}),$$

where A_i is the absorbance at wavelength i nm.

(5) Observation log

Seawater samples were collected at 24 stations.

(6) Preliminary results

The repeatability of this system was provisionally 1.1 µmol kg^{-1} (n = 48), which was calculated from replicate samples. A range control chart of TA measurement is illustrated in Figure 4.5-1

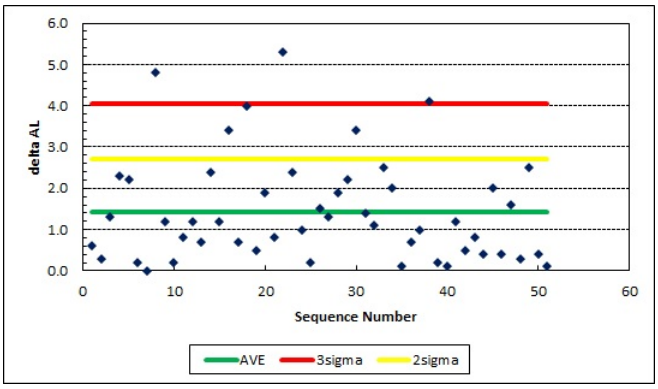

Figure 4.5-1. Range control chart of the absolute differences of replicate measurements of TA. The AVE indicates average. The 2 and 3 sigma indicate the upper control limits of sigma × 2 and that × 3, respectively.

(7) Date archives

These data obtained in this cruise will be submitted to the Data Management Group (DMG) of JAMSTEC, and will be opened to the public via "Data Research System for Whole Cruise Information in JAMSTEC (DARWIN)" in JAMSTEC web site.
<http://www.godac.jamstec.go.jp/darwin/e>

4.6. CH_4

(1) Personnel

Sohiko Kameyama (Hokkaido University) – Principal investigator, Not on board
Xinyuan Zheng (Hokkaido University)
Amane Fujiwara (JAMSTEC)

(2) Objective

Methane (CH_4) is a potent greenhouse gas and its greenhouse effect is second only to carbon dioxide. In the past few decades, its concentration in the atmosphere has also increased rapidly. The ocean is the source of CH_4 release, although the CH_4 released by it does not account for a large proportion of the total atmospheric inventory. Its emissions vary greatly over time and space, which reflects the complex biogeochemical dynamics of the Arctic Ocean. Especially in the Arctic region, the CH_4 stored in the marine sediments probably exceeds the total inventory of atmospheric CH_4. We study CH_4 in the Arctic environment to investigate the factors controlling the spatiotemporal variability of CH_4 concentrations and carbon isotope distributions in the Arctic Ocean, and to understand the potential for large-scale CH_4 emissions from the melting of residual seafloor permafrost due to climate warming.

(3) Parameters

Dissolved CH_4 concentration
Carbon isotopic composition of CH_4

(4) Instruments and methods

(4-1) Discrete bottle sampling

Discrete water samples for each station (Table 4.4) were collected at multiple depths using 12-L Niskin bottles mounted on a CTD system. For each sample, an aliquot of 100 mL seawater was transferred from the Niskin bottles to an amber vial (100 mL). The vial was filled smoothly from the bottom with seawater using a drawing tube that extended from the Niskin drain to the bottom of the vial. The seawater was allowed to overflow by an amount of approximately one and a half times the vial volume. After sampling, 0.5 mL saturated mercuric chloride was added to poison the sample. Then, the vial was crimp-sealed with a butyl-rubber stopper and aluminum cap.

(4-2) Sample storage

The samples were stored at 4°C in the dark onboard the R/V Mirai, and transported chilled to laboratories on land for analysis when the R/V Mirai returned to Japan.

(4-3) Sample measurement

The samples will be measured using gas chromatography-isotope ratio mass

spectrometry (GC-IRMS) coupled with a purge and trap extraction system in Nagoya University, Japan.

(5) Station list

A list of the water sampling stations for CH_4 is presented in Table 4.4.

Table 4.4. List of sampling stations for water column CH_4.

Stn.	Sampling date (UTC)	Latitude (N)	Longitude (W)
010	11 Oct.	74°-33.03”	161°-53.06”
011	11 Oct.	74°-58.81”	158°-07.55”
012	12 Oct.	75°-10.95”	160°-00.17”
013	14 Oct.	73°-17.32”	160°-00.66”
015	14 Oct.	72°-47.32”	157°-59.98”
017	15 Oct.	71°-19.18”	158°-26.24”
020	15 Oct.	71°-58.34”	153°-59.67”
022	18 Oct.	75°-00.88”	164°-57.48”
023	18 Oct.	75°-00.17”	167°-14.30”
024	18 Oct.	75°-00.04”	169°-38.22”
025	18 Oct.	75°-00.20”	174°-59.65”
026	19 Oct.	75°-00.05”	172°-00.23”
027	19 Oct.	74°-36.00”	170°-11.94”
029	19 Oct.	73°-29.97”	168°-48.83”
030	20 Oct.	73°-00.08”	168°-49.55”
031	20 Oct.	72°-00.00”	168°-49.98”
033	20 Oct.	69°-59.98”	168°-48.79”
034	20 Oct.	69°-00.22”	168°-49.64”
035	21 Oct.	68°-00.00”	168°-49.99”

(6) Data archives

These data obtained in this cruise will be submitted to the Data Management Group (DMG) of JAMSTEC, and will be opened to the public via “Data Research System for Whole Cruise Information in JAMSTEC (DARWIN)” in JAMSTEC web site.
<http://www.godac.jamstec.go.jp/darwin/e>)

4.7. ^{129}I

(1) Personnel

Yuichiro Kumamoto (JAMSTEC) – Principal investigator, Not on board

(2) Objective

Determination of activity concentrations of ^{129}I in the Arctic Ocean, Bering Sea, and northern North Pacific Ocean.

(3) Parameters

^{129}I

(4) Instruments and Methods

a. Sampling

Seawater samples for ^{129}I were collected using 12-liter PVC bottles. Surface seawater was collected from continuous pumped-up water at about 4-m depth. The seawater sample was collected into a 1-L plastic bottle after two-time rinsing.

b. Preparation and analysis

Iodine in the seawater samples is extracted by the solvent extraction technique. Extracted iodine is then precipitated as silver iodide by the addition of the silver nitrate. Iodine isotopic ratios ($^{129}I/^{127}I$) of the silver iodide are measured by the Accelerator Mass Spectrometry (AMS). To evaluate the ^{129}I concentration in the seawater samples, iodine concentration (^{127}I) will be measured by the inductively coupled plasma mass spectrometry (ICP-MS) and/or the voltammetry.

(5) Sample list

We collected 80 seawater samples for ^{129}I measurements in the Arctic Ocean, Bering Sea, and northern North Pacific Ocean during this cruise (Table 4.7-1).

(6) Data archives

These data obtained in this cruise will be submitted to the Data Management Group (DMG) of JAMSTEC, and will be opened to the public via "Data Research System for Whole Cruise Information in JAMSTEC (DARWIN)" in JAMSTEC web site.
<http://www.godac.jamstec.go.jp/darwin/e>

Table 4.7-1. Seawater samples collected for the ^{129}I measurement.

No.	Station	Depth (m)	Method	Latitude	Longitude	Date (UTC)
1	Stn.01	10	bottle	32.00N	147.00E	2020/09/21
2	Stn.01	50	bottle	32.00N	147.00E	2020/09/21
3	Stn.01	100	bottle	32.00N	147.00E	2020/09/21
4	Stn.01	150	bottle	32.00N	147.00E	2020/09/21
5	Stn.01	199	bottle	32.00N	147.00E	2020/09/21
6	Stn.01	300	bottle	32.00N	147.00E	2020/09/21
7	Stn.01	400	bottle	32.00N	147.00E	2020/09/21
8	Stn.01	600	bottle	32.00N	147.00E	2020/09/21
9	Stn.01	802	bottle	32.00N	147.00E	2020/09/21
10	Stn.04	9	bottle	47.01N	160.05E	2020/10/01
11	Stn.04	50	bottle	47.01N	160.05E	2020/10/01
12	Stn.04	101	bottle	47.01N	160.05E	2020/10/01
13	Stn.04	150	bottle	47.01N	160.05E	2020/10/01
14	Stn.04	200	bottle	47.01N	160.05E	2020/10/01
15	Stn.04	299	bottle	47.01N	160.05E	2020/10/01
16	Stn.04	400	bottle	47.01N	160.05E	2020/10/01
17	Stn.04	600	bottle	47.01N	160.05E	2020/10/01
18	Stn.04	801	bottle	47.01N	160.05E	2020/10/01
19	Stn.10	20	bottle	74.55N	161.88W	2020/10/10
20	Stn.10	50	bottle	74.55N	161.88W	2020/10/10
21	Stn.10	100	bottle	74.55N	161.88W	2020/10/10
22	Stn.10	150	bottle	74.55N	161.88W	2020/10/10
23	Stn.10	199	bottle	74.55N	161.88W	2020/10/10
24	Stn.10	249	bottle	74.55N	161.88W	2020/10/10
25	Stn.10	297	bottle	74.55N	161.88W	2020/10/10
26	Stn.10	400	bottle	74.55N	161.88W	2020/10/10
27	Stn.10	601	bottle	74.55N	161.88W	2020/10/10
28	Stn.10	800	bottle	74.55N	161.88W	2020/10/10
29	Stn.10	1001	bottle	74.55N	161.88W	2020/10/10
30	Stn.10	1501	bottle	74.55N	161.88W	2020/10/10
31	Stn.10	1731	bottle	74.55N	161.88W	2020/10/10
32	Stn.12	20	bottle	75.18N	160.01W	2020/10/12
33	Stn.12	50	bottle	75.18N	160.01W	2020/10/12
34	Stn.12	100	bottle	75.18N	160.01W	2020/10/12
35	Stn.12	150	bottle	75.18N	160.01W	2020/10/12
36	Stn.12	200	bottle	75.18N	160.01W	2020/10/12

Table 4.7-1. (continued)

No.	Station	Depth (m)	Method	Latitude	Longitude	Date (UTC)
37	Stn.12	250	bottle	75.18N	160.01W	2020/10/12
38	Stn.12	300	bottle	75.18N	160.01W	2020/10/12
39	Stn.12	401	bottle	75.18N	160.01W	2020/10/12
40	Stn.12	601	bottle	75.18N	160.01W	2020/10/12
41	Stn.12	800	bottle	75.18N	160.01W	2020/10/12
42	Stn.12	1000	bottle	75.18N	160.01W	2020/10/12
43	Stn.12	1501	bottle	75.18N	160.01W	2020/10/12
44	Stn.12	1993	bottle	75.18N	160.01W	2020/10/12
45	Stn.13	20	bottle	73.29N	160.01W	2020/10/13
46	Stn.13	50	bottle	73.29N	160.01W	2020/10/13
47	Stn.13	100	bottle	73.29N	160.01W	2020/10/13
48	Stn.13	151	bottle	73.29N	160.01W	2020/10/13
49	Stn.13	202	bottle	73.29N	160.01W	2020/10/13
50	Stn.13	249	bottle	73.29N	160.01W	2020/10/13
51	Stn.13	300	bottle	73.29N	160.01W	2020/10/13
52	Stn.13	401	bottle	73.29N	160.01W	2020/10/13
53	Stn.13	501	bottle	73.29N	160.01W	2020/10/13
54	Stn.13	751	bottle	73.29N	160.01W	2020/10/13
55	Stn.13	1000	bottle	73.29N	160.01W	2020/10/13
56	Stn.13	1209	bottle	73.29N	160.01W	2020/10/13
57	Stn.25	20	bottle	75.00N	175.00W	2020/10/18
58	Stn.25	50	bottle	75.00N	175.00W	2020/10/18
59	Stn.25	100	bottle	75.00N	175.00W	2020/10/18
60	Stn.25	150	bottle	75.00N	175.00W	2020/10/18
61	Stn.25	200	bottle	75.00N	175.00W	2020/10/18
62	Stn.25	249	bottle	75.00N	175.00W	2020/10/18
63	Stn.25	268	bottle	75.00N	175.00W	2020/10/18
64	surface-1	4	pump	35.40N	141.24E	2020/09/26
65	surface-2	4	pump	39.98N	142.43E	2020/09/27
66	surface-3	4	pump	43.00N	154.35E	2020/09/30
67	surface-4	4	pump	48.03N	162.00E	2020/10/01
68	surface-5	4	pump	52.03N	169.08E	2020/10/03
69	surface-6	4	pump	54.03N	171.49E	2020/10/03
70	surface-7	4	pump	57.99N	177.50E	2020/10/05
71	surface-8	4	pump	60.97N	177.52W	2020/10/05
72	surface-9	4	pump	62.01N	175.70W	2020/10/06

Table 4.7-1. (continued)

No.	Station	Depth (m)	Method	Latitude	Longitude	Date (UTC)
73	surface-10	4	pump	74.54N	161.89W	2020/10/10
74	surface-11	4	pump	75.18N	160.00W	2020/10/12
75	surface-12	4	pump	73.29N	160.01W	2020/10/13
76	surface-13	4	pump	75.02N	175.00W	2020/10/18
77	surface-14	4	pump	73.01N	168.83W	2020/10/20
78	surface-15	4	pump	69.51N	168.83W	2020/10/21
79	surface-16	4	pump	67.00N	168.83W	2020/10/21
80	surface-17	4	pump	64.68N	170.03W	2020/10/22

4.8. Radiocesium (^{134}Cs and ^{137}Cs)

(1) Personnel

Yuichiro Kumamoto (JAMSTEC) – Principal investigator, Not on board

(2) Objective

Determination of activity concentrations of radiocesium (^{134}Cs and ^{137}Cs) in the Arctic Ocean, Bering Sea, and northern North Pacific Ocean.

(3) Parameters

^{134}Cs, ^{137}Cs

(4) Instruments and Methods

a. Sampling

Seawater samples for radiocesium were collected using 12-liter PVC bottles. Surface seawater was collected from continuous pumped-up water at about 4-m depth. The sample volumes is 40 L (two 20-L plastic containers).

b. Preparation and analysis

The seawater sample for radiocesium measurement was not filtered and was acidified by adding nitric acid. Radiocesium in the seawater sample is concentrated using ammonium phosphomolybdate (AMP) that forms an insoluble compound with cesium. The radiocesium (^{134}Cs and ^{137}Cs) in the compound is measured using Ge gamma-ray spectrometers.

(5) Sample list

We collected 34 seawaters for the radiocesium measurements in the Arctic Ocean, Bering Sea, and northern North Pacific Ocean during this cruise (Table 4.8-1).

(6) Data archives

These data obtained in this cruise will be submitted to the Data Management Group (DMG) of JAMSTEC, and will be opened to the public via "Data Research System for Whole Cruise Information in JAMSTEC (DARWIN)" in JAMSTEC web site.
<http://www.godac.jamstec.go.jp/darwin/e>

Table 4.8-1. Seawater samples collected for radiocesium measurements.

No.	Station	Depth (m)	Method	Latitude	Longitude	Date (UTC)
1	Stn.01	10	bottle	32.00N	147.00E	2020/09/21
2	Stn.01	50	bottle	32.00N	147.00E	2020/09/21
3	Stn.01	100	bottle	32.00N	147.00E	2020/09/21
4	Stn.01	150	bottle	32.00N	147.00E	2020/09/21
5	Stn.01	199	bottle	32.00N	147.00E	2020/09/21
6	Stn.01	300	bottle	32.00N	147.00E	2020/09/21
7	Stn.01	400	bottle	32.00N	147.00E	2020/09/21
8	Stn.01	600	bottle	32.00N	147.00E	2020/09/21
9	Stn.01	802	bottle	32.00N	147.00E	2020/09/21
10	Stn.04	9	bottle	47.01N	160.05E	2020/10/01
11	Stn.04	50	bottle	47.01N	160.05E	2020/10/01
12	Stn.04	101	bottle	47.01N	160.05E	2020/10/01
13	Stn.04	150	bottle	47.01N	160.05E	2020/10/01
14	Stn.04	200	bottle	47.01N	160.05E	2020/10/01
15	Stn.04	299	bottle	47.01N	160.05E	2020/10/01
16	Stn.04	400	bottle	47.01N	160.05E	2020/10/01
17	Stn.04	600	bottle	47.01N	160.05E	2020/10/01
18	Stn.04	801	bottle	47.01N	160.05E	2020/10/01
19	Stn.10	10	bottle	74.55N	161.88W	2020/10/10
20	Stn.10	50	bottle	74.55N	161.88W	2020/10/10
21	Stn.10	100	bottle	74.55N	161.88W	2020/10/10
22	Stn.10	150	bottle	74.55N	161.88W	2020/10/10
23	Stn.10	200	bottle	74.55N	161.88W	2020/10/10
24	Stn.10	300	bottle	74.55N	161.88W	2020/10/10
25	Stn.10	400	bottle	74.55N	161.88W	2020/10/10
26	Stn.10	600	bottle	74.55N	161.88W	2020/10/10
27	Stn.10	801	bottle	74.55N	161.88W	2020/10/10
28	surface-5	4	pump	52.03N	169.08E	2020/10/03
29	surface-8	4	pump	60.97N	177.52W	2020/10/05
30	surface-11	4	pump	75.18N	160.00W	2020/10/12
31	surface-12	4	pump	73.29N	160.01W	2020/10/13
32	surface-13	4	pump	75.02N	175.00W	2020/10/18
33	surface-15	4	pump	69.51N	168.83W	2020/10/21
34	surface-17	4	pump	64.68N	170.03W	2020/10/22

4.9. Underway surface water monitoring

(1) Personnel

Amane Fujiwara (JAMSTEC) – Principal investigator

Masahiro Orui (Marine Works Japan Ltd.; MWJ) – Operation leader

Misato Kuwahara (MWJ)

Haruka Sato (MWJ)

(2) Objective

Our purpose is to continuously obtain temperature, salinity, dissolved oxygen, fluorescence, and total dissolved gas pressure data of near-sea surface water.

(3) Parameters

Temperature

Salinity

Dissolved oxygen

Fluorescence

Turbidity

Total dissolved gas pressure

(4) Instruments and Methods

The Continuous Sea Surface Water Monitoring System (Marine Works Japan Co. Ltd.) has four sensors and automatically measures temperature, salinity, dissolved oxygen, chlorophyll-a fluorescence, and turbidity in near-sea surface water every one minute. This system is located in the "sea surface monitoring laboratory" and connected to shipboard LAN-system. Measured data, time, and location of the ship were stored in a data management PC. Sea water was continuously pumped up to the laboratory from an intake placed at the approximately 4.5 m below the sea surface and flowed into the system through a vinyl-chloride pipe. The flow rate of the surface seawater was adjusted to 10 dm^3 min^{-1}.

a. Instruments

Software

SeaMoni Ver.1.2.0

Sensors

Specifications of each sensor in this system are listed below.

Temperature and Conductivity sensor

Model:	SBE-45, SEA-BIRD ELECTRONICS, INC.
Serial number:	4563325-0362
Measurement range:	Temperature -5 °C - +35 °C
	Conductivity 0 S m^{-1} - 7 S m^{-1}
Initial accuracy:	Temperature 0.002 °C
	Conductivity 0.0003 S m^{-1}
Typical stability (per month):	Temperature 0.0002 °C
	Conductivity 0.0003 S m^{-1}
Resolution:	Temperature 0.0001 °C
	Conductivity 0.00001 S m^{-1}

Bottom of ship thermometer

Model:	SBE 38, SEA-BIRD ELECTRONICS, INC.
Serial number:	3857820-0540
Measurement range:	-5 °C – +35 °C
Initial accuracy:	±0.001 °C
Typical stability (per 6 month):	0.001 °C
Resolution:	0.00025 °C

Dissolved oxygen sensor

Model:	RINKO II, JFE ADVANTECH CO. LTD.
Serial number:	13
Measuring range:	0 mg L^{-1} – 20 mg L^{-1}
Resolution:	0.001 mg L^{-1} – 0.004 mg L^{-1} (25 °C)
Accuracy:	Saturation ± 2 % F.S. (non-linear) (1 atm, 25 °C)

Fluorescence & Turbidity sensor

Model:	C3, TURNER DESIGNS
Serial number:	2300707
Measuring range:	Chlorophyll in vivo 0 µg L^{-1} – 500 µg L^{-1}
Minimum Detection Limit:	Chlorophyll in vivo 0.03 µg L^{-1}
Measuring range:	Turbidity 0 NTU - 1500 NTU
Minimum Detection Limit:	Turbidity 0.05 NTU

Total dissolved gas pressure sensor

Model:	HGTD-Pro, PRO OCEANUS
Serial number:	37-394-10
Temperature range:	-2 °C – 50 °C
Resolution:	0.0001 %
Accuracy:	0.01 % (Temperature Compensated)
Sensor Drift:	0.02 % per year max (0.001 % typical)

(5) Observation log

Periods of measurement, maintenance, and problems during this cruise are listed in Table 4.9-1.

Table 4.9-1. Events list of the Sea surface water monitoring during MR20-05C.

System Date [UTC]	System Time [UTC]	Events	Remarks
2020/09/19	11:20	All the measurements started and data was available.	Start
2020/09/26	01:01-01:56	All the measurements stopped.	Filter Cleaning System Maintenance
2020/09/28	01:01-08:49	All the measurements stopped.	Pump stopped
2020/10/04	02:35-02:39	All the measurements stopped.	Software Maintenance
2020/10/06	07:32-08:02	Filter Cleaning	-
2020/10/10	01:03-01:10	Filter Cleaning	-
2020/10/16	01:25-01:42	Filter Cleaning	-
2020/10/20	03:34-03:40	Filter Cleaning	-
2020/10/25	21:05	All the measurements stopped.	End

We took the surface water samples from this system once a day to compare sensor data with bottle data of salinity, dissolved oxygen, and chlorophyll a. The results are shown in Figure 4.9 -2. All the salinity samples were analyzed by the Model 8400B "AUTOSAL" manufactured by Guildline Instruments Ltd. (see 3.12), dissolve oxygen samples were analyzed by Winkler method (see 4.1), and chlorophyll a were analyzed by 10-AU manufactured by Turner Designs. (see 4.11).

(a)

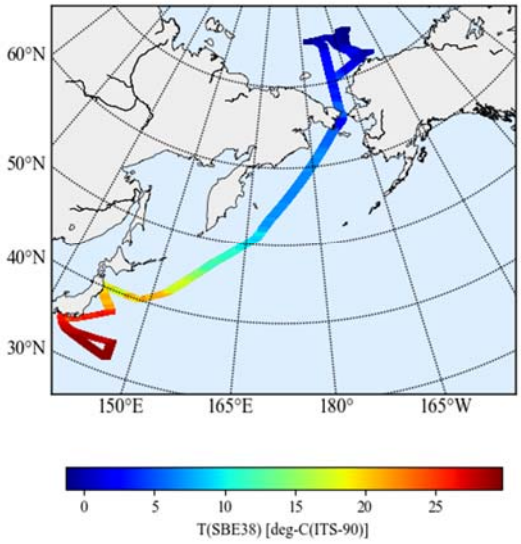
60°N
50°N
40°N
30°N
150°E
165°E
180°
165°W
0
5
10
15
20
25
T(SBE38) [deg-C(ITS-90)]

(b)

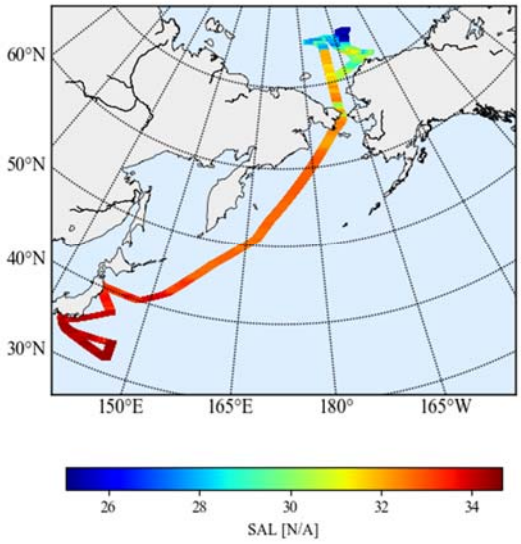
60°N
50°N
40°N
30°N
150°E
165°E
180°
165°W
26
28
30
32
34
SAL [N/A]

(c)

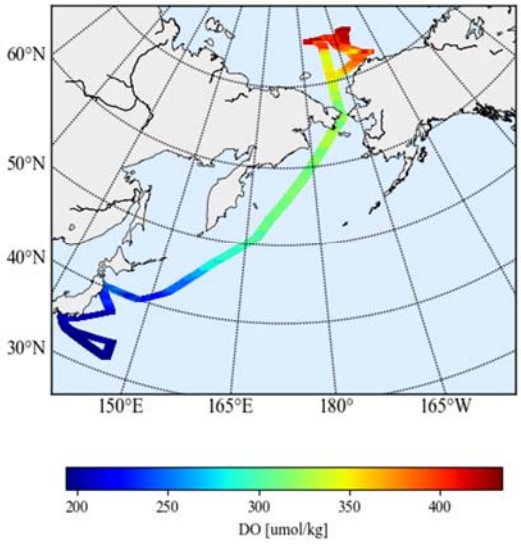

(d)

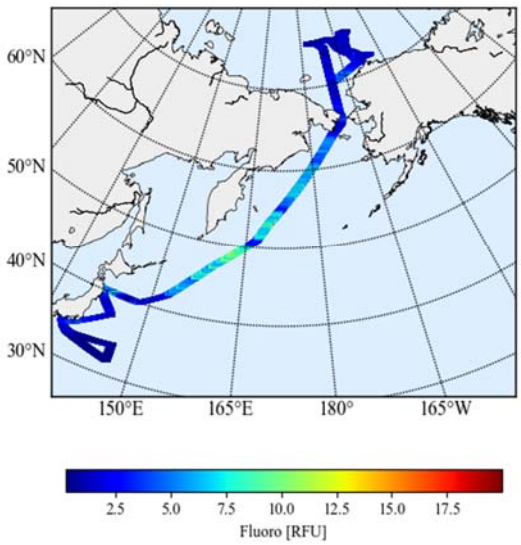

Figure 4.9-1. Spatial distribution of (a) temperature, (b) salinity, (c) dissolved oxygen, and (d) chlorophyll-a fluorescence in MR20-05C cruise.

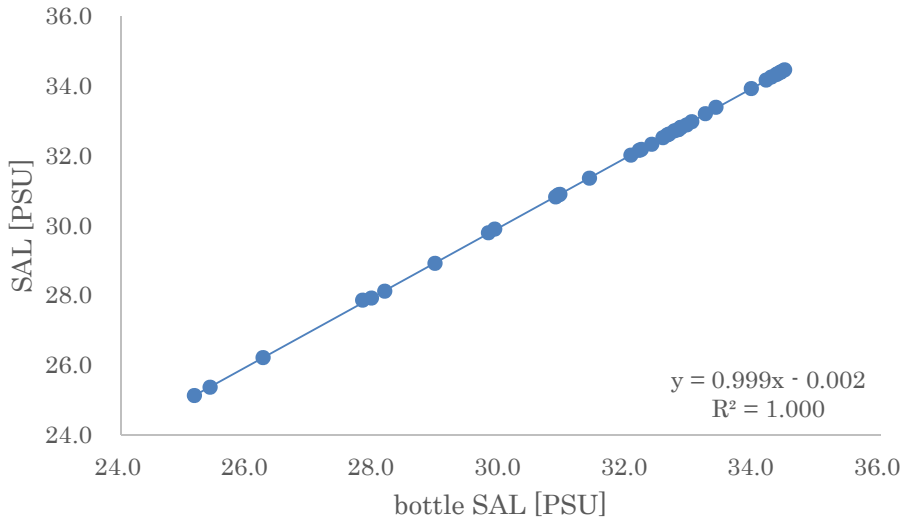

Figure 4.9-2-1. Correlation of salinity between sensor data and bottle data.

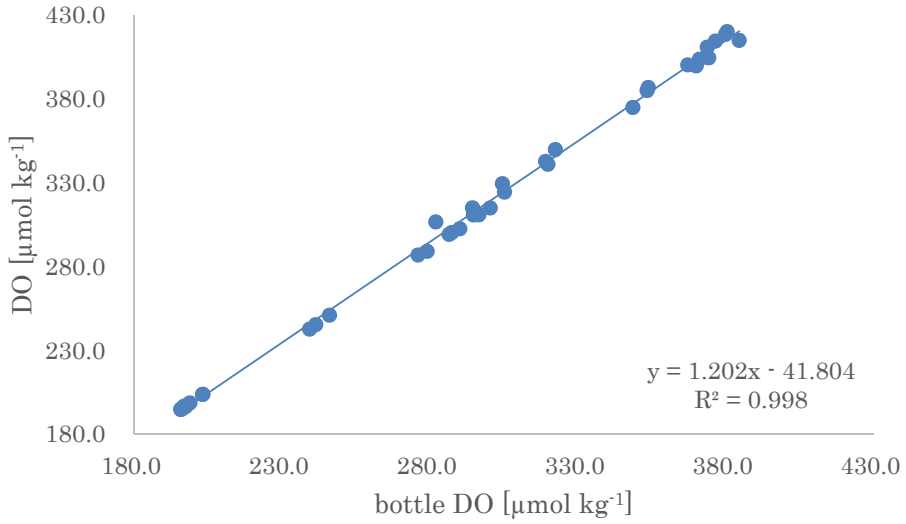

Figure 4.9-2-2. Correlation of dissolved oxygen between sensor data and bottle data.

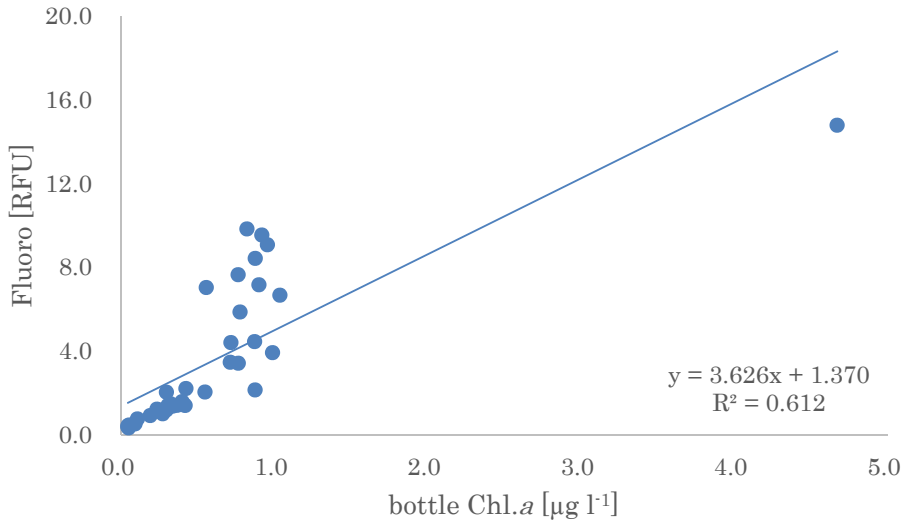

Figure 4.9-2-3. Correlation of fluorescence between sensor data and bottle data.

(6) Data archives

These data obtained in this cruise will be submitted to the Data Management Group (DMG) of JAMSTEC, and will opened to the public via "Data Research System for Whole Cruise Information in JAMSTEC (DARWIN)" in JAMSTEC web site.
<http://www.godac.jamstec.go.jp/darwin/e>

4.10. Continuous measurement of pCO_2

(1) Personnel

Akihiko Murata (JAMSTEC) – Principal investigator, Not on board

Nagisa Fujiki (Marine Works Japan Ltd.; MWJ) – Operation leader

Yuta Oda (MWJ)

Hiroshi Hoshino (MWJ)

(2) Objective

To survey spatial distributions of surface seawater pCO_2 in the western Arctic Ocean.

(3) Parameters

Partial pressures of CO_2 (pCO_2)

(4) Methods, Apparatus and Performance

Atmospheric and surface seawater pCO_2 were measured with a system having the off-axis integrated-cavity output spectroscopy gas analyzer (Off-Axis ICOS; 911-0011, Los Gatos Research). The CO_2 concentrations of the standard gases used for calibration were measured every about 4 hours to calibrate the system. The CO_2 concentrations in air taken from the bow of the ship (approx.13 m above the sea level) were measured every about two hours. Seawater was taken from an intake placed at the approximately 4.5 m below the sea surface and introduced into the equilibrator at the flow rate of 4 – 5 L min^{-1} by a pump. The equilibrated air was circulated in a closed loop by a pump at flow rate of 0.6 - 0.7 L min^{-1} through two electric cooling units, a starling cooler, and the Off-Axis ICOS.

(5) Preliminary result

Distributions of surface seawater CO_2 were shown in Figure 4.10-1, along with those of sea surface temperature (SST).

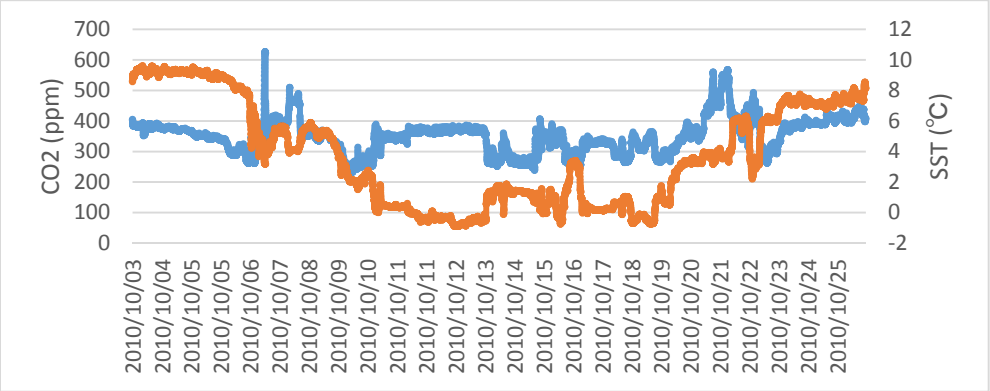

Figure 4.10-1. Distributions of surface seawater CO_2 (blue) and SST (orange) as a function of observation time.

(6) Date archives

These data obtained in this cruise will be submitted to the Data Management Group (DMG) of JAMSTEC, and will be opened to the public via "Data Research System for Whole Cruise Information in JAMSTEC (DARWIN)" in JAMSTEC web site.
<http://www.godac.jamstec.go.jp/darwin/e>

4.11. Chlorophyll *a*

(1) Personnel

Amane Fujiwara (JAMSTEC) – Principal investigator
Hiroaki Sakoh (Marine Works Japan Ltd.; MWJ) – Operation leader
Erii Irie (MWJ)

(2) Objectives

Chlorophyll-a, a major photosynthetic pigment of phytoplankton, is widely used as a proxy of phytoplankton biomass. The objective of the sampling of chlorophyll-a concentration is to investigate the vertical and horizontal distribution of phytoplankton bulk and size fractionated biomass in the Arctic Ocean.

(3) Parameters

Total chlorophyll *a*
Size-fractionated chlorophyll *a*
Comparison of Trapped efficiency by filters

(4) Instruments and methods

We collected samples for total chlorophyll *a* (chl-*a*) concentration from 7 to 13 depths and size-fractionated chl-*a* from 6 depths between the surface and 200 m depth including a chl-*a* maximum layer. The chl-*a* maximum layer was determined by a fluorometer (Seapoint Sensors, Inc.) attached to the CTD system. Replicate water sample was taken at chl-a maximum depth from the same Niskin bottle in order to assess our precision of chl-*a* measurement.

Water samples for total chl-*a* were vacuum-filtrated (<0.02MPa) through 25mm-diameter ADVANTEC GF-75 filter. Water samples for size-fractionated chl-*a* were passed through 20 μm pore-size nylon filter (47 mm in diameter), 2μm pore-size nuclepore filters (47 mm in diameter), and ADVANTEC GF-75 filter (25 mm in diameter) under gentle vacuum (<0.02MPa).

The filter samples were immediately soaked in 7 ml of N,N-dimethylformamide (DMF) in a polypropylene tube. The tubes were stored at –20°C under the dark condition to extract chl-*a* at least for 24 hours. Some tubes were kept at –80°C under the dark condition until the extraction.

Chl-*a* concentrations were measured by a fluorometer (10-AU, TURNER DESIGNS) following to the method of Welschmeyer (1994). The 10-AU fluorometer was calibrated against a pure chl-*a* (Sigma-Aldrich Co., LLC) prior to the analysis.

We also evaluated the trapped efficiency between different brand of glass fiber filter, ADVANTEC GF-75 filter (standard chl-*a* filter for the SAS project) and Whatman GF/F filter (historically used filter for Mirai cruises). 20 replicate water samples were collected from chl-*a* maximum layer or surface for the comparison.

(5) Sampled location

Samples for total chl-*a* were collected at 21 sites in the Arctic Ocean, 1 site in the subarctic zone, and 3 sites in the subtropical zone (Figure 4.11-1). Samples for size-fractionated chl-*a* were collected at 11 sites in the Arctic Ocean and 1 site in the subarctic zone (Figure 4.11-1).

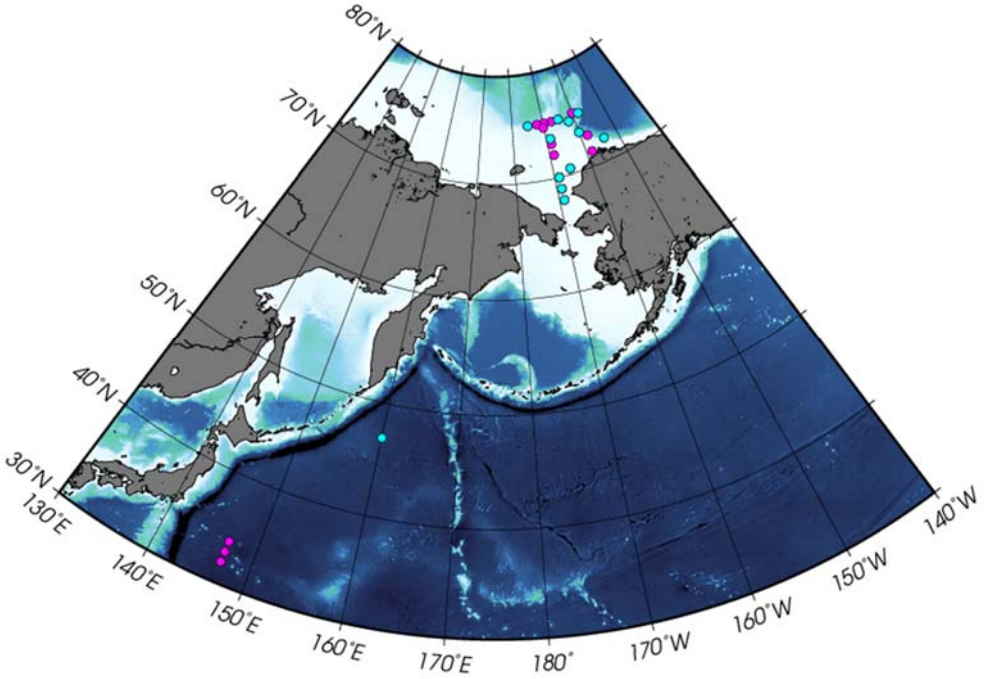

Figure 4.11-1. Sampling positions of total chl-*a* and both total and size-fractionated chl-a were taken are shown in magenta and cyan circles, respectively.

(6) Preliminary results

Vertical distributions of total chl-*a* along 75°N are shown in Figure 4.11-2.

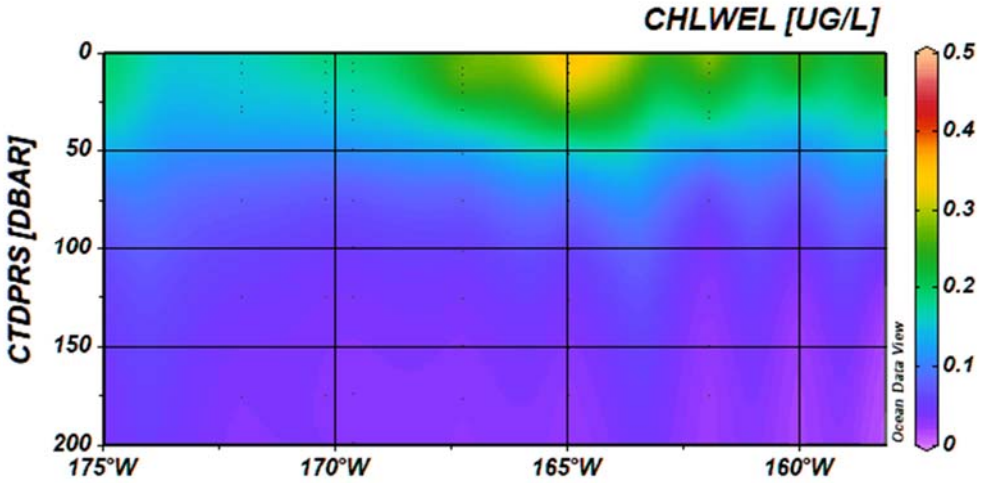

Figure 4.11-2. Vertical section of total chl-*a* concentration along 75°N.

The result of comparison of the trapped efficiency between the different filters is shown in Figure 4.11-3 and Table 4.11-1. There was no statistically significant difference between chl-*a* concentrations obtained by the different glass fiber filters (*p*-value = 0.92, t-test).

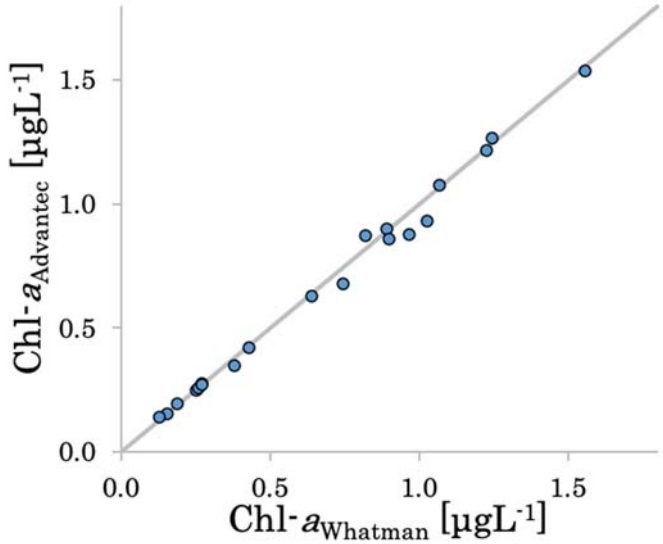

Figure 4.11-3. Comparison of chl-a concentration obtained by Advantec GF-75 and Whatman GF/F filters. Gray line indicates 1:1. Statistics are also shown in Table 4.11-1.

Table4.11-1. Results of the trapped efficiency experiment.

	min	max	Avg.	S.D.
Difference in Chl-*a* concentration (µgL^{-1})	-0.094	0.051	-0.014	0.035

The result of the evaluation of our measurement precision is summarized in Table 4.11-2. The standard deviation of absolute difference among 15 pairs of chl-*a* concentration was 0.023 (µg L^{-1}) and relative error was 4.3%.

Table 4.11-2. Result of the measurement precision experiment.

Number of replicate sample pairs	Standard deviation (µgL^{-1})	Relative error (%)
15	0.023	4.3

(7) Data archives

These data obtained in this cruise will be submitted to the Data Management Group (DMG) of JAMSTEC, and will be opened to the public via "Data Research System for Whole Cruise Information in JAMSTEC (DARWIN)" in JAMSTEC web site.
<http://www.godac.jamstec.go.jp/darwin/e>

(8) Reference

Welschmeyer, N. A. (1994): Fluorometric analysis of chlorophyll *a* in the presence of chlorophyll *b* and pheopigments. Limnol. Oceanogr., 39, 1985–1992.

4.12. Bio-optical observations

(1) Personnel

Amane Fujiwara (JAMSTEC) – Principal Investigator

(2) Objectives

The objective of these observations is to develop and evaluate ocean color algorithms to estimate phytoplankton community composition and algal size using optical properties of seawater as well as investigating in-situ phytoplankton community structure and in-water optical properties. Results from these investigations will be applied to satellite remote sensing and used to clarify the responses of phytoplankton to the recent climate change in the western Arctic Ocean.

(3) Parameters

A. Surface and underwater spectral radiance and irradiance
B. Phytoplankton pigments and absorption coefficient
C. Underway measurement of Multi-spectral excitation/emission fluorescence

(4) Instruments and methods

A) Surface and underwater spectral radiance and irradiance

Underwater spectral downwelling planar irradiance, $E_d(\lambda, z)$ [μW cm^{-2} nm^{-1}], and upwelling radiance, $L_u(\lambda, z)$ [μW cm^{-2} nm^{-1} str^{-1}], at 17 wavelengths over the spectral range 380 – 765 nm were measured with a C-OPS spectroradiometer (Biospherical Instrument Inc.). The C-OPS was deployed in free-fall mode up to ~100 m deep at a distance from the stern of ship to avoid ship shadows. Downwelling irradiance incident upon the sea surface $E_d(\lambda, z = 0+)$ was also monitored by a reference sensor with the same specifications as the underwater sensor. Before each deployment of the instrument, 30 seconds of averaged dark values were recorded. Underwater photosynthetically available radiation (PAR) was also calculated by converting the $E_d(\lambda, z)$ to quantum units, $E_{d,q}(\lambda, z)$ [μmol photons m^{-2} s^{-1}], and integrating the $E_{d,q}(\lambda, z)$ from 395 to 710 nm.

B) Seawater samples for phytoplankton pigments were collected from the sea surface and other depths using a bucket or Niskin-X bottles on the CTD/R. 1 – 4 L of water sample were filtered on a glass fiber filter (GF/F, 47 mm) and stored in a super freezer (-80 °C). Pigment concentrations will be analyzed on land using high performance liquid chromatography (HPLC) (Agilent Technologies 1300 series) following to the method of van Heukelem and Thomas (2001) after the cruise, and will provide information on phytoplankton biomass and community structure.

Seawater samples for absorption coefficients measurement were collected from the sea surface. For measurements of spectral absorption coefficient of particles, particles in 1-4 liter(s) of water sample were concentrated on a glass fiber filter (Whatman GF/F, 25 mm). Filter samples were stored in a super freezer (-80˚C). Optical density (OD) of

particles on the filter pad will be measured on land with a spectrophotometer following to the method of Stramski et al. (2015), and then, absorption coefficient of particles ($a_p(\lambda)$), detritus ($a_d(\lambda)$), and phytoplankton ($a_{ph}(\lambda, z)$) we be determined. For measurements of spectral absorption coefficient of CDOM ($a_{CDOM}(\lambda)$), ~300 ml of water sample was filtrated through a 0.2 μm Nuclepore filter (Whatman, 47 mm). Filtered water samples were stored in a refrigerator until analysis on land. $a_{CDOM}(\lambda)$ will also be measured using a spectrophotometer.

C) Horizontal distribution of multi-spectral excitation/emission fluorescence was measured using a *Multi-Exciter* instrument (JFE-Advantech Inc.). *Multi-Exciter* detects fluorescence signals from 630 to 1000 nm which excited at 9 bands (375, 400, 420, 435, 470, 505, 525, 570, and 590 nm). The *Multi-Exciter* was attached to the continuous surface water monitoring system and measured the spectral fluorescence of surface water for every 15 minutes along the cruise track. 22 HPLC samples were also taken from continuous surface water monitoring system to compare the fluorometric signals and phytoplankton pigment composition.

(5) Station list and sampling location

Table 4.12-1. Number of instrument deployments or discrete water samples collected for each parameter on the cruise.

Instrument	*Number of stations*
C-OPS	13
Parameter	*Number of samples*
$a_p(\lambda)$, $a_d(\lambda)$, $a_{ph}(\lambda)$,	13
$a_{CDOM}(\lambda)$	13
Phytoplankton pigments (HPLC)	86 (64 for vertical, 22 for surface)

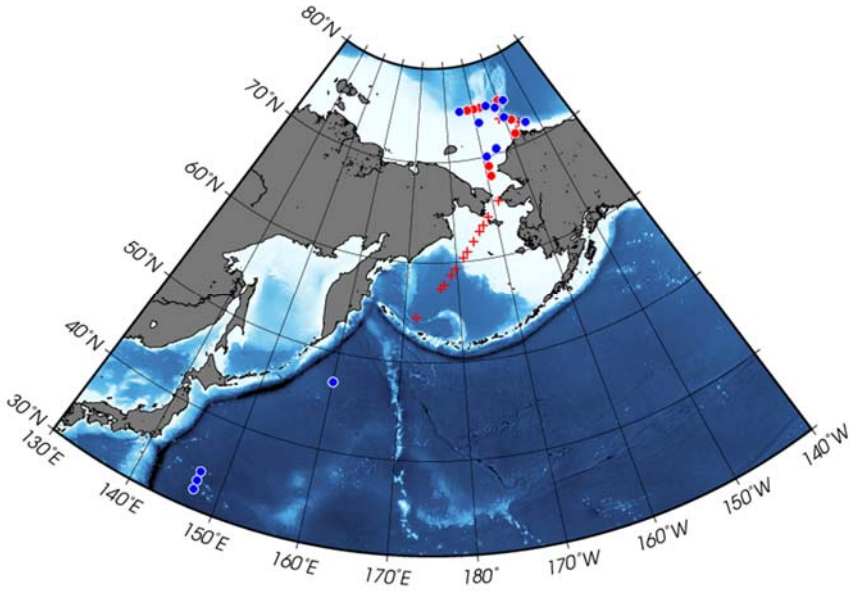

Figure 4.12-1. Sampling locations of bio-optical observations. Red crosses and circles indicate the sites where HPLC samples were collected from surface and vertical water column, respectively. Blue circles indicate the cites where both HPLC and bio-optical parameters were taken.

(6) Data archives

These data obtained in this cruise will be submitted to the Data Management Group (DMG) of JAMSTEC, and will be opened to the public via "Data Research System for Whole Cruise Information in JAMSTEC (DARWIN)" in JAMSTEC web site.
<http://www.godac.jamstec.go.jp/darwin/e>

(7) Reference cited

Stramski, D., R. A. Reynolds, S. Kaczmarek, J. Uitz and G. Zheng. 2015. Correction of pathlength amplification in the filter-pad technique for measurements of particulate absorption coefficient in the visible spectral region. *Appl. Opt.*, 54, 6763-6782. doi: 10.1364/AO.54.006763.

Van Heukelem, L, Thomas C. S. 2001. Computer-assisted high-performance liquid chromatography method development with applications to the isolation and analysis of phytoplankton pigments. *J Chromatogr A*, 910, 31–49.

4.13. Nitrogen cycle

4.13.1. Nitrogen cycle in the Chukchi and Beaufort Seas

(1) Personnel

Takuhei Shiozaki (The University of Tokyo) – Principal investigator

Yuki Sato-Takabe (The University of Tokyo) – Not on board

(2) Objectives

The Arctic Ocean has been experiencing the sharpest decline in sea ice, with summer sea ice extent decreasing at a rate of 13% per decade (Serreze & Meier, 2019). The sea ice reduction leads to an increase in light in the sea. This allows phytoplankton, which has been limited by light, to flourish, and their production is now increasing across the Arctic Ocean (Lewis et al., 2020). This increase in light in the sea may have unexpected effects on the marine ecosystem, which is a decrease in nitrification (Shiozaki et al., 2019). Nitrification is the process by which microbes convert ammonia to nitrite, and then to nitrate is known to be limited by light (Ward, 2008). We showed that light is the main regulatory factor for nitrifiers in the Arctic Ocean, and that even very low light level can suppress nitrification (Shiozaki et al., 2019). The sea ice reduction may therefore alter the nitrogen cycle, and consequently Arctic marine ecosystem since nitrogen is major limiting nutrient for biological production in the Arctic Ocean (Trembley et al., 2015). However, our knowledge about the nitrogen cycle in the Arctic Ocean is still limited, which makes it difficult to predict the impact of environment changes on marine ecosystem. To examine the changes in nitrogen cycle and primary production, we have monitored the following parameters in the Chukchi and Beaufort Seas since 2015.

(3) Parameters

Nitrogen fixation rate

Nitrate assimilation rate

Ammonium assimilation rate

Ammonia oxidation rate

Primary production

Chlorophyll *a*

Nutrients

Microbial community (DNA and RNA)

Abundance of Aerobic anoxygenic phototrophic bacteria (AAnPB)

(4) Instruments and methods

Water samples for incubation experiments, nutrients, chlorophyll *a*, DNA, and RNA analysis were collected from depths corresponding to 100, 10, 1, and 0.1% of surface light intensity, and from near bottom in the shelf or from 100 m in the off-shelf with acid-cleaned Niskin-X bottles and a bucket (from surface sample). Further, samples for

ammonia oxidation and DNA were collected from additional depths (1000 m or bottom depth minus 10 m) in the off-shelf region. The depth profiles of light intensity were obtained using a C-OPS (Biospherical Instruments) before the sampling.

Nitrogen fixation, nitrate and ammonium assimilation, and ammonia oxidation rates were evaluated using ^{15}N tracer. Nitrogen fixation rate was determined by the gas dissolution method (Mohr et al., 2010). Primary production was determined using ^{13}C tracer. After addition of the tracers, the incubation bottles were placed into on-deck incubators cooled by flowing surface seawater. Light levels were adjusted using neutral-density screens. The samples from below the euphotic zone were wrapped in aluminum foil and incubated in a thermostatic incubator. Samples of 1 or 2 L collected for estimating the initial ^{15}N and ^{13}C enrichment of particulate organic matter were filtered immediately at the beginning of the incubation. The incubations for nitrogen fixation, nitrate and ammonia assimilation were terminated by gentle vacuum filtration of the seawater samples through a precombusted GF/F filter. Those for ammonia oxidation were terminated by filtration using 0.2 μm pore-size filters, and filtrate was collected. The filters and filtrate were kept frozen (-20 °C) for on-shore analysis.

Samples for nutrients analysis were collected in 10 mL acrylic tubes and were immediately determined on board using a QuAAtro system (see a report of S. Nishino and colleagues in this issue). Samples for chlorophyll *a* of 290 ml were filtered onto 25-mm Whatman GF/F filters, and the chlorophyll *a* concentration were measured fluorometrically using a Turner Design 10-AU fluorometer after extraction with *N*, *N*-dimethylformamide on board. Samples for DNA and RNA analyses were filtered onto Sterivex-GP pressure filter units with a 0.22 μm pore size (Millipore). RNA samples were filtered within 30 min and then added to RNA*later* Stabilization Solution (Life Technologies). The Sterivex filter units were frozen at -80°C until onshore analyses. Samples for AAnPB were collected in 25-mL centrifuge tubes and were fixed with glutaraldehyde filtered by 0.2-μm pore-size fileters. The samples were stored >3 hr at 4 °C in the dark, and filtered onto a Nuclepore black polycarbonate membrane filters (0.2-μm pore-size) under gentle vacuum (≤20 cm Hg).

(5) Data archives

These data obtained in this cruise will be submitted to the Data Management Group (DMG) of JAMSTEC, and will be opened to the public via "Data Research System for Whole Cruise Information in JAMSTEC (DARWIN)" in JAMSTEC web site.
<http://www.godac.jamstec.go.jp/darwin/e>

4.13.2. N nutrient addition experiment

(1) Personnel

Takuhei Shiozaki (The University of Tokyo) – Principal investigator

Amane Fujiwara (JAMSTEC)

(2) Objective

We recently showed that Arctic nitrification is primarily regulated by the light environment and may have experienced a decreasing trend over the last two decades (Shiozaki et al., 2019). The suppression of nitrification may alter the composition of inorganic N nutrient. Here we examined how microbial ecosystem change with different inorganic N nutrient composition by microcosm experiments.

(3) Parameters

Chlorophyll *a*

Nutrients

Abundance of pico- and nano-sized phytoplankton

Abundance of bacteria

Phytoplankton pigments

Microbial community (DNA)

(4) Instruments and methods

The experiments were performed using seawater collected from 68 m at Sta. 11 and 28 m at Sta. 13. The seawater was sieved by 100 μm-mesh to reduce grazing pressure and dispensed into nine 10 L polyethylene bags at each station. Three different triplicate treatments were set up: control without any nutrient addition, nitrate addition treatment (final concentration: ~5 μM), and ammonium addition treatment (final concentration: ~5 μM). These bags were treated under dim light condition (10 μmol photon s^{-1} m^{-2}) representing 1% light levels relative to the surface with a 10:14 light:dark cycle in a thermostatic room (4 °C). Experiments were lasted for 16 and 14 days at Sta. 11 and 13, respectively. Sampling frequencies of each parameter are listed as follows (Tables 4.13.2-1 and 2).

Table 4.13.2-1. Sampling frequency of each parameters for samples collected at Sta. 11.

Day	0	2	4	6	8	10	12	14	16
Chla	○	○	○	○	○	○	○	○	○
Nutrients	○	○	○	○	○	○	○	○	○
Pico-Nano	○		○	○	○	○	○	○	○
Bacteria	○		○	○	○	○	○	○	○
Pigments	○				○				○
DNA	○				○				○

Table 4.13.2-2. Sampling frequency of each parameters for samples collected at Sta. 13.

Day	0	2	4	6	8	10	12	14
Chla	○	○	○	○	○	○	○	○
Nutrients	○	○	○	○	○	○	○	○
Pico-Nano	○	○	○	○	○	○	○	○
Bacteria	○	○	○	○	○	○	○	○
Pigments	○				○			○
DNA	○				○			○

(5) Data archives

These data obtained in this cruise will be submitted to the Data Management Group (DMG) of JAMSTEC, and will be opened to the public via "Data Research System for Whole Cruise Information in JAMSTEC (DARWIN)" in JAMSTEC web site.
<http://www.godac.jamstec.go.jp/darwin/e>.

References

Lewis, K. M., van Dijken, G. L., & Arrigo, K. R. (2020). Changes in phytoplankton concentration now drive increased Arctic Ocean primary production. Science, 369, 198-202.

Serreze, M. C., & Meier, W. N. (2019). The Arctic's sea ice cover: trends, variability, predictability, and comparisons to the Antarctic. Annals of the New York Academy of Sciences, 1436, 36-53. https://doi.org/10.1111/nyas.13856.

Shiozaki, T., Ijichi, M., Fujiwara, A., Makabe, A., Nishino, S., Yoshikawa, C., et al. (2019). Factors regulating nitrification in the Arctic Ocean: Potential impact of sea ice reduction and ocean acidification. Global Biogeochemical Cycles, 33, 1085-1099.

Tremblay, J-É, Anderson, L. G., Matrai, P., Coupel, P., Bélanger, S., Michel, C., et al. (2015). Global and regional drivers of nutrient supply, primary production and CO2 drawdown in the changing Arctic Ocean. Progress in Oceanography, 139, 171-196.

Ward, B. B. (2008). Nitrification in marine systems. In D. G. Capone, D. A. Bronk, M. R. Mulholland, & E. J. Carpenter (Eds.), Nitrogen in the Marine Environment, (2nd ed.), pp. 199–261. Burlington, MA: Academic Press. https://doi.org/10.1016/B978-0-12-372522-6.00005-0.

4.14. Environmental DNA

(1) Personnel

Akihide Kasai (Hokkaido University) – Principal investigator, Not on board

Tatsuya Kawakami (Hokkaido University)

(2) Objectives

To depict the aquatic biodiversity is essential to reveal the substantial impacts of climate change on the Arctic marine ecosystems. Fishes are one of the major components of the ecosystem and can be very susceptible to climate warming. Elevating temperature, sea-ice cover reduction, and changes in primary production seasonality would induce pole-ward shifts of their distributions and anomalous fluctuations in the abundances. Fishes also include major fishery species (e.g., cods, flatfishes, rockfishes, salmons). Because they are important for the Arctic culture and economy, their ecological changes will also influence human activity. However, comprehensive research of fish diversity in the Arctic region has often been difficult by conventional methods (e.g., bottom trawling and visual census) because those are labor-intensive and have limitations in operating in the ice-covered area.

Analyzing environmental DNA (eDNA) is an emerging method to assess aquatic community composition. eDNA originated from aquatic organisms in various forms (e.g., cells, feces, gametes) can be retrieved from seawater and used in quantitative PCR (qPCR) assay or metabarcoding to identify organisms present in the study site. Because the eDNA approach has successfully been applied to various environments (river, lake, coastal area), it can also be considered a promising tool for Arctic studies.

Therefore, this cruise's primary aim is to collect eDNA samples to analyze the fish community in the Arctic Ocean. eDNA samples were also collected in the North Pacific Ocean and the Bering Sea to enabling latitudinal comparison in the fish community. However, many technical issues, such as eDNA capture efficiency, PCR inhibition, and optimization of sampling effort, still need to be solved. So, replicate sampling was conducted to estimate the optimal sampling effort.

(3) Parameters

eDNA

(4) Instruments and methods

(4.1) Pumped surface water

(4.1.1) Routine sampling

Surface seawater continuously pumped up from about 4.5 m depth for the underway sea-surface monitoring was routinely collected. The water was pre-filtered using a metal scrub brush along the way of intake. The collection was performed once a day at around sunset (in the North Pacific Ocean and the Bering Sea) or twice a day around sunrise and sunset (in the Arctic Ocean). The water was collected in two sterilized 10 l plastic

bags for every collection. Accordingly, filtered samples were obtained from 55 sites (Table 4.14-1).

Water samples were vacuum-filtered onto 0.45 μm Sterivex™-HV PVDF filters (Millipore) in duplicate, with an aspirator (As-one, GAS-1N) connected to a manifold (Rocker, Multivac 310-MS). The filtration was terminated when the filter was clogged. So, the filtering volumes differed among the sampling sites and even between the replicates (between 2.35 and 12 l per filter). After filtration, the filters were filled with 1.6 ml of RNAlater and then stored at −20 °C.

(4.1.2) Replicate sampling

Additional water collection was performed at four sites (Table 4.14-1: St. 03 in the subtropic, St. 04 in the frigid, and St. 10 and 35 in the Arctic region) to obtain samples for optimization of sampling effort. Eight filtering replicates of the 0.45 μm filter were collected at each site. The water was collected in eight sterilized 10 l plastic bags and sub-sampled from each bag. Filtering volume was equal among the replicates within the site (3 or 5 l), and a total of 24–40 l of water was filtered at each site.

Small experiments to compare eDNA capture efficiency between two filters having different pore sizes were also conducted at three sites (St. 03, St. 04, and St. 35). The same seawater filtered in the above was also filtered using 0.22 μm Sterivex™-GV PVDF filters in this experiment. Because the filter was easily clogged, the filtering volume was set at a smaller volume than the 0.45 μm filter (1.5 or 3 l). The total amount of volume filtered was 12–24 l.

Filtration and sample preservation were conducted in the same manner as the routine collection.

(4.2) Niskin water sampler

Seawater samples were also collected using 12 l Niskin bottles mounted on the CTD/Carousel Water Sampling System at six stations (Table 4.14-1). At these stations, pumped surface water was also collected as a routine sampling. Collection depths were determined as the bottom of the mixed layer or the depth showing the highest light attenuation rate (it is expected to be the most turbid layer). Two replicates were collected in each sampled depth. Water collection, filtration, and sample preservation were conducted in the same manner as the routine collection.

(4.3) Prevention of contamination

All sampling equipment and working space were decontaminated using bleach solution before use, and new nitrile gloves were worn at each water sampling to minimize cross-contamination.

Further, 500 ml of Milli-Q water were also filtered as a negative control (filtration blank) for every 10–12 seawater samples to check for cross-contamination during the filtration process.

(5) Station list

Table 4.14-1. List of sampling sites for eDNA sample collection.

No.	Site	Sampling depth (m)	Method	Latitude (N)	Longitude (E)	Date (UTC)
1	NP01	4.5	Pump	32.45	144.95	2020/9/20
2	NP02	4.5	Pump	32.01	146.98	2020/9/21
3	NP03	4.5	Pump	31.99	146.98	2020/9/22
4	NP04	4.5	Pump	33.00	147.00	2020/9/23
5	St. 03 (P03)	4.5	Pump	34.00	147.00	2020/9/23
6	NP05	4.5	Pump	34.01	147.00	2020/9/24
7	NP06	4.5	Pump	33.59	141.39	2020/9/25
8	BP01	4.5	Pump	34.66	139.56	2020/9/26
9	BP02	4.5	Pump	34.77	139.91	2020/9/26
10	BP03	4.5	Pump	34.90	140.33	2020/9/26
11	BP04	4.5	Pump	35.12	140.72	2020/9/26
12	NP07	4.5	Pump	37.56	145.32	2020/9/27
13	NP08	4.5	Pump	40.29	149.18	2020/9/29
14	NP09	4.5	Pump	43.62	155.22	2020/9/30
15	St. 04 (K2)	4.5	Pump	47.00	160.03	2020/10/1
16	NP10	4.5	Pump	47.01	160.03	2020/10/1
17	NP11	4.5	Pump	48.85	163.61	2020/10/2
18	NP12	4.5	Pump	51.87	168.91	2020/10/3
19	BS01	4.5	Pump	55.13	173.12	2020/10/4
20	BS02	4.5	Pump	58.44	178.23	2020/10/5
21	BS03	4.5	Pump	61.95	184.20	2020/10/6
22	BS04	4.5	Pump	65.37	191.53	2020/10/7
23	AO01	4.5	Pump	67.51	191.17	2020/10/7
24	AO02	4.5	Pump	69.00	191.17	2020/10/8
25	St.07	46	Niskin	69.01	191.17	2020/10/8
26	AO03	4.5	Pump	70.24	192.74	2020/10/8
27	AO04	4.5	Pump	70.79	196.96	2020/10/9
28	AO05	4.5	Pump	71.28	202.29	2020/10/9
29	AO06	4.5	Pump	72.89	200.43	2020/10/10
30	AO07	4.5	Pump	74.52	198.08	2020/10/10
31	St. 10 (NAP)	4.5	Pump	74.53	198.07	2020/10/10
32	AO08	4.5	Pump	74.54	198.06	2020/10/11
33	AO09	4.5	Pump	74.99	200.73	2020/10/11
34	AO10	4.5	Pump	75.17	199.99	2020/10/12
35	St. 12 (Ice side)	15	Niskin	75.18	199.99	2020/10/12

Table 4.14-1. (Continued)

No.	Site	Sampling depth (m)	Method	Latitude (N)	Longitude (E)	Date (UTC)
36	AO11	4.5	Pump	75.19	201.60	2020/10/12
37	AO12	4.5	Pump	75.00	201.33	2020/10/13
38	AO13	4.5	Pump	73.80	200.35	2020/10/13
39	AO14	4.5	Pump	72.61	202.58	2020/10/14
40	AO15	4.5	Pump	71.32	201.60	2020/10/14
41	St. 17 (B4)	29	Niskin	71.32	201.56	2020/10/15
42	St. 17 (B4)	110	Niskin	71.32	201.56	2020/10/15
43	AO16	4.5	Pump	71.36	201.88	2020/10/15
44	AO17	4.5	Pump	71.80	207.01	2020/10/15
45	AO18	4.5	Pump	72.36	203.35	2020/10/16
46	AO19	4.5	Pump	73.24	198.42	2020/10/16
47	AO20	4.5	Pump	74.93	195.11	2020/10/17
48	AO21	4.5	Pump	75.00	194.99	2020/10/17
49	St.22	26	Niskin	75.01	195.04	2020/10/17
50	AO22	4.5	Pump	75.00	192.33	2020/10/18
51	AO23	4.5	Pump	75.00	185.05	2020/10/18
52	AO24	4.5	Pump	74.94	188.30	2020/10/19
53	AO25	4.5	Pump	73.49	191.21	2020/10/19
54	St.29	110	Niskin	73.50	191.19	2020/10/19
55	AO26	4.5	Pump	72.00	191.17	2020/10/20
56	St.31	4.5	Pump	72.00	191.17	2020/10/20
57	AO27	4.5	Pump	70.43	191.17	2020/10/20
58	AO28	4.5	Pump	68.50	191.17	2020/10/21
59	St.35	45	Niskin	68.00	191.17	2020/10/21
60	AO29	4.5	Pump	66.50	191.17	2020/10/21
61	BS05	4.5	Pump	64.63	189.85	2020/10/22
62	BS06	4.5	Pump	63.00	186.08	2020/10/22
63	BS07	4.5	Pump	60.36	181.39	2020/10/23
64	BS08	4.5	Pump	56.84	175.68	2020/10/24
65	BS09	4.5	Pump	53.39	170.58	2020/10/25
66	NP13	4.5	Pump	52.33	169.36	2020/10/25

(6) Preliminary results

During this cruise, a total of 110 eDNA samples were obtained from 55 sites across the North Pacific Ocean (17 sites), the Bering Sea (9 sites), and the Arctic Ocean (29 sites) (Figure 4.14-1). These samples will be the subject of metabarcoding analysis to clarify the species composition of fishes and their regional differences. Comparing the results

from the surface water to that from a deeper layer would be worth to estimate vertical distribution of fishes and how hydrographic condition possibly affects the eDNA detection.

The replicated samples can also be used for metabarcoding. Its components would be analyzed using species accumulation curve and various indices (e.g., species richness and detection rate with Chao II estimator, the dissimilarity between replicates and sites with Jaccard's index) to find optimal sampling effort in the Arctic Ocean. How the use of different filters would affect to eDNA detection can be testified similarly.

These future works intend to provide an essential basis for facilitating the use of eDNA in the Arctic region and uncover the climate-induced changes in the Arctic ecosystem.

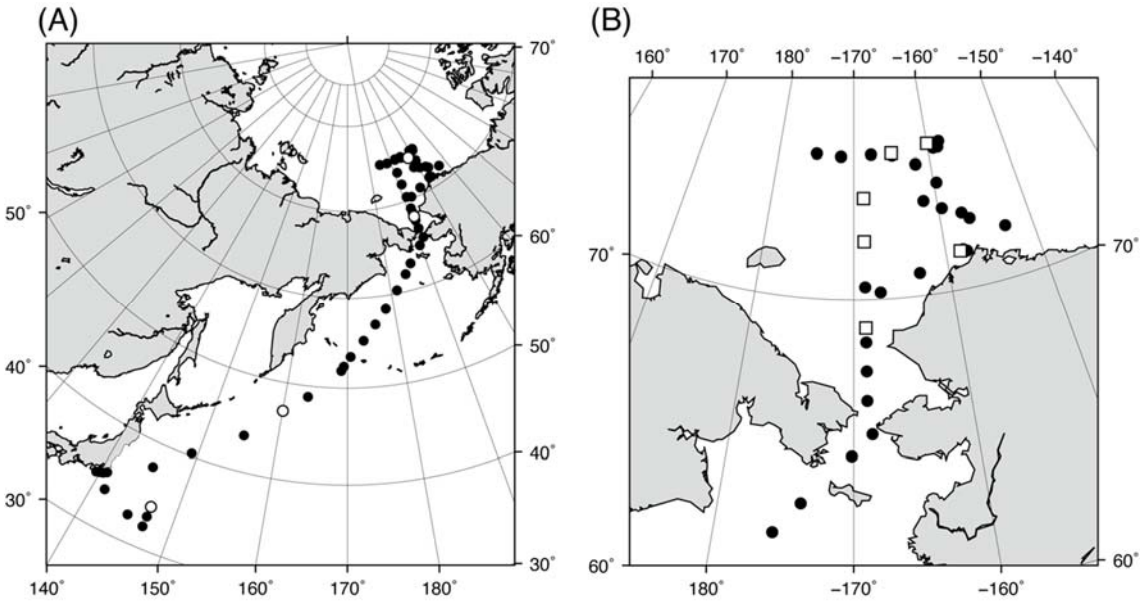

Figure 4.14-1. Map showing the sites where eDNA samples were collected. (A) Locations of the sites for routine collection (black circles) and the sites where additional replicate sampling was performed (white circles). (B) Locations of the sites for routine collection (black circles) and Niskin sampling with routine sampling (white squares) in the Arctic region.

(7) Data archives

These data obtained in this cruise will be submitted to the Data Management Group (DMG) of JAMSTEC, and will be opened to the public via "Data Research System for Whole Cruise Information in JAMSTEC (DARWIN)" in JAMSTEC web site.
<http://www.godac.jamstec.go.jp/darwin/e>

4.15. Microplastic sampling

(1) Personnel

Ryota Nakajima (JAMSTEC) – Principal investigator, Not on board
Sanae Chiba (JAMSTEC) – Not on board
Amane Fujiwara (JAMSTEC)
Junko Toyoshima (The Ocean Policy Research Institute; OPRI)

(2) Objective

The distribution of microplastic in the open ocean of the Arctic Ocean is largely undocumented. Substantial numbers of studies on microplastics have been reported in the Pacific and Atlantic Oceans, yet very few data are available in the polar oceans. In the present study, we conducted microplastic surveys along the cruise track to fill gaps in the Arctic Ocean.

(3) Method

Neuston net sampling for surface microplastic analysis

Floating microplastic samples were collected at Stns 1,2,3,4,29 and 35 using a neuston net with a square mouth opening of 75 cm height and 75 cm width, equipped with a 333 μm mesh opening net with a collecting bottle attached at the cod end. At each station, the net was towed three times for 20 min each along the surface of the starboard side. At the stns 29 and 35, each tow was carried out for 15 min due to a logistical reason. The trawl speed ranged between 1 and 2 knots. A flow meter was installed at the net mouth to estimate the volume of water filtered during each tow. The collected samples were fixed with 5% formalin and stored at room temperature until analysis.

Seawater sampling for subsurface microplastic analysis

Sea subsurface (ca. 7 m depth below sea surface) microplastic samples were collected using a pumped seawater system of the ship throughout the cruise. The pumped unfiltered seawater was continuously filtered through a 333 μm mesh screen and then 100 μm mesh screen at a flow rate about 3–4 L/min, enabling ca. 5,000 L per day. These meshes were collected and replaced every 24 hours, and the collected meshes were wrapped with an aluminum foil and stored in a vacuum sealed aluminum bag at room temperature until analysis. Time and position of the mesh replacement are shown in Table 4.15-1.

Microplastic samples from both the neuston net and pumped seawater will be subjected to enumeration and identification of plastic types using a microscope and FT-IR. The microplastics will also be weighed for mass calculation. The distribution, density and concentration of microplastic in this study will be compared with the previous reports in the Arctic Ocean.

Table 4.15-1. Time and position of the mesh replacement. Accumulated flow volume is also shown.

Date (UTC)	Time (UTC)	Latitude	Longitude	Accumulated flow volume (L)
2020/9/20	1:10	32-49.47211N	143-10.03129E	Start
2020/9/21	1:02	32-01.18668N	146-59.20985E	5382
2020/9/22	1:10	32-00.90939N	146-59.62326E	10561
2020/9/23	1:15	32-59.48536N	146-59.81290E	15486
2020/9/24	1:20	34-00.10186N	146-59.62465E	20343
2020/9/25	1:19	33-45.47763N	143-33.61966E	24942
2020/9/26	1:05	35-02.11960N	138-31.89661E	29495
2020/9/27	1:12	36-42.40742N	143-37.91143E	31769
2020/9/28	23:09	40-16.82645N	146-17.78529E	36587
2020/9/29	23:12	42-10.74435N	153-14.41791E	42388
2020/9/30	23:11	46-13.85455N	158-54.29688E	48675
2020/10/1	23:12	48-02.01803N	161-59.61870E	54470
2020/10/2	23:12	50-38.57145N	167-15.92658E	59994
2020/10/3	22:13	53-57.72466N	171-23.94120E	64328
2020/10/4	23:03	57-21.49107N	176-29.18682E	67797
2020/10/5	23:04	60-50.88697N	177-44.79767W	72342
2020/10/6	23:06	64-28.66261N	170-34.99179W	76939
2020/10/8	0:08	67-59.98236N	168-49.97848W	81811
2020/10/9	1:01	70-34.24230N	164-53.65759W	86408
2020/10/10	1:15	72-12.58940N	158-39.57761W	91148
2020/10/11	1:16	74-32.22804N	161-59.57393W	96216
2020/10/12	1:14	74-59.18043N	159-18.43630W	101486
2020/10/13	1:12	75-10.83506N	158-07.26119W	107081
2020/10/14	1:11	73-04.27095N	159-08.26691W	112845
2020/10/15	1:16	71-19.30728N	158-24.16714W	118994
2020/10/16	1:14	72-03.83620N	154-59.36231W	124810
2020/10/17	1:12	74-10.41285N	163-41.60068W	129905
2020/10/18	1:16	75-00.02354N	166-33.30772W	134964
2020/10/19	1:20	74-59.95140N	172-42.08173W	140115
2020/10/20	1:11	72-59.93509N	168-49.60896W	145301
2020/10/21	1:14	69-18.68741N	168-50.09839W	149723
2020/10/22	5:06	65-16.50501N	168-50.33841W	152447
2020/10/23	5:33	61-43.94192N	176-12.58858W	153445
2020/10/24	5:44	57-57.52929N	177-26.74369E	157591
2020/10/25	5:32	54-18.26921N	171-53.02789E	162112

(4) Data archives

These data obtained in this cruise will be submitted to the Data Management Group (DMG) of JAMSTEC, and will be made available to the public via "Data Research System for Whole Cruise Information in JAMSTEC (DARWIN)" in JAMSTEC web site.
<http://www.godac.jamstec.go.jp/darwin/e>

4.16. Plankton net sampling

(1) Personnel

Kohei Matsuno (Hokkaido University) – Principal investigator, Not on board
Atsushi Yamaguchi (Hokkaido University) – Not on board
Koki Tokuhiro (Hokkaido University)
Yuri Fukai (Hokkaido University)

(2) Objectives

The goals of this study were as follows:

1) Clarify the horizontal distribution of the zooplankton community analyzed by microscopy
2) Evaluate physical condition (stable isotope, stomach contents, fatty acid, egg production) of Arctic copepods and ostracods in the Arctic Ocean
3) Evaluate the spatial distribution of abundance and biomass of jelly fish
4) Clarify the differences of stable isotope of pacific copepods between north Pacific Ocean and western Arctic Ocean

(3) Parameters

Microscopic observation, stable isotope, stomach contents, fatty acid, egg production, photograph of jelly fish

(4) Instruments and methods

Zooplankton samples were collected by vertical haul of Quad-NORPAC nets at 26 stations in the north Pacific Ocean and the western Arctic Ocean. The Quad-NORPAC net (mesh size: 335, 150 and two 63 μm [one is for fixed sample ad the other has large size cod-end to collected fresh samples for incubation], mouth diameter: 45 cm) was towed between surface and 150 m depth or bottom -10 m (stations where the bottom was shallower than 150 m) at all stations (Figure 4.16-1 and Table 4.16-1). The zooplankton samples collected by the NORPAC net with 335, 150 and one 63 μm mesh were immediately fixed with 5% buffered formalin for zooplankton structure analysis. Jelly fishes collected by a bucket net with large size cod-end (mesh: 62 μm, mouth diameter: 45 cm) were taken pictures (Figure 4.16-2) and the bucket-net sample was fixed with 99.5% ethanol for analysis on DNA of jelly fishes (investigator: Dr. Charlotte Havermans [AWI]). The volume of water filtered through the net was estimated based on readings from a flow meter mounted in the mouth ring of the net.

An 80-cm ring net (mesh size: 335 μm, mouth diameter: 80 cm) was towed between the surface and the depth of 300 m (or the bottom -10 m) at 26 stations (Figure 4.16-1 and Table 4.16-2). The fresh samples were used for evaluation of copepod and ostracod physiological activities (i.e. stable isotope, stomach contents, fatty acid and egg production). After sorting, the remaining subsamples were fixed with 99.5% ethanol.

A closing PCP net (mesh size: 63 μm, mouth diameter: 45 cm) was towed at one deep station with five layers (0-50, 50-100, 100-250, 250-500, 500-1000 and 1000-1600 m). The volume of water filtered through the net was estimated based on reading from a flow meter mounted in the mouth ring. The zooplankton samples collected by the closing PCP net were immediately fixed with 5% buffered formalin for zooplankton structure analysis (Figure 4.16-1 and Table 4.16-3).

A large closing PCP net (mesh size: 335 μm, mouth diameter: 80 cm) was towed at one deep station in one layer (1000-1600 m). Fresh samples were used for evaluation of copepod and ostracod physiological activities (i.e., stable isotope, stomach contents, fatty acid and egg production). After sorting, the remaining zooplankton subsample collected by the large closing PCP net were fixed with 99.5% ethanol.

(5) On-board treatment

[stable isotope, stomach contents and fatty acid]

Fresh zooplankton samples collected with a bucket net or ring net were immediately added 10% soda water (CO_2 water) for analysis of stable isotope, stomach contents and fatty acid. We sorted the late copepodite stage of the Pacific copepods (*Neocalanus cristatus*, *N. plumchrus*, *N. flemingeri*, *Eucalanus bungii*, *Metridia pacifica*) and the Arctic copepods (*Calanus glacialis*, *C. hyperboreus*, *M. longa*, *Paraeuchaeta glacialis*). Some specimens were rinsed with Milli-Q water, transferred into 24-hole microplate and stored at -20□ for stable isotope and fatty acid analysis. For stomach contents analysis, the Arctic copepods (*C. glacialis*, *C. hyperboreus*, *M. longa*) and deep-sea copepods (*Gaetanus tenuispinus*, *G. brevispinus*, *Chiridius obtusifrons*, *Scaphocalanus magnus*) were sorted and incubated in DNA-free sea water (0.2 μm filtered sea water) collected with a Niskin bottle. After several hours, the evacuated fecal pellets were picked up and preserved at -20□.

[egg production of Ostracod]

We immediately sorted some ostracod from fresh zooplankton samples collected with a bucket net or ring net. A female ostracod was sorted in 50 ml bottle filled with water from chlorophyll *a* maximum layer, and incubated at cool incubator set at 3, 5, 7□. After spawning eggs, the number of eggs were counted and transferred into 24-hole microplate. The eggs were incubated at cool incubator set at 3, 5, 7□ for analysis of hatching ratio.

(6) Station list

Table 4.16-1: Data on plankton samples collected by vertical hauls with a Quad-NORPAC net

Table 4.16-2: Data on plankton samples collected by vertical hauls with a ring net (mesh size: 335 μm)

Table 4.16-3: Data on plankton samples collected by vertical hauls with a closing net (mesh size: 63 μm) and a large closing net (mesh size: 335 μm)

Table 4.16-1. Data on plankton sample collected by vertical haul with Quad-NORPAC net.

Station No.	Position				S.M.T		Length of wire (m)	Angle of wire (°)	Depth estimated by wire angle (m)	Kind of cloth	Flowmeter		Estimated volume of water filtered (m^3)	Remark
	Lat. (N)		Lon.		Date	Hour					No.	Reading		
Sta. 001	31	59.92	147	0.05 E	2020/9/22	21:06	151	6	150	335 μm	2560	1420	23.91	
										150 μm	1333	1410	22.67	
										63 μm	1632	1138	15.71	
										63 μm				for experiment
Sta. 002	32	59.95	147	0.08 E	2020/9/23	20:57	158	18	150	335 μm	2560	1250	21.04	
										150 μm	1333	1360	21.86	
										63 μm	1632	1150	15.87	
										63 μm				for experiment
Sta. 003	34	0.08	146	59.87 E	2020/9/24	20:57	152	10	150	335 μm	2560	1641	27.63	
										150 μm	1333	1719	27.63	
										63 μm	1632	1784	24.63	
										63 μm				for experiment
Sta. 004	47	0.97	160	2.26 E	2020/10/1	22:00	150	2	150	335 μm	2560	1641	27.63	
										150 μm	1333	1719	27.63	
										63 μm	1632	1738	23.99	
										63 μm				for experiment
Sta. 007	69	0.02	168	49.93 W	2020/10/7	18:52	42	5	42	335 μm	2560	515	8.67	UTC-11h
										150 μm	1333	630	10.13	
										63 μm	1632	632	8.72	
										63 μm				for experiment, remaining ethanol
Sta. 008	69	59.57	168	49.75 W	2020/10/8	2:47	29	6	29	335 μm	2560	372	6.26	
										150 μm	1333	340	5.47	
										63 μm	1632	310	4.28	
										63 μm				for experiment, remaining ethanol
Sta. 009	70	29.97	165	29.87 W	2020/10/8	12:10	33	7	33	335 μm	2560	436	7.34	
										150 μm	1333	410	6.59	
										63 μm	1632	320	4.42	
										63 μm				for experiment, remaining ethanol
Sta. 010	74	31.37	161	55.43 W	2020/10/10	6:05	151	7	150	335 μm	2560	1480	24.92	
(NAPt)										150 μm	1333	1400	22.51	
										63 μm	1632	960	13.25	
										63 μm				for experiment, remaining ethanol
Sta. 011	74	58.88	158	7.9 W	2020/10/11	11:24	153	12	150	335 μm	2560	1315	22.14	
(ICE)										150 μm	1333	1271	20.43	
										63 μm	1632	909	12.55	
										63 μm				for experiment, remaining ethanol
Sta .12B	75	0	158	40.18 W	2020/10/12	18:10	150	2	150	335 μm	2560	1325	22.31	
										150 μm	1333	1276	20.51	
										63 μm	1632	879	12.13	
										63 μm				for experiment, remaining ethanol
Sta. 13	73	17.26	160	1.06 W	2020/10/13	11:52	151	8	150	335 μm	2560	1252	21.08	
										150 μm	1333	1230	19.77	
										63 μm	1632	840	11.60	
										63 μm				for experiment, remaining ethanol
Sta. 15	72	47.28	157	59.96 W	2020/10/13	19:00	151	5	150	335 μm	2560	1282	21.58	
										150 μm	1333	1271	20.43	
										63 μm	1632	752	10.38	
										63 μm				for experiment, remaining ethanol
Sta. 18	71	40.78	152	29.87 W	2020/10/15	4:40	152	10	150	335 μm	2560	1259	21.20	
										150 μm	1333	1200	19.29	
										63 μm	1632	745	10.28	
										63 μm				for experiment, remaining ethanol
Sta. 20	71	58.74	153	58.76 W	2020/10/15	12:02	151	8	150	335 μm	2560	1270	21.38	
										150 μm	1333	1380	22.18	
										63 μm	1632	792	10.93	
										63 μm				for experiment, remaining ethanol
Sta. 22	75	0.08	164	58.14 W	2020/10/17	9:25	151	7	150	335 μm	2560	1519	25.57	Strong wind and wave
										150 μm	1333	1880	30.22	
										63 μm	1632	1450	20.02	
										63 μm				for experiment, remaining ethanol

Table 4.16-1. (continued)

Station No.	Position				S.M.T		Length of wire (m)	Angle of wire (°)	Depth estimated by wire angle (m)	Kind of cloth	Flowmeter		Estimated volume of water filtered (m^3)	Remark
	Lat. (N)		Lon.		Date	Hour					No.	Reading		
Sta. 23	75	0.66	167	14.83 W	2020/10/17	17:00	151	7	150	335 μm	2560	1910	32.16	Strong wind and wave
										150 μm	1333	2139	34.39	
										63 μm	1632	1839	25.39	
										63 μm				for experiment, remaining ethanol
Sta. 24	75	0.74	169	37.86 W	2020/10/17	23:05	151	8	150	335 μm	2560	1455	24.50	Strong wind and wave
										150 μm	1333	1595	25.64	
										63 μm	1632	1152	15.90	
										63 μm				for experiment, remaining ethanol
Sta. 25	75	0	175	0.24 W	2020/10/18	8:39	152	13	150	335 μm	2560	1403	23.62	
										150 μm	1333	1935	31.11	
										63 μm	1632	1118	15.43	
										63 μm				for experiment, remaining ethanol
Sta. 26	75	0.41	171	58.91 W	2020/10/18	17:12	152	10	150	335 μm	2560	1344	22.63	
										150 μm	1333	1372	22.06	
										63 μm	1632	952	13.14	
										63 μm				for experiment, remaining ethanol
Sta. 27	74	36.04	170	11.98 W	2020/10/18	22:40	151	8	150	335 μm	2560	1305	21.97	
										150 μm	1333	1272	20.45	
										63 μm	1632	820	11.32	
										63 μm				for experiment, remaining ethanol
Sta. 29	73	29.5	168	47.44 W	2020/10/19	8:40	109	16	105	335 μm	2560	1080	18.18	
										150 μm	1333	1120	18.00	
										63 μm	1632	771	10.64	
										63 μm				for experiment, remaining ethanol
Sta. 30	72	59.98	168	49.53 W	2020/10/19	13:55	55	1	54	335 μm	2560	610	10.27	
										150 μm	1333	600	9.65	
										63 μm	1632	475	6.56	
										63 μm				for experiment, remaining ethanol
Sta. 31	72	0.02	168	50.01 W	2020/10/19	19:46	40	3	40	335 μm	2560	392	6.60	
										150 μm	1333	385	6.19	
										63 μm	1632	289	3.99	
										63 μm				for experiment, remaining ethanol
Sta. 32	71	0.01	168	49.94 W	2020/10/20	2:45	34	8	34	335 μm	2560	352	5.93	
										150 μm	1333	360	5.79	
										63 μm	1632	318	4.39	
										63 μm				for experiment, remaining ethanol
Sta. 33	70	0.11	168	49.95 W	2020/10/20	8:35	28	8	28	335 μm	2560	332	5.59	
										150 μm	1333	338	5.43	
										63 μm	1632	265	3.66	
										63 μm				for experiment, remaining ethanol
Sta. 35	68	0	168	49.98 W	2020/10/20	23:00	47	8	47	335 μm	2560	418	7.04	
										150 μm	1333	435	6.99	
										63 μm	1632	300	4.14	
										63 μm				for experiment, remaining ethanol

Table 4.16-2: Data on plankton samples collected by vertical hauls with a ring net

Station No.	Position					S.M.T		Length of wire (m)	Angle of wire (°)	Depth estimated by wire angle (m)	Kind of cloth	Remark
	Lat. (N)		Lon.			Date	Hour					
Sta. 003	34	0.08	146	59.87	E	2020/9/24	21:15	300	3	300	335 µm	for experiment, remaining ethanol
							21:41	150	1	150	335 µm	for Go pro test, remaining ethanol
Sta. 004	47	0.97	160	2.26	E	2020/10/1	22:00	150	2	150	335 µm	for experiment, remaining ethanol
Sta. 007	69	0.02	168	49.93	W	2020/10/7	19:02	43	10	42	335 µm	UTC -11 hour, for experiment, remaining ethanol
Sta. 008	69	59.57	168	49.75	W	2020/10/8	2:47	29	6	29	335 µm	Clogging jelly fish
Sta. 009	70	29.97	165	29.87	W	2020/10/8	12:10	33	7	33	335 µm	for experiment, remaining ethanol
Sta. 010 (NAPt)	74	31.37	161	55.43	W	2020/10/10	6:17	300	2	300	335 µm	for experiment, remaining ethanol
Sta. 011 (ICE)	74	58.88	158	7.9	W	2020/10/11	11:35	153	12	150	335 µm	for experiment, remaining ethanol
Sta. 12B	75	0	158	40.18	W	2020/10/12	18:32	300	2	300	335 µm	for experiment, remaining ethanol
Sta. 13	73	17.26	160	1.06	W	2020/10/13	12:04	151	8	150	335 µm	for experiment, remaining ethanol
Sta. 15	72	47.28	157	59.96	W	2020/10/13	19:15	307	12	300	335 µm	for experiment, remaining ethanol
Sta. 18	75	0.08	164	58.14	W	2020/10/17	4:53	303	8	300	335 µm	for experiment, remaining ethanol
Sta. 20	71	58.74	153	58.76	W	2020/10/15	12:13	307	12	300	335 µm	for experiment, remaining ethanol
Sta. 22	75	0.08	164	58.14	W	2020/10/17	9:42	301	4	300	335 µm	for experiment, remaining ethanol
Sta. 23	75	0.66	167	14.83	W	2020/10/17	17:18	234	10	232	335 µm	for experiment, remaining ethanol
Sta. 24	75	0.74	169	37.86	W	2020/10/17	23:24	228	3	228	335 µm	for experiment, remaining ethanol
Sta. 25	75	0	175	0.24	W	2020/10/18	8:52	255	2	255	335 µm	for experiment, remaining ethanol
Sta. 26	75	0.41	171	58.91	W	2020/10/18	17:26	302	6	300	335 µm	for experiment, remaining ethanol
Sta. 27	74	36.04	170	11.98	W	2020/10/18	23:00	198	8	196	335 µm	for experiment, remaining ethanol
Sta. 29	73	29.5	168	47.44	W	2020/10/19	8:52	107	12	105	335 µm	for experiment, remaining ethanol
Sta. 30	72	59.98	168	49.53	W	2020/10/19	14:04	53	6	53	335 µm	for experiment, remaining ethanol
Sta. 31	72	0.02	168	50.01	W	2020/10/19	19:52	40	3	40	335 µm	for experiment, remaining ethanol
Sta. 32	71	0.01	168	49.94	W	2020/10/20	3:00	34	8	34	335 µm	for experiment, remaining ethanol
Sta. 33	70	0.11	168	49.95	W	2020/10/20	8:42	28	8	28	335 µm	for experiment, remaining ethanol
Sta. 35	68	0	168	49.98	W	2020/10/20	23:15	47	4	47	335 µm	for experiment, remaining ethanol

Table 4.16-3. Data on plankton samples collected by vertical hauls with a closing net and a large closing net

Station No.	Position					S.M.T		Length of wire (m)	Angle of wire (°)	Depth estimated by wire angle (m)	Closed net depth (m)	Kind of cloth	Flowmeter		Estimated volume of water filtered (m^3)	Remark
	Lat. (N)		Lon.			Data	Hour						No.	Reading		
Sta. 010	74	31.37	161	55.43	W	2020/10/10	16:37	50	4	50	0	63 µm	1852	221	3.68	
(NAPt)							16:40	101	6	100	51	63 µm	1852	362	6.02	
							16:52	251	6	250	103	63 µm	1852	932	15.51	
							17:12	502	5	500	257	63 µm	1852	1630	27.12	
							17:30	1005	7	1000	517	63 µm	1852	3009	50.07	
							18:10	1601	2	1600	1033	63 µm	1852	3090	51.41	
							19:25	1602	3	1600	1043	335 µm				for experiment, remaining ethanol

(7) Preliminary results

As an indication of the preliminary results, we present the following item.

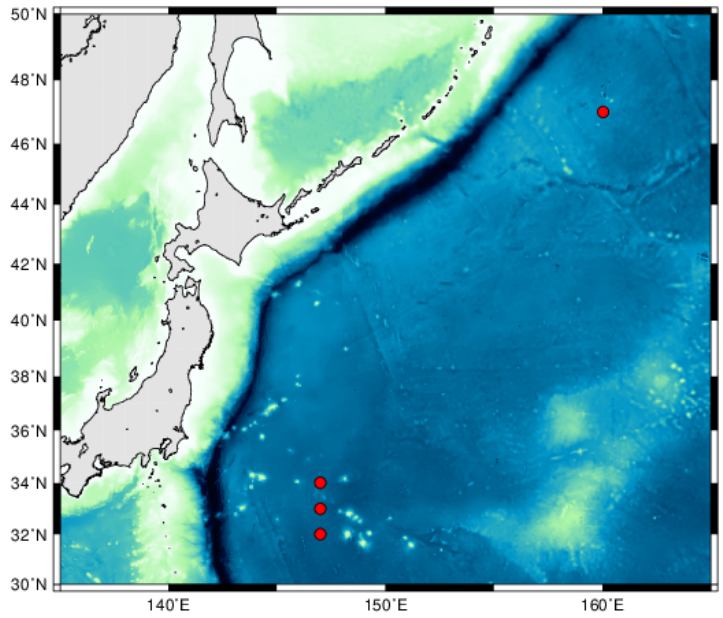

Figure 4.16-1. Location of the sampling stations in the Pacific sector of Arctic Ocean (circles: NORPAC net + ring net, stars: NORPAC net + ring net + closing net).

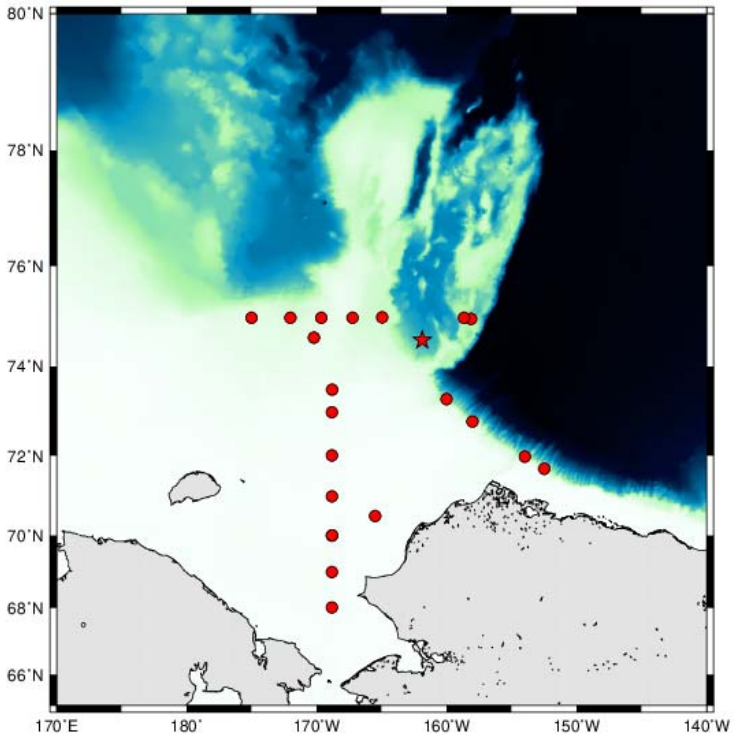

Figure 4.16-1. (continued)

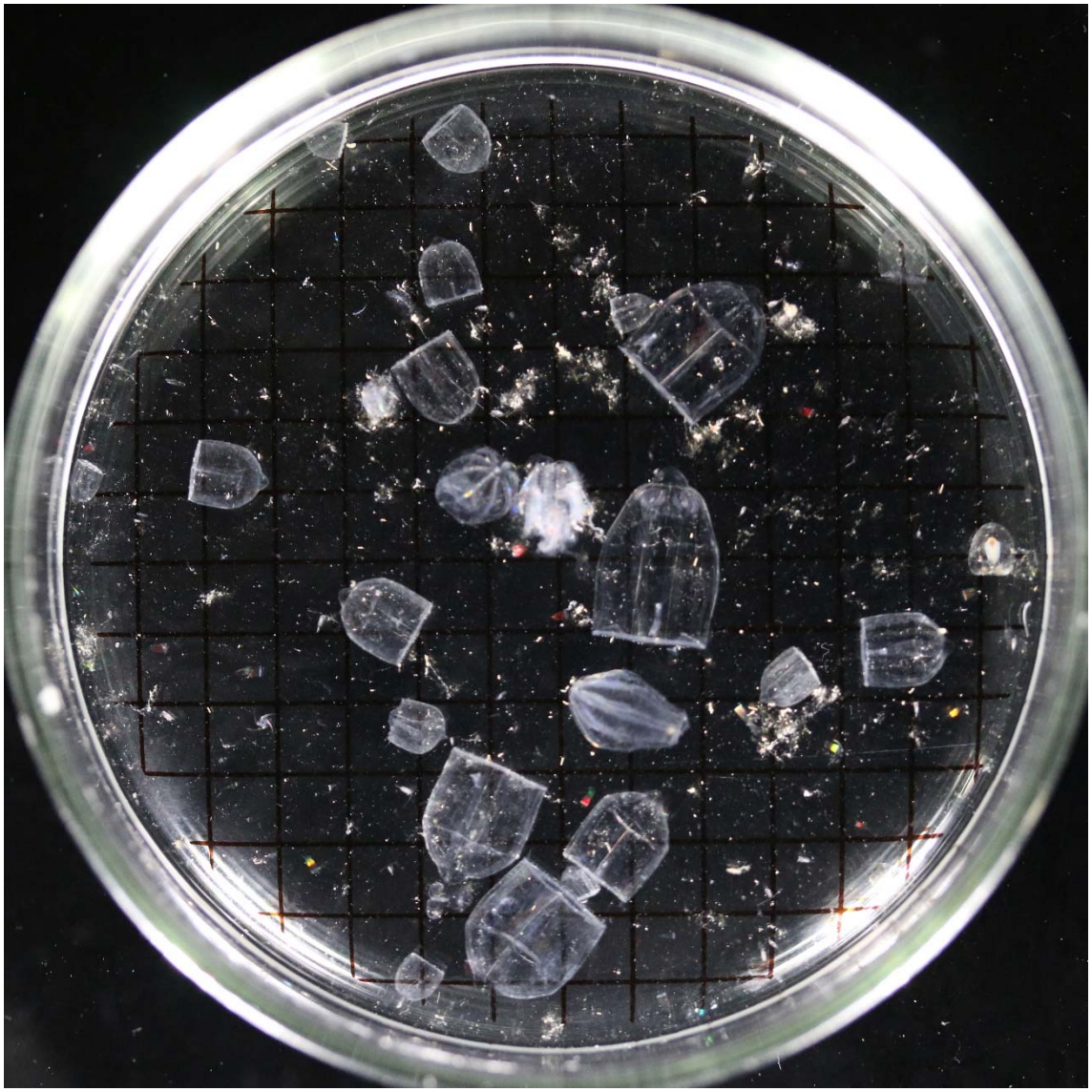

Figure 4.16-2. Photograph of jelly fish collected by bucket net.

(8) Data archives

These data obtained in this cruise will be submitted to the Data Management Group (DMG) of JAMSTEC, and will be opened to the public via "Data Research System for Whole Cruise Information in JAMSTEC (DARWIN)" in JAMSTEC web site.
<http://www.godac.jamstec.go.jp/darwin/e>

4.17. Water sampling for plankton

(1) Personnel

Kohei Matsuno (Hokkaido University) – Principal investigator, Not on board
Atsushi Yamaguchi (Hokkaido University) – Not on board
Koji Suzuki (Hokkaido University) – Not on board
Koki Tokuhiro (Hokkaido University)
Yuri Fukai (Hokkaido University)

(2) Objectives

The goals of this study were as follows:

1) Clarifying the spatial distribution of phytoplankton and microprotist assemblages by multispectral excitation–emission fluorometer (MFL), microscopy and eDNA.
2) Clarifying the horizonal distribution of phytoplankton assemblages by UHPLC and evaluate their conditions by the maximum photochemical efficiency (Fv/Fm).
3) Quantifying diatom assemblages using DNA (18S V4 region) analysis and SEM, and evaluate their activities by the analyses of *rbcL* and *NR* gene expression.
4) Evaluate the spatial and horizontal distribution of *C. glacialis* in the western Arctic Ocean using eDNA

(3) Parameters

MFL, microscopic observation, environmental DNA, UHPLC, Fv/Fm, SEM, gene expression of *rbc*L and *NR*

(4) Instruments and methods

Sea water samples (1L) were collected from depths of 0, 10, 20, 30, 40 and 50 m for determination of the chlorophyll *a* maximum layer using a bucket and Niskin water sampler at 21 stations (Figure 4.17-1, Table 4.17-1). The water samples were fixed by acid lugol (1% final concentration). The samples will be concentrated to 20 mL with a syphon in the land laboratory and microprotists will be enumerated and identified under an inverted microscopy. An MFL (Multi-Exciter, JFE-Advantech Co. Ltd) was attached to the CTD frame to measure the vertical profile of chlorophyll *a* fluorescence.

For the analysis of phytoplankton and diatom distributions and their conditions, sea water samples were collected from 0 m and sub-surface chlorophyll-*a* maximum layer (SCM) using a bucket and Niskin water sampler. Sea water samples (170–1200 mL) for the analyses of UHPLC, DNA and *rbcL* and *NR* gene expression were filtered by GF/F or 2.0 μm membrane filter. All filtered samples were preserved at -80□. In the land laboratory, they will be analyzed. The Fv/Fm was measured each station and layer using a pulse-amplitude modulated fluorometer (Water-PAM; Walz, Effeltrich, Germany). Samples (3 mL) for this analysis were placed in a quartz cuvette and illuminated by red-

LED with a peak illumination at 655 nm, and the Fv/Fm of each sample was determined. The measurements of the Fv/Fm were repeated three to five times for each sample.

Sea water samples (1L) collected from depth of 0, 10, 20, 30, 50 m using a bucket and Niskin water sampler at 8 stations for analysis of spatial and horizontal distribution of *C. glacialis* (Figure 4.17-1 and Table 4.17-1). The waters were filtered through 0.2 μm filters for *in situ* environmental DNA analysis. All filters were preserved at -20□.

(5) Station list

Table 4.17-1. Log of water samples collected by Niskin sampler and bucket. Circles indicate an MFL was attached to the CTD frame.

	Date	Latitude (°N)	Longitude (°W)	Sampling depth (m)	MFL
St. 007	2020/10/8	69.01	168.83	0, 10, 20, 30, 46, 14	○
St. 009	2020/10/8	70.50	165.50	0, 10, 20, 30, 38, 11	○
St. 010	2020/10/10	74.55	161.88	0, 10, 20, 30, 50, 100, 200, 300	
St. 011	2020/10/11	74.98	158.13	0, 10, 20, 30, 50, 15	
St. 012	2020/10/12	75.18	160.01	0, 10, 20, 30, 50, 15	
St. 013	2020/10/13	73.29	160.01	0, 10, 20, 30, 50, 32	
St. 015	2020/10/14	72.79	158.02	0, 10, 20, 30, 50, 15	
St. 017	2020/10/15	71.32	158.44	0, 10, 20, 30, 50, 22	○
St. 020	2020/10/15	71.97	153.99	0, 10, 20, 30, 50, 15	
St. 022	2020/10/17	75.01	164.96	0, 10, 20, 30, 50, 26	
St. 023	2020/10/18	75.00	167.24	0, 10, 20, 30, 50, 16	
St. 024	2020/10/18	75.00	169.64	0, 10, 20, 30, 50, 34	○
St. 025	2020/10/18	75.00	175.00	0, 10, 20, 30, 50, 27	○
St. 026	2020/10/19	75.00	172.02	0, 10, 20, 30, 50, 27	○
St. 027	2020/10/19	74.60	170.21	0, 10, 20, 30, 50, 25	○
St. 029	2020/10/19	73.50	168.81	0, 10, 20, 30, 50, 100, 18	○
St. 030	2020/10/20	73.00	168.83	0, 10, 20, 30, 50	○
St. 031	2020/10/20	72.00	168.83	0, 10, 20, 30, 12	○
St. 033	2020/10/20	70.00	168.81	0, 10, 20, 30, 15	○
St. 034	2020/10/20	69.03	168.83	0, 16	
St. 035	2020/10/21	68.01	168.83	0, 10, 20, 30, 50, 26	○

(6) Preliminary results

As an indication of the preliminary results, we present following items.

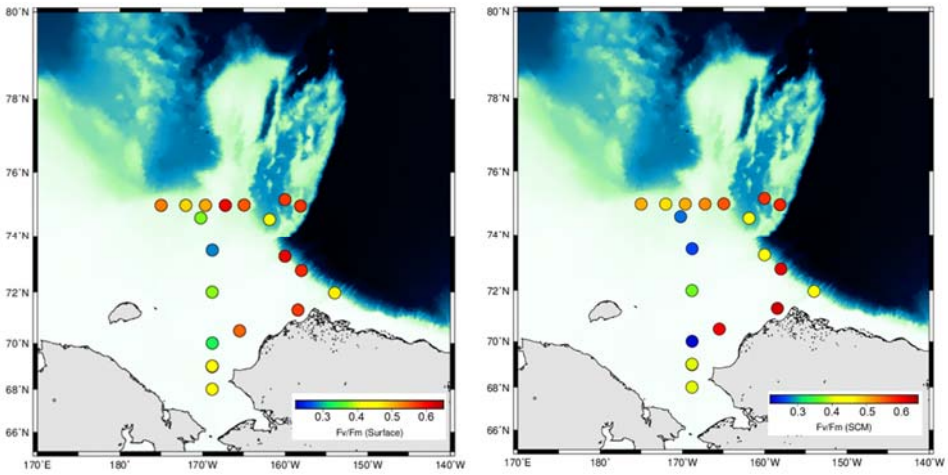

Figure 4.17-1. Spatial values of the maximum photochemical efficiency (Fv/Fm) in the surface layer and the sub-surface chlorophyll-*a* maximum layer (SCM).

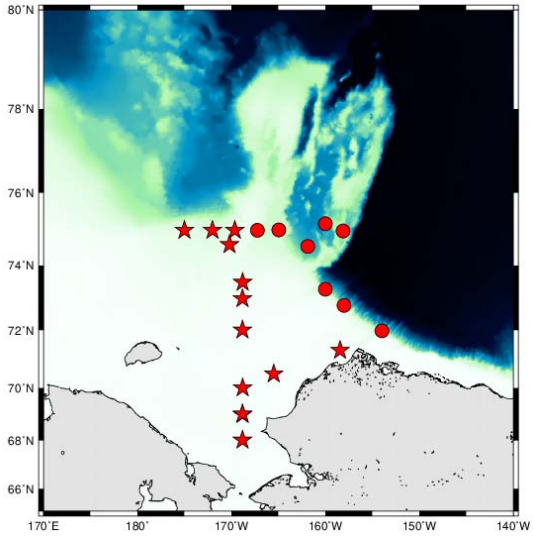

Figure 4.17-2. Locations of the water sampling and MFL stations in the Pacific sector of the Arctic Ocean (circles: Niskin+bucket, stars: Niskin+bucket+MFL).

(7) Data archives

These data obtained in this cruise will be submitted to the Data Management Group (DMG) of JAMSTEC, and will be opened to the public via "Data Research System for Whole Cruise Information in JAMSTEC (DARWIN)" in JAMSTEC web site.
<http://www.godac.jamstec.go.jp/darwin/e>

4.18. Sea bottom sediments

(1) Personnel

Kohei Matsuno (Hokkaido University) – Principal investigator, Not on board
Atsushi Yamaguchi (Hokkaido University) – Not on board
Koji Suzuki (Hokkaido University) – Not on board
Koki Tokuhiro (Hokkaido University)
Yuri Fukai (Hokkaido University)

(2) Objectives

The goals of this study were as follows:

1) Clarify the spatial distribution of diatom resting stages in the sediments of Pacific-Arctic Ocean.
2) Evaluate the impact of diatom resting stages as a seed of primary production.

(3) Parameters

Microscopic observation of diatom resting stages in the sediments

(4) Sampling

Sea bottom sediment samplings were conducted using a Smith–McIntyre sampler at nine stations in the Pacific sector of the Arctic Ocean (Figure 4.18-1), but at station 33, we did not collect sediment samples because of sandy bottom condition. We inserted a liner tube (diameter: 3.6 cm) and cut the sediment from the surface to the depth of 3 cm; all samples were sorted in dark cool (~4 °C) conditions. After a period of more than one month, their containing diatom resting stages will be quantified by incubation (most probable number method). In addition, the impact of diatom resting stages as a seed of primary production will be evaluated by land-experiment.

Another aliquot (depth: 0–1 cm) was cut and preserved in dark cool conditions for analysis of dinoflagellates (investigator: Dr. So-Young Kim [KOPRI]).

(5) Station list

Table 4.18-1. List of stations for sediment samples collected using a Smith–McIntyre sampler in the Pacific sector of the Arctic Ocean during this cruise.

Station no.	Date	Latitude (°N)	Longitude (°W)	Bottom depth (m)
St. 007	2020/10/7	69.00	168.83	49.2
St. 008	2020/10/8	70.00	168.83	36.5
St. 009	2020/10/8	70.50	165.50	39.2
St. 029	2020/10/19	73.50	168.81	112.0
St. 030	2020/10/19	73.00	168.83	59.9
St. 031	2020/10/19	72.00	168.83	48.2
St. 032	2020/10/20	71.00	168.83	39.7
St. 033	2020/10/20	70.00	168.81	38.7
St. 035	2020/10/20	68.01	168.83	53.9

(6) Preliminary results

As an indication of preliminary results, we present the following item.

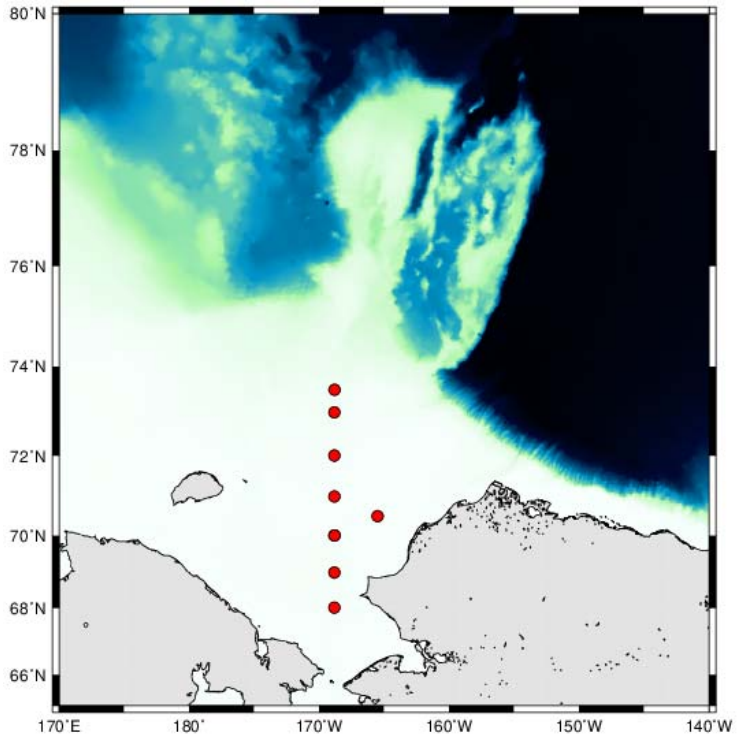

Figure 4.18-1. Locations of the sampling stations for the collection of bottom sediments in the Pacific sector of the Arctic Ocean during this cruise. Black dots indicate sampling stations.

(7) Data archives

These data obtained in this cruise will be submitted to the Data Management Group (DMG) of JAMSTEC, and will be opened to the public via "Data Research System for Whole Cruise Information in JAMSTEC (DARWIN)" in JAMSTEC web site.
<http://www.godac.jamstec.go.jp/darwin/e>

5. Geology

5.1. Sea bottom topography measurements

(1) Personnel

Shigeto Nishino (JAMSTEC) – Principal investigator
Ryo Oyama (Nippon Marine Enterprises, Ltd.; NME) – Operation leader
Souichiro Sueyoshi (NME)
Wataru Tokunaga (NME)
Masanori Murakami (NME)
Yoichi Inoue (MIRAI Crew)

(2) Objective

R/V MIRAI is equipped with the Multi Beam Echo Sounding system (MBES; SEABEAM 3012 (L3 Communications ELAC Nautik, Germany)). The objective of MBES is collecting continuous bathymetric data along ship track to make a contribution to geological and geophysical studies.

(3) Instruments and Methods

The "SEABEAM 3012" on R/V MIRAI was used for bathymetry mapping during this cruise.

To get accurate sound velocity of water column for ray-path correction of acoustic beams, we determined sound velocities at the depth of 6.62m, the bottom of the ship, by a surface sound velocimeter. We made sound velocity profiles based on the observations of CTD, XCTD and Argo float conducted in this cruise by the equation in Del Grosso (1974).

The system configuration and performance are shown in Table 5.1-1.

Table 5.1-1. SEABEAM 3012 System configuration and performance.

Frequency:	12 kHz
Transmit beam width:	2.0 degree
Transmit power:	4 kW
Transmit pulse length:	2 to 20 msec.
Receive beam width:	1.6 degree
Depth range:	50 to 11,000 m
Number of beams:	301 beams (Spacing mode: Equi-angle)
Beam spacing:	1.5 % of water depth (Spacing mode: Equi-distance)
Swath width:	60 to 150 degrees
Depth accuracy:	< 1 % of water depth (average across the swath)

(4) Observation Period

19 Sep. 2020 - 1 Nov. 2020 (UTC)

(5) Preliminary Results

The results will be published after the primary processing.

(6) Data archives

These data obtained in this cruise will be submitted to the Data Management Group (DMG) of JAMSTEC, and will be opened to the public via "Data Research System for Whole Cruise Information in JAMSTEC (DARWIN)" in JAMSTEC web site.
<http://www.godac.jamstec.go.jp/darwin/e>

(7) Remarks

1. The following periods, data acquisition was suspended due to the shallow sea area.

20:15UTC 05 Oct. 2020 - 05:31UTC 10 Oct. 2020
10:44UTC 14 Oct. 2020 - 16:33UTC 14 Oct. 2020
17:20UTC 14 Oct. 2020 - 13:56UTC 15 Oct. 2020
08:50UTC 16 Oct. 2020 - 23:31UTC 16 Oct. 2020
10:58UTC 19 Oct. 2020 - 16:26UTC 23 Oct. 2020

2. During the observation of microstructure measurement (T-MAP), sonar pinging was stopped due to preventing contamination noise to the shear probes of T-MAP.

5.2. Sea surface gravity measurements

(1) Personnel

Shigeto Nishino (JAMSTEC) – Principal investigator
Ryo Oyama (Nippon Marine Enterprises, Ltd.; NME) – Operation leader
Souichiro Sueyoshi (NME)
Wataru Tokunaga (NME)
Masanori Murakami (NME)
Yoichi Inoue (MIRAI Crew)

(2) Objective

The local gravity is an important parameter in geophysics and geodesy. The gravity data were collected during this cruise.

(3) Parameters

Relative Gravity [CU: Counter Unit]
[mGal] = (coefl: 0.9946) * [CU]

(4) Instruments and Methods

The relative gravity using LaCoste and Romberg air-sea gravity meter S-116 (Micro-g LaCoste, LLC) was measured during the cruise. To convert the relative gravity to absolute one, we measured gravity, using portable gravity meter (Scintrex gravity meter CG-5), at Shimizu port as the reference points.

(5) Observation Period

18 Sep. 2020 - 3 Nov. 2020 (UTC)

(6) Preliminary Results

Absolute gravity table is shown in Table 5.2-1.

Table 5.2-1. Absolute gravity table of the MR20-05C cruise.

No.	Date	UTC	Port	Absolute Gravity [mGal]	Sea Level [cm]	Ship Draft [cm]	Gravity at Sensor * [mGal]	S-116 Gravity [mGal]
#1	18-Sep. 12010.45	07:57	Shimizu	979,728.98	143	644	979,729.67	
#2	03-Nov. 12007.46	23:46	Shimizu	979,728.98	161	623	979,729.68	

*: Gravity at Sensor
= Absolute Gravity + Sea Level*0.3086/100 + (Draft-530)/100*0.2222

(7) Data archives

These data obtained in this cruise will be submitted to the Data Management Group (DMG) of JAMSTEC, and will be opened to the public via "Data Research System for Whole Cruise Information in JAMSTEC (DARWIN)" in JAMSTEC web site.
<http://www.godac.jamstec.go.jp/darwin/e>

5.3. Surface magnetic field measurements

(1) Personnel

Shigeto Nishino (JAMSTEC) – Principal investigator
Ryo Oyama (Nippon Marine Enterprises, Ltd.; NME) – Operation leader
Souichiro Sueyoshi (NME)
Wataru Tokunaga (NME)
Masanori Murakami (NME)
Yoichi Inoue (MIRAI Crew)

(2) Objective

Measurement of magnetic force on the sea is required for the geophysical investigations of marine magnetic anomaly caused by magnetization in upper crustal structure. We measured geomagnetic field using a three-component magnetometer during this cruise.

(3) Instruments and Methods

A shipboard three-components magnetometer system (SFG2018, Tierra Tecnica) is equipped on-board R/V MIRAI. Three-axes flux-gate sensors with ring-cored coils are fixed on the fore mast. Outputs from the sensors are digitized by a 20-bit A/D converter (1 nT/LSB) and sampled at 8 times per second. Yaw (heading), Pitch and Roll are measured by the Inertial Navigation Unit (INU) for controlling attitude of a Doppler radar. Ship's position, speed over ground (Differential GNSS) and gyro data are taken from LAN every second.

The relation between a magnetic-field vector observed on-board, $\mathbf{H}_{\mathrm{ob}}$, (in the ship's fixed coordinate system) and the geomagnetic field vector, $\mathbf{F}$, (in the Earth's fixed coordinate system) is expressed as:

$$\mathbf{H}_{\mathrm{ob}} = \tilde{\mathbf{A}}\ \tilde{\mathbf{R}}\ \tilde{\mathbf{P}}\ \tilde{\mathbf{Y}}\ \mathbf{F} + \mathbf{H}_{\mathrm{p}} \qquad \text{(a)}$$

where $\tilde{\mathbf{R}}$, $\tilde{\mathbf{P}}$ and $\tilde{\mathbf{Y}}$ are the matrices of rotation due to roll, pitch and heading of a ship, respectively. $\tilde{\mathbf{A}}$ is a 3 x 3 matrix which represents magnetic susceptibility of the ship, and $\mathbf{H}_{\mathrm{p}}$ is a magnetic field vector produced by a permanent magnetic moment of the ship's body. Rearrangement of Eq. (a) makes

$$\tilde{\mathbf{B}}\,\mathbf{H}_{\mathrm{ob}} + \mathbf{H}_{bp} = \tilde{\mathbf{R}}\ \tilde{\mathbf{P}}\ \tilde{\mathbf{Y}}\ \mathbf{F} \qquad \text{(b)}$$

where $\tilde{\mathbf{B}} = \tilde{\mathbf{A}}^{-1}$, and $\mathbf{H}_{bp} = -\tilde{\mathbf{B}}\,\mathbf{H}_{\mathrm{p}}$. The magnetic field, $\mathbf{F}$, can be obtained by measuring , $\tilde{\mathbf{R}}$, $\tilde{\mathbf{P}}$, $\tilde{\mathbf{Y}}$ and $\mathbf{H}_{\mathbf{ob}}$, if $\tilde{\mathbf{B}}$ and $\mathbf{H}_{bp}$ are known. Twelve constants in $\tilde{\mathbf{B}}$ and $\mathbf{H}_{\mathbf{bp}}$ can be determined by measuring variation of $\mathbf{H}_{\mathbf{ob}}$ with , $\tilde{\mathbf{R}}$, $\tilde{\mathbf{P}}$, and, $\tilde{\mathbf{Y}}$ at a place where the geomagnetic field, $\mathbf{F}$, is known.

(4) Observation Period

19 Sep. 2020 - 1 Nov. 2020 (UTC)

(5) Preliminary Results

The results will be published after the primary processing.

(6) Data archives

These data obtained in this cruise will be submitted to the Data Management Group (DMG) of JAMSTEC, and will be opened to the public via "Data Research System for Whole Cruise Information in JAMSTEC (DARWIN)" in JAMSTEC web site.
<http://www.godac.jamstec.go.jp/darwin/e>

(7) Remarks

1. For calibration of the ship's magnetic effect, "figure-eight" turns (a pair of clockwise and anti-clockwise rotation) were held at the following period and positions.
   07:30 - 07:52 21 Sep. 2020 (UTC) around 32-01N, 146-58E
   12:35 - 12:55 14 Oct. 2020 (UTC) around 72-00N, 157-36W
   19:09 - 19:31 19 Oct. 2020 (UTC) around 73-30N, 168-44W
   01:02 - 01:25:30 Oct. 2020 (UTC) around 40-01N, 149-16E

6. Notice on using

This cruise report is preliminary but it represents final documentation as of the end of the cruise. This report might not be corrected even if changes regarding its content (e.g., taxonomic classifications) are found after its publication. Moreover, this report might also be changed without notice. Data in this cruise report might be raw or unprocessed. If you intend to use or to refer to the data presented in this report, please ask the Chief Scientist for the latest information.
Users of information on this report are requested to submit Publication Report to JAMSTEC.
http://www.godac.jamstec.go.jp/darwin/explain/1/e#report
E-mail: submit-rv-cruise@jamstec.go.jp